UNIVERSITY OF CALIFORNIA, SAN DIEGO

Seasonal precipitation at a 3.97 Ma *Australopithecus anamensis* site, Allia Bay, Kenya

A dissertation submitted in partial satisfaction of the requirements for the degree
Doctor of Philosophy

in

Anthropology with a Specialization in Anthropogeny

by

Melanie M. Beasley

Committee in charge:

Professor Margaret J. Schoeninger, Chair
Professor Carolyn M. Kurle
Professor Thomas E. Levy
Professor Joanna M. McKittrick
Professor Katerina Semendeferi

2016

The Dissertation of Melanie M. Beasley is approved and it is acceptable in quality and form for publication on microfilm and electronically:

_____

_____

_____

_____

_____

Chair

University of California, San Diego

2016

DEDICATION

For the man who taught me to love teaching and
was a huge supporter of my education:

Turhon A. Murad, PhD, ABFA
(July 27, 1944 – August 15, 2015)

Mentor, adopted father, and gingerbread house builder.

TABLE OF CONTENTS

LIST OF FIGURES

LIST OF TABLES

ACKNOWLEDGEMENTS

I would like to thank my family, friends and collaborators because without their love and support this dissertation would never have been pursued or completed. First, I am eternally grateful to my advisor and mentor, Margaret Schoeninger, for her guidance, wisdom, patience, and understanding as I battled my through the process of forming a dissertation project and completing this exciting research. It has been an honor to work with her on the Koobi Fora collection she started assembling the year I was born and her extensive body of work on stable isotopes and paleoenvironment reconstructions were the inspiration for the present study. Margaret, whatever success I achieve as a biological anthropologist is in large part due to your mentorship and I can never thank you enough for accepting me as a student. I also thank my committee members Carolyn Kurle, Tom Levy, Joanna McKittrick, and Katerina Semendeferi for supporting this project and their insightful comments.

This project would not have been possible without the support of John Valley, the Director of the WiscSIMS Laboratory in the Department of Geoscience at University of Wisconsin, Madison. His guidance and insights about the project has been transformative and I am honored to be able to continue the collaboration between Margaret and John, as this project built on previous investigations at Allia Bay about paleoenvironment and diagenesis. I owe a huge debt of gratitude to Ian Orland, “my post-doc”, the amazing research scientist assigned to my project during visits to WiscSIMS. Everything I know about SIMS I learned from Ian and I appreciate his thoughtful answers to every question I had during those long analytical sessions. This project would never have gone from an idea to a completed dissertation without all his help figuring out sample mounts, imaging, and SIMS analyses. I appreciate the amazing team of people at UW-Madison who helped me during every campus visit to complete this project: Brian Hess, Noriko Kita, Kouki Kitajima, Jim Kern, John Fournelle, Phillip Gopon, and Lance Rodenkirch. I also thank Meave Leakey, Henry Bunn, and Alan Walker for access to fossil and

modern East African material that they gave to Margaret. Meave's continued support of this project after Margaret's initial isotopic investigations at Allia Bay provided the necessary fossil material to further investigate diagenesis and seasonal rainfall. A special thanks to Dr. Bruce Deck for help with the bulk isotopic analysis and for many lovely conversations about trains.

This dissertation would not have been possible without the following funding sources: The Wenner-Gren Foundation Dissertation Research Grant, Department of Anthropology Project Bucks, UCSD Academic Senate Grant, and Sigma-Xi Grant-in-Aid of Research. Thanks to these sources for providing support for this research. A special thanks to the following friends who allowed me to crash on couches in order to stretch my research funds: Alexana Hickmott (and Zorro), Mike and Rebecca Fouquette, Maggie Trumbly, Jen Harris (RIP), Jeff and Yvonne Wilson, Jake and Codye Cammack, Turhon and Jackie Murad, Courtney and Alex Daniels, and Erin Linde. Free places to stay allowed for more money for spot analyses, my deepest thanks. Two valuable experiences during my graduate career also need to be acknowledged because the experiences greatly enhanced my perspective about this dissertation project. First, a huge thanks to the Center for Academic Research and Training in Anthropogeny (CARTA) for the funding support, the symposia, and the trip to East Africa. Being able to experience the Miombo woodland at Ugalla and the arid environment of East Africa, greatly aided my understanding of East African environments and the importance of ecotone transitions. My thinking has been greatly shaped by that experience and my valuable interactions with the other CARTA students and especially conversations with Jim Moore and Alyssa Crittenden. CARTA symposia have brought together amazing anthropologists that have become valuable mentors and friends, such as Linda Marchant, Katie Hinde, and Carol Ward. To Linda especially, I am so grateful for our "shared wall" during your time at UCSD and you are the most amazing and supportive academia-Aunt. Second, a huge thanks to Jean-Jacques Hublin and Mike Richards for arranging two research trips to the Max Planck Institute for Evolutionary Anthropology in Leipzig and

providing funds for strontium analysis. My time in Leipzig was a highlight of my time in graduate school.

Additionally there are several people whose friendship and support during graduate school helped maintain my sanity and were invaluable during the rollercoaster of this research project. To my first mentor, Eric Bartelink, I would not be where I am without you; it is an honor to be your first student, friend, and colleague. I will be forever grateful to my labmate, who has been a friend, a mentor, my true brother in research, Andrew Somerville you are a model of the academic I hope to be and the lucky foot to my rabbit. From day one my partner in crime, my ginger wife, my rock has been Kari Hanson for whom I would never have been able to survive without. You have been my strongest advocate every time I stick my foot in my mouth and you make me want to be more fashionable, thanks for all the dresses. You bring out the best in me and I love you to death – but I am sorry that Africa hated you. By the power of Grayskull! There are no cats in America! And thankfully to round out the Bio Babes of Bones and Brains, we were gifted with Baboon Behavior, the ever gorgeous inside and out, Corinna Most. Corinna, who has been forever the epitome of support and kindness, you are a beautiful sole and my life has been enriched by your friendship. Baby Roo lives on forever in our hearts. Additionally, I thank the fellow graduate students who have made my time memorable at UCSD over beers, games, and debates: Matt Howland, Brady Liss, Ellen Kozelka, Mark Irish, Sam Streuli, Misha Miller-Sisson, Melanie McComsey, Jess Novak, Craig Smitheram, Matt Sitek, and many others that have participated in the fun times. But to those who know me, my anthropology family extends far beyond UCSD. Conferences (my favorite season of the year) have given me an anthropology family that has provided constant support and inspiration, I could never name them all but to my adopted academic families at Chico, UF, UNLV, MPI, UW, MSU, NYU, GW, and all my other conference buddies at SCA, Eagle Lake, WeBIG, SWABA, SAA and AAPA, I thank you for so

many beers, good conversations, and shared hotel rooms. All of you make being an anthropologist my favorite thing in the world.

On a personal note I thank Abra Pitters, my best friend in the world for being my rock, my roommate, and my constant touchstone over the years. You are my one true cheerleader that has been there longest throughout my growth as an anthropologist. Abra, Gerhard, and Zoey were the best roommates during every stress of graduate school, I will always cherish our time together. This PhD would never have happened without the support of Jon Hardes, who has given words of wisdom and been a true friend through the good and bad times. Thank you Jon for giving me my love of the National Park Service and rhinos, you made my life better. To the following people, I am so grateful for your friendship through this process: Mangan Golden, Jenn Rossiter, Traci Van Deest, Sarah Weil, Kyle McCormick, Jessica Dimka, Alli Bouwman, Nick Stevens, Stephanie Schnorr, Chelsea Leonard, Angela Perri, Geraldine Fahy, Carlos Zambrano, Katie Skorpinski, Katie Rubin, Katie Baustian, Katie Kulhavy, Amanda Friend, Michala Stock, Myra Laird, my academic brothers (Nick Passalacqua, Chris Rainwater, and Mike Kenyhercz), and countless others. Justin Seleska, thanks for all the distraction during the final year of my dissertation because every concert, baseball game, and hockey game was necessary for my writing process.

To my family, Mom, Jill, and Katie, well I don't know what to say. Too many feelings to express, there has been support, there has been silence, but I hope they are proud. Whatever happens, there is love in my heart for our family of four. To my adopted Knight family, Ray, Trista, Kendyl and Ryder, thank you for taking me in every Christmas, during every fight, and I will always be Dr. Knight-Beasley in my heart. To the rest of my adopted family, Judy Harper, Steve Gale, the Hooks (Eileen, Melissa, and Jeff), Turhon (RIP) and Jackie Murad, and John and Barb Thomas, you have all made me a better person and I am grateful to each of you for the unwavering support, shoulders to cry on, and always being there when I call. And finally to my

father, Marcial Garcia, thank you for all of our wonderful conversations, your enthusiasm for history, and support of my pursuit of a PhD. I am thankful for the time as an adult that we have had together and I hope you are proud.

Chapter 2 is currently being prepared for submission for publication with co-author Margaret Schoeninger. Chapter 3 is currently being prepared for submission for publication with co-authors Margaret Schoeninger, Ian Orland, and John Valley. Chapter 4 is currently being prepared for submission for publication with co-authors Margaret Schoeninger, Ian Orland, and John Valley. The dissertation author was the primary investigator and author of the material for all three chapters.

CURRICULUM VITAE

EDUCATION

2016 Doctor of Philosophy, Anthropology with a Specialization in Anthropogeny, University of California, San Diego
2011 Iso-Camp: Stable Isotope Ecology Short Course, University of Utah
2008 Master of Arts, Anthropology, California State University, Chico
2003 Bachlor of Science, Anthropology, University of California, Davis

PUBLISHED ARTICLES

Jaouen, K, Beasley MM, Schoeninger MJ, Hublin JJ, Richards MP. (2016) Zinc isotope ratios of bones and teeth as new dietary indicators: results from a modern food web (Koobi Fora, Kenya). Scientific Reports 6:26281.

Beasley MM, Bartelink EJ, Taylor LL, Miller RM. (2014) Comparison of transmission FTIR, ATR, and DRIFT: Implications for assessment of diagenesis of bone. J Archaeol Sci. 46:16-22.

Good SP, Kennedy CD, Stalker JC, Chesson LA, Valenzuela LO, Beasley MM, Ehleringer JR, Bowen GJ. (2014) Patterns of local and nonlocal water resource use across the western U.S. determined via stable isotope intercomparisons. Water Resour. Res. 50(10):8034-8049.

Bartelink EJ, Berg GE, Beasley MM, Chesson LA. (2014) Application of stable isotope forensics for predicting region-of-origin of human remains from past wars and conflicts. Annals of Anthropological Practice, special volume (invited): "Practicing Forensic Anthropology: A Human Rights Approach to the Global Problem of Missing and Unidentified Persons". 38(1):124-136.

Beasley MM, Martinez AM, Simons DD, Bartelink EJ. (2013) Paleodietary analysis of a San Francisco Bay area shellmound: stable carbon and nitrogen isotope analysis of late Holocene humans from the Ellis Landing site (CA-CCO-295). J Archaeol Sci.40:2084-2094.

AWARDS, GRANTS, AND FELLOWSHIPS

2016 Dean of Social Science Student Travel Grant, UCSD ($374)

2015 UCSD President's Dissertation Year Diversity Fellowship (1 year of $22,000 stipend plus university fees)

2015 European Society for the Study of Human Evolution, ESHE Student Travel Grant (€550)

2015 UCSD Graduate Student Association Travel Grant ($500)

2014 Student Poster Award, Honorable Mention, Western Bioarchaeology Interest Group Annual Meeting (book prize)

2013 Wenner-Gren Foundation Dissertation Fieldwork Grant ($19,940)

2013 Project Bucks Grant, Department of Anthropology, UCSD ($3,600)

2013 Dean of Social Science Student Travel Grant, UCSD, ($250)

2012 Sigma Xi Grants-in-Aid of Research ($1,000)

2012 Dean of Social Science Student Travel Grant, UCSD, ($125)

2011 Dean of Social Science Student Travel Grant, UCSD, ($250)

2011 Student Paper Award, Society for American Archaeology Annual Meeting in Sacramento

2011 CARTA Fellowship, UCSD (3 years of $35,000 stipend and university fees)

2010 James A. Bennyhoff Award, from SCA ($1000, 4 AMS date, 50 obsidian sourcing)

2009 San Diego Fellowship, UCSD (4 years of $20,000 stipend plus university fees)

2008 Outstanding Master's Thesis Award, CSU Chico ($500)

2008 Outstanding Student Paper Award, Society for California Archaeology ($200)

2008 BSS Student Travel Grant, CSU Chico, for AAFS Conference ($200)

2007 CSU Chico Graduate School Student Research Grant ($500)

2006 BSS Student Travel Grant, CSU Chico, for AAFS Conference ($75)

2005 BSS Student Travel Grant, CSU Chico, for AAFS Conference ($200)

ACADEMIC APPOINTMENTS (Instructor of Record; *Upper Division Course)

The Human Skeleton*
Summer 2012-2016: University of California, San Diego, Associate Instructor

Human Origins
Summer 2013: University of California, San Diego, Associate Instructor

Intro to Physical Anthropology
Summer 2014: Saddleback Community College, Associate Part-Time Faculty
Spring 2009: California State University, Chico, Part-time Adjunct Faculty
Spring 2008, 2009: Butte Community College, Associate Faculty

Survey of Forensic Science*
Fall 2007, Spring 2008: California State University, Chico, Part-time Adjunct Faculty

ABSTRACT OF THE DISSERTATION

Seasonal precipitation at a 3.97 Ma *Australopithecus anamensis* site,
Allia Bay, Kenya

by

Melanie M. Beasley

Doctor of Philosophy in Anthropology with a Specialization in Anthropogeny

University of California, San Diego, 2016

Professor Margaret J. Schoeninger, Chair

This dissertation explores the link between habitat and human evolution by examining the mosaic habitat and its seasonal variation in rainfall at the single fossil locality of Allia Bay, Kenya (3.97±0.03 MA) using stable carbon ($\delta^{13}C$) and oxygen ($\delta^{18}O$) isotope ratios in fossil faunal tooth enamel. Serial $\delta^{18}O$ values from 10µm spot analyses in contrast to data from bulk powdered samples, this dissertation uses browsing and grazing faunal enamel to document prolonged periods of environmental stability with mild seasonality and periods of marked fluctuating seasonality during the drier phases at Allia Bay when *Au. anamensis* occupied the region.

Traditional bulk $\delta^{13}C$ and $\delta^{18}O$ values of fossil Allia Bay compared to modern Koobi Fora fauna indicate that the local environment at Allia Bay was distinctly wetter and more closed compared to the arid open grassland of the modern region. Despite regional interpretations of a continuously arid open Turkana Basin over the past 4 Ma, the Allia Bay fauna suggest that local habitats surrounding Lake Turkana were ecologically distinct with different microclimates. Enamel from fossil localities used for isotopic analysis to reconstruct the paleoenvironment are often considered impervious to diagenesis, however at Allia Bay mineral structure changes in enamel indicate that diagenesis is an issue at this fossil locality. While the complex process of enamel diagenesis is not understood completely, the high-resolution sampling of $\delta^{18}O_{en}$ values documented a relationship between mineral structure change and diagenesis of $\delta^{18}O_{en}$. Confocal laser fluorescent microscopy imaging identified evidence of mineral structure change documented by far-red fluorophores that correlate with alteration of $\delta^{18}O_{en}$, while other inclusions identified by green and red fluorophores have limited impact to $\delta^{18}O_{en}$. Ultimately, this dissertation documented the first evidence of variation in seasonal rainfall patterns at Allia Bay during intra-annual cycles (~10-17 months of time recorded in enamel). The $\delta^{18}O_{en}$ values documented in fossil hippopotamids and suids show a 6-8‰ baseline difference during the occupation of Allia Bay, suggesting the ecosystem shifted significantly. As rainfall patterns fluctuated, animal and plant communities were impacted and the early hominins would have required adaptive flexibility to cope with the changing habitat.

CHAPTER 1: INTRODUCTION

Our understanding of the forces selecting for human bipedalism, the distinctive mode of human locomotion, was upended in 2009, when White and colleagues (*Science*, 326:64), described the 4.4 million year old *Ardipithecus ramidus* at Aramis, Ethiopia as the earliest facultative biped and a human ancestor. In contrast to expectations, the species inhabited open woodland not savanna grassland (although see Moore 1996). Prior to this find, the general consensus was that bipedalism arose in conjunction with the spreading of savanna grassland environments as climate became drier at the end of the Miocene Epoch (5-7 million years ago, MA) (Cerling et al. 1997). Isbell and Young (1996) proposed that bipedalism was more efficient energetically for reaching widely dispersed resource patches of fruit- or nut-producing trees compared to the knuckle-walking of chimpanzee ancestors who remained in forest refugia. While many people question the placement of *Ardipithecus* within our lineage and many others question its mode of locomotion, the types of environments inhabited by our earliest facultative and, subsequently, obligate bipedal ancestors are now open to question.

Remains of *Australopithecus anamensis*, the earliest confirmed obligate hominin bipedal species, have been recovered from Allia Bay, Kenya (3.97±0.03 MA) on the eastern shore of Lake Turkana in the Koobi Fora Region, and from southwest of the lake at Kanapoi, Kenya (4.17-4.07 MA) (Brown and McDougall 2011; Leakey et al. 1995; Leakey et al. 1998; Wood and Leakey 2011). Phylogenetic analyses indicate that the *Au. anamensis* populations found at Kanapoi and Allia Bay represent part of an anagenetically evolving lineage in which a sudden transition from *Ardipithecus* led to *Au. anamensis* and another, later transition gave rise to *Au. afarensis* (Haile-Selassie et al. 2010; Kimbel et al. 2006; White et al. 2006). Kimbel et al. (2006) suggest that each site-sample captures a different point along the evolutionary trajectory of early hominins, so it is critical to reconstruct the paleoenvironment of each site to evaluate the interplay between habitat and human evolution.

This dissertation tests hypotheses regarding the link between habitat and human evolution at Allia Bay, Kenya (3.97±0.03 MA) by exploring the mosaic habitat and seasonal variation in rainfall within a "local" environment using stable carbon ($\delta^{13}C$) and oxygen ($\delta^{18}O$) isotopes from fossil fauna tooth enamel. The $\delta^{13}C$ and $\delta^{18}O$ values in bulk samples of powdered enamel will establish the general paleoenvironment indicating the canopy cover/feeding ecology, relative humidity, and moisture regime experienced by an animal depending on the feeding and drinking behavior that is averaged over the duration of the development of a tooth (i.e., months or years) and therefore might mask the amount of variation in intra-annual isotope values. Subsequently, high-resolution serial sampling of $\delta^{18}O$ values generated by secondary ion mass spectrometry (SIMS) will provide estimates about the variability of patterns of seasonal rainfall amount and duration at Allia Bay experienced by browsing and grazing fauna.

Over the years, many hypotheses have suggested links among climate, the environment, and significant morphological adaptations in hominins, especially bipedalism (e.g., deMenocal 2004; Domínguez -Rodrigo 2014; Potts 1998). Unfortunately, paleoenvironmental reconstructions in East Africa often rely on surface-collected fossil fauna that are not *in situ* and which combine multiple temporal and geographically dispersed components. Such a framework lacks the temporal-spatial resolution to develop solid causal links between evolution and the environment (Kingston 2007). By focusing on the fauna from a single excavation (locality 261-1) with good temporal resolution, this dissertation will provide evidence of the level of variability in seasonal precipitation patterns at the sole hominin fossil site dating to 3.97 Ma currently known along our evolutionary tree.

In the East African Rift System, debates continue over how wet or dry and how tree-covered or open was the environment at the period in human evolution when early hominins shifted their mode of locomotion to bipedalism (Cerling et al. 2010; White et al. 2009a; WoldeGabriel et al. 2009). Isotopic data from paleosols typically indicate open, xeric habitats

with little woody canopy cover (Cerling et al. 2011b; Passey et al. 2010). There is, however, a warm-season bias in carbonate formation (Peters et al. 2013) which could account for these patterns. In contrast, isotopic data generated from fossil tooth enamel, which reflects the environment recorded by a single individual, often suggest more mixed mosaic, mesic habitats 4 Ma in the Turkana Basin (Drapeau et al. 2014; Schoeninger et al. 2003b).

In 2008, Codron and colleagues suggested that early *Australopithecus* was a hominin genus uniquely adapted to arid regions As mentioned above, paleosol carbonate data indicate that Allia Bay during *Au. anamensis* times was as arid as today's bush and grassland savanna in the Turkana Basin (Cerling et al. 2011a). In addition to the previously noted complications of paleosol carbonate data, faunal assemblages suggest that *Au. anamensis* survived in a variety of ecosystems from wetter, closed woodlands with patches of open grassland to more arid woodland and shrubland regions (Behrensmeyer and Reed 2013). Extensive geological mapping revealed that in contrast to the Turkana Basin of today, the ancestral Omo River flowed continuously through the region with Allia Bay situated on a channel of this river system, at the time of *Au. anamensis* (Brown and Feibel 1991). Recent work on extant chimpanzee samples collected from a range of habitats (closed canopy to open savanna woodlands) reveals that animals living along a continuously flowing river channel have lower (i.e., wetter) $\delta^{13}C$ values than expected based on the region's Mean Annual Precipitation (Schoeninger et al. 2015). In the East African Rift System, transition between different biomes (for example, closed canopy forest transitioning into open grassland) can be sudden (Ward et al. 1999). During the fluvial phase when *Au. anamensis* occupied Allia Bay, the Omo River could have dominated an otherwise arid environment to the extent that only narrow ecotones (transitions between biomes) existed between desert and forest niches (Ward et al. 1999).

The following dissertation chapters aim to investigate the mosaic habitat and seasonal rainfall patterns at Allia Bay. Chapter 2 tests whether the Turkana Basin has been continuously

arid or if there were local ecological niches (i.e., Allia Bay) of more mesic habitats available to early hominins. A previous pilot study of bulk $\delta^{18}O$ and $\delta^{13}C$ from fossil fauna enamel samples from Allia Bay (n =22) showed a general paleoenvironment signature of a wetter mosaic habitat with significantly more woodland compared to the modern arid environment (Schoeninger et al. 2003b). In Chapter 2, an additional 48 fossil fauna bulk enamel samples from seven animal families are compared to the $\delta^{13}C$ and $\delta^{18}O$ of their modern analogs collected in the Koobi Fora region by Dr. Margaret Schoeninger in 1984 and 1993. This chapter serves as a background for the paleoenvironment reconstruction of Allia Bay using traditional bulk stable isotope carbonate preparation methods. The modern data (n = 70) set is the largest carbonate record of ten modern species representing five animal families living within the Turkana Basin along the northeastern shore of Lake Turkana analyzed to date.

Chapter 3 addresses the issue of diagenesis in tooth enamel that was previously identified by cathodoluminescence (CL) (Schoeninger et al. 2003a) and ion microprobe data (Kohn et al. 1999). It is unclear whether changes identified by CL correspond to altered isotope ratios at the altered/unaltered boundary of enamel mineral structure change. It was not until technological advancements in high-resolution sampling capabilities, such as with the SIMS, that the question of diagenesis of $\delta^{18}O$ in enamel identified by CL could be tested. The SIMS ability to generate serial spot analyses at a scale of 10 µm spots *in situ* ensures the boundary between altered and unaltered tooth enamel can be accurately characterized for changes in $\delta^{18}O_{en}$ values. This chapter presents data on the identification of altered $\delta^{18}O_{en}$ values that corresponds to predicted diagenetically altered regions based on imaging of enamel with confocal laser fluorescence microscopy (CLFM). The results from this experiment highlight the complexity of diagenesis as tooth enamel moves from the biosphere to the geosphere.

Based on the results from diagenesis identification determined in Chapter 3, Chapter 4 analyzes the $\delta^{18}O$ values recorded in the unaltered regions in enamel to reconstruct the seasonal

patterns of rainfall at an early hominin site. Previous analysis of stress lines recorded in tooth enamel suggest that browsers and grazers from Allia Bay experienced intra-annual periods of stress, leading Macho et al. (2003) to conclude that hominins at Allia Bay experienced a seasonal environment with periods of resource stress in a climate similar to modern Masai Mara (i.e., two rainy seasons – one long, one short). This chapter presents the SIMS high-resolution $\delta^{18}O$ analysis that suggests browsers and grazers recorded seasonal shifts in source $\delta^{18}O$ values, which may affect the vegetation seasonally available in the mosaic channel river system at Allia Bay.

By exploring the impact of seasonality on human evolution, this dissertation attempts to provide a new scale of analysis to explore the links between the paleoenvironment and bipedalism. The ultimate aim of the dissertation is to refine the definition of the mosaic habitat at Allia Bay and for the first time provide information on the intra-annual variation in rainfall at an early fossil hominin locality within a biologic time-scale.

References

Behrensmeyer AK, and Reed KE. 2013. Reconstructing the habitats of *Australopithecus*: Paleoenvironments, site taphonomy, and faunas. In: Reed KE, Fleagle JG, and Leakey RE, editors. The Paleobiology of *Australopithecus*. London: Springer. p 41-60.

Brown F, and Feibel C. 1991. Stratigraphy, depositional environments and palaeogeography of the Koobi Fora Formation. In: Harris J, editor. Koobi Fora Research Project. Oxford: Clarendon Press. p 1-30.

Brown FH, and McDougall I. 2011. Geochronology of the Turkana depression of northern Kenya and southern Ethiopia. Evolutionary Anthropology: Issues, News, and Reviews 20(6):217-227.

Cerling TE, Harris JM, MacFadden BJ, Leakey MG, Quade J, Eisenmann V, and Ehleringer JR. 1997. Global vegetation change through the Miocene/Pliocene boundary. Nature 389(6647):153-158.

Cerling TE, Levin NE, and Passey BH. 2011a. Stable Isotope Ecology in the Omo-Turkana Basin. Evolutionary Anthropology: Issues, News, and Reviews 20(6):228-237.

Cerling TE, Levin NE, Quade J, Wynn JG, Fox DL, Kingston JD, Klein RG, and Brown FH. 2010. Comment on the paleoenvironment of *Ardipithecus ramidus*. Science 328(5982):1105.

Cerling TE, Wynn JG, Andanje SA, Bird MI, Korir DK, Levin NE, Mace W, Macharia AN, Quade J, and Remien CH. 2011b. Woody cover and hominin environments in the past 6 million years. Nature 476(7358):51-56.

Codron D, Lee-Thorp JA, Sponheimer M, De Ruiter D, and Codron J. 2008. What insights can baboon feeding ecology provide for early hominin niche differentiation? International Journal of Primatology 29(3):757-772.

deMenocal PB. 2004. African climate change and faunal evolution during the Pliocene–Pleistocene. Earth and Planetary Science Letters 220(1-2):3-24.

Domínguez-Rodrigo M. 2014. Is the "Savanna Hypothesis" a dead concept for explaining the emergence of the earliest hominins? Current Anthropology 55(1):59-81.

Drapeau M, Robe R, Wynn J, and Geraads D. 2014. The Omo Mursi Formation reconsidered: a window into the East African Pliocene. Journal of Human Evolution 75:64-79.

Haile-Selassie Y, Saylor BZ, Deino A, Alene M, and Latimer BM. 2010. New hominid fossils from Woranso-Mille (Central Afar, Ethiopia) and taxonomy of early *Australopithecus*. American Journal of Physical Anthropology 141(3):406-417.

Isbell LA, and Young TP. 1996. The evolution of bipedalism in hominids and reduced group size in chimpanzees: alternative responses to decreasing resource availability. Journal of Human Evolution 30(5):389-397.

Kimbel WH, Lockwood CA, Ward CV, Leakey MG, Rak Y, and Johanson DC. 2006. Was *Australopithecus anamensis* ancestral to *A. afarensis*? A case of anagenesis in the hominin fossil record. Journal of Human Evolution 51(2):134-152.

Kingston JD. 2007. Shifting adaptive landscapes: progress and challenges in reconstructing early hominid environments. American Journal of Physical Anthropology 134(S45):20-58.

Kohn MJ, Schoeninger MJ, and Barker WW. 1999. Altered states: Effects of diagenesis on fossil tooth chemistry. Geochimica et Cosmochimica Acta 63(18):2737-2747.

Leakey MG, Feibel CS, McDougall I, and Walker A. 1995. New four-million-year-old hominid species from Kanapoi and Allia Bay, Kenya. Nature 376(6541):565-571.

Leakey MG, Feibel CS, McDougall I, Ward C, and Walker A. 1998. New specimens and confirmation of an early age for *Australopithecus anamensis*. Nature 393(6680):62-66.

Macho GA, Leakey M, Williamson D, and Jiang Y. 2003. Palaeoenvironmental reconstruction: evidence for seasonality at Allia Bay, Kenya, at 3.9 million years. Palaeogeography, Palaeoclimatology, Palaeoecology 199(1):17-30.

Moore J. 1996. Savanna chimpanzees, referential models and the last common ancestor. In: McGrew WC, Marchant LF, and Nishida T, editors. Great Ape Societies. Cambridge: Cambridge University Press. p 275-292.

Passey BH, Levin NE, Cerling TE, Brown FH, and Eiler JM. 2010. High-temperature environments of human evolution in East Africa based on bond ordering in paleosol carbonates. Proceedings of the National Academy of Sciences 107(25):11245-11249.

Peters NA, Huntington KW, and Hoke GD. 2013. Hot or not? Impact of seasonally variable soil carbonate formation on paleotemperature and O-isotope records from clumped isotope thermometry. Earth and Planetary Science Letters 361:208-218.

Potts R. 1998. Environmental hypotheses of hominin evolution. American Journal of Physical Anthropology 107(s27):93-136.

Schoeninger MJ, Hallin K, Reeser H, Valley JW, and Fournelle J. 2003a. Isotopic alteration of mammalian tooth enamel. International Journal of Osteoarchaeology 13(1-2):11-19.

Schoeninger MJ, Most CA, Moore JJ, and Somerville AD. 2015. Environmental variables across *Pan troglodytes* study sites correspond with the carbon, but not the nitrogen, stable isotope ratios of chimpanzee hair. American Journal of Primatology. DOI: 10.1002/ajp.22496

Schoeninger MJ, Reeser H, and Hallin K. 2003b. Paleoenvironment of *Australopithecus anamensis* at Allia Bay, East Turkana, Kenya: evidence from mammalian herbivore enamel stable isotopes. Journal of Anthropological Archaeology 22(3):200-207.

Ward C, Leakey M, and Walker A. 1999. The new hominid species *Australopithecus anamensis*. Evolutionary Anthropology 7(6):197-205.

White TD, Ambrose SH, Suwa G, Su DF, DeGusta D, Bernor RL, Boisserie J-R, Brunet M, Delson E, Frost S et al. . 2009a. Macrovertebrate Paleontology and the Pliocene Habitat of *Ardipithecus ramidus*. Science 326(5949):67-93.

White TD, Asfaw B, Beyene Y, Haile-Selassie Y, Lovejoy CO, Suwa G, and WoldeGabriel G. 2009b. *Ardipithecus ramidus* and the Paleobiology of Early Hominids. Science 326(5949):64-86.

White TD, WoldeGabriel G, Asfaw B, Ambrose S, Beyene Y, Bernor RL, Boisserie J-R, Currie B, Gilbert H, Haile-Selassie Y et al. . 2006. Asa Issie, Aramis and the origin of *Australopithecus*. Nature 440(7086):883-889.

WoldeGabriel G, Ambrose SH, Barboni D, Bonnefille R, Bremond L, Currie B, DeGusta D, Hart WK, Murray AM, and Renne PR. 2009. The geological, isotopic, botanical, invertebrate, and lower vertebrate surroundings of *Ardipithecus ramidus*. Science 326(5949):65-65e65.

Wood B, and Leakey M. 2011. The Omo-Turkana Basin Fossil Hominins and Their Contribution to Our Understanding of Human Evolution in Africa. Evolutionary Anthropology: Issues, News, and Reviews 20(6):264-292.

CHAPTER 2: MIOMBO WOODLANDS AND EARLY HOMININS: A COMPARISON OF CARBONATE STABLE ISOTOPE FAUNAL DATA FROM MODERN KOOBI FORA AND 3.97MA ALLIA BAY, EAST LAKE TURKANA, KENYA

Introduction

Many important early hominin fossil sites that shape our understanding about the root of our ancestral lineage occur in East Africa, which is currently one of the hottest regions in the world. The Turkana-Omo Basin has some of the oldest hominin fossil-bearing localities, including on the eastern shore of Lake Turkana from Allia Bay, Kenya (3.97 ± 0.03 Ma) (Leakey et al. 1995; Leakey et al. 1998; Ward et al. 1999; Ward et al. 2001; Wood and Leakey 2011) and from southwest of the lake at Kanapoi, Kenya (4.17-4.07 Ma) (Brown and McDougall 2011; Leakey et al. 1995; Leakey et al. 1998). There *Australopithecus anamenesis*, the earliest confirmed obligate biped within the hominin lineage, has been recovered.

The ecological niche exploited by early hominins is assumed to have played an essential role in the origins of bipedalism, a distinguishing characteristic of hominins among mammals. Therefore, reconstructing the paleoenvironment at early hominin sites is essential for understanding the selective forces that resulted in such a significant morphological change. A phylogenetic analysis supports the idea that *Au. anamensis* represents part of an anagenetically evolving lineage, arising from a sudden transition out of the preceding *Ardipithecus* genus and giving rise to the later *Au. afarensis* species (Haile-Selassie et al. 2010; Kimbel et al. 2006; White et al. 2006). Currently, *Au. anamensis* has been recovered at three fossil sites in the Omo-Turkana Basin (Allia Bay, Kanapoi, and Fejej) and possibly four sites in the Afar Rift of Ethiopia (Aramis, Asa Issie, Woranso-Mille and Galili) (Haile-Selassie et al. 2010; Kappelman et al. 1996; Kullmer et al. 2008; Leakey et al. 1995; Van Couvering 2000; Ward et al. 1999; Ward et al. 2001; Ward 2014; White et al. 2006; Wood and Leakey 2011). Kimbel et al. (2006) suggest that each site-sample captures a different point along the evolutionary trajectory of early hominins, so it is

critical to reconstruct the paleoenvironment of each site to evaluate the interplay between habitat and human evolution.

Over the years, many hypotheses have suggested links among climate, the environment, and significant morphological adaptations in hominins, especially bipedalism (Behrensmeyer 2006; deMenocal 2004; Domínguez-Rodrigo 2014; Potts 1998). Unfortunately, paleoenvironmental reconstructions in East Africa often rely on surface-collected fossil fauna that combine multiple temporal and geographically dispersed components that are not *in-situ*. As a result global or regional trends are most often discussed. On a global scale, cooling in the Neogene Period (23-2.6 Ma) resulted in the aridification of Africa (deMenocal and Rind 1993; Tiedemann et al. 1994; Zachos et al. 2001) with arid-adapted C_4 plants spreading between 8 and 6 Ma (Cerling 1992; Cerling et al. 1997; Morgan et al. 1994; Ségalen et al. 2007). Fossil faunal, floral, and paleosol assemblages suggest a general trend of increasingly open-arid environments with pulses of species turnover during the past 4 Ma (Behrensmeyer et al. 1997; Bobe et al. 2002; Bonnefille 1995; Bonnefille and Mohammed 1994; Bonnefille et al. 2004; Cerling et al. 2015; Cerling et al. 1988; Fernández and Vrba 2006; Passey et al. 2010; Reed 1997; Vrba et al. 1995; Vrba 1985; Vrba 1988). In the last 4 Ma, paleosol data indicate that the dominant environment in East Africa was wooded grassland with significant areas of open habitat, represented by 10-40% woody canopy cover (Cerling et al. 2011a; Cerling et al. 2011b). Generally, the Plio-Pleistocene environment in East Africa became more open with less continuous tree cover compared to earlier periods and continued to shift towards the arid environment that is experienced today in modern East Africa.

The general nature of this framework, however, lacks the temporal-spatial resolution to develop solid causal links between evolution and the environment (Kingston 2007). In fact, at the West Turkana fossil localities, the mammalian assemblages indicate a sufficiently humid climate to support perennial rivers during the past 4 Ma (Harris et al. 1988). It is clear from the fossil

mammal assemblages from localities surrounding Lake Turkana that despite regional climatic shifts in the Turkana Basin, the local habitats surrounding the lake were distinct ecologically to the extent that differences in the nature and abundance of species was maintained (Harris et al. 1988). Outside of the Turkana Basin at fossil localities in the Kenya Rift Valley from the past 4 Ma, a heterogeneous environment of mixed C_3 and C_4-plants persisted with no evidence of a shift from closed to more open habitats (Kingston et al. 1994). Yet, carbon isotope data indicate a dependence by *Au. bahrelghazali* from Chad on C_4-plant resources as early as 3 Ma suggesting that open habitat environments were critical for subsistence strategies of this early hominin (Lee-Thorp et al. 2012). Recent studies reviewed by Kingston (2007) highlight that short-term ecological changes might match or even exceed the influence of long-term changes on evolution; assuming this is correct, then it is no longer reasonable to frame human evolution within long-term global or regional trends, but instead the focus must be on smaller, more local sites and time scales.

This debate about scale of ecological influence on human evolution is highlighted in the ongoing different interpretations of how wet or dry and how tree-covered or open was the environment at the period in human evolution when early hominins shifted their mode of locomotion to bipedalism (Cerling et al. 2010; White et al. 2009a; WoldeGabriel et al. 2009). In the Turkana Basin, the prevailing assumption is the region was continually hot during the past 4 Ma as arid-adapted C_4 plants spread throughout Africa with soil temperatures typically above 30°C year round supporting an early opening of the habitat (Cerling 1992; Cerling et al. 2015; Cerling et al. 1997; Passey et al. 2010). Recent analysis of the bulk enamel $\delta^{13}C$ by Cerling et al. (2015) suggests that in the Turkana Basin 4 Ma there were more mixed feeding species compared to the more distinct C_3 browsers or C_4 grazers that occur today. Kanapoi, the earliest documented site of *Au. anamensis* and the type locality for the species, has a diverse mammalian fauna including cercopithecid, elephantid, rhinocerotid, suid, giraffid, and bovid species, which have

been used in approximating the paleoenvironment of this early hominin species as dry, possibly open, wooded or bushland conditions (Harris and Leakey 2003; Leakey et al. 1995). Kanapoi has also been characterized as having an open arid to semi-arid climate based on paleosol carbon isotope data (Wynn 2000) supporting the interpretation of a continually hot arid climate in the Turkana Basin over the past 4 Ma. However, recent reevaluation of the fauna (Geraads et al. 2013) and ecological structure analysis (Harris and Leakey 2003) suggests that Kanapoi had a mosaic habitat of woodland and open grassland possibly closer to a closed woodland similar to the habitat proposed for *Ardipithecus ramidus* (Harris and Leakey 2003; White et al. 2009b).

In contrast to the continuously hot arid reconstruction of the climate from paleosol data, an early pilot study at Allia Bay of the $\delta^{18}O$ and $\delta^{13}C$ values from fossil fauna tooth enamel suggested that the local paleoenvironment was more mesic than today with a habitat similar to modern Miombo woodlands (Schoeninger et al. 2003b). A Miombo-like savanna woodland is an ecosystem dominated by *Brachystegia* spp., with approximately 25-75% canopy cover (Moore 1996). This is supported by the four paleosol samples from Allia Bay, three of which have the lowest $\delta^{13}C$ values of any samples from the Turkana Basin, indicative of significant woody cover (>40%) (Levin et al. 2011; Levin et al. 2015). Additionally, a proxy climate method using strontium isotope ratios of lacustrine fish fossil remains from the Koobi Fora region demonstrate that between ~2 and 1.85 Ma the Turkana Basin remained well-watered and was possibly an aridity refugium for obligate drinking fauna when other basins in the East African Rift System were impacted by droughts (Joordens et al. 2011). These conflicting interpretations of paleoenvironments both at the local scale based on soils and fauna and the regional scale emphasize the need for multiple lines of evidence from fossil localities across the Turkana Basin in order to better understand the proximal and causal links impacting the selection for the defining morphological features of our ancestral lineage.

When considering the multiple lines of evidence accumulated from sites across East Africa, it seems that there is a general trend for fossil fauna assemblages and isotopic data generated from enamel (which reflects the environment recorded by a single individual) to point toward mixed mosaic mesic habitats compared to isotopic data from paleosols, which indicate more open xeric habitats with significantly less woody canopy cover. Perhaps this is the result of warm-season bias in carbonate formation which would impact interpretations generated from paleosol carbonate data (Peters et al. 2013). The paleosol carbonate value depends on the temperature of carbonate formation and the $\delta^{18}O$ value of the water from which it is formed (Peters et al. 2013). It is possible that overprinting of the ^{13}C-^{18}O ordering in the paleosol carbonates that might homogenize the isotopic values occurs due to a warm-season bias (Peters et al. 2013; Quade et al. 2007). It is assumed that carbonate formation temperatures reflect mean-annual air temperatures in past environments, but if there is a seasonal bias toward warm-season carbonate formation, then it is possible that interpreted air and soil temperature records are biased in the Turkana Basin where seasonal fluctuations are currently unknown (Breecker et al. 2009; Passey et al. 2010; Peters et al. 2013; Quade et al. 2007).

The seemingly conflicting interpretation of soil and faunal data result in the term "mosaic" being associated with multiple interpretations of varied paleoenvironments (Reed et al. 2014). By invoking the term "mosaic" to define a variety of paleoenvironments, the specific differences in the composition of openness compared to more densely tree-covered areas can be overlooked but might be key in understanding the environmental variables that promoted selection for bipedalism. The question is, within a mosaic habitat was *Au. anamensis* associated more specifically with one habitat, either densely tree-covered woodlands or more open grassland savannas, or were they occupying the fringe ecotones between woodlands and grasslands exploiting a variety of resources favoring a flexible ecological adaptation?

Chimpanzees often act as a referential model for our early hominin ancestors (Moore 1996; Sponheimer et al. 2006). A recent study of modern chimpanzee habitats reconstructed from biological tissues ($\delta^{13}C$ in hair) indicate that modern environmental model expectations will not conform to known ecological habitats when individuals are living within a riverine gallery forest in a region of low rainfall (Schoeninger et al. 2015). This has serious implications for paleoenvironment reconstructions because when chimpanzees occupying a habitat with a variety of ecosystem types they have been shown to feed only in the more densely tree-covered ecological niches (Schoeninger et al. 2015). In this instance recovered fauna might indicate a 'mosaic' habitat, while to the chimpanzees there was only one habitat they were feeding in. Perhaps early hominins similarly had narrow ecological niches with a specific feeding ecology or possibly early hominins overcame this and occupied areas with a variety of habitats to exploit multiple ecosystem types. It is possible that the key to the success of early hominins was their adaptive flexibility to exploit the variety of ecosystem types within a single geographic region. Therefore it is critical to understand the nature of a 'mosaic' habitat at a local site scale.

To test whether the Turkana Basin has been uniformly an arid landscape dominated by grasslands 4 Ma, we focus on Allia Bay, Kenya (site 261-1, 3.97 ± 0.03 Ma) where *Au. anamensis* and other non-hominin primates are found associated with fossil hippos, elephants, giraffes, suids, deinotheres, bovids, and equids. Here we present new bulk $\delta^{18}O$ and $\delta^{13}C$ data of tooth enamel from 48 fossil fauna, compared with 22 in the earlier study (Schoeninger et al. 2003b). We compare these fossil data to enamel and bone carbonate from 70 modern fauna collected within the larger Koobi Fora region on the eastern shore of Lake Turkana. We expect the bulk $\delta^{18}O$ values from modern and fossil faunal enamel will support the pilot data conclusion that Allia Bay was significantly more mesic compared to today's environment (contra Passey et al. 2010). By focusing on a single site within the greater Turkana Basin, we hope to better understand the mosaic habitat at a single local site that *Au. anamensis* inhabited.

We also compare the Allia Bay fossil $\delta^{13}C$ and $\delta^{18}O$ data to other Pliocene sites in the Omo-Turkana Basin that have published comparative $\delta^{13}C$ and $\delta^{18}O$ data, specifically Kanapoi (Harris et al. 2003) and the Omo Mursi Formation (Figure 2.1; Drapeau et al. 2014). The hominin fossil site of Kanapoi has *Au. anamensis* remains with a suggested paleoenvironment of an arid to semi-arid climate with seasonal moisture in a mosaic of gallery forest to closed woodland opening into open grassland patches (Bobe 2011; Geraads et al. 2013; Wynn 2000). In the Omo Valley, the Omo Mursi Formation with fossils collected from Cholo and Yellow Sands, has yet to yield any primate remains, including hominins, but is an approximately contemporary site to Kanapoi and Allia Bay dating to more than 4 Ma (Drapeau et al. 2014). Drapeau et al. (2014) interpret the Omo Mursi paleoenvironment as more humid and closed compared to the lower Turkana Basin acting as a mesic refugium for closed-habitat species. Drapeau et al. (2014) postulate that the absence of hominins at the Omo Mursi localities is that the wetter tree-covered habitat was not favored by the hominins that might be more adapted to open drier environments similar to Kanapoi.

The five Ethiopian localities (Fejej, Aramis, Asa Issie, Woranso-Mille and Galili) (Haile-Selassie et al. 2010; Kappelman et al. 1996; Kullmer et al. 2008; Leakey et al. 1995; Van Couvering 2000; Ward et al. 1999; Ward et al. 2001; Ward 2014; White et al. 2006; Wood and Leakey 2011) were omitted from this study because of the lack of enamel stable carbon and oxygen isotope data or the fossil locality was outside of the Omo-Turkana Basin with a different water source. Paleoenvironmental reconstructions of the sites based on fossil fauna assemblages indicate that all the localities were mosaic habitats with varied amount of canopy cover and different moisture regimes. Quite possibly *Au. anamensis* was adaptively flexible (Behrensmeyer and Reed 2013; Wynn 2000). We expect this comparison to expand our information on the types of habitats that *Au. anamensis* inhabited and, quite possibly, highlight adaptive flexibility in a species that may have flourished in a wide variety of environments.

Paleoenvironmental reconstruction of the Omo-Turkana Basin

Faunal analyses of fossil species in the Omo-Turkana Basin suggest differences in the habitats across the region. The lower Omo Valley between 4-2 Ma had high proportions of tragelaphini (kudu, bushbuck, eland) and aepycerotini (impala), which are bovids associated with woodlands or edge environments between woodlands and grasslands (Bobe 2011). Additionally, some reduncini (waterbuck and reedbuck) and bovini (buffalo) species were represented in the Omo Valley that have modern analogs associated with grasslands in environments close to water (Bobe 2011). The mix of species in the Omo Valley seem to indicate a more forested and stable environment than those in other parts of the basin, because the east and west sides of Lake Turkana have higher proportions of alcelaphini (hartebeest, topi) and antilopini (gerenuk, gazelle), which are associated more often with open country (Bobe 2011). Specific fossil fauna data from Kanapoi suggests that *Au. anamensis* was associated with a mosaic environment dominated by wooded habitats with a mixture of woodlands and grasslands (Bobe 2011; Geraads et al. 2013; Harris and Leakey 2003). As environments changed through time, early hominins would have had to cope with the altered spatial distribution of resources in the surrounding landscape as shifting precipitation patterns affected plant and animal distribution.

The fossil megafauna at Kanapoi (Geraads et al. 2013; Harris et al. 2003) and pilot bulk stable isotope data from Allia Bay (Schoeninger et al. 2003b) suggest that the Turkana Basin environment of the time was dominated by wooded habitats with a mixture of woodlands and grasslands. In contrast, however, Bobe (2011) suggest the two sites were relatively dry and open based on the rodent faunal assemblage at Allia Bay and comparable patterns of cercopithecines to colobines at the two sites (3:1 ratio). Paleosol carbon data at Kanapoi suggests that during *Au. anamensis* occupation the site had an arid to semi-arid climate with seasonal moisture with woodlands or gallery forests available in a relatively open grassland savanna region of the basin (Wynn 2000). However, recent reevaluation of the ruminant fauna suggests that Kanapoi is less

clearly an open habitat because of the abundance of tragelaphins and the presence of giraffes combined with the relatively low frequency of antilopins and reduncins (Geraads et al. 2013). The large mammal terrestrial fauna suggests a more closed woodland environment based on modern analogs, while the paleosol isotope data suggests a more dry open habitat (Behrensmeyer and Reed 2013; Wynn 2000).

Unfortunately, little is known about the faunal assemblage at Allia Bay because only the primates and hominins have been described in detail (Bobe 2011; Wood and Leakey 2011). Only two studies have been published on the Allia Bay megafauna, Schoeninger et al. (2003b) describing the isotopic data from tooth enamel and Macho et al. (2003) using stress lines in enamel to describe seasonality. The Allia Bay browser (*Deinotherium, Hexaprotodon, Tragelapjus, Hippopotamus*) and grazer (*Alcelaphus*, *Nyanzachoerus*) enamel experienced intra-annual periods of stress, suggesting that hominins at Allia Bay experienced a seasonal environment with periods of resource stress in a climate similar to modern Masai Mara (i.e., two rainy seasons – one long, one short) (Macho et al. 2003). The paleosol $\delta^{13}C$ values from Allia Bay have the lowest values in the Turkana Basin indicating significant woody cover (>40%) at the site compared to samples from the western side of the lake in the Nachukui Formation at 4 Ma (Levin et al. 2011; Levin et al. 2015).

The third *Au. anamensis* locality in the Omo-Turkana Basin is located in southern Ethiopia at Fejej (4.18-4.00 Ma) (Kappelman et al. 1996; Van Couvering 2000; Ward 2014). Little is known about the paleoenvironment at Fejej because the paleoecology has not been published in detail. However, the fauna used to date the site indicate browsing (*Nyanzachoerus*) and grazing (*Hipparion* and Gompotheriidae) species were present in what was likely a mosaic habitat that was well-watered to accommodate Hippopotamidae and Crocodilia (Asfaw et al. 1991). The relative mosaic nature of the paleoenvironment at Fejej of woodland and grassland

habitats and the climate is still unknown, so for the purpose of this analysis the site will not be considered.

It is clear that as climate changes occurred different parts of the Omo-Turkana Basin responded by creating locally diverse ecological niches. This project contributes new isotopic data from Allia Bay fossil fauna to compare with other *Au. anamensis* and non-hominin bearing sites in the Omo-Turkana Basin approximately 4 Ma to interrogate whether Allia Bay is consistent with the interpretation of an arid opening habitat in the Turkana Basin starting 4 Ma similar to the modern Koobi Fora environment or if Allia Bay was a more mesic environment indicating the presence of locally distinct ecological niches across the region. It is likely that Allia Bay had a distinct ecological niche in the basin because of the difference in canopy cover on the eastern shores of the lake compared to the western as indicated by the $\delta^{13}C$ paleosol data.

Principles of stable isotope analysis

Oxygen

The $^{18}O/^{16}O$ ratio, expressed as $\delta^{18}O$, varies in meteoric water due to differences in mean annual precipitation, ambient temperature, distance from the sea, altitude, and humidity (Dansgaard 1964; Luz et al. 1984; Poage and Chamberlain 2001; Rozanski et al. 1993; Sponheimer and Lee-Thorp 2014; Yurtsever and Gat 1981). Stable oxygen isotope ratios ($\delta^{18}O$) are regularly used to interpret past environments because δ18O values imprinted in soil carbonates (Cerling and Quade 1993) and biogenic apatites (e.g. tooth enamel or bone apatite) (Longinelli 1984; Luz and Kolodny 1985; Luz et al. 1984) serve as proxies for prevailing climatic conditions (i.e., annual rainfall, seasonality, and aridity) (Fricke et al. 1998; Fricke and O'Neil 1999; Hallin et al. 2012; Harris and Cerling 2002; Harris et al. 2008; Souron et al. 2012; Vogel 1983). The $\delta^{18}O$ value in enamel is mainly controlled by the isotopic composition of ingested water (Luz et al. 1984; Podlesak et al. 2008; Sponheimer and Lee-Thorp 1999). Modern animals

show that the $\delta^{18}O$ signal in body tissues (e.g., hair, bone, teeth) is strongly correlated with the $\delta^{18}O$ signal of local precipitation ($\delta^{18}O_{ppt}$) (Podlesak et al. 2008).

The physiology and adaptive behavior of mammals further affect the resulting $\delta^{18}O$ values recorded in enamel ($\delta^{18}O_{en}$) because both the phosphate (PO_4) and carbonate (CO_3) fractions in tooth enamel reflect the $\delta^{18}O$ value of their body water ($\delta^{18}O_{bw}$), which depends on the oxygen isotope composition of the source water (Bryant and Froelich 1995; Bryant et al. 1996; Cerling et al. 2008; Huertas et al. 1995; Luz et al. 1984; Quinn 2015). In mammal species that satisfy their water needs by drinking (e.g., suids, equids, elephants, and hippos), $\delta^{18}O_{en}$ correlates with the oxygen stable isotope composition of precipitation ($\delta^{18}O_{ppt}$) (Levin et al. 2006), which in turn correlates with temperature (Dansgaard 1964; Huertas et al. 1995; Rozanski et al. 1992; Yurtsever and Gat 1981; alternative view about correlation with temperature see Fricke and O'Neil, 1999). During periods of greater amount of rainfall, $\delta^{18}O_{ppt}$ values are generally lower, while higher $\delta^{18}O_{ppt}$ values indicate more arid conditions (Balasse et al. 2003; Kohn and Welker 2005; Rozanski et al. 1992). One complication is when large mammals that drink mainly from a drinking source that is itself evaporated (e.g., lakes), then their drinking water would also be enriched relative to local meteoric water (Cerling et al. 2008). Cerling et al. (2008) demonstrated this enrichment difference between river-dwelling hippos (more depleted in $\delta^{18}O_{en}$ values) versus lake-dwelling hippos (more enriched in $\delta^{18}O_{en}$ values) in the Turkana Basin. While modern Lake Turkana has been shown to be well mixed and isotope values are not subject to evaporative effects, the samples from Allia Bay Area 261-1 (3.97 ± 0.03MA) represent a fluvial period when drinking surface water from a paleolake was not available.

In contrast, mammal species that obtain their water mainly from food (e.g., leaf water), $\delta^{18}O_{en}$ values monitor relative humidity, which strongly influences $\delta^{18}O$ values of leaf water (Ayliffe and Chivas 1990; Kohn et al. 1996; Levin et al. 2006). The stable isotope composition of plant leaf water is enriched during transpiration because lighter isotopes preferentially evaporate

from the stomatal pores more readily than the heavy isotopes during the stomatal conductance of water vapor, resulting in leaf water $\delta^{18}O$ values being significantly higher than $\delta^{18}O_{ppt}$ values (Dongmann et al. 1974; Flanagan et al. 1991; Sternberg 1988). Certain plants are hygroscopic and will hold water molecules from the environment during various times of the day due to the surrounding climate (Taylor 1968). This is key for animals that live in environments with variable availability of water because they can adjust feeding times to take food when it is full of free water, making the animal nearly independent of surface water (Taylor 1968; Yakir 1992). The negative correlation between leaf water $\delta^{18}O$ values and relative humidity (RH) results in a corresponding negative correlation between $\delta^{18}O_{en}$ of non-drinking species and average RH that has been demonstrated for Australian marsupials (Ayliffe and Chivas 1990), East African mammals (Levin et al. 2006), and North American deer (Luz et al. 1990).

Carbon

In the simplest terms, carbon is incorporated into the food-web through chemical reactions involving the exchange of carbon from the ocean to atmospheric carbon dioxide (CO^2); then CO^2 reacts during photosynthesis in plants, which incorporates the stable isotope forms of carbon in plants and then subsequently consumed by animals which record the $\delta^{13}C$ in bones and enamel. There are three metabolizing pathways of photosynthesis that occur in plants known as C_3, C_4, and crassulacean acid metabolism (CAM) (DeNiro and Epstein 1978; Schoeninger and Deniro 1984). Each photosynthetic pathway incorporates varying amounts of ^{13}C and ^{12}C because of the different reaction rates of each isotope when processed through the varying pathways (O' Leary 1981; O' Leary 1988). The resulting $\delta^{13}C$ values from each photosynthetic pathway are distinct because of the differences in the incorporation of ^{13}C via the C_3-plant pathway (Calvin and Benson 1948) or the C_4-plant pathway (Hatch and Slack 1966). The discrimination against the heavier carbon isotope in C_3 plants results in a depletion of ^{13}C, so the fractionation of the carbon yields $\delta^{13}C$ values that range from -35 to -20‰, with an average of -

27.1 ±2.0‰ (Heaton 1999; O' Leary 1981; O' Leary 1988; O' Leary 1995). Most types of trees, shrubs, legumes, and tubers are examples of C_3 plants that are typical of temperate regions. Since C_4 plants discriminate less against the heavy ^{13}C, a greater amount of ^{13}C is incorporated and the result is that the plant is enriched in ^{13}C, causing a less negative value. The $\delta^{13}C$ values for C_4 plants range from -14 to -9‰, with an average of -13.1 ±1.2‰ (O' Leary 1988; O' Leary 1995). C_4 plants include maize, millet, amaranth, and sugarcane, all of which grow in hot and arid climates.

CAM plants are succulents (i.e. cactus) with photosynthetic pathways that can either metabolize carbon from the atmosphere like C_3 plants or in a time-separated C_4-like pathway, depending on the environmental conditions (O' Leary 1981; Ransom and Thomas 1960). Since CAM plants metabolize carbon along similar pathways as C_3 and C_4 plants, $\delta^{13}C$ values that range from -20 to -10‰, so they are usually isotopically distinct from C_3 plants but not from C_4 plants (O' Leary 1988). CAM plants are not regularly consumed by East African fauna, so browsers and grazers can be distinguished by the two main photosynthetic plant pathways.

In modern and paleoenvironment reconstructions, $\delta^{13}C$ values have not only been used to identify the diet of an animal, but also the type of environment an animal is feeding in (i.e. the canopy effect, amount of woody cover) (Cerling et al. 2011b; van der Merwe and Medina 1991). It has been shown in Amazonian rainforest leaves (van der Merwe and Medina 1991), New World primate hair (Schoeninger et al. 1997; Schoeninger et al. 1998), and from paleosol data from hominin-bearing fossils sites in East Africa (Cerling et al. 2011b), that animals feeding in more closed-canopy environments will have depleted $\delta^{13}C$ values relative to those from more open habitats. Additionally, C_3 plants will have enriched $\delta^{13}C$ values under drought conditions, especially in more xeric environments like the modern Turkana Basin (Garten Jr and Taylor Jr 1992; Schoeninger et al. 1998). Today in East Africa, carbon can be used to distinguish between C_4 grazers and C_3 browsers because in the hot arid climate of the Turkana Basin all the grasses

are C_4 and all trees and shrubs are C_3 (Cerling et al. 2015; Schoeninger et al. 2003b). Similar environmental observations of feeding position beneath a canopy and drought effects have been recorded in $\delta^{13}C_{en}$ values of ungulates from varying habitats (Cerling and Harris 1999), suggesting fossil fauna $\delta^{13}C_{en}$ values can be used for dietary and paleoenvironment reconstruction in conjunction with $\delta^{18}O_{en}$.

Materials and methods

Fossil sample

Enamel fragments (n = 48) from Allia Bay site 261-1 (beneath the Moiti Tuff) were available for $\delta^{13}C_{en}$ and $\delta^{18}O_{en}$ analysis. Tooth samples are limited to family level taxonomic identification and tooth types were unknown for the species considered drinking (n = 32; hippopotamid, equids, suids, deinotheriidae and elephantidae), non-drinking (n = 2; giraffids), and flexible-drinking (n = 14; bovids) species (sample distribution reflects the only available enamel fragments from Allia Bay for the current study; see Table 2.1). Unlike the previous bulk stable isotope study at Allia Bay, the bovids are included in our analysis because their feeding ecology varies widely and our modern comparison samples have a good representation of varied diets and body sizes.

Although tooth enamel is assumed to be resistant to post-burial chemical alteration (diagenesis) (Koch et al. 1997; Lee-Thorp 2002; Zazzo et al. 2004), recent isotopic studies of bulk enamel suggest this might not be true for older fossil localities (Jacques et al. 2008; Zazzo 2014). Previous cathodoluminescence (CL) results on samples from Allia Bay indicate that portions of the outer layer of enamel have altered crystal structure (Schoeninger et al. 2003a) and ion microprobe data confirm the alteration of the biogenic apatite (Kohn et al. 1999). It is unclear whether changes identified by CL correspond to altered isotope ratios in tooth enamel. Therefore,

the bulk samples analyzed in this study were collected after removal of at least the outer 0.5 mm, similar to the method used by Schoeninger et al. (2003a).

Modern sample

A modern fauna sample from the Turkana Basin of varied diet and water dependency is a necessary control sample. Currently, as when *Au. anamensis* occupied the Turkana Basin, the Omo River provides the most important water source for the lake and fluvial system in the region, which has consistently originated in the Ethiopian Highlands (Feibel 2011; Kohn et al. 1998; Yuretich 1979). The consistent origins of the Turkana Basin water source means that a modern sample from the region will serve as an ideal control for the paleoenvironmental reconstruction and understanding a mosaic habitat in the past. Today, the known seasonal environment of the area consists of an open arid region adjacent to Lake Turkana with one rainy season, which is recorded in tooth enamel $\delta^{18}O$ values (Kohn et al. 1998; Meteorological Office 1983).

In 1984 and 1993, MS collected recently-deceased modern fauna from the eastern shores of Lake Turkana in the Koobi Fora region (Figure 2.2). Of the available modern Koobi Fora fauna, eleven species serve as analogs for the Allia Bay fossil sample. Since the fossils are only identified to family, the following families are represented for the modern sample: Bovidae (n = 56), Equidae (n = 9), Giraffidae (n = 7), Hippopotamidae (n = 5), and Suidae (n = 6). Table 2.2 indicates the specific species, water dependency (obligate drinkers or non-obligate drinkers), diet (grazers, browsers and mixed feeders), and isotope data for the modern sample. Unfortunately, no bone or tooth Proboscidea (the extinct Deinotheriidae or extant Elephantidae) samples were collected from the Koobi Fora region because they have not recently inhabited the area. The ungulates available do represent a range of body size and variable feeding ecology. Of the modern samples collected and analyzed for comparison in this study, only the bovid and equid species had modern enamel available, while the girraffid, hippopotamid, and suid samples collected are limited to bone samples. For modern samples with only bone available, bone values

were corrected to enamel values by +2.3‰ for carbon and +1.7‰ for oxygen (Warinner and Tuross 2009) because despite the correction being generated for pigs from a feeding experiment, for the purpose of this study it was more important to maintain continuity of species from the Koobi Fora region over using published enamel values from outside of the region. To account for changes in $\delta^{13}C_{en}$ values dues to changes in atmospheric carbon due to human activities starting with the Industrial Revolution, all the modern Koobi Fora $\delta^{13}C_{en}$ were corrected for the Suess effect by +1.0‰ to match fossil values (Keeling 1979). Table 2.2 also includes 32 previously published modern enamel samples collected in the Koobi Fora region to increase the sample size of the grazing fauna for comparison (Harris and Cerling 2002; Jehle 2013; Levin et al. 2006).

Laboratory preparation

The outer 0.5 mm layer of a sample was dremeled to remove any macroscopic contaminants and ultrasonically cleaned in washes of ddH_2O and acetone. Samples were ground with a mortar and pestle into a powder and sieved through a mesh screen (234μm). The organics were removed from the bioapatite sample through treatment with a 2% sodium hypochlorite (NaOCl) solution and 0.1M acetic acid (CH_3COOH) solution, following a 0.04 ml solution/mg sample ratio (Koch et al. 1997). Samples were treated with the NaOCl for a total of 48 hours, with a change of the solution at 24 hours; following the ddH_2O rinse, samples were treated with acetic acid for a total of 24 hours. This preparation method was used after a subsample of fossil enamel was prepared following three different sample preparations and found to yield the same $\delta^{18}O$ and $\delta^{13}C$ values within range of the instrument precision. The other two preparation methods tested (Balasse et al. 2002; Sponheimer et al. 2005) were used by White et al. (2009a) for the Aramis fossil material, by Lee-Thorp et al. (2012) for the Chad fossil material, and Cerling et al. (2013) for the Turkana Basin material.

Stable isotope analyses of fossil enamel and modern bone were conducted at the Scripps Institution of Oceangraphy's Analytical Facility on a gas bench Thermo MAT 253 coupled to a

Thermo-Finnigan Delta XP Plus mass spectrometer with an established analytical precision of ± 0.2‰ for both $\delta^{18}O$ and $\delta^{13}C$ based on an internal lab carbonate standard. Samples were calibrated to NBS-18 and NBS-19 and reported relative to the international standards Vienna Pee Dee Belemnite (PBD) for $\delta^{13}C$ and Standard Mean Ocean Water (SMOW) for $\delta^{18}O$. The $\delta^{18}O$ values are also converted to PDB ($\delta^{18}O_{PDB} = (0.97006 \times \delta^{18}O_{SMOW}) - 29.94$) because the enamel samples are a bioapatite rather than a water sample and it is common practice to report enamel carbonate relative to PDB.

Statistical analysis

The $\delta^{13}C_{en}$ and $\delta^{18}O_{en}$ values for each family of species were evaluated statistically to compare between the fossil and modern samples. Based on sample size and previous ecological reconstructions, it was expected that the data would be non-normally distributed which was confirmed by testing for normality using the Shapiro-Wilk's and K-S Lilliefors test of normality. Therefore, comparing the two temporal data sets was done using a Mann-Whitney U test, which is a nonparametric test that does not require normality of the distributions of a sample.

Results

Comparison with pilot study

The larger overall sample size of the Allia Bay fossils compared to the previous pilot data and the additional analog speciesprovide a clearer representation of the difference between the paleoenvironmental conditions at Allia Bay when *Au. anamensis* inhabited the region compared to those existing today. Table 2.3 compare the current study samples to the samples published in Schoeninger et al. (2003b). While the means for each family are within 1‰ (except the $\delta^{13}C_{en}$ of the Elephantidae because of one sample from the current study that plots with the Deinotheriidae and is possibly misidentified), the ranges for some families increase and the new samples fill in a continuous spectrum of isotopic values for each family. Although all new enamel fragments were

sampled for the current study, due to only family level identifications for the samples it is quite possible the same individuals were sampled from the 2003 study. For this reason, and because the mean $\delta^{13}C_{en}$ and $\delta^{18}O_{en}$ ratios are similar, only the 48 new fossil samples will be considered in the following analysis.

Paleolandscape at Allia Bay

By comparing Allia Bay fossil fauna to their modern analogs at Koobi Fora (Figure 2.3), it is clear there has been a significant shift in the environment from 4 Ma to today and that at least one portion of the Turkana Basin was not as hot and arid as the modern Koobi Fora region. All of the fossil fauna are, on average, lower in both $\delta^{18}O$ and $\delta^{13}C$ than are their modern contemporaries suggesting that 4 Ma the ecological setting was more mesic with more closed canopy compared to the modern east Lake Turkana environment at Allia Bay. Table 2.4 presents the Mann-Whitney U comparisons for the five fossil family groups that had modern species from the Turkana Basin available for comparison. The aggregation of modern species into family taxonomic level allowed direct comparison with the fossil Allia Bay sample. The mean $\delta^{13}C_{en}$ ratios in the modern Koobi Fora samples were higher compared to the fossil Allia Bay sample. There is a similar trend with the $\delta^{18}O_{en}$ ratios of the modern sample having higher mean values compared to the fossil sample. While there are no modern Koobi Fora analogs for the Proboscidea families, the mean $\delta^{13}C_{en}$ ratios are consistent with previously published carbon data for the families in East Africa (Uno et al. 2011) and the $\delta^{18}O_{en}$ ratios are consistent with the other obligate drinking families represented at Allia Bay (Figure 2.2F).

Fossil Hippopotamidae at Allia Bay have significantly lower bulk carbonate $\delta^{18}O_{en}$ and $\delta^{13}C_{en}$ values compared to the modern common hippo inhabiting Lake Turkana, and the fossil hippos show a bigger range in carbon values compared to the modern ones (Figure 2.2A). At Allia Bay the lowest mean $\delta^{18}O_{en}$ values among the mammals were the hippopotatmid family, which is consistent with what occurs in modern ecosystems where it likely reflects their semi-

aquatic habitat (Cerling et al. 2008). East Africa is the source of most of the known information about the evolution of the hippo family where there was an explosion in the diversity that occurred around 4Ma, the same time period represented by the Allia Bay material. Present at Allia Bay in the lower part of the Koobi Fora Formation, are the common hippo, aff. *Hippopotamus* cf. *H. protamphibius* and a larger *Hippopotamus* species (Harris et al. 2008). Modern isotopic data of the common hippo across Africa suggest it is an opportunistic rather than an obligate grazer (Boisserie et al. 2005). The combined bulk $\delta^{18}O$ and $\delta^{13}C$ values suggest a wide range of feeding ecologies for Hippopotamidae at Allia Bay. Browsers have the expected higher $\delta^{18}O$ combined with lower $\delta^{13}C$ values and grazers have lower $\delta^{18}O$ combined with higher $\delta^{13}C$ values. In addition, there are a number of mixed feeders (i.e., C_3 and C_4). This might indicate one species with a wide feeding ecology range. Alternatively, the two previously identified species of *Hippopotamus* (Harris et al. 2008) had different but overlapping dietary adaptations: one with an emphasis on browse with some individuals feeding on mixed browse and graze, and the second with an emphasis on graze with some mixed-feeding individuals.

The giraffids have the lowest $\delta^{13}C_{en}$ values of the entire Allia Bay fossil sample combined with some of the highest $\delta^{18}O_{en}$ values, as expected for a non-obligate drinking browser (Figure 2.3B). Two of the suid samples have similarly high $\delta^{18}O_{en}$ values compared to the giraffids, but a much larger range of $\delta^{13}C_{en}$ values (11.7‰), which indicates multiple species feeding in a variety of ecological niches at Allia Bay (Figure 2.3C). The suid family $\delta^{18}O_{en}$ values are the only family that doesn't exhibit a significant depletion in the oxygen values compared to the modern Koobi Fora samples. In fact two of the fossil Allia Bay suids plot with the modern warthogs, which are grazers that are less water dependent compared to modern bushpigs and forest hogs in East and Central Africa (Harris and Cerling 2002). It is possible that two Suidae species are represented in the Allia Bay fossil sample, a species of the kolpochoere lineage (extant browsing and mixed feeder forest hogs) and a species of the metridiochoere lineage (extant grazing warthog) because

both linages were recovered from other fossil localities in the Turkana Basin (Harris and Cerling 2002). Similar to the hippos and giraffes, the two equid samples have significantly lower bulk carbonate $\delta^{18}O_{en}$ and $\delta^{13}C_{en}$ values compared to the modern zebras (Figure 2.3D). The bovid family $\delta^{13}C_{en}$ values have a range of 13.6‰, which is evidence for browsers, grazers, and mixed feeders being present on the landscape (Figure 2.3E). The modern bovids have a wider range of $\delta^{13}C_{en}$ values, but this is likely because the five modern species (dik-dik, gerenuk, lesser kudu, oryx, and topi) are likely different species than those represented in the fossil assemblage.

Allia Bay vs. Kanapoi and Omo Mursi

For comparing the Allia Bay isotope data to the previously published data on Kanapoi (Harris et al. 2003) and Omo Mursi (Drapeau et al. 2014), all species were combined into family groups in the same way as was done previously with the modern species (Figure 2.4). Not all families were represented from each site and some lacked the sample size for statistical comparison. At Kanapoi, the Elephantidae (*Elephas ekorensis* and *Loxodonta adaurora*) and Suidae (*Nyanzachoerus pattersoni* and *Notochoerus jageri*) had enough samples to compare statistically to the corresponding Allia Bay fauna (Table 2.5). The only significant difference was the significantly higher $\delta^{13}C_{en}$ ratios of the Elephantidae family with Kanapoi (-2.1 ± 0.7‰ [n = 7]) having significantly higher values compared to Allia Bay. The single sample of a Giraffidae (*Sivatherium* cf. *S. hendeyi*) and Equidae (*Eurygnathohippus* sp.) could not be compared statistically to Allia Bay, but when the values were plotted (Figure 2.4B and 2.4D) they were consistent with the corresponding modern species at Koobi Fora, which had higher $\delta^{13}C_{en}$ and $\delta^{18}O_{en}$ values. The comparison of the fauna from Kanapoi to Allia Bay indicates that Kanapoi was likely less humid with more open woodlands compared to Allia Bay.

At Omo Mursi, the Elephantidae (*Loxodonta adaurora*), Hippopotamid (*Hippopotamus* cf. *protamphibius*), and Suidae (*Nyanzachoerus kanamensis* and *Notochoerus jageri*) had enough samples to compare statistically to the corresponding Allia Bay fauna (Table 2.5). Similar to the

Kanapoi comparison, the only significant differences were the significantly higher $\delta^{13}C_{en}$ ratios of the Elephantidae family with Omo Mursi (-4.0 ± 1.8‰ [n = 18]) having significantly higher values compared to Allia Bay. Although there weren't enough Deinotheriidae samples for statistical comparison, the Omo Mursi individuals exhibited lower $\delta^{13}C_{en}$ and $\delta^{18}O_{en}$ values indicating that for the species occupying the most closed-canopy niches, they also recorded a wetter environment from those ecological zones compared to the grazing species (Figure 2.4F). Overall, it appears that Allia Bay and Omo Mursi have a similar woodland environment with Omo Mursi possibly having a slightly more humid environment signaled by the depleted Deinotheriidae and two of the Bovidae samples (Figure 2.4E and 2.4F).

Discussion

Hippopotamidae-Giraffidae Offset

Among East African large mammals recovered from fossil localities, often Hippopotamidae have the lowest $\delta^{18}O_{en}$ values and Giraffidae have the highest (Bedaso et al. 2013; Levin et al. 2015; Levin et al. 2008; White et al. 2009a; Wynn et al. 2013). This pattern holds true at Allia Bay, but unfortunately can not be calculated for Kanapoi and Omo Mursi since each site has only one species present. The Hippopotamidae-Giraffidae (H-G) offset is used to indicate the relative wetness of a fossil locality, with drier sites interpreted as having larger offsets, while wetter sites have smaller offsets (Levin et al. 2015). However, the offset might not suggest a wetter environment, but rather an indicator of habitat variability suggesting greater variability between the hippo ecological niche compared to the giraffe ecological niche within an ecoregion. Levin et al. (2015) reported the H-G offset for Woranso-Mille (3.76-3.57 Ma) compared to Aramis (4.4 Ma) and Hadar (3.8-3.24 Ma) as evidence that Woranso-Mille had a wetter paleoenvironment (Table 2.6). While all the sites have high standard errors suggesting a lot of variability within each habitat, the H-G offset suggests that Aramis would be the driest site,

Woranso-Mille the wettest site, and Allia Bay similar to Hadar as an intermediate climate between Aramis and Woranso-Mille. However, the H-G offset of the modern Koobi Fora environment, known to be an arid region with little rainfall, has the lowest offset and lowest standard error which calls into question what the H-G offset is indicating about an environment.

To check if the H-G offset is a good measure of the relative wet versus dry measure of a fossil locality, the hippos and giraffes from the four fossil sites were statistically compared (Table 2.7). It was expected that Woranso-Mille and Aramis should be significantly different from all other fossil localities and that Allia Bay and Hadar would be similar, however this is not the case. Woranso-Mille and Hadar giraffes and hippos are statistically similar, Allia Bay and Aramis hippos are statistically similar, and Aramis and Woranso-Mille are statistically similar (although approaching a difference $p = 0.0673$). By looking at the comparison of the hippo and giraffe $\delta^{18}O_{en}$ values, it appears that the H-G offset does not accurately reflect the relative wetness of a fossil locality. The lowest H-G offset calculated is for Koobi Fora, which is arid and has little habitat variability. Perhaps the H-G offset is a better reflection of the mosaic nature of an ecoregion, a possible mosaic habitat index with higher values suggesting increasing heterogeneity and lower values suggesting increasing homogeneity in a paleolandscape. Further research across more fossil and modern localities are needed to better understand what the H-G offset indicates in a paleoenvironment.

Omo-Turkana Basin 4.2 to 3.9 MA

Cerling et al. (2015) reports mean $\delta^{13}C_{en}$ values for 14 taxa in the Turkana Basin (TB) between 4.0 and 3.4 MA, but the number of samples and site locations within the basin are not reported. By comparing the Allia Bay (AB) percentage of taxa with $\delta^{13}C_{en}$ values designated as browser (<-8‰), mixed feeder (>-8‰ to <-1‰), and grazers (>-1‰) (following Cerling et al. 2015) to the percentage of corresponding feeders represented by the 14 taxa analyzed by Cerling et al (2015), Allia Bay has more browsers and mixed feeders than other sites represented in their

study (browsers: AB = 35.4% vs TB = 21.4%; mixed feeders: AB = 54.2% vs TB = 50%; grazers: AB = 10.4% vs TB = 28.6%). This suggests that Allia Bay had significantly more browsing closed canopy habitats at 3.97 MA compared to the aggregated samples from the larger Turkana Basin region over a 600 KYA span of time. At Allia Bay during the period when *Au. anamensis* occupied the site, there was significantly less open grassland in the immediate vicinity based on the dietary ecology of the large bodied mammals recovered from the site. This highlights the importance of looking at site-specific paleoenvironment indicators at short time scales because there can be a great amount of variability.

Au. anamensis occupied Kanapoi and Allia Bay, so we expected the mosaic nature of Allia Bay and Kanapoi to be more similar compared to the Omo Mursi environment where no hominin remains have been recovered. However, by comparing the isotope data from the three sites in the Omo-Turkana Basin, it is likely that Allia Bay and Omo Mursi were more similar in climate and the mosaic nature of the habitats. The absence of hominins at the Omo Mursi localities is more likely due to sampling, than the fact that hominins did not favor the wetter tree-covered habitat as Drapeau et al. (2014) postulated. Unfortunately, since the Allia Bay fauna have not been analyzed and published, abundance mammal species data is not available for comparison. It is possible that with further analyses there will be other distinct differences between the two sites to better understand why primates have yet to be recovered from Omo Mursi.

The most common bovid at Kanapoi is tragelaphins, while reduncins are rare in the taxa list, which is the opposite of what has been found at Koobi Fora where reduncins are abundant and tragelaphins are rare (Geraads et al. 2013). Geraads et al. (2013) suggest that Kanapoi is not as open an environment as was previously thought based on isotopic data (Harris et al. 2003; Wynn 2000), but rather had an environment with significant amounts of shrubs, bushes, and trees to accommodate tragelaphin and giraffe species. In fact the only two bovid isotope samples from

Kanapoi were impalas (a woodland edge species) that had browsing $\delta^{13}C_{en}$ values. The arid signal from the $\delta^{18}O_{en}$ values of the giraffid and equid samples at Kanapoi correspond to the modern Koobi Fora samples indicate that the overall region of Kanapoi was likely more arid compared to Omo Mursi and Allia Bay despite well-watered patches of woodland.

Reconstructing mosaic habitats and Au. anamensis

It is important when reconstructing paleoenvironments to appreciate the potential biases of relying on one type of data over another. By looking at modern environmental reconstructions from biological animal data, we gain further appreciation for how difficult reconstructing past ecosystems over periods of millions of years can be if researchers only relied on few lines of evidence. Recently, Schoeninger et al. (2015) analyzed modern chimp $\delta^{13}C$ and $\delta^{15}N$ from hair collected at a savanna chimpanzee research site (Ugalla, Tanzania) compared to other published chimpanzee isotopic data from across a variety of ecosystems (Figure 2.4). They found a strong correlation ($r^2 = 0.56$, $p < 0.001$) between mean annual precipitation (MAP) and the $\delta^{13}C$ values of the hair confirming that local site ecology influenced the source plant tissues consumed and recorded by the chimpanzees (Schoeninger et al. 2015). However, two sites did not record the expected values in the hair. Ishasha chimpanzees recorded lower $\delta^{13}C$ values for the predicted MAP and is a habitat where the chimpanzees lived and feed in a more humid gallery forest along a perennially flowing river (Schoeninger et al. 2015; Sept et al. 1992). Ugalla chimpanzees recorded higher $\delta^{13}C$ values for the predicted MAP and is a habitat of continuous leguminous trees with a very open canopy and enough light for C_4 grasses to grow which possibly causes the MAP to be an unreliable indicator of canopy cover (Schoeninger et al. 2015). This example highlights how if biological isotopes alone were relied upon to reconstruct the paleoenvironments of hominins, it is possible that specific local site ecology or behavioral adaptations for exploiting particular niches within a larger mosaic habitat might not yield a complete picture of the past. In the East African Rift, transition between different biomes (for example, closed canopy forest

transitioning into open grassland) can be sudden (Ward et al. 1999). During the fluvial phase of *Au. anamensis*, the Omo River could have dominated an otherwise arid environment to the extent that only narrow ecotones existed between desert and forest niches (Ward et al. 1999).

Paleoprecipitation, specifically MAP, can be estimated from the measured depth to the top of a soil's calcic horizon (Retallack 1994) and has been applied to 33 paleosols of the composite Turkana Basin record (Wynn 2004). However, the presence of noncalcic soils in the Turkana Basin during certain intervals (4-3.6MA; when Allia Bay is occupied by *Au. anamensis*) prevents the use of this method for some localities (Wynn 2004). At Kanapoi, a calcic horizon is present and paleosol data indicates a seasonal climate regime with paleoprecipitation estimated at approximately 620 ± 100 mm/year (1SD; Wynn 2004). Currently, 12 individuals of *Au. anamensis* at Kanapoi have $\delta^{13}C_{en}$ and $\delta^{18}O_{en}$ values published (n = 17; Cerling et al. 2013) and unlike other later hominins they exhibit a narrow range of $\delta^{13}C_{en}$ values indicating a C_3-based diet similar to the earlier *Ar. ramidus* (White et al. 2009a). Using 620 mm as the estimated MAP for Kanapoi, the *Au. anamensis* $\delta^{13}C$ mean falls on the predicted trendline (Firgure 2.5) for the local ecology of these early hominins similar to arid chimpanzee sites categorized as a Tropical and Subtropical Savannas, Grasslands, and Shrublands (TSGSS) biome (Schoeninger et al. 2015), supporting the interpretation of Kanapoi as a semi-arid to arid paleoclimate. As an ecoregion, if Kanapoi had an arid climate with niches of denser woodland, then it is likely that within that mosaic habitat *Au. anamensis* was exploiting food resources primarily along a narrow riparian corridor (Cerling et al. 2013).

The noncalcic soil formation during the Allia Bay occupation suggest that the site experienced little seasonal precipitation or MAP values greater than 1,000mm (Wynn 2004). The data from this study suggests that Allia Bay was more mesic compared to Kanapoi, suggesting MAP >620 mm, but other proxies are needed to characterize the amount of paleoprecipitation and level of seasonality. If Allia Bay *Au. anamensis* populations had a similar feeding ecology as

Kanapoi hominins but a greater MAP, then it is possible that Allia Bay hominins would plot similar to the Ugalla chimpanzees (Figure 2.5). This would indicate that early hominins were occupying open Miombo woodlands similar to the environment at Ugalla (MAP = 1050 mm). The Allia Bay fauna isotope data clearly indicates a mosaic of habitats available to early hominins who could have been exploiting dietary resources from a more densely covered woodland along a riverine channel that was more mesic, situated in an ecoregion with areas that were arid and open grassland.

Conclusion

In summation, after applying correction factors (i.e., Suess effect, converting bone to enamel values) to the modern fauna, the fossil fauna exhibit lower oxygen values and lower carbon isotope values indicating a very different paleoenvironment at Allia Bay compared to the modern Koobi Fora region. The isotope data may indicate minor diagenetic alteration (Schoeninger et al. 2003b), which we are currently investigating further with new analytical techniques, but these new fossil sample data support the earlier Schoeninger et al. (2003b) interpretation of a more mesic environment at Allia Bay during the occupation of *Au. anamensis*. The oxygen isotope data indicate a wetter paleoenvironment and the carbon signal from the fauna of mostly browsing and mixed feeding species suggests more tree cover compared to the modern Koobi Fora region. It is critical to evaluate multiple lines of evidence when reconstructing paleoenvironments of early hominins and each fossil locality should be considered at the local scale within a broader region. The data we present here supports the idea that within the Turkana Basin there were a variety of ecological niches with different climate regimes and it should not be considered one large arid open grassland system over the past 4 Ma. From the fossil fauna tooth enamel it is clear that Allia Bay was a mesic woodland environment with associated open grasslands, much different than the modern environment.

Acknowledgments

This chapter is currently being prepared for submission for publication of the material with co-author Margaret J. Schoeninger. The dissertation author was the primary investigator and author of this material.

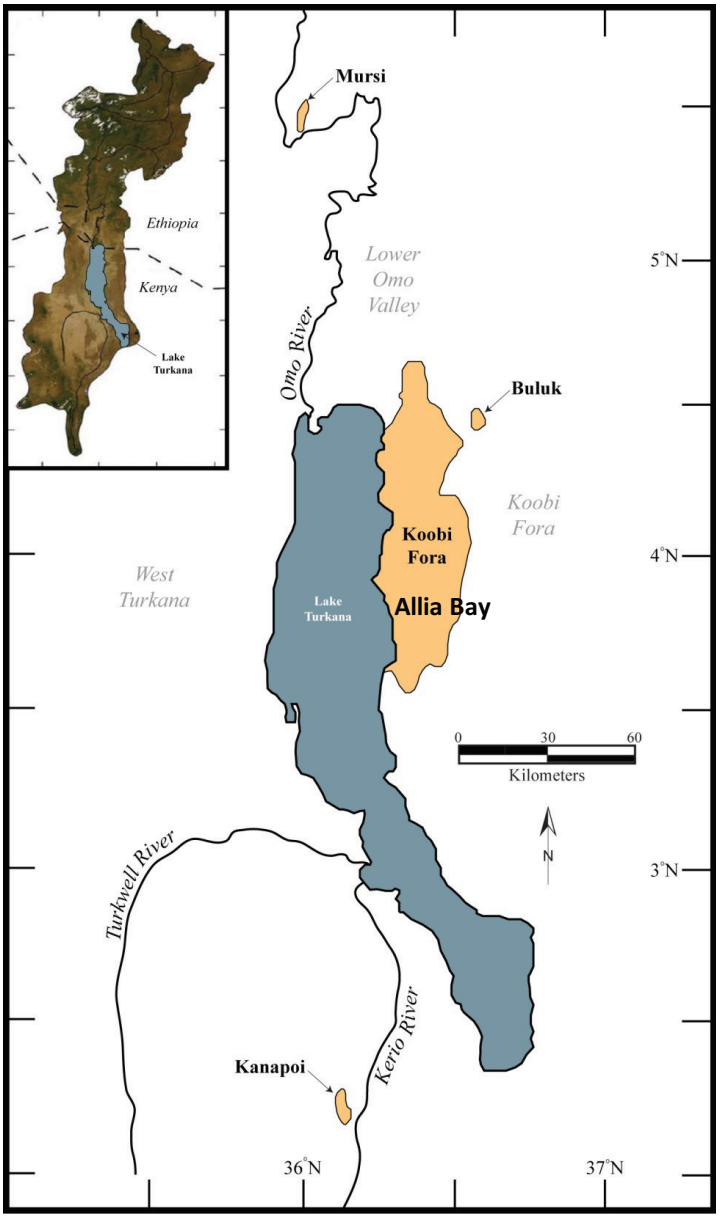

Figure 2.1. Map of the Omo-Turkana Basin highlighting fossil localities.
[adapted from Feibel 2011]

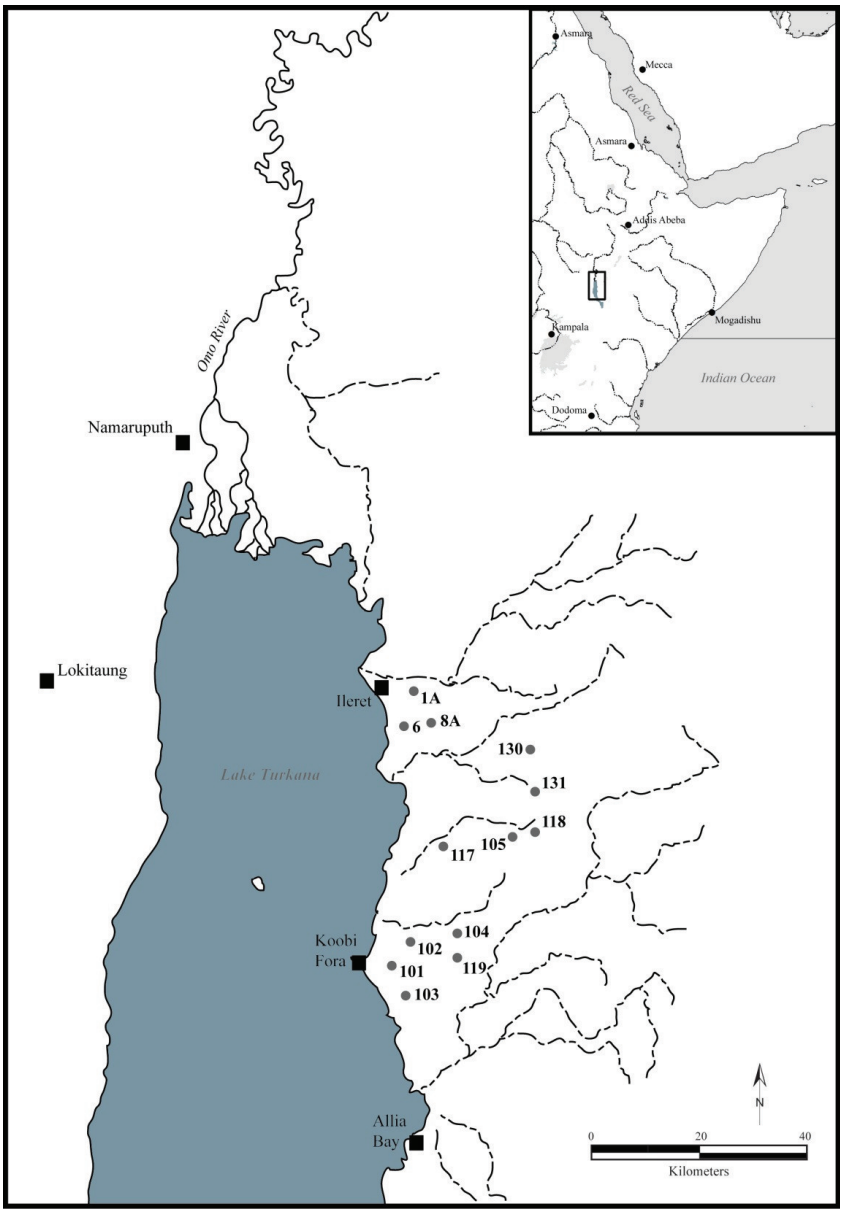

Figure 2.1. Map of the Omo-Turkana Basin. Numbers indicate modern sample collection areas.
[adapted from Brown et al. 2006]

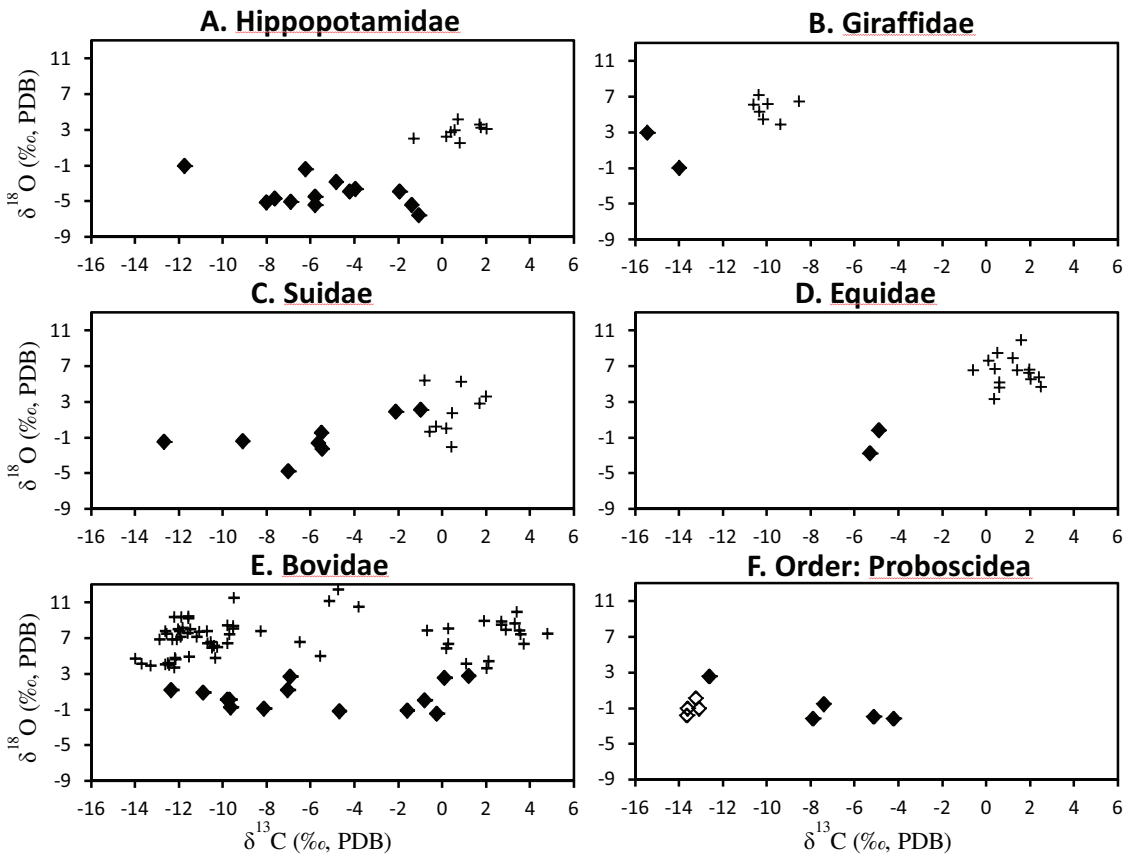

Figure 2.3. Scatterplot of $\delta^{13}C$ and $\delta^{18}O$ of modern Koobi Fora and Allia Bay fauna. Figure A-E compares $\delta^{13}C$ and $\delta^{18}O$ modern Koobi Fora fauna (+) to fossil Allia Bay fauna (♦). The Allia Bay fauna $\delta^{13}C$ and $\delta^{18}O$ values are consistently depleted for the five families compared to the modern analogs. Figure F compares Allia Bay fossil Deinotheriidae (◊) and Elephantidae (♦). There are no extant proboscidea at Koobi Fora to compare with the fossil data. One of the Allia Bay Elephantidae samples plots with the hyper-browser Deinotheriidea, it is possible that this family level identification is inaccurate.

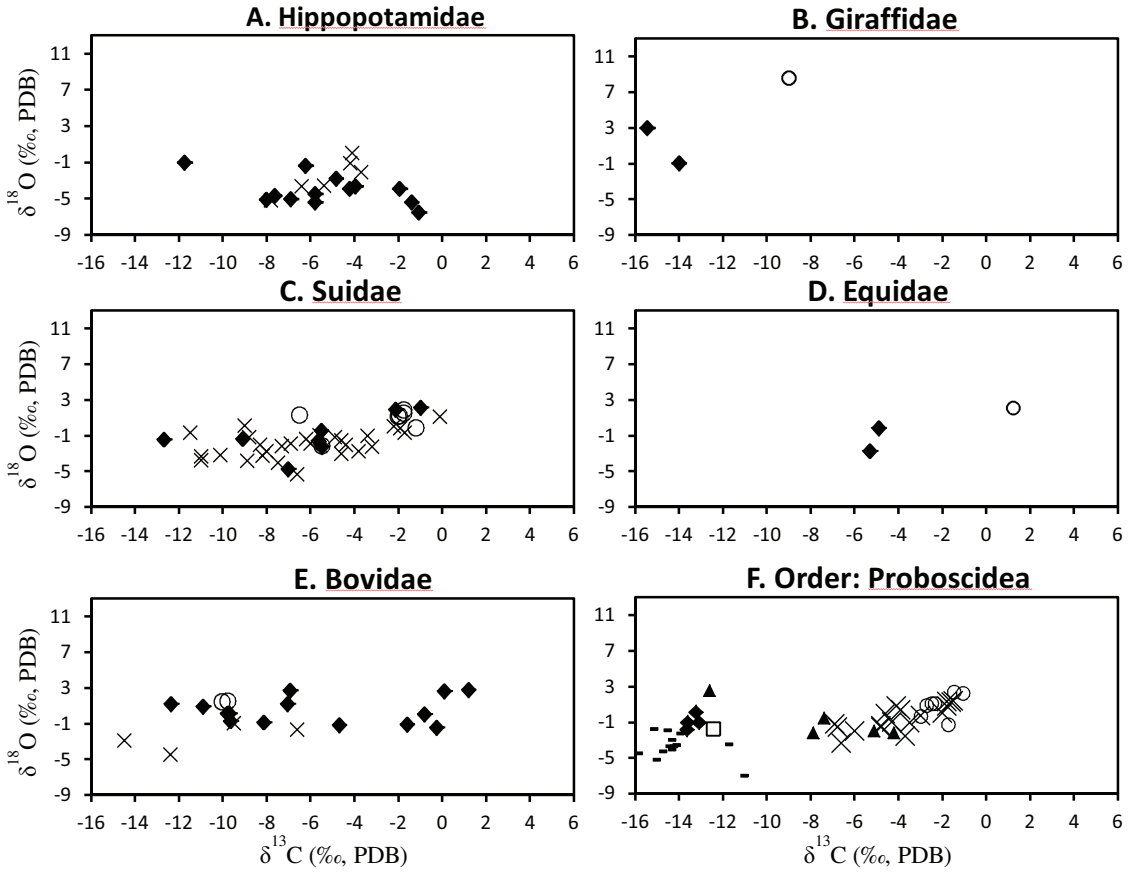

Figure 2.4. Scatterplot of $\delta^{13}C$ and $\delta^{18}O$ of Allia Bay, Omo Mursi, and Kanapoi fauna. Figure A-F compares $\delta^{13}C$ and $\delta^{18}O$ values from Allia Bay fossil fauna (♦, ▲) to equivalent taxa from other early Pliocene sites in the Omo-Turkana Basin. The Omo Mursi formation fauna (Drapeau et al. 2014) are plotted with the line-symbols (x, -) and the fossil fauna from Kanapoi (Harris et al. 2003) are represented by the open-symbols (○, □). Figure F is a plot of fossil Deinotheriidae (♦, -, □) and Elephantidae (▲, x, ○).

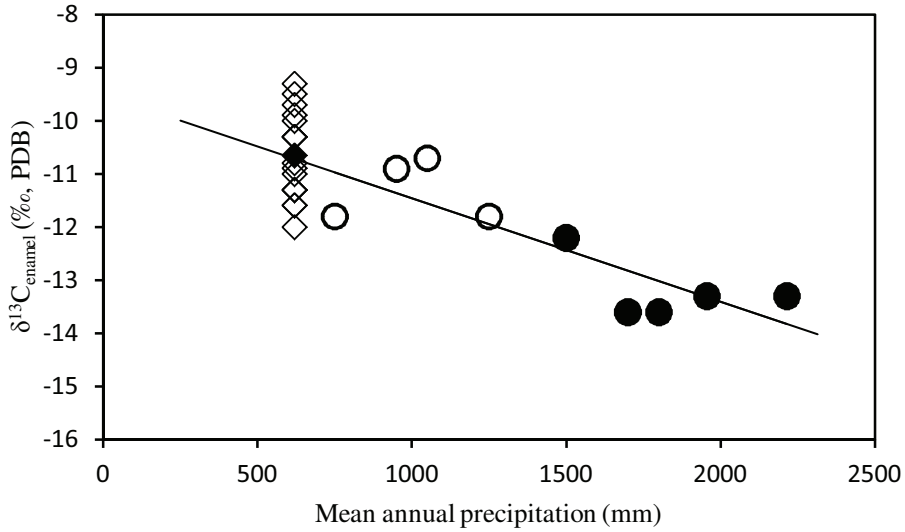

Figure 2.5: Plot of mean annual precipitation (MAP) vs. $\delta^{13}C_{enamel}$. Carbon ($\delta^{13}C_{enamel}$) stable isotope ratios in chimpanzee enamel (Schoeninger et al. 2015; converted from hair values following Sponheimer et al. 2006) and *Au. anamensis* enamel from Kanapoi (open diamond symbols, ◊, with the mean as a filled diamond, ♦; Cerling et al. 2013) plotted against Mean Annual Precipitation (MAP). Schoeninger et al. (2015) showed a statistically significant negative correlation between $\delta^{13}C$ and the MAP (trendline: $y = -0.0021x - 20.648$; $R^2 = 0.55796$). Chimpanzee sites with an open circle symbol (○) are Ishasha, Fongoli, Ugalla, and Gombe (in order from lowest to highest MAP), classified as Tropical and Subtropical Savanna, Grassland, and Shrubland (TSGSS) Biomes. Chimpanzee sites with filled circle (●) are Kibale, Cameroon, Taï, Ganta, and Logango (in order from lowest to highest MAP), classified as Tropical and Subtropical Moist Broadleaf Forest (TSMBF) Biomes.

Table 2.1. Allia Bay fossil sample

Family	Sample Number	Water Dependency**	Diet*	$\delta^{13}C$ (‰, PDB)	$\delta^{18}O$ (‰, VSMOW)	$\delta^{18}O$ (‰, PDB)
Bovidae (n = 14)						
	4865.4	Flexible	Browse	-12.4	32.1	1.2
	4864d	Flexible	Browse	-10.9	31.8	0.9
	4865.6	Flexible	Browse	-9.8	30.9	0.1
	4869a	Flexible	Browse	-9.7	30.9	0.1
	4865.2	Flexible	Browse	-9.6	30.0	-0.8
	4865.5	Flexible	Browse	-8.1	29.9	-0.9
	4865.3	Flexible	Mixed	-7.1	32.0	1.1
	4865.1	Flexible	Mixed	-6.9	33.6	2.7
	4864.1	Flexible	Mixed	-4.7	29.6	-1.2
	4877b2	Flexible	Mixed	-1.6	29.7	-1.2
	4874a2	Flexible	Grazer	-0.8	30.9	0.0
	4877	Flexible	Grazer	-0.3	29.3	-1.5
	4867.1	Flexible	Grazer	0.1	33.5	2.6
	4875a2	Flexible	Grazer	1.2	33.7	2.8
Mean				**-5.8**	**31.3**	**0.4**
Standard Deviation				**4.7**	**1.5**	**1.5**
Giraffidae (n = 2)						
	4860.1	Non-Obligate	Browse	-15.5	33.9	3.0
	4859b3	Non-Obligate	Browse	-14.0	29.8	-1.0
Mean				**-14.7**	**31.9**	**1.0**
Standard Deviation				**1.0**	**2.9**	**2.8**
Deinotheriidae (n = 4)						
	4857.2	Obligate	Browse	-13.7	29.0	-1.8
	4858b2	Obligate	Browse	-13.6	29.8	-1.0
	4858.1	Obligate	Browse	-13.2	30.9	0.1
	4857.1	Obligate	Browse	-13.1	29.8	-1.1
Mean				**-13.4**	**29.9**	**-1.0**
Standard Deviation				**0.3**	**0.8**	**0.8**
Elephantidae (n = 5)						
	4901.2	Obligate	Browse	-12.6	33.5	2.5
	4902b2	Obligate	Mixed	-7.9	28.6	-2.2
	4908a3	Obligate	Mixed	-7.4	30.3	-0.6
	4901.1	Obligate	Mixed	-5.1	28.8	-2.0
	4905	Obligate	Mixed	-4.2	28.6	-2.2
Mean				**-7.5**	**29.9**	**-0.9**
Standard Deviation				**3.3**	**2.1**	**2.0**
Equidae (n = 2)						
	4854a4	Obligate	Mixed	-4.9	30.7	-0.2
	4853a3	Obligate	Mixed	-5.3	28.0	-2.8
Mean				**-5.1**	**29.3**	**-1.5**
Standard Deviation				**0.3**	**1.9**	**1.9**

Table 2.1. Allia Bay fossil sample (continued)

Family	Sample Number	Water Dependency**	Diet*	$\delta^{13}C$ (‰, PDB)	$\delta^{18}O$ (‰, VSMOW)	$\delta^{18}O$ (‰, PDB)
Hippopotamidae (n = 13)						
	4892.1	Obligate	Browse	-11.7	29.8	-1.0
	4891.5	Obligate	Browse	-8.0	25.6	-5.1
	4896	Obligate	Mixed	-7.6	26.0	-4.7
	4891.6	Obligate	Mixed	-6.9	25.6	-5.1
	4892.2	Obligate	Mixed	-6.2	29.4	-1.4
	4891.7	Obligate	Mixed	-5.8	26.2	-4.5
	4891.4	Obligate	Mixed	-5.8	25.3	-5.4
	4891.3	Obligate	Mixed	-4.8	27.9	-2.9
	4891.1	Obligate	Mixed	-4.2	26.8	-3.9
	4895.1	Obligate	Mixed	-4.0	27.1	-3.7
	4891.2	Obligate	Mixed	-2.0	26.8	-3.9
	4891.9	Obligate	Mixed	-1.4	25.2	-5.4
	4891.8	Obligate	Mixed	-1.1	24.1	-6.6
Mean				**-5.3**	**26.6**	**-4.1**
Standard Deviation				**3.0**	**1.7**	**1.6**
Suidae (n = 8)						
	4884a3	Obligate	Browse	-12.7	29.3	-1.5
	4887.1	Obligate	Browse	-9.1	29.4	-1.4
	4881	Obligate	Mixed	-7.0	25.9	-4.8
	4882.1	Obligate	Mixed	-5.7	29.1	-1.7
	4879.1	Obligate	Mixed	-5.5	30.4	-0.5
	4889a2	Obligate	Mixed	-5.5	28.5	-2.3
	4879.2	Obligate	Mixed	-2.1	32.8	1.8
	4883	Obligate	Grazer	-1.0	33.0	2.1
Mean				**-6.1**	**29.8**	**-1.0**
Standard Deviation				**3.7**	**2.3**	**2.2**

*Diet determined based on bulk $\delta^{13}C$ value following Cerling et al (2015): C_3 browser (<-8‰); mixed C_3/C_4 diet (>-8‰ to <-1‰); C_4 grazer (>-1‰).

** Water dependency based on modern analog families (Bovidae considered flexible because species within Bovidae are both obligate and non-obligate drinkers).

Table 2.2. Turkana Basin (Koobi Fora) modern species data

Family Sample #	Location (Area #)	Year Collected	Water Dependency[3]	Diet[3]	$\delta^{13}C$ (‰, PDB)[1]	$\delta^{18}O$ (‰, VSMOW)[2]	$\delta^{18}O$ (‰, PDB)[2]
Bovidae, Dik-dik (*Madoqua sp.*) n = 39							
2202	101	1984	Non-Obligate	Browser	-12.6	38.8	7.7
2251	117	1984	Non-Obligate	Browser	-11.5	35.9	4.9
2256	117	1984	Non-Obligate	Browser	-12.4	34.9	3.9
2274	101	1984	Non-Obligate	Browser	-10.3	37.0	6.0
2318	104	1984	Non-Obligate	Browser	-5.6	36.0	4.9
2340	102	1984	Non-Obligate	Browser	-10.7	38.9	7.7
2342	102	1984	Non-Obligate	Browser	-9.5	39.4	8.3
2347	102	1984	Non-Obligate	Browser	-8.3	38.9	7.8
2375	Ileret	1984	Non-Obligate	Browser	-11.1	38.8	7.7
2463	117	1984	Non-Obligate	Browser	-12.2	34.7	3.7
2465	117	1984	Non-Obligate	Browser	-11.6	38.7	7.6
2467	117	1984	Non-Obligate	Browser	-13.7	35.1	4.1
2743	Omo	1984	Non-Obligate	Browser	-11.8	39.3	8.1
4401	101	1993	Non-Obligate	Browser	-9.5	39.2	8.0
4420	Karari	1993	Non-Obligate	Browser	-13.3	34.9	3.9
4421	Karari	1993	Non-Obligate	Browser	-12.9	37.9	6.8
4433	Karari	1993	Non-Obligate	Browser	-12.2	35.8	4.8
4441	Ileret (1A)	1993	Non-Obligate	Browser	-10.6	37.6	6.5
4447	Ileret (1A)	1993	Non-Obligate	Browser	-11.5	39.0	7.9
4460	Ileret (6)	1993	Non-Obligate	Browser	-11.9	40.5	9.3
4462	Ileret (6)	1993	Non-Obligate	Browser	-12.6	38.5	7.5
4463	Ileret (6)	1993	Non-Obligate	Browser	-11.6	40.3	9.2
4470	105	1993	Non-Obligate	Browser	-11.6	40.6	9.4
4474	Karari	1993	Non-Obligate	Browser	-10.7	37.4	6.4
4485	Karari	1993	Non-Obligate	Browser	-11.9	38.2	7.1
4502	130	1993	Non-Obligate	Browser	-12.0	38.9	7.8
4504	118	1993	Non-Obligate	Browser	-12.6	35.0	4.0
4513	Karari	1993	Non-Obligate	Browser	-10.5	36.9	5.9
4514	130	1993	Non-Obligate	Browser	-10.3	35.7	4.7

Table 2.2. Turkana Basin (Koobi Fora) modern species data (continued)

Family	Sample #	Location (Area #)	Year Collected	Water Dependency[3]	Diet[3]	$\delta^{13}C$ (‰, PDB)[1]	$\delta^{18}O$ (‰, VSMOW)[2]	$\delta^{18}O$ (‰, PDB)[2]
	4521	131	1993	Non-Obligate	Browser	-12.2	35.6	4.6
	4523	131	1993	Non-Obligate	Browser	-12.3	37.9	6.8
	K00-KF-320*		2000	Non-Obligate	Browser	-12.5	35.2	4.2
	85-KF-K00*		2000	Non-Obligate	Browser	-11.2	38.2	7.1
	K00-KF-316*		2000	Non-Obligate	Browser	-10.4	37.2	6.1
	K00-KF-319*		2000	Non-Obligate	Browser	-9.8	39.6	8.4
	96-KF-K00*		2000	Non-Obligate	Browser	-9.8	37.5	6.4
	K00-KF-317*		2000	Non-Obligate	Browser	-9.7	38.5	7.4
	86-KF-K00*		2000	Non-Obligate	Browser	-9.5	42.8	11.5
	K00-KF-318*		2000	Non-Obligate	Browser	-6.5	37.6	6.5
Mean						**-11.0**	**37.8**	**6.7**
Standard Deviation						**1.7**	**1.9**	**1.8**
Bovidae, Gerenuk (*Litocranius walleri*) n = 3								
	2170	101	1984	Non-Obligate	Browser	-14.0	35.7	4.7
	2235	101	1984	Non-Obligate	Browser	-12.2	40.5	9.3
	2457	117	1984	Non-Obligate	Browser	-12.0	39.1	8.0
Mean						**-12.7**	**38.4**	**7.3**
Standard Deviation						**1.1**	**2.5**	**2.4**
Bovidae, Lesser Kudu (*Tragelaphus imberbis*) n = 3								
	4407	Ileret	1993	Non-Obligate	Browser	-4.8	43.7	12.4
	4438	Karari	1993	Non-Obligate	Browser	-12.1	37.9	6.8
	4443	Ileret (1A)	1993	Non-Obligate	Browser	-5.2	42.3	11.1
Mean						**-7.3**	**41.3**	**10.1**
Standard Deviation						**4.1**	**3.0**	**2.9**
Giraffidae, Giraffe (*Giraffe cameleopardolos*) n = 7								
	771 (bone)	Buluk	1984	Non-Obligate	Browser	-8.6	37.5	6.4
	2076 (bone)	107	1984	Non-Obligate	Browser	-10.0	37.2	6.1

Table 2.2. Turkana Basin (Koobi Fora) modern species data (continued)

Family Sample #	Location (Area #)	Year Collected	Water Dependency[3]	Diet[3]	$\delta^{13}C$ (‰, PDB)[1]	$\delta^{18}O$ (‰, VSMOW)[2]	$\delta^{18}O$ (‰, PDB)[2]
2266 (bone)	Camp	1984	Non-Obligate	Browser	-10.4	38.3	7.2
2281 (bone)	Camp	1984	Non-Obligate	Browser	-10.3	36.4	5.3
2330 (bone)	119	1984	Non-Obligate	Browser	-10.6	37.2	6.1
2383 (bone)	207	1984	Non-Obligate	Browser	-9.4	34.9	3.9
2407 (bone)	Camp	1984	Non-Obligate	Browser	-10.2	35.4	4.4
Mean					**-9.9**	**36.7**	**5.6**
Standard Deviation					**0.7**	**1.2**	**1.2**
Bovidae, Oryx (*Oryx beisa*) n = 8							
2120	102	1984	Non-Obligate	Grazer	2.0	34.6	3.6
2131	102	1984	Non-Obligate	Grazer	0.3	37.4	6.3
2132	102	1984	Non-Obligate	Grazer	0.3	39.1	8.0
ORYX-1 KF*		1999	Non-Obligate	Grazer	-0.7	38.9	7.8
TEC-K89.9E*		1974	Non-Obligate	Grazer	0.2	36.8	5.8
OM 1530*		1968	Non-Obligate	Grazer	1.1	35.1	4.1
ORYX-2 KF*		1999	Non-Obligate	Grazer	2.9	39.0	7.9
72-KF-K00*		2000	Non-Obligate	Grazer	3.5	38.9	7.8
Mean					**1.2**	**37.5**	**6.4**
Standard Deviation					**1.5**	**1.8**	**1.8**
Bovidae, Topi (*Damaliscus (lunatus) korrigum*) n = 9							
2085	101	1984	Flexible	Grazer	3.7	37.4	6.3
2094	103	1984	Flexible	Grazer	2.1	35.4	4.4
2175	101	1984	Flexible	Grazer	3.6	38.5	7.4
TOPI-1 K.FORA*		1999	Flexible	Grazer	1.9	40.0	8.9
K97-121-KF M2*		1997	Flexible	Grazer	2.7	39.6	8.5
K97-120-KF M1*		1997	Flexible	Grazer	2.7	39.9	8.8
K97-120-KF M2*		1997	Flexible	Grazer	3.3	39.7	8.6
TOPI-3 K.FORA*		1999	Flexible	Grazer	3.4	41.1	9.9
75-KF-K00*		2000	Flexible	Grazer	4.8	38.6	7.5

Table 2.2. Turkana Basin (Koobi Fora) modern species data (continued)

Family	Sample #	Location (Area #)	Year Collected	Water Dependency[3]	Diet[3]	$\delta^{13}C$ (‰, PDB)[1]	$\delta^{18}O$ (‰, VSMOW)[2]	$\delta^{18}O$ (‰, PDB)[2]
Mean						**3.1**	**38.9**	**7.8**
Standard Deviation						**0.9**	**1.7**	**1.7**
Equidae, Burchell's Zebra (*Equus burchelli*) n = 9								
	2116	101	1984	Obligate	Grazer	2.4	36.8	5.7
	2142	101	1984	Obligate	Grazer	2.0	36.6	5.5
	2144	Camp	1984	Obligate	Grazer	1.9	37.3	6.2
	2306	102	1984	Obligate	Grazer	2.0	37.7	6.6
	71-KF-K00*		2000	Obligate	Grazer	0.4	37.8	6.7
	74-KF-K00*		2000	Obligate	Grazer	0.5	39.6	8.5
	TEC.K89.6*		1974	Obligate	Grazer	0.6	35.6	4.6
	99-KF-K00*		2000	Obligate	Grazer	1.2	39.0	7.9
	73-KF-K00*		2000	Obligate	Grazer	1.4	37.6	6.5
Mean						**1.4**	**37.5**	**6.5**
Standard Deviation						**0.8**	**1.2**	**1.2**
Equidae, Grevy's Zebra (*Equus grevyi*) n = 6								
	2243	105	1984	Flexible	Grazer	2.5	35.7	4.7
	2364	Kokoi	1984	Flexible	Grazer	0.1	38.7	7.6
	2432	117	1984	Flexible	Grazer	0.4	34.3	3.3
	2434	117	1984	Flexible	Grazer	-0.6	37.6	6.6
	2435	117	1984	Flexible	Grazer	0.6	36.2	5.2
	20134*		1974	Flexible	Grazer	1.6	41.1	9.9
Mean						**0.8**	**37.3**	**6.2**
Standard Deviation						**1.1**	**2.4**	**2.3**
Hippopotamidae, Hippo (*Hippopotamus amphibius*) n = 9								
	2096 (bone)	103	1984	Obligate	Grazer	0.8	32.4	1.5
	2249 (bone)	117	1984	Obligate	Grazer	0.6	33.9	3.0
	2408 (bone)	Camp	1984	Obligate	Grazer	1.7	34.6	3.6

Table 2.2. Turkana Basin (Koobi Fora) modern species data (continued)

Family	Sample #	Location (Area #)	Year Collected	Water Dependency[3]	Diet[3]	$\delta^{13}C$ (‰, PDB)[1]	$\delta^{18}O$ (‰, VSMOW)[2]	$\delta^{18}O$ (‰, PDB)[2]
	2409 (bone)	Camp	1984	Obligate	Grazer	2.0	34.0	3.1
	2410 (bone)	Camp	1984	Obligate	Grazer	1.8	34.2	3.2
	ET-161*		1971	Obligate	Grazer	-1.3	32.9	2.0
	ET-162*		1990	Obligate	Grazer	0.2	33.1	2.2
	TEC.K89.2*		1974	Obligate	Grazer	0.4	33.6	2.7
	OM-6102B*		1975	Obligate	Grazer	0.7	35.2	4.2
Mean						**0.8**	**33.8**	**2.8**
Standard Deviation						**1.0**	**0.9**	**0.8**
Suidae, Warthog (*Phacochoerus sp.*) n = 9								
	4382 (bone)	102	1993	Obligate	Grazer	0.9	36.3	5.2
	4416 (bone)	Ileret (8A)	1993	Obligate	Grazer	0.4	32.6	1.7
	4444 (bone)	Ileret (1A)	1993	Obligate	Grazer	-0.3	31.1	0.2
	4445 (bone)	Ileret (1A)	1993	Obligate	Grazer	0.2	30.9	0.0
	4446 (bone)	Ileret (1A)	1993	Obligate	Grazer	0.4	28.7	-2.1
	4458 (bone)	Ileret (6)	1993	Obligate	Grazer	-0.6	30.5	-0.4
	TEC.K89.5*		1974	Obligate	Grazer	-0.8	36.4	5.4
	K00-KF-322*		2000	Obligate	Grazer	1.7	33.7	2.8
	100-KF-K00*		2000	Obligate	Grazer	2.0	34.6	3.6
Mean						**0.4**	**32.8**	**1.8**
Standard Deviation						**1.0**	**2.7**	**2.6**

[1] $\delta^{13}C$ values from this study corrected for Suess effect (+1) and bone converted to enamel (+2.3) (Warinner and Tuross 2009)

[2] $\delta^{18}O$ (SMOW & PDB) bone values converted to enamel (+1.7) (Warinner and Tuross 2009)

[3] Water dependency and diet based on observation of modern species (Dorst and Dandelot 1970; Estes 1991)

* Samples from the Koobi Fora, Turkana Basin previously reported in (Harris and Cerling 2002; Jehle 2013; Levin et al. 2006)

The 'Camp' designation for the location is for samples collected at the Koobi Fora Base Camp.

Table 2.3. Comparison of current study Allia Bay fossil fauna to Schoeninger et al. (2003)

			$\delta^{13}C$ (‰, PDB)				$\delta^{18}O$ (‰, PDB)			
	Family	**N**	**Mean**	**Max**	**Min**	**Range**	**Mean**	**Max**	**Min**	**Range**
Current Study										
	Deinotheriidae	4	-13.4	-13.1	-13.7	0.6	-1	0.1	-1.8	1.9
	Elephantidae	5	-7.5	-4.2	-12.6	8.4	-0.9	2.5	-2.2	4.7
	Giraffidae	2	-14.7	-14	-15.5	1.5	1	3	-1	4
	Suidae	8	-6.1	-1	-12.7	11.7	-1	2.1	-4.8	6.9
	Hippopotamidae	13	-5.3	-1.1	-11.7	10.6	-4.1	-1	-6.6	5.6
Schoeninger et al. (2003)										
	Deinotheriidae	2	-13.9	-13.1	-14.7	1.6	-1.1	-0.5	-1.6	1.1
	Elephantidae	5	-4.6	-3.0	-6.8	3.9	-1.8	-0.6	-2.9	2.3
	Giraffidae	3	-14.5	-13.4	-15.2	1.8	0.0	1.2	-2.1	3.3
	Suidae	5	-5.4	-0.2	-12.9	12.7	-1.7	1.1	-4.1	5.2
	Hippopotamidae	7	-6.4	-1.5	-12.6	11.1	-3.1	2.8	-7.2	10.0

Table 2.4 Mann-Whitney U results for modern Koobi Fora compared to fossil Allia Bay fauna.

	Family	N	Z	p value[1]	Trend[2]
$\delta^{13}C$	Bovid	57	-2.78	**0.0054**	KF>AB
	Equid[3]				KF>AB
	Giraffid[3]				KF>AB
	Hippopotamid	18	-3.1543	**0.00164**	KF>AB
	Suid	14	-3.0338	**0.00244**	KF>AB
$\delta^{18}O$	Bovid	57	5.57	**0.0001**	KF>AB
	Equid[3]				KF>AB
	Giraffid[3]				KF>AB
	Hippopotamid	18	-3.1543	**0.00164**	KF>AB
	Suid	14	-1.2264	0.2187	

[1] Statistically significant results ($p<.05$) are indicated by bold-faced type in the table

[2] Direction of trend indicate which skeletal sample has a higher stable isotope value

[3] Fossil sample size (n = 2) is too small to statistically compare but trend was noted

Table 2.5 Mann-Whitney U Results for Fossil Locality Comparisons

	Family	N	Z	p value[1]	Trend[2]
Allia Bay vs Kanapoi					
$\delta^{13}C$	Elephantidae	13	2.76	**0.0058**	K>AB
	Suid	15	-1.79	0.0735	
$\delta^{18}O$	Elephantidae	13	1.46	0.1443	
	Suid	15	-1.1	0.2713	
Allia Bay vs Omo Mursi					
$\delta^{13}C$	Elephantidae	23	2.42	**0.0155**	AB<M
	Hippopotamid	19	-0.09	0.9283	
	Suid	36	-0.21	0.8337	
$\delta^{18}O$	Elephantidae	23	0.82	0.4122	
	Hippopotamid	19	-1.7103	0.0873	
	Suid	36	-1.08	0.2801	

[1] Statistically significant results ($p<.05$) are indicated by bold-faced type in the table

[2] Direction of trend indicate which skeletal sample has a higher mean stable isotope values

Table 2.6. Comparison of Hippopotamidae-Giraffidae offset in East Africa

		$\delta^{18}O_{gir}$			$\delta^{18}O_{hip}$			$\Delta^{18}O_{gir\text{-}hip}$	$\varepsilon_{gir\text{-}hip}$	$\varepsilon_{gir\text{-}hip}$
Fossil Locality	**Age (Ma)**	**N**	**mean**	**1SD**	**N**	**mean**	**1SD**		**(offset)**	**(SE)**
Aramis	4.4	8	5.4	1.1	9	-3.9	2.8	9.3	9.3	3.0
Allia Bay	3.97	2	1.0	2.8	13	-4.1	1.6	5.1	5.1	3.2
Hadar (Dikika)	3.8-3.24	24	-1.4	3.1	18	-7.1	2.5	5.7	5.8	4.0
Woranso-Mille	3.76-3.57	8	-2.4	3.3	8	-6.2	1.8	3.8	3.8	3.8
Koobi Fora	Modern	7	5.6	1.2	9	2.8	0.8	2.8	2.8	1.4

Table 2.7 Mann-Whitney U Results for Hippopotamidae and Giraffidae Comparisons

Localities	N	Z	p value[1]	Trend[2]
Hippopotamidae $\delta^{18}O$				
Allia Bay vs Aramis	22	-0.53	0.5961	
Allia Bay vs Hadar	31	-3.9	**0.0001**	AB>H
Allia Bay vs Woranso-Mille	21	2.21	**0.0271**	AB>W-M
Aramis vs Woranso-Mille	17	1.83	0.0673	
Hadar vs Woranso-Mille	26	-1.64	0.1010	
Hadar vs Aramis	27	-2.75	**0.0060**	A>H
Giraffidae $\delta^{18}O$				
Aramis vs Woranso-Mille	16	3.05	**0.0023**	A>W-M
Hadar vs Woranso-Mille	32	0.85	0.3953	
Hadar vs Aramis	32	-4.07	**0.0001**	A>H

[1] Statistically significant results ($p<.05$) are indicated by bold-faced type in the table

[2] Direction of trend indicate which skeletal sample has a higher mean stable isotope values

References

Asfaw B, Beyene Y, Semaw S, Suwa G, White T, and WoldeGabriel G. 1991. Fejej: a new paleoanthropological research area in Ethiopia. Journal of Human Evolution 21(2):137-143.

Ayliffe LK, and Chivas AR. 1990. Oxygen isotope composition of the bone phosphate of Australian kangaroos: potential as a palaeoenvironmental recorder. Geochimica et Cosmochimica Acta 54(9):2603-2609.

Balasse M, Ambrose SH, Smith AB, and Price TD. 2002. The Seasonal Mobility Model for Prehistoric Herders in the South-Western Cape of South Africa Assessed by Isotopic Analysis of Sheep Tooth Enamel. Journal of Archaeological Science 29(9):917-932.

Balasse M, Smith AB, Ambrose SH, and Leigh SR. 2003. Determining sheep birth seasonality by analysis of tooth enamel oxygen isotope ratios: The late stone age site of Kasteelberg (South Africa). Journal of Archaeological Science 30(2):205-215.

Bedaso ZK, Wynn JG, Alemseged Z, and Geraads D. 2013. Dietary and paleoenvironmental reconstruction using stable isotopes of herbivore tooth enamel from middle Pliocene Dikika, Ethiopia: Implication for Australopithecus afarensis habitat and food resources. Journal of human evolution 64(1):21-38.

Behrensmeyer AK. 2006. Climate change and human evolution. Science(Washington) 311(5760):476-478.

Behrensmeyer AK, and Reed KE. 2013. Reconstructing the habitats of *Australopithecus*: Paleoenvironments, site taphonomy, and faunas. In: Reed KE, Fleagle JG, and Leakey RE, editors. The Paleobiology of *Australopithecus*. London: Springer. p 41-60.

Behrensmeyer AK, Todd NE, Potts R, and McBrinn GE. 1997. Late Pliocene faunal turnover in the Turkana Basin, Kenya and Ethiopia. Science 278(5343):1589-1594.

Bobe R. 2011. Fossil Mammals and Paleoenvironments in the Omo-Turkana Basin. Evolutionary Anthropology: Issues, News, and Reviews 20(6):254-263.

Bobe R, Behrensmeyer AK, and Chapman RE. 2002. Faunal change, environmental variability and late Pliocene hominin evolution. Journal of Human Evolution 42(4):475-497.

Bonnefille R. 1995. A reassessment of the Plio-Pleistocene pollen record of East Africa. In: Vrba E, Denton G, Partridge T, and Buckle LH, editors. Paleoclimate and Evolution with Emphasis on Human Origins. New Haven: Yale University Press. p 299-310.

Bonnefille R, and Mohammed U. 1994. Pollen-inferred climatic fluctuations in Ethiopia during the last 3000 years. Palaeogeography, Palaeoclimatology, Palaeoecology 109(2-4):331-343.

Bonnefille R, Potts R, Chalié F, Jolly D, and Peyron O. 2004. High-resolution vegetation and climate change associated with Pliocene *Australopithecus afarensis*. Proceedings of the National Academy of Sciences 101(33):12125-12129.

Breecker D, Sharp Z, and McFadden LD. 2009. Seasonal bias in the formation and stable isotopic composition of pedogenic carbonate in modern soils from central New Mexico, USA. Geological Society of America Bulletin 121(3-4):630-640.

Brown FH, and McDougall I. 2011. Geochronology of the Turkana depression of northern Kenya and southern Ethiopia. Evolutionary Anthropology: Issues, News, and Reviews 20(6):217-227.

Bryant JD, and Froelich PN. 1995. A model of oxygen isotope fractionation in body water of large mammals. Geochimica et Cosmochimica Acta 59(21):4523-4537.

Bryant JD, Koch PL, Froelich PN, Showers WJ, and Genna BJ. 1996. Oxygen isotope partitioning between phosphate and carbonate in mammalian apatite. Geochimica et Cosmochimica Acta 60(24):5145-5148.

Calvin M, and Benson AA. 1948. The path of carbon in photosynthesis. Science 107:476-480.

Cerling T, Harris J, Hart J, Kaleme P, Klingel H, Leakey M, Levin N, Lewison R, and Passey B. 2008. Stable isotope ecology of the common hippopotamus. Journal of Zoology 276(2):204-212.

Cerling TE. 1992. Development of grasslands and savannas in East Africa during the Neogene. Palaeogeography, Palaeoclimatology, Palaeoecology 97(3):241-247.

Cerling TE, Andanje SA, Blumenthal SA, Brown FH, Chritz KL, Harris JM, Hart JA, Kirera FM, Kaleme P, and Leakey LN. 2015. Dietary changes of large herbivores in the Turkana Basin, Kenya from 4 to 1 Ma. Proceedings of the National Academy of Sciences 112(37):11467-11472.

Cerling TE, Bowman JR, and O'Neil JR. 1988. An isotopic study of a fluvial-lacustrine sequence: the Plio-Pleistocene Koobi Fora sequence, East Africa. Palaeogeography, palaeoclimatology, palaeoecology 63(4):335-356.

Cerling TE, and Harris JM. 1999. Carbon Isotope Fractionation Between Diet and Bioapatite in Ungulate Mammals and Implications for Ecological and Paleoecological Studies. Oecologia 120:347-363.

Cerling TE, Harris JM, MacFadden BJ, Leakey MG, Quade J, Eisenmann V, and Ehleringer JR. 1997. Global vegetation change through the Miocene/Pliocene boundary. Nature 389(6647):153-158.

Cerling TE, Levin NE, and Passey BH. 2011a. Stable Isotope Ecology in the Omo-Turkana Basin. Evolutionary Anthropology: Issues, News, and Reviews 20(6):228-237.

Cerling TE, Levin NE, Quade J, Wynn JG, Fox DL, Kingston JD, Klein RG, and Brown FH. 2010. Comment on the paleoenvironment of *Ardipithecus ramidus*. Science 328(5982):1105.

Cerling TE, Manthi FK, Mbua EN, Leakey LN, Leakey MG, Leakey RE, Brown FH, Grine FE, Hart JA, and Kaleme P. 2013. Stable isotope-based diet reconstructions of Turkana Basin hominins. Proceedings of the National Academy of Sciences 110(26):10501-10506.

Cerling TE, and Quade J. 1993. Stable carbon and oxygen isotopes in soil carbonates. Climate Change in Continental Isotopic Records, Geophysical Monograph 78: American Geophysical Union. p 217-231.

Cerling TE, Wynn JG, Andanje SA, Bird MI, Korir DK, Levin NE, Mace W, Macharia AN, Quade J, and Remien CH. 2011b. Woody cover and hominin environments in the past 6 million years. Nature 476(7358):51-56.

Dansgaard W. 1964. Stable isotopes in precipitation. Tellus 16(4):436-468.

deMenocal PB. 2004. African climate change and faunal evolution during the Pliocene–Pleistocene. Earth and Planetary Science Letters 220(1-2):3-24.

deMenocal PB, and Rind D. 1993. Sensitivity of Asian and African climate to variations in seasonal insolation, glacial ice cover, sea surface temperature, and Asian orography. Journal of Geophysical Research: Atmospheres 98(D4):7265-7287.

DeNiro MJ, and Epstein S. 1978. Influence of Diet on Distribution of Carbon Isotopes in Animals. Geochimica et Cosmochimica Acta 42(5):495-506.

Domínguez-Rodrigo M. 2014. Is the "Savanna Hypothesis" a dead concept for explaining the emergence of the earliest hominins? Current Anthropology 55(1):59-81.

Dongmann G, Nürnberg H, Förstel H, and Wagener K. 1974. On the enrichment of $H_2{}^{18}O$ in the leaves of transpiring plants. Radiation and environmental biophysics 11(1):41-52.

Drapeau M, Robe R, Wynn J, and Geraads D. 2014. The Omo Mursi Formation reconsidered: a window into the East African Pliocene. Journal of Human Evolution 75:64-79.

Feibel CS. 2011. A geological history of the Turkana Basin. Evolutionary Anthropology: Issues, News, and Reviews 20(6):206-216.

Fernández MH, and Vrba ES. 2006. Plio-Pleistocene climatic change in the Turkana Basin (East Africa): evidence from large mammal faunas. Journal of Human Evolution 50(6):595-626.

Flanagan LB, Comstock JP, and Ehleringer JR. 1991. Comparison of modeled and observed environmental influences on the stable oxygen and hydrogen isotope composition of leaf water in *Phaseolus vulgaris L.* Plant Physiology 96(2):588-596.

Fricke HC, Clyde WC, and O'Neil JR. 1998. Intra-tooth variations in $\delta^{18}O$ (PO_4) of mammalian tooth enamel as a record of seasonal variations in continental climate variables. Geochimica et Cosmochimica Acta 62(11):1839-1850.

Fricke HC, and O'Neil JR. 1999. The correlation between $^{18}O/^{16}O$ ratios of meteoric water and surface temperature: its use in investigating terrestrial climate change over geologic time. Earth and Planetary Science Letters 170(3):181-196.

Garten Jr CT, and Taylor Jr G. 1992. Foliar $\delta^{13}C$ within a temperate deciduous forest: spatial, temporal, and species sources of variation. Oecologia 90(1):1-7.

Geraads D, Bobe R, and Manthi FK. 2013. New ruminants (Mammalia) from the Pliocene of Kanapoi, Kenya, and a revision of previous collections, with a note on the Suidae. Journal of African Earth Sciences 85:53-61.

Haile-Selassie Y, Saylor BZ, Deino A, Alene M, and Latimer BM. 2010. New hominid fossils from Woranso-Mille (Central Afar, Ethiopia) and taxonomy of early *Australopithecus*. American Journal of Physical Anthropology 141(3):406-417.

Hallin KA, Schoeninger MJ, and Schwarcz HP. 2012. Paleoclimate during Neandertal and anatomically modern human occupation at Amud and Qafzeh, Israel: the stable isotope data. Journal of Human Evolution 62(1):59-73.

Harris JM, Brown F, Leakey M, Walker A, and Leakey R. 1988. Pliocene and Pleistocene hominid-bearing sites from west of Lake Turkana, Kenya. Science 239(4835):27-33.

Harris JM, and Cerling TE. 2002. Dietary adaptations of extant and Neogene African suids. J Zool Lond 256:45-54.

Harris JM, Cerling TE, Leakey M, and Passey B. 2008. Stable isotope ecology of fossil hippopotamids from the Lake Turkana Basin of East Africa. Journal of Zoology:1-9.

Harris JM, and Leakey M. 2003. Introduction. In: Harris J, and Leakey M, editors. Contributions in Science: Geology and Vertebrate Paleontology of the Early Pliocene Site of Kanapoi, Northern Kenya Los Angeles: Natural History Museum of Los Angeles County. p 1-7.

Harris JM, Leakey M, Cerling T, and Winkler A. 2003. Early Pliocene tetrapod remains from Kanapoi, Lake Turkana Basin, Kenya. In: Harris J, and Leakey M, editors. Contributions in Science: Geology and Vertebrate Paleontology of the Early Pliocene site of Kanapoi, Northern Kenya Natural History Museum of Los Angeles County. p 39-114.

Hatch M, and Slack C. 1966. Photosynthesis by sugarcane leaves. A new carboxylation reaction and the pathway of sugar formation. Biochemical Journal 101:103-111.

Heaton THE. 1999. Spatial, Species, and Temporal Variations in the $^{13}C/^{12}C$ ratios of C_3 Plants: Implications for Palaeodiet Studies. Journal of Archaeological Science 26(6):637-649.

Huertas AD, Iacumin P, Stenni B, Chillón BS, and Longinelli A. 1995. Oxygen isotope variations of phosphate in mammalian bone and tooth enamel. Geochimica et Cosmochimica Acta 59(20):4299-4305.

Jacques L, Ogle N, Moussa I, Kalin R, Vignaud P, Brunet M, and Bocherens H. 2008. Implications of diagenesis for the isotopic analysis of Upper Miocene large mammalian herbivore tooth enamel from Chad. Palaeogeography, Palaeoclimatology, Palaeoecology 266(3):200-210.

Jehle GE. 2013. An Ecological Snapshot of the Early Pleistocene at Kokiselei, Kenya. Salt Lake City: The University of Utah.

Joordens JC, Vonhof HB, Feibel CS, Lourens LJ, Dupont-Nivet G, van der Lubbe JH, Sier MJ, Davies GR, and Kroon D. 2011. An astronomically-tuned climate framework for hominins in the Turkana Basin. Earth and Planetary Science Letters 307(1):1-8.

Kappelman J, Swisher III CC, Fleagle JG, Yirga S, Bown TM, and Feseha M. 1996. Age of *Australopithecus afarensis* from Fejej, Ethiopia. Journal of Human Evolution 30(2):139-146.

Keeling CD. 1979. The Suess Effect: ^{13}Carbon-^{14}Carbon Interrelations. Enviornmental International 2:229-300.

Kimbel WH, Lockwood CA, Ward CV, Leakey MG, Rak Y, and Johanson DC. 2006. Was *Australopithecus anamensis* ancestral to *A. afarensis*? A case of anagenesis in the hominin fossil record. Journal of Human Evolution 51(2):134-152.

Kingston JD. 2007. Shifting adaptive landscapes: progress and challenges in reconstructing early hominid environments. American Journal of Physical Anthropology 134(S45):20-58.

Kingston JD, Marino BD, and Hill A. 1994. Isotopic evidence for Neogene hominid paleoenvironments in the Kenya Rift Valley. Science 264(5161):955-958.

Koch PL, Tuross N, and Fogel ML. 1997. The Effects of Sample Treatment and Diagenesis on the Isotopic Integrity of Carbonate in Biogenic Hydroxylapatite. Journal of Archaeological Science 24(5):417-429.

Kohn MJ, Schoeninger MJ, and Barker WW. 1999. Altered states: effects of diagenesis on fossil tooth chemistry. Geochimica et Cosmochimica Acta 63(18):2737-2747.

Kohn MJ, Schoeninger MJ, and Valley JW. 1996. Herbivore tooth oxygen isotope compositions: Effects of diet and physiology. Geochimica et Cosmochimica Acta 60(20):3889-3896.

Kohn MJ, Schoeninger MJ, and Valley JW. 1998. Variability in oxygen isotope compositions of herbivore teeth: reflections of seasonality or developmental physiology? Chemical Geology 152(1-2):97-112.

Kohn MJ, and Welker JM. 2005. On the temperature correlation of δ^{18}O in modern precipitation. Earth and Planetary Science Letters 231(1):87-96.

Kullmer O, Sandrock O, Viola TB, Hujer W, Said H, and Seidler H. 2008. Suids, elephantoids, paleochronology, and paleoecology of the Pliocene hominid site Galili, Somali Region, Ethiopia. Palaios 23(7):452-464.

Leakey MG, Feibel CS, McDougall I, and Walker A. 1995. New four-million-year-old hominid species from Kanapoi and Allia Bay, Kenya. Nature 376(6541):565-571.

Leakey MG, Feibel CS, McDougall I, Ward C, and Walker A. 1998. New specimens and confirmation of an early age for *Australopithecus anamensis*. Nature 393(6680):62-66.

Lee-Thorp J. 2002. Two decades of progress towards understanding fossilization processes and isotopic signals in calcified tissue minerals. Archaeometry 44:435-446.

Lee-Thorp J, Likius A, Mackaye HT, Vignaud P, Sponheimer M, and Brunet M. 2012. Isotopic evidence for an early shift to C_4 resources by Pliocene hominins in Chad. Proceedings of the National Academy of Sciences 109(50):20369-20372.

Levin NE, Cerling T, Passey B, Harris J, and Ehleringer J. 2006. A stable isotope aridity index for terrestrial environments. Proceedings of the National Academy of Sciences 103(30):11201-11205.

Levin NE, Brown FH, Behrensmeyer AK, Bobe R, and Cerling TE. 2011. Paleosol carbonates from the Omo Group: Isotopic records of local and regional environmental change in East Africa. Palaeogeography, Palaeoclimatology, Palaeoecology 307(1):75-89.

Levin NE, Haile-Selassie Y, Frost SR, and Saylor BZ. 2015. Dietary change among hominins and cercopithecids in Ethiopia during the early Pliocene. Proceedings of the National Academy of Sciences 112(40):12304-12309.

Levin NE, Simpson SW, Quade J, Cerling TE, and Frost SR. 2008. Herbivore enamel carbon isotopic composition and the environmental context of Ardipithecus at Gona, Ethiopia. Geological Society of America Special Papers 446:215-234.

Longinelli A. 1984. Oxygen isotopes in mammal bone phosphate: a new tool for paleohydrological and paleoclimatological research? Geochimica et Cosmochimica Acta 48(2):385-390.

Luz B, Cormie AB, and Schwarcz HP. 1990. Oxygen isotope variations in phosphate of deer bones. Geochimica et Cosmochimica Acta 54(6):1723-1728.

Luz B, and Kolodny Y. 1985. Oxygen isotope variations in phosphate of biogenic apatites, IV. Mammal teeth and bones. Earth and Planetary Science Letters 75(1):29-36.

Luz B, Kolodny Y, and Horowitz M. 1984. Fractionation of oxygen isotopes between mammalian bone-phosphate and environmental drinking water. Geochimica et Cosmochimica Acta 48(8):1689-1693.

Macho GA, Leakey M, Williamson D, and Jiang Y. 2003. Palaeoenvironmental reconstruction: evidence for seasonality at Allia Bay, Kenya, at 3.9 million years. Palaeogeography, Palaeoclimatology, Palaeoecology 199(1):17-30.

Meteorological Office. 1983. Tables of Temperature, Relative Humidity, Precipitation and Sunshine for the World: Part IV. Africa, the Atlantic Ocean South of 35°N and the Indian Ocean. London: Her Majesty's Stationary Office.

Moore J. 1996. Savanna chimpanzees, referential models and the last common ancestor. In: McGrew WC, Marchant LF, and Nishida T, editors. Great Ape Societies. Cambridge: Cambridge University Press. p 275-292.

Morgan ME, Kingston JD, and Marino BD. 1994. Carbon isotopic evidence for the emergence of C_4 plants in the Neogene from Pakistan and Kenya. Nature 367(6459):162-165.

O' Leary MH. 1981. Carbon Isotope Fractionation in Plants. Phytochemistry 20(4):553-567.

O' Leary MH. 1988. Carbon Isotopes in Photosynthesis. Bioscience 38(5):328-335.

O' Leary MH. 1995. Environmental effects on carbon isotope fractionation in terrestrial plants. In: Wada E, editor. Stable Isotopes in the Biosphere. Japan: Kyoto University Press. p 78-91.

Passey BH, Levin NE, Cerling TE, Brown FH, and Eiler JM. 2010. High-temperature environments of human evolution in East Africa based on bond ordering in paleosol carbonates. Proceedings of the National Academy of Sciences 107(25):11245-11249.

Peters NA, Huntington KW, and Hoke GD. 2013. Hot or not? Impact of seasonally variable soil carbonate formation on paleotemperature and O-isotope records from clumped isotope thermometry. Earth and Planetary Science Letters 361:208-218.

Poage MA, and Chamberlain CP. 2001. Empirical relationships between elevation and the stable isotope composition of precipitation and surface waters: Considerations for studies of paleoelevation change. American Journal of Science 301(1):1-15.

Podlesak D, Torregrossa A, Ehleringer J, Dearing M, Passey B, and Cerling T. 2008. Turnover of oxygen and hydrogen isotopes in the body water, CO_2, hair, and enamel of a small mammal. Geochimica et Cosmochimica Acta 72:19-35.

Potts R. 1998. Environmental hypotheses of hominin evolution. American Journal of Physical Anthropology 107(s27):93-136.

Quade J, Garzione C, and Eiler J. 2007. Paleoelevation reconstruction using pedogenic carbonates. Reviews in Mineralogy and Geochemistry 66(1):53-87.

Quinn RL. 2015. Influence of Plio-Pleistocene basin hydrology on the Turkana hominin enamel carbonate $\delta^{18}O$ values. Journal of Human Evolution 86:13-31.

Ransom S, and Thomas M. 1960. Crassulacean acid metabolism. Annual Review of Plant Physiology 11:81-110.

Reed KE, Rowan J, and Kamilar J. 2014. African vegetation structure: Modern analogs and hominin habitat reconstructions. American Journal of Physical Anthropology 153(S58):218.

Reed KE. 1997. Early hominid evolution and ecological change through the African Plio-Pleistocene. Journal of Human Evolution 32(2):289-322.

Retallack G. 1994. The environmental factor approach to the interpretation of paleosols. In: Amundson R, Harden J, and Singer M, editors. Factors of soil formation: a fifieth annerversary perspective. Madison: Soil Science Society of America. p 31-64.

Rozanski K, Araguás-Araguás L, and Gonfiantini R. 1992. Relation between long-term trends of oxygen-18 isotope composition of precipitation and climate. Science 258:981-984.

Rozanski K, Araguás-Araguás L, and Gonfiantini R. 1993. Isotopic patterns in modern global precipitation. In: Swart P, Lohmann K, McKenzie J, and Savin E, editors. Climate Change in Continental Isotopic Records. Washington: Geophysical Monograph AGU. p 1-36.

Schoeninger MJ, and Deniro MJ. 1984. Nitrogen and Carbon Isotopic Composition of Bone Collagen from Marine and Terrestrial Animals. Geochimica et Cosmochimica Acta 48(4):625-639.

Schoeninger MJ, Hallin K, Reeser H, Valley JW, and Fournelle J. 2003a. Isotopic alteration of mammalian tooth enamel. International Journal of Osteoarchaeology 13(1-2):11-19.

Schoeninger MJ, Iwaniec UT, and Glander KE. 1997. Stable isotope ratios indicate diet and habitat use in New World monkeys. American Journal of Physical Anthropology 103(1):69-83.

Schoeninger MJ, Iwaniec UT, and Nash LT. 1998. Ecological attributes recorded in stable isotope ratios of arboreal prosimian hair. Oecologia 113(2):222-230.

Schoeninger MJ, Most CA, Moore JJ, and Somerville AD. 2015. Environmental variables across *Pan troglodytes* study sites correspond with the carbon, but not the nitrogen, stable isotope ratios of chimpanzee hair. American Journal of Primatology. DOI: 10.1002/ajp.22496.

Schoeninger MJ, Reeser H, and Hallin K. 2003b. Paleoenvironment of *Australopithecus anamensis* at Allia Bay, East Turkana, Kenya: evidence from mammalian herbivore enamel stable isotopes. Journal of Anthropological Archaeology 22(3):200-207.

Ségalen L, Lee-Thorp J, and Cerling T. 2007. Timing of C_4 grass expansion across sub-Saharan Africa. Journal of Human Evolution 53:549-559.

Sept JM, King BJ, McGrew W, Moore J, Paterson JD, Strier KB, Uehara S, Whiten A, and Wrangham RW. 1992. Was There No Place Like Home?: A New Perspective on Early Hominid Archaeological Sites From the Mapping of Chimpanzee Nests [and Comments and Reply]. Current Anthropology 33(2):187-207.

Souron A, Balasse M, and Boisserie J-R. 2012. Intra-tooth isotopic profiles of canines from extant *Hippopotamus amphibius* and late Pliocene hippopotamids (Shungura Formation, Ethiopia): insights into the seasonality of diet and climate. Palaeogeography, Palaeoclimatology, Palaeoecology 342:97-110.

Sponheimer M, and Lee-Thorp J. 2014. Hominin Paleodiets: The Contribution of Stable Isotopes. In: Henke W, and Tattersall I, editors. Handbook of Paleoanthropology. Berlin: Springer. p 1-27.

Sponheimer M, Lee-Thorp J, de Ruiter D, Codron D, Codron J, Baugh AT, and Thackeray F. 2005. Hominins, sedges, and termites: new carbon isotope data from the Sterkfontein Valley and Kruger National Park. Journal of Human Evolution 48(3):301-312.

Sponheimer M, and Lee-Thorp JA. 1999. Oxygen isotopes in enamel carbonate and their ecological significance. Journal of Archaeological Science 26(6):723-728.

Sponheimer M, Loudon J, Codron D, Howells M, Pruetz JD, Codron J, De Ruiter D, and Lee-Thorp JA. 2006. Do "savanna" chimpanzees consume C_4 resources? Journal of Human Evolution 51(2):128-133.

Sternberg L. 1988. Oxygen and hydrogen isotope ratios in plant cellulose: mechanisms and applications. In: Rundel P, Ehleringer J, and Nagy K, editors. Stable Isotopes in Ecological Research. Berlin: Springer-Verlag. p 124-141.

Taylor C. 1968. Hygroscopic food: a source of water for desert antelopes? Nature 21:181-182.

Tiedemann R, Sarnthein M, and Shackleton NJ. 1994. Astronomic timescale for the Pliocene Atlantic $\delta^{18}O$ and dust flux records of Ocean Drilling Program Site 659. Paleoceanography 9(4):619-638.

Uno KT, Cerling TE, Harris JM, Kunimatsu Y, Leakey MG, Nakatsukasa M, and Nakaya H. 2011. Late Miocene to Pliocene carbon isotope record of differential diet change among East African herbivores. Proceedings of the National Academy of Sciences 108(16):6509-6514.

Van Couvering J. 2000. Fejej. In: Delson E, Tattersall I, Van Couvering J, and Brooks A, editors. Encyclopedia of human evolution and prehistory (2nd Edition). New York: Garland. p 267-268.

van der Merwe NJ, and Medina E. 1991. The Canopy Effect, Carbon Isotope Ratios and Foodwebs in Amazonia. Journal of Archaeological Science 18(3):249-259.

Vogel J. 1983. Isotopic evidence for the past climates and vegetation of southern Africa. Bothalia 14(3/4):391-394.

Vrba ES, Denton G, Partridge T, and Burckle L. 1995. Paleoclimate and Evolution with Emphasis on Human Origins. New Haven: Yale University Press.

Vrba ES. 1985. Ecological and adaptive changes associated with early hominid evolution. In: Delson E, editor. Ancestors: The hard evidence. New York: Alan R Liss. p 63-71.

Vrba ES. 1988. Late Pliocene climatic events and hominid evolution. In: Grine F, editor. Evolutionary History of the "Robust" Australopithecines. New York: Aldine de Gruyter. p 405-426.

Ward CV, Leakey M, and Walker A. 1999. The new hominid species *Australopithecus anamensis*. Evolutionary Anthropology 7(6):197-205.

Ward CV, Leakey M, and Walker A. 2001. Morphology of *Australopithecus anamensis* from Kanapoi and Allia Bay, Kenya. Journal of Human Evolution 41:255-368.

Ward CV. 2014. Taxonomic affinity of the Pliocene hominin fossils from Fejej, Ethiopia. Journal of human evolution(73):98-102.

Warinner C, and Tuross N. 2009. Alkaline cooking and stable isotope tissue-diet spacing in swine: archaeological implications. Journal of Archaeological Science 36(8):1690-1697.

White TD, Ambrose SH, Suwa G, Su DF, DeGusta D, Bernor RL, Boisserie J-R, Brunet M, Delson E, Frost S et al. . 2009a. Macrovertebrate Paleontology and the Pliocene Habitat of *Ardipithecus ramidus*. Science 326(5949):67-93.

White TD, Asfaw B, Beyene Y, Haile-Selassie Y, Lovejoy CO, Suwa G, and WoldeGabriel G. 2009b. *Ardipithecus ramidus* and the Paleobiology of Early Hominids. Science 326(5949):64-86.

White TD, WoldeGabriel G, Asfaw B, Ambrose S, Beyene Y, Bernor RL, Boisserie J-R, Currie B, Gilbert H, Haile-Selassie Y et al. . 2006. Asa Issie, Aramis and the origin of *Australopithecus*. Nature 440(7086):883-889.

WoldeGabriel G, Ambrose SH, Barboni D, Bonnefille R, Bremond L, Currie B, DeGusta D, Hart WK, Murray AM, and Renne PR. 2009. The geological, isotopic, botanical, invertebrate, and lower vertebrate surroundings of *Ardipithecus ramidus*. Science 326(5949):65-65e65.

Wood B, and Leakey M. 2011. The Omo-Turkana Basin Fossil Hominins and Their Contribution to Our Understanding of Human Evolution in Africa. Evolutionary Anthropology: Issues, News, and Reviews 20(6):264-292.

Wynn JG. 2000. Paleosols, stable carbon isotopes, and paleoenvironmental interpretation of Kanapoi, Northern Kenya. Journal of Human Evolution 39(4):411-432.

Wynn JG. 2004. Influence of Plio-Pleistocene aridification on human evolution: Evidence from paleosols of the Turkana Basin, Kenya. American Journal of Physical Anthropology 123(2):106-118.

Wynn JG, Sponheimer M, Kimbel WH, Alemseged Z, Reed K, Bedaso ZK, and Wilson JN. 2013. Diet of *Australopithecus afarensis* from the Pliocene Hadar formation, Ethiopia. Proceedings of the National Academy of Sciences 110(26):10495-10500.

Yakir D. 1992. Variations in the natural abundance of oxygen-18 and deuterium in plant carbohydrates. Plant, Cell & Environment 15(9):1005-1020.

Yuretich RF. 1979. Modern sediments and sedimentary processes in Lake Rudolf (Lake Turkana) eastern rift valley, Kenya. Sedimentology 26(3):313-331.

Yurtsever Y, and Gat J. 1981. Stable isotope hydrology: Deuterium and Oxygen-18 in the water cycle. Atmospheric Waters:103-142.

Zachos J, Pagani M, Sloan L, Thomas E, and Billups K. 2001. Trends, rhythms, and aberrations in global climate 65 Ma to present. Science 292(5517):686-693.

Zazzo A. 2014. Bone and enamel carbonate diagenesis: a radiocarbon prospective. Palaeogeography, Palaeoclimatology, Palaeoecology 416:168-178.

Zazzo A, Lecuyer C, and Mariotti A. 2004. Experimentally-controlled carbon and oxygen isotope exchange between bioapatites and water under inorganic and microbially-mediated conditions. Geochimica et Cosmochimica Acta 68(1):1-12.

CHAPTER 3: DIAGENESIS OF FOSSIL TOOTH ENAMEL: FLUORESCENCE AND SECONDARY ION MASS SPECTROMTRY (SIMS) REVEAL ALTERED MINERAL STRUCTURE AFFECTS $\delta^{18}O$ VALUES IN FAUNAL ENAMEL

Introduction

Since the late 1970s, techniques developed in isotope geochemistry have become increasingly popular tools for archaeologists and paleoanthropologists when reconstructing ancient diets, environments, climate, and migration patterns. DeNiro and Epstein (1976, 1978, 1981), van der Merwe and Vogel (1978), and Vogel and van der Merwe (1977) pioneered the use of stable carbon and nitrogen isotope ratios from bone collagen to interpret diet. DeNiro and Epstein (1976) gave new meaning to the phrase "you are what you eat" when they established that the isotopic signatures of food items in an organism's diet are incorporated into its bodily tissues. Early studies using the carbonate component of bone mineral (bioapatite) for paleodiet reconstruction, however, were initially rejected because the biogenic values can be obscured by diagenesis (Nelson et al. 1986; Schoeninger and Deniro 1982a; Schoeninger and Deniro 1982b; Schoeninger and Deniro 1983; Sullivan and Krueger 1981; Sullivan and Krueger 1983).

Subsequent research on bioapatite in bones and teeth suggested that diagenetic contaminants and exogenous carbonates could be successfully removed by pretreatment in many samples (Garvie-Lok et al. 2004; Koch et al. 1997; Krueger 1991; Lambert et al. 1990; Lee-Thorp and van der Merwe 1987; Nielsen-Marsh and Hedges 2000a; Nielsen-Marsh and Hedges 2000b; Sillen 1989; Sillen et al. 1989; Yoder and Bartelink 2010). Pretreatment methods that have been used on bioapatite include heating a sample in an oxygen atmosphere in specific steps to separate CO^2 fractions from different sources (Haas and Banewicz 1980; Surovell 2000); fast treatment with strong acids (Hedges et al. 1995); and treatment with weak acids (Garvie-Lok et al. 2004; Yoder and Bartelink 2010). The apparent success of pretreatment methods for stable carbon isotope analysis of bioapatite led to a common practice of incorporating the analysis as a

complement to stable isotope analysis of archaeological bone collagen, thus providing an additional measure of dietary composition (Beasley et al. 2013; Kellner and Schoeninger 2007; Lee-Thorp and Sponheimer 2003a; Wright and Schwarcz 1996). For bioapatite $\delta^{13}C$, enamel is considered the gold standard for pre-Quaternary research but recent studies have shown that bone can be as reliable as enamel for samples from the past 40,000 years (Zazzo 2014). Mineral alteration (Schoeninger et al. 2003), rare earth element incorporation (Kohn et al. 1999), comparisons between the carbonate and phosphate fractions (Kolodny et al. 1983; Longinelli 1966; Longinelli 1984; Longinelli and Nuti 1973), and oxide additions during fossilization indicate a greater potential for isotopic alteration to the oxygen values in enamel ($\delta^{18}O_{en}$) than previously appreciated (Jacques et al. 2008), so the debate regarding diagenetic alteration to enamel continues.

Although tooth enamel is often assumed to be resistant to diagenesis overprinting of isotopic values (Koch et al. 1997; Lee-Thorp 2002; Wang and Cerling 1994; Zazzo et al. 2004), previous cathodoluminescence (CL), an imaging method that utilizes photon emissions to identify elements in minerals, indicate that portions of the outer layer of enamel from fossil fauna at Allia Bay, Kenya (a 3.97±0.03 MA hominin fossil locality) have altered crystal structure (Schoeninger et al. 2003) and ion microprobe data confirm the alteration of the biogenic apatite (Kohn et al. 1999). It is unclear whether changes identified by CL correspond to altered isotope ratios at the altered/unaltered boundary (Figure 3.1). It is possible that bulk $\delta^{18}O_{en}$ analyses of fossil enamel are systematically biased by ±1‰ because of the diagenetic precipitation of secondary minerals in biogenic apatite identified by ion microprobe, electron microprobe, and transmission electron microscope in some Allia Bay fossil samples (Kohn et al. 1999). Zazzo et al. (2004) found that current pretreatment methods similar to the Krueger (1991) protocol using dilute acetic acid failed to adequately remove the exogenous material and restore pristine biogenic values of $\delta^{13}C$ and $\delta^{18}O$ ratios of fossil enamel bioapatite. Jacques et al. (2008) identified alteration in Chadian

fossil enamel that altered $\delta^{13}C$ and $\delta^{18}O$ ratios towards the more positive direction by as much as +6‰ and +22‰, respectively, depending on the mass spectrometers used for analysis of traditional bulk enamel samples. Therefore, it is still necessary to evaluate enamel bioapatite samples independently of pretreatment methods for potential diagenetic contaminants. The alteration of $\delta^{18}O_{en}$ values of the Chadian fossil enamel by as much as +22‰ suggests that there is a large range of variation in the effects of diagenesis on $\delta^{18}O_{en}$ depending on the burial environment, but it is unclear what is the proximate cause of the shift of $\delta^{18}O_{en}$ values. In studies focusing on fossil tooth enamel, this is especially important because the bioapatite fraction is solely relied on as preserving biogenic meaningful values and the focus of much of the paleoenvironmental reconstructions at early hominin sites (Cerling et al. 2013; Lee-Thorp et al. 2012; Levin et al. 2015; White et al. 2009).

In this study, we interrogate further the diagenesis of fossil fauna tooth enamel, the specimens used in the previous CL and ion microprobe work, from the Allia Bay fossil locality (Kohn et al. 1999; Schoeninger et al. 2003). At Allia Bay, the fossil fauna was excavated from a single locality (Area 261-1) with good temporal resolution on the eastern shore of Lake Turkana in the Koobi Fora Region associated with *Australopithecus anamensis*, the earliest confirmed obligate hominin bipedal species (Leakey et al. 1995; Leakey et al. 1998; Wood and Leakey 2011). Area 261-1 contains material from fluvial deposits of the Lokochot Member of the Koobi Fora Formation near the base of the Moiti Tuff (Bobe 2011; Brown and McDougall 2011; Wood and Leakey 2011). The fossil material was recovered from a single excavation (give citation).

The larger aim of this project tests hypotheses regarding the link between habitat and human evolution by exploring the seasonal variation in rainfall within a "local" environment (see Chapter 4). This study uses fossil Giraffidae, Elephantidae, and Deinotheriidae enamel fragments to characterize diagenesis in tooth enamel identified by the previous CL and ion microprobe analyses. This study is the first to apply secondary ion mass spectrometry (SIMS) analysis to

fossil fauna to address issues of diagenesis of $\delta^{18}O_{en}$ values. The high-resolution sampling capability of SIMS, with analysis spots 10-13 µm *in situ* (Valley and Kita 2009), provide a new scale of analysis, which can collect data from zones of mineral alteration identified by CL and microprobe as well as unaltered mineral structure zones. Traditional isotopic mass spectrometers used in previous diagenesis studies of $\delta^{13}C$ and $\delta^{18}O$ values (Jacques et al. 2008; Zazzo 2014), cannot serial sample at a high-resolution compared to the SIMS capability. By conducting SIMS analyses on fossil fauna enamel we investigate if $\delta^{18}O_{en}$ values are diagenetically altered in regions of mineral structure change. Or conversely, do $\delta^{18}O_{en}$ values maintain a biogenic signature in the zones of mineral structure change.

Fossilization and diagenesis of biological material

The fossilization process of bones and teeth has long been studied and is recognized as a complex process (Lee-Thorp 2000; Lee-Thorp and Sponheimer 2003b; Lee-Thorp and van der Merwe 1991; Schoeninger and Deniro 1982a). In the case of bone and tooth fossilization, there are two basic types of diagenesis that are recognized: the addition of new material to an existing matrix and the alteration of the existing matrix itself (Krueger 1991). Electron microprobe and scanning electron microscope analysis shows fossil mammalian tooth enamel having large amounts of secondary Fe-, Si-, Mn-, and Al-bearing oxides, fluorine and sulphur contamination, and Ca, P, Cl. Na, and Mg depletion (Jacques et al. 2008; Kohn et al. 1999). In enamel, the most common material added is a simple carbonate (typically calcite, $CaCO_3$), carbonate ions affixed on bioapatite surfaces, or carbonate ions substituting at hydroxyl and phosphate sites within the hydroxyapatite (Krueger 1991; Sponheimer and Lee-Thorp 1999). The incorporation of carbonate in apatite results in increased solubility because of the reduced crystal size resulting in relatively increased surface area with an increase in strain on the bonds (LeGeros and Tung 1983; LeGeros et al. 1971; Sillen and LeGeros 1991). In contrast, the incorporation of fluorine ions in apatite

results in decreased solubility as a result of increased crystallinity and relatively decreased surface area (LeGeros 1981; Moreno et al. 1977; Sillen and LeGeros 1991).

The particular incorporation of diagenetic material is highly dependent of site-specific characteristics of the soil matrix and groundwater. In the Rift Valley, the East African Plio-Pleistocene fossils are typically characterized by relatively large crystal size and high levels of fluoride content because of the alkaline nature of the depositional environment (Sillen 1986). For the South African Pleistocene fossils largely found in karstic cave deposits, the fossils are characterized by saturation with carbonate and the deposition of calcite with low levels of fluoride (Sillen and LeGeros 1991). Other carbonate based material, such as corals, incorporate a considerable amount of Rare Earth Elements (REEs) with a preference for light elements resulting from the reaction of the carbonates with groundwater (Scherer and Seitz 1980). The mineral changes observed during diagenesis are often suggested to occur early in the fossilization process, after which saturation and stabilization occurs, with, presumably, little notable change occurring subsequently (Sponheimer and Lee-Thorp 1999). But the timing of diagenetic alteration is open to significant debate and outside the scope of this paper.

High-resolution $\delta^{18}O_{en}$ values generated by SIMS

Recent studies in geochemistry and cosmochemistry that serial sample small geologic zoned material (i.e., single crystalline structures) has used a large radius secondary ionization mass spectrometer (SIMS) technique to evaluate high-resolution patterns of zoned isotope differences. SIMS techniques use far less material compared with techniques that rely on mechanically shaved/drilled powder for analysis using conventional acid-digestion and measurement by CO^2-gas source mass spectrometry (Kita et al. 2009; Valley and Kita 2009). When sequential measurements are made along the growth axis of materials with chronological depositional growth (i.e., otoliths and speleothems), a spatial resolution of approximately 10-13

μm is routinely achievable for detecting zoned isotopic differences even for samples of uncertain homogeneity (Kolodny et al. 2003; Orland et al. 2009; Treble et al. 2007; Valley et al. 1998; Weidel et al. 2007).

For enamel, diagenesis studies of $\delta^{18}O_{en}$ and $\delta^{13}C_{en}$ values generated by traditional bulk sampling require a larger quantity of powder enamel (1-5 mg; Jacques et al. 2008; Zazzo et al. 2014) that would aggregate material from unaltered and altered zones identified by CL (Schoeninger et al. 2003). The primary beam (^{+}Cs) of the SIMS analyzes a pit in samples only about ~2-μm-deep and 10-μm-wide, so the sample area can cross altered/unaltered boundaries to address the issue of possible diagenesis to $\delta^{18}O_{en}$ values in enamel where the mineral structure has changed. Unfortunately, the CL method previously used by Schoeninger et al. (2003) to identify zones of mineral structure alteration burns the polished surface of an enamel mount during analysis. This results in the sample mounts needing to be repolished prior to SIMS analysis, which effectively removes the surfaces (greater than ~2-μm) that the CL imaged for diagenesis. In order to use SIMS analysis for accessing diagenesis in $\delta^{18}O_{en}$, an imaging technique must be used to 1) identify zones of potential diagenesis similar to CL, and 2) not require extra sample preparation (i.e., further polishing) after the imaging is completed prior to SIMS analysis.

Fluorescence in Teeth

During the 20th century there have been many suggestions as to the cause of natural fluorescence in teeth, including suggestions that it is due to the mineral phase of teeth (Glasser and Fonda 1938), organic compounds (Hartles and Leaver 1953), pyrimidine-containing moieties (Hartles and Leaver 1953), the inorganic complexes of some organic substances or combination of amino acid, peptide, or pyrimidine (Armstrong 1963), calcified proteins in tyrosine or tryptophan (Mancewicz and Hoerman 1964), not tryptophan but some unspecified organic compound (Spitzer and Ten Bosch 1976), and that fluorescence is not due to a single compound

but is due to the interaction between different fluorophores (mineral or organic substances that absorb light at a specific wavelength and re-emit it with a lower energy that is shifted to a longer wavelength) within the dental tissue (Hefferren et al. 1971). The fluorescent properties of teeth have been used as a non-invasive diagnostic way of detecting dental caries (Garcia-Herraiz et al. 2012; Hall et al. 1970; Horibe et al. 1974). Subsequent enamel research in dentistry using fluorescent properties of teeth has focused on the effects of bleaching treatments to enamel and the resulting structural changes to teeth (Götz et al. 2007).

Most minerals do not fluoresce and those that do (only about 15%) usually fluoresce when specific impurities, known as "activators", are present within the mineral (Valeur and Berberan-Santos 2012). Fluorescence can also be caused by crystal structure defects or organic impurities, but which can occur as a result of mineral exchange and interaction with groundwater during the fossilization process in teeth and bones. A fluorescent activator in a mineral is typically a metal cation such as tungsten, molybdenum, lead, boron, titanium, manganese, uranium, and chromium or trace and REEs such as samarium, europium, terbium, dysprosium, and yttrium (Valeur and Berberan-Santos 2012). The presence of certain metallic ions will alter the intensity of fluorescence such as iron or copper that decreases fluorescence or aluminum which depending on the bond will either quench or increase fluorescence (McGarry and Baker 2000). Fluorescence intensity will also increase with increasing pH (Coble 1996; Senesi et al. 1991). For the purpose of this study, it is presumed that as calcite is precipitated in tooth enamel during the fossilization process, that the interaction observed during calcite crystallization in speleothems would be similar to the recrystallization of calcite in enamel during groundwater interaction in the post-depositional environment.

Imaging Fossil Teeth to Identify Diagenesis

Confocal laser fluorescence microscopy (CLFM) is a microscopic technique that produces an image with information about the structure of a material in question because it delineates the fluoresced region (i.e., the spatial distribution of a molecule of interest). Confocal laser microscopy has long been used to obtain histotomographic images that can provide highly sensitive evidence of structural changes within hard tissue such as teeth (Duschner et al. 2000; Götz et al. 2007). The system produces fluorescent excitation at three excitation wavelengths to identify fluorescence at the following intensities: 488-nm for green fluorophores, 568-nm for red fluorophores, and 647-nm for far-red fluorophores.

Two initial tests were performed on modern and fossil teeth using the CLFM to confirm its usefulness in assessing enamel altered zones: 1) comparing non-destructive imaging methods (CLFM and scanning electron microscope, SEM) to CL images, and 2) using CLFM to image modern and fossil enamel. A suid fossil sample from Allia Bay was imaged by CL, scanning electron microscope (SEM), and CLFM (Figure 3.2). The CL image identified an altered area in the enamel, but the SEM image did not identify any features of mineral structure change. The CLFM image of the same location identified that same altered zone identified by CL with additional detail of unknown origins (i.e., it could be biogenic or diagenetic).

The success of identifying zoned alteration in the fossil enamel that was similar to the CL image initiated the second test to compare a modern and fossil enamel fragment to determine if the fluorescence identified by CLFM was due to the properties of enamel or diagenetic inclusions in the mineral structure. During enamel deposition, ameloblast cells experience cyclic variations during their secretion process that lead to the formation of incremental features, such as cross-striations, Retzius lines (brown striae of Retzius), perikymata, and laminations that remain visible in enamel (Boyde et al. 1988; Dean 1987; Gustafson and Gustafson 1967; Hillson 2005; Tafforeau et al. 2007). The modern enamel imaged by CLFM does not fluoresce any of these

enamel features. However, in the fossil enamel, incremental features in the form of crystalline rod-like structures and lines are illuminated in the less intense fluoresced regions, while the most intensely fluoresced regions have these incremental morphological features obscured by fluorophores. This is likely because precipitation of inclusions and recrystallization of hydroxyapatite with mineral inclusions is occurring along the incremental features. The most intense fluoresced regions where morphological features are obscured are likely indicating the most altered regions in the apatite matrix. In regions where there is intense fluorescence of green fluorophores, the red fluorophores are also most intense in the same zone while any morphological features highlighted by the green fluorophores are decreased in red fluorophores with a quenching of the fluorescence. Similarly, the far-red fluorophores are only emitted in the most intense regions indicated by the red and green fluorophores, with none of the incremental morphological features fluoresced at all (Figure 3.3). Together, the three wavelength excitation lasers contribute information about the most altered regions of enamel by the inclusion of mineral structure alteration.

It is important to note that the fluorescence in the fossil enamel appears to be a stable signal within the teeth lacking loss of the fluorescence signal days after repeated viewing. For the fossil teeth confocal images, the brightest fluorescence is observed with the 488 nm laser and is thought to be evidence of organic matter or REEs inclusions from the calcite precipitation during the fossilization process similar to the banding observed in speleothems at that excitation wavelength. The green fluorophores are most intensely emitted along the outer edges of the enamel (i.e., the surface of the tooth and at the dentine-enamel junction, DEJ) and along cracks in the enamel. The cracks exhibit varying degrees of fluorescence, likely associated to when the post-mortem crack occurred in relation to the groundwater interaction.

Models of diagenesis: Expectations for SIMS and CLFM analyses

If intra-tooth isotope ratios follow a smooth curve and no change in the pattern occurs at the altered/unaltered boundary identified by CLFM, then alteration of the $\delta^{18}O$ values is unlikely a result of mineral structure changes. However, if zoned isotopic differences are detected and the changes between zones correspond to altered/unaltered boundaries identified by CLFM, then it is likely there is post-burial alteration and only unaltered regions should be used for paleoenvironment reconstructions at Allia Bay. Since the CLFM images captures green, red, and far-red fluorophores, if a difference in $\delta^{18}O$ values occurs at an alteration boundary identified by one laser-line but not another, this might help identify the cause of mineral structure change altering the $\delta^{18}O$ values.

Materials and Methods

Modern Sample

Although the SIMS instrument has been applied to biological materials that exhibit periodic growth to identify zoned isotopic patterns (i.e., otoliths), there is currently only a single study on modern woodrats (Blumenthal et al. 2014) applying the SIMS method to enamel and no prior studies have applied the method to fossil fauna. Blumenthal et al. (2014) found that sampling internal enamel near the dentine along the growth axis of the tooth (i.e., from the occlusal surface to the cementum-enamel junction, CEJ) recorded $\delta^{18}O$ seasonal data. However, as the aim of this diagenesis study is to focus on fossil enamel, a modern unaltered sample is necessary to understand the relationship between SIMS generated $\delta^{18}O_{en}$ and CLFM images identifying mineral structure change. To ensure that the high-resolution data generated by the SIMS will track seasonal precipitation patterns in large bodied herbivores when sample transects are placed transversally to the growth axis for future paleoenvironmental studies at Allia Bay, a modern fauna sample of varied diet and water dependency is a necessary control sample.

Currently, as well as when *Au. anamensis* occupied the Turkana Basin, the Omo River provides the most important water source for the lake and fluvial system in the region and has consistently originated in the Ethiopian Highlands (Feibel 2011; Kohn et al. 1998; Yuretich 1979). The consistent origins of the Turkana Basin water source means that a modern sample from the region will serve as an ideal modern control for identifying seasonal patterns generated by the SIMS data once the diagenetically altered analyses have been identified. Today, the known seasonal environment of the area consists of an open arid region adjacent to Lake Turkana with one rainy season that has been documented in traditional bulk $\delta^{18}O_{en}$ patterns of large bodied herbivores (Kohn et al. 1998). To test the application of SIMS in conjunction with CLFM, two modern animals, a Burchell's zebra (*Equus burchelli*) and a Grant's gazelle (*Nanger granti*) from Koobi Fora (collected in 1984 by MJS) were selected as control samples representing an obligate drinking grazer and a non-obligate drinking mixed feeder, respectively.

Fossil Sample

A total of twelve fossil samples have been analyzed by SIMS to reconstruct the paleoenvironment at Allia Bay. This study examines a total of five fossil fauna enamel fragment samples from Allia Bay representing three families (Deinotheriidae, Elephantidae, and Giraffidae) because they represented different ways that diagenesis can alter $\delta^{18}O_{en}$ patterns. These fossil samples were selected to test the question of how evidence of mineral structure change in enamel influences $\delta^{18}O_{en}$ patterns because the CLFM images indicated brightly fluoresced regions in the enamel (Figure 3.4). A transverse transect was planned for SIMS analysis with pits spaced 30-µm apart to bisect the identified fluoresced zone on two samples, Elephantidae (4901.2) and Giraffidae (4860.1). Based on the results of the two pilot samples (discussed below), spacing between analysis pits were increased from 60 to 240 µm apart in an effort to cover more area. A second parallel transverse transect was placed near the initial transect

in a non-fluoresced zone to analyze the unaltered $\delta^{18}O_{en}$ patterns that correspond to the $\delta^{18}O_{en}$ values generated in the fluoresced zone.

Sample preparation, confocal laser fluorescent microscopy (CLFM)

Each enamel fragment was bisected in a longitudinal direction (occlusal surface to root tip) and mounted, along with 4-6 grains of UWA-1 (fluorapatite standard; $\delta^{18}O = 12.70‰$, VSMOW), in polished 2.5-cm-diameter epoxy plugs. To minimize instrumental bias associated with sample position, the region of interest for SIMS analysis was placed within 5mm of the center of the plug (Kita et al. 2009; Treble et al. 2007). Confocal laser fluorescent microscopy (CLFM) was subsequently completed at the Keck Bioimaging Laboratory at UW-Madison using a Bio-Rad MRC-1024 scanning confocal microscope operated with a 40-mW three laser line imaging system. The Bio-Rad MRC-1024 confocal system uses an inverted Nikon Diaphot 200 equipped for standard widefield fluorescent, brightfield, and differential interference contrast (DIC) microscopy attached to a side-mounted scanhead, krypton/argon mixed-gas laser, interface box, and Dell PowerEdge 1800 computer with dual displays running LaserSharp 5.2. The system produces fluorescent excitation through the use of argon/krypton mixed gas laser lines: 488-nm for green fluorophores, 568-nm for red fluorophores, and 647-nm for far-red fluorophores. The fluorescent emission is directed to three highly sensitive photomultiplier tubes (PMTs) to collect emitted green, red, and far-red light. Unlike film or CCD cameras, the PMTs collect a single pixel at a time as the laser scans across the sample. Before the emitted light reaches the PMTs, however, it passes through a confocal pinhole to remove out-of-focus light and either a bandpass (BP) or longpass (LP) filter to remove unwanted wavelengths. Each sample was imaged by the 488-nm (green fluorophores), 568-nm (red fluorophores), and 647-nm (far-red fluorophores) laser lines to detect potential diagenetically altered regions. Images of enamel fluorescence were collected and processed with Image-J software to add a threshold of 85, 210, and 50 for the green, red, and far-red fluorophores, respectively, to distinguish the likely diagenetically altered areas to

bisect during SIMS analysis (Figure 3.5). A total of 24 fossil samples were prepared and CLFM imaged, but only five samples are discussed in this study because three samples met the sample criteria of a distinct fluoresced zone corresponding to a nearby non-fluoresced zone to place parallel transects and two samples represented unique forms of diagenesis discussed below (Figure 3.3).

Secondary ion mass spectrometry (SIMS)

Oxygen isotope data were acquired at the UW-Madison WiscSIMS Laboratory using a CAMECA ims-1280 high resolution, large radius multicollector ion microprobe using a ~1.9 nA primary beam of $^{133}Cs^{+}$ focused to approximately 12 to 13-µm beam-spot size (Kita et al. 2011; Kita et al. 2009; Valley and Kita 2009). The primary beam sputtered a ~2-µm-deep pit in the enamel for analyses of the secondary oxygen ions. Charging of the sample surface was compensated by a gold coat on the epoxy mount, which was applied following cleaning in deionized water and ethyl alcohol.

A total of 413 oxygen analyses were made of the 2 modern (n = 68) and 5 fossil (n = 345) fauna samples in transverse transects across the enamel fragments spaced 30-µm apart (see Appendix 3.1). Throughout the analysis sessions, 4-5 consecutive measurements of UWA-1 fluorapatite standard were analyzed before and after every 8-16 sample analyses for determination of the standard deviation of each sample analysis (Appendix 3.1). The ion microprobe instrumental mass fractionation factor (IMF = $\delta^{18}O_{measured} - \delta^{18}O_{VSMOW}$) in fluorapatite is calculated from each bracketing set of UWA-1 measurements and was typically 1.01‰. The precision of a set of bracketing standard analyses, on average equals to 0.38‰ (2 standard deviations, SD; Appendix 3.1), was used to estimate the spot-to-spot reproducibility of the enamel sample analyses. The 2SD for each bracket is the best estimate of the analytical uncertainty of individual sample analyses.

A typical secondary $^{16}O^-$ ion intensity was $2.4x10^9$ cps. The mass resolving power was 2200 and the $^{18}O^-$ and $^{16}O^-$ ions were simultaneously collected by two Faraday Cup detectors in the multicollection system. Each analysis lasted approximately 4 min, including a pre-sputtering burn through the gold coat (10 s), an automatic recentering of secondary ions in the field aperture (~60 s), and 20 cycles of 4-s integrations of oxygen ions for isotopic measurements (80 s). Detailed analytical conditions of the WiscSIMS system are described by previous workers (Valley and Kita 2009).

It is important to note that the $\delta^{18}O$ values generated from this analysis are not confidently tied to the VSMOW scale because of the range of acid-digestion $\delta^{18}O$ values accepted for the UWA-1 fluorapatite standard. The UWA-1 standard is a geological fluorapatite, while enamel is a biological hydroxyapatite ($Ca_{10}(PO_4)_6(OH)_2$) with possible ion substitutions of fluoride, chloride, or carbonate. Matrix differences between fluorapatite to hydroxyapatite prohibit accurate correction of enamel to VSMOW. The SIMS primary beam sputters all the oxygen ions contained within an analysis pit, which includes PO_4, CO_3 and OH, in the enamel and we assume a fractionation occurs for "bulk oxygen ions" versus the oxygen analyzed by traditional bulk enamel carbonate methods. Additionally, phosphates are more complex systems than carbonates and there is no nationally recognized standard for tooth enamel phosphate, meaning that results need to be compared with others from the site to obtain relative differences (Aubert et al. 2012; Bryant et al. 1996; Fricke and O'Neil 1996; Iacumin et al. 1996; Zazzo et al. 2004). All sample $\delta^{18}O$ values generated in this study are corrected to the UWA-1 standard and the relative variability between values is the focus of the following interpretations. Until a uniform biological apatite standard is found for SIMS analyses, interpretations of $\delta^{18}O$ values should not be related to bulk carbonate stable isotopic absolute $\delta^{18}O$ values. However, internal $\delta^{18}O$ patterns within a single tooth and the $\delta^{18}O$ differences between individuals in this study are

the focus of the subsequent diagenesis discussion. All $\delta^{18}O$ values and figures reported in this study are relative to UWA-1 ($\delta^{18}O = 12.7‰$).

Sample pit quality evaluation

To ensure only reliable $\delta^{18}O$ values are obtained from the SIMS analysis for this enamel diagenesis study, two sample quality checks were employed to each sample pit analysis: SEM pit imaging and relative yield analysis. After oxygen isotope analysis at WiscSIMS, every analysis pit (standards and samples) were examined with SEM to ensure each analysis pit was a uniform "regular" pit with reliable $\delta^{18}O$ values generated. Pits that are classified as "irregular" were eliminated from the diagenesis investigation because irregular pit margins might alter $\delta^{18}O$ values due to an irregularity with the primary beam or a diagenetic inclusion in the enamel. Pits should be uniform because if the pit exposed a "pocket" or "crack" of other material within the enamel, then there might be excess oxygen ions released by the primary beam which would alter the $\delta^{18}O$ values (Figure 3.6). A total of 18 pits were excluded based on the SEM sample quality check.

To check the performance of the primary beam (i.e., the efficiency of the beam sputtering oxygen ions) during an analysis session, the oxygen ion yield for each analysis was analyzed as a relative yield throughout an entire analytical session. The relative yield of each sample is compared to the average yield of the bracketing standards and based on the Tukey definition of an outlier, all samples with relative yields outside the accepted range determined for the analytical session were excluded. A total of 13 pits were excluded based on the relative yield analysis sample quality check. Some of the sample pits analyzed were determined as generating unreliable $\delta^{18}O$ values based on both sample quality checks, so out of 413 enamel sample analyses a total of 386 was used for this diagenesis study.

Results and Discussion

The results of each line transect in a sample are presented in Table 3.1. When the $\delta^{18}O_{en}$ values that are non-biogenic are removed for each transect line, the range difference between the biogenic values versus including the non-biogenic values have a varying degree of impact to the $\Delta^{18}O$ (0 to 8.11‰) for a single transect line. Most pits determined to be non-biogenic have values relatively similar to the biogenic values of $\delta^{18}O_{en}$ and the mean for a line transect does not change significantly. However, in an extreme case (Giraffidae 4859b3, discussed below) $\delta^{18}O_{en}$ values can shift by ~10‰, which would result in a significant change for the paleoenvironment interpretation. In the following sections each sample will be discussed in terms of how diagenetic alterations were determined by the pattern of $\delta^{18}O_{en}$ and the corresponding CLFM images.

Modern Koobi Fora fauna: SIMS and recording seasonal shifts in $\delta^{18}O_{en}$

Figure 3.7 plots the $\delta^{18}O_{en}$ values for the modern Koobi Fora fauna SIMS transects. Neither the zebra nor the Grant's gazelle had any fluoresced zones in the enamel identified by any of the CLFM laser lines. Both modern species exhibit a continuous smooth curve pattern in $\delta^{18}O_{en}$ values across the enamel from the outer edge to the DEJ. The pattern is reminiscent of a sinusoidal curve oscillating between wet and dry seasons that has been observed in other serial sampling of $\delta^{18}O_{en}$ values from modern fauna in the Koobi Fora region (Kohn et al. 1998). The zebra, a grazing obligate drinker, shows less variation across the SIMS analysis transect ($\Delta^{18}O_{en}$ = 2.24‰) compared to the gazelle ($\Delta^{18}O_{en}$ = 3.87‰), a mixed C_3/C_4 feeding non-obligate drinker. This would suggest that the zebra had a more constant water source available during the period recorded in the $\delta^{18}O_{en}$ values compared to the gazelle. Since the gazelle obtains most of its water from the browse vegetation it consumes, the gazelle will be more subject to the changing aridity in the hot arid climate of the modern Turkana Basin resulting in the greater fluctuation in $\delta^{18}O_{en}$ values. The lack of diagenesis in the modern enamel and the expected fluctuating seasonal pattern in $\delta^{18}O_{en}$ values indicate that SIMS analysis sampling transverse transects across the enamel will

record meaningful $\delta^{18}O_{en}$ values that can be used for paleoenvironment reconstructions. A known growth rate in enamel is necessary to translate the SIMS data into meaningful seasonal patterns of rainfall amount and duration, but in the absence of a known growth rate the patterns are still meaningful for discussions of climate stability (see Chapter 4 for discussion).

CLFM images and Diagenesis

Two samples, Elephantidae (4901.2) and Giraffidae (4860.1), were analyzed by SIMS every 30-µm in two parallel line transects bisecting fluoresced zones identified by CLFM green fluorophores excited by the 488-nm laser line. The green fluorophore laser line was relied on because of its success in identifying the banding in speleothems (Orland et al. 2009). Figure 3.8 and 3.9 plot the relative $\delta^{18}O_{en}$ patterns for each transect line of 4901.2 and 4860.1 for the three laser lines. Each laser line excitation at a different wavelength causes a different emission of fluorophores which are exhibited by different fluorescence patterns for each transect laser line images. In some case the fluoresced zone occurs in all three laser line images, just two laser line images, or a single laser line will identify a possible diagenesis zone. Based on overlapping unaltered areas of enamel that represent the same $\delta^{18}O_{en}$ patterns in parallel transects, it appears that the far-red fluorophores are best at distinguishing diagenetic alteration (see Figure 10 and 11). The far-red fluorophores are the best-fit line of the three CLFM images for identifying the $\delta^{18}O_{en}$ values that do not follow the expected pattern. This is further supported by current dental research that indicates the green 488-nm laser line will excite both healthy and decayed dental tissue (McConnell et al. 2007). Bacterially infected dental tissue exhibit greater intensity fluorescence emission by the 647-nm far-red laser line compared to healthy enamel, dentine, and cementum (Buchalla 2005; Koenig et al. 1993; McConnell et al. 2007; Taubinsky et al. 2000). However, fluorescence studies in dental research most often deal with living dental tissue and the modern enamel samples from Koobi Fora exhibited no fluorescence emissions at any of the three

excitation states, so it cannot be assumed that fossil teeth will fluoresce similar to healthy dental tissue.

Changes in mineral structure that might cause fluorescence can come from a number of metals, trace elements, and REEs. The excitation laser lines used in CLFM images will cause a wide range of fluorescing emission of materials that react at the following wavelengths: green 488-nm (emission = 505-600-nm), red 568-nm (emission = 580-630-nm), and far-red (emission 665-765-nm). Identifying the specific cause of the fluorescence in fossil enamel is outside the scope of this study and will be pursued in future research. The best explanation for the current study is that mineral structure changes to fossil enamel occur in all the zones that fluoresce for each CLFM laser line, but not each laser line identifies changes that alter the $\delta^{18}O_{en}$ values. The best-fit of the far-red laser line corresponding to $\delta^{18}O_{en}$ values that have altered values from the expected pattern suggests that the minerals causing the fluorescent emissions in the far-red regions are likely the cause of the alteration. Until further research with electron microprobe analysis, far-red fluorophore zones will be considered diagenetically altered and these values will be excluded from paleoenvironment reconstructions at Allia Bay (see Chapter 4).

Once diagenesis was identified and determined to be associated with far-red fluorophores in 4901.2 and 4860.1 when analyzed with a high-resolution sampling protocol, a lower-resolution sampling was conducted on other samples to maximize coverage across the fossil assemblage. The Deinotheriidae (4857.1) sample was analyzed with SIMS pits every 240µm in a region with minimal fluorescence to maximize the pristine paleoenvironment $\delta^{18}O_{en}$ signatures (Figure 3.12). The Deinotheridae sample highlights an important example of diagenesis of values altering in the more positive and negative direction within the same sample (Figure 3.13). This suggests that as a tooth fossilizes the interaction of the outer enamel and inner enamel at the DEJ are being affected by different diagenetic factors possibly at different times as the tooth transitions from the biosphere to the geosphere.

The seemingly continuous pattern in $\delta^{18}O_{en}$ values (see Figure 3.10, 3.11, and 3.13) as the biogenic enamel transitions to zones of enamel diagenesis would suggest that isotopic overprinting is occurring during the recrystallization of the mineral structure, possibly mixing the biogenic value with the altered $\delta^{18}O$ signature of the burial environment. This means that even when values from far-red fluorophore regions are analyzed, they possibly hold important information about the post-depositional burial environment. The question remains of when during that post-depositional period does the overprinting occur of the recrystallization and change to the $\delta^{18}O$ signature. It could occur early in the fossilization process, after which saturation and stabilization occurs (Sponheimer and Lee-Thorp 1999), or it could be a continuous process that gradually changes different zones of the enamel be successive interactions over millions of years. It is possible the pattern of $\delta^{18}O_{en}$ values in the diagenetic zones record the process of alteration. A stable pattern with little change ($\Delta^{18}O$ = ~0.5‰), like the Giraffidae 4860.1, Line 2 (Figure 3.11) might indicate one recrystallization event, while gradually changing patterns with a lot of variation ($\Delta^{18}O$ = ~2.5‰), like the Elephantidae 4901.2, Line 4 (Figure 3.10), might represent successive interactions with groundwater continually causing isotopic overprinting and a gradually changing value. This is all speculation and outside the scope of this paper, but it is important to recognize the value in the non-biogenic $\delta^{18}O_{en}$ values from the diagenetically altered zones.

Diagenesis not identified by CLFM images

After it was determined that far-red fluorophores were the best indicator of diagenetic alteration to $\delta^{18}O_{en}$ values, the samples for the larger paleoenvironment study using SIMS were analyzed avoiding zones of suspected diagenesis. However, two unique patterns were observed in Giraffidae (4859b3) and Elephantidae (4908a3) where three transect lines were sampled and in each sample one line had a unique unexpected pattern (Figure 3.14 and 3.15). The Giraffidae (4859b3) Line 3 had the most altered section of enamel observed for Allia Bay fossil fauna

(Figure 3.15). Some of the values decreased in $\delta^{18}O_{en}$ by ~10‰ and instead of the diagenesis alteration occurring at the edge of the outer enamel or at the DEJ, the impacted enamel was in the center of transect across the enamel. In the case of this extreme alteration observed in the $\delta^{18}O_{en}$ values, there was no fluorescent zone in the corresponding CLFM region. Instead, when the gold coat was removed for post-CLFM analysis, an altered region in the internal enamel was observed by transmitted light microscopy. This is the only sample that exhibited such an alteration and caused an excess of oxygen ions sputtered by the primary beam because the relative yield indicated they were outliers. The SEM analysis of the pits indicated the area was different from biogenic enamel because the pits in the area illuminated by transmitted light microscopy had irregular pits. It is unknown what the cause of this illuminated area is in the enamel, but it did significantly alter the $\delta^{18}O_{en}$ values.

The Elephantidae (4908a3) sample is another example of unexpected change in the $\delta^{18}O_{en}$ pattern that did not occur in a fluoresced zone on enamel. In the Line 1, there is a distinct decrease in the $\delta^{18}O_{en}$ values over 30 µm of 1.4‰, followed by a sharp increase in values in a diagenetically altered region near the DEJ (Figure 3.15). This was a more sudden change in the $\delta^{18}O$ value than observed in any other transect that was in a non-fluoresced zone. Sharp shifts by that degree in the $\delta^{18}O_{en}$ over a short distance is only observed in areas determined to be diagenetically altered. Additionally, the transect does not follow the expected pattern of the other two transects in the enamel fragment, supporting the interpretation that some unknown cause that does not fluoresce is altering the $\delta^{18}O_{en}$ values along the transect. The Giraffidae and Elephantidae samples with evidence of diagenesis that is not identified by the CLFM images, highlights the complexity of diagenesis in tooth enamel and that caution in interpreting the paleoenvironment at hominin sites is necessary. It is critical to evaluate enamel samples for the potential of diagenetic alteration to ensure biogenic values are generated.

Conclusion

This study used CLFM images to identify diagenesis in tooth enamel suggesting that it is a valid method for pre-screening enamel samples for high-resolution SIMS analysis. However, further testing is needed to determine what causes the fluorescing in fossil enamel with the different laser lines. The inclusion excited by the far-red laser line provides the best approximation for what is causing the most significant diagenetic alteration to $\delta^{18}O_{en}$ values in the Allia Bay samples. The analysis of the modern Koobi Fora samples indicate that seasonal patterns of the $\delta^{18}O$ variation are recorded in the enamel in the transverse direction of enamel deposition and can be used to for environment reconstructions. If fluoresced regions in enamel are avoided during SIMS $\delta^{18}O$ analysis, then researchers are most likely to generate valuable high-resolution seasonal records of $\delta^{18}O_{en}$ from fossil fauna at hominin sites. Seasonality has been implicated as a key factor in the evolution of humans (Foley 1993; Kingston 2005; Moore 1996; Nelson 2005; Potts 1998; Reed and Fish 2005). By generating high-resolution $\delta^{18}O_{en}$ data from fossil fauna, SIMS analyses will offer a new scale of analysis from which we can estimate the levels of seasonality at a biological time scale, rather than a geologic time scale.

Acknowledgements

This chapter is currently being prepared for submission for publication of the material with co-authors Margaret J. Schoeninger, Ian Orland, and John Valley. The dissertation author was the primary investigator and author of this material.

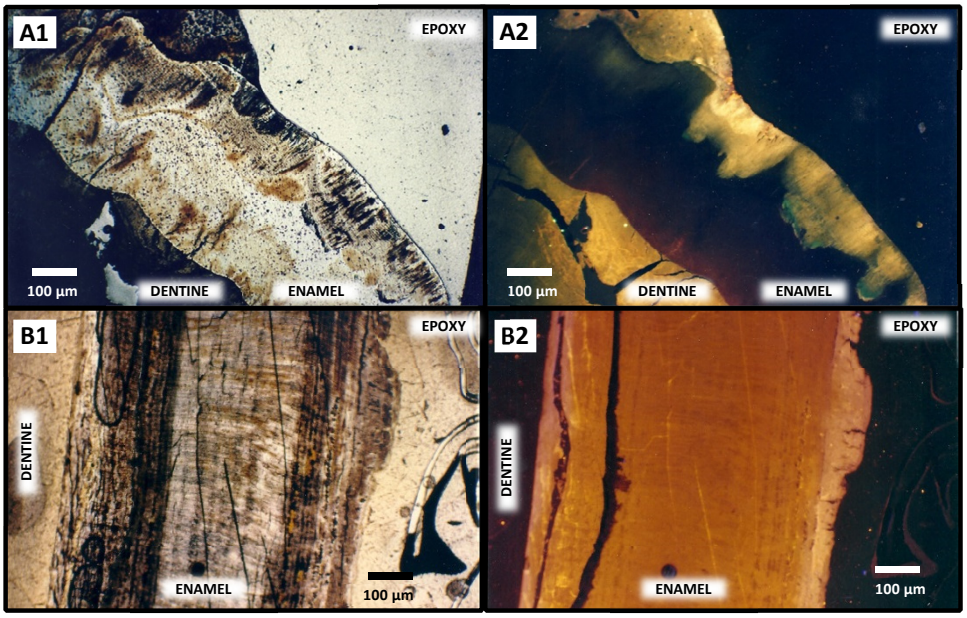

Figure 3.1: Transmitted light and cathodoluminescence images of enamel. Two examples of transmitted light (**1**) and cathodoluminescence (**2**) images from a (**A**) Suidae (4880.3) and (**B**) Hippopotamidae (4894a) sample from Allia Bay (Schoeninger et al. 2003). In the cathodoluminescence image (**A2**), the dark area of enamel is unaltered and the yellow area of enamel represents mineral structure changes from manganese inclusions. However, in some fossil fauna enamel the alteration completely changes the enamel (**B2**), which for the hippo is due to silica-bearing minerals (bright orange alteration).
[photos courtesy of Margaret Schoeninger]

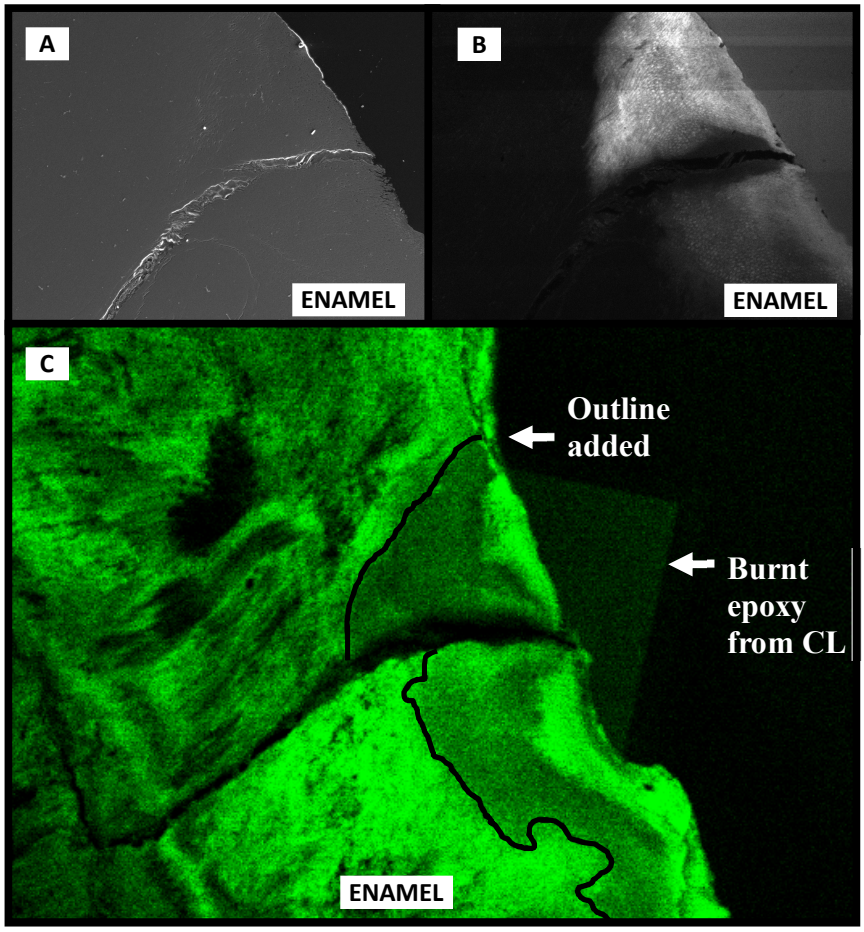

Figure 3.2: Comparison of three imaging methods of a fossil Suidae sample from Allia Bay. (**A**) The SEM image does not identify any potential diagenesis in the enamel. (**B**) The CL image identifies an altered area in the enamel, but it burns the surface of the sample mount requiring further polishing prior to SIMS analysis. (**C**) The CLFM image of a larger area of enamel. The same altered area identified by CL is delineated in the CLFM image (outlined in black line) along with additional detail of unknown origins (i.e., it could be biogenic or diagenetic). [Image C appears pixelated because the sample was not polished for SIMS analysis, this was a test sample.]

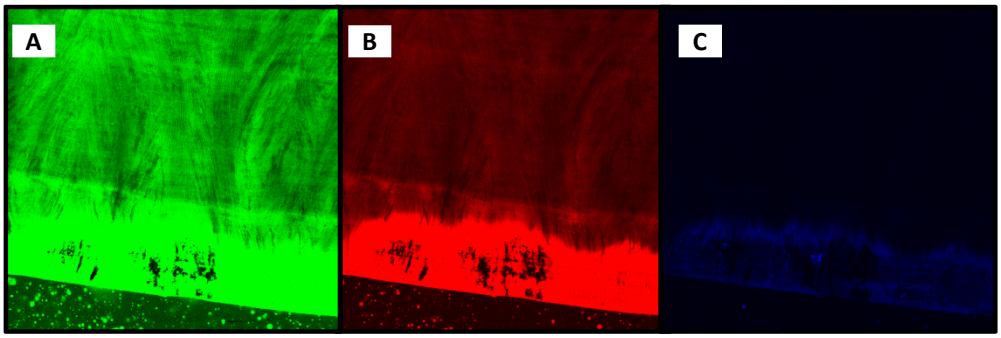

Figure 3.3: Comparison of CLFM three laser line images. The Bio-Rad MRC-1024 confocal system (CLFM) produces fluorescent excitation through the use of argon/krypton mixed gas laser lines: (**A**) 488-nm for green fluorophores, (**B**) 568-nm for red fluorophores, and (**C**) 647-nm for far-red fluorophores.

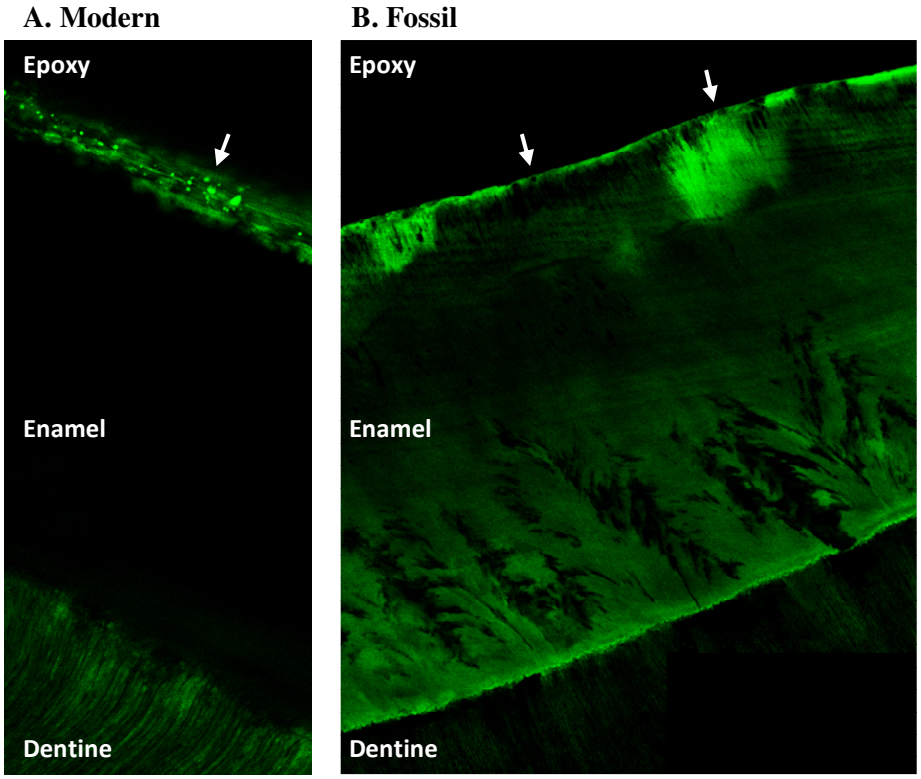

Figure 3.4: Modern and fossil enamel CLFM green fluorophore images. An example of CLFM 488-nm (green fluorophore) laser line images of a modern and fossil tooth sample used to select SIMS analysis transect lines (white arrows).
[Sample: (**A**) Zebra 2142 and (**B**) Elephantidae 4901.2]

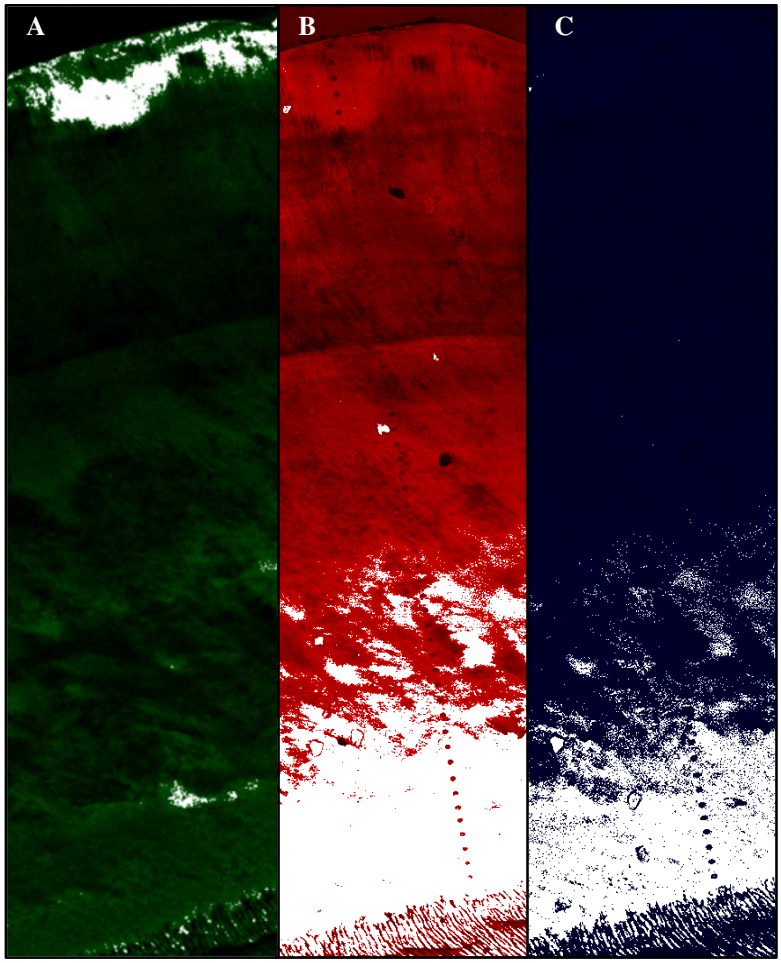

Figure 3.5: CLFM laser line images of a SIMS transect. An example of a CLFM image of the (**A**) 488-nm (green fluorophores), (**B**) 568-nm (red fluorophores), and (**C**) 647-nm (far-red fluorophores) laser lines to detect potential diagenetically altered regions. Each image is post-processed with Image-J software to add a threshold of 85, 210, and 50 for the green, red, and far-red fluorophores, respectively. The green fluorophores image (**A**) is pre-SIMS analysis used to determine the transect of interest, while the red (**B**) and far-red (**C**) fluorophores images are post-SIMS analysis and the analysis pits can be identified.
[Sample: Giraffidae 4860.1 (Line1)]

1. Giraffidae (4859b3)

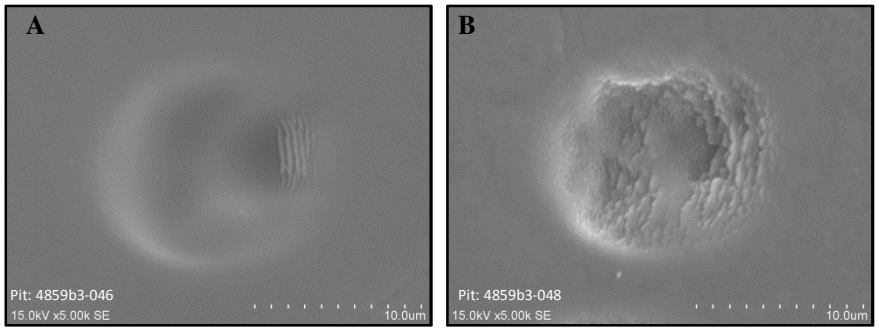

2. Giraffidae (4860.1)

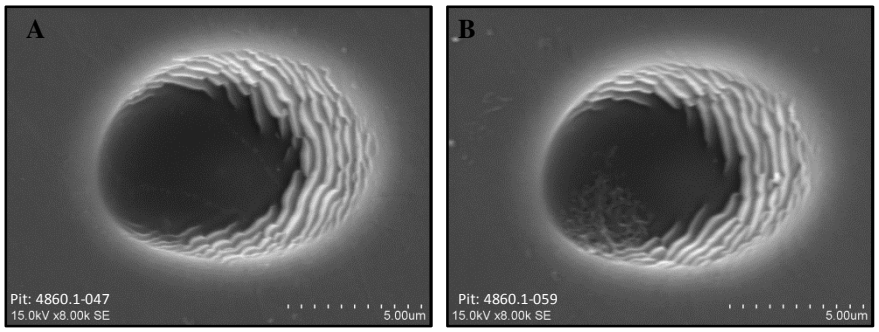

3. Elephantidae (4908a3)

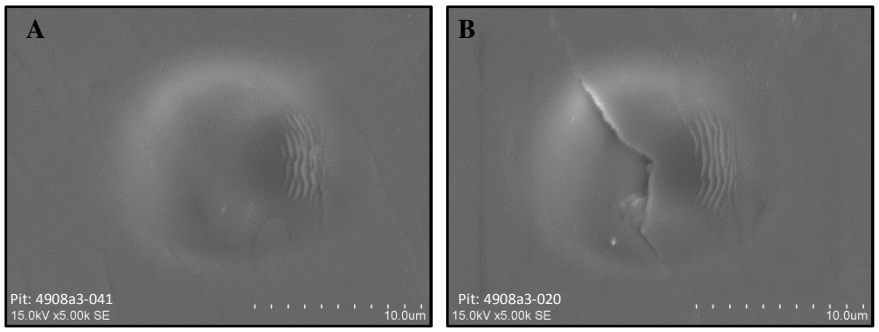

Figure 3.6: SEM images of SIMS analysis pits. Regular pits (**A**) and irregular pits (**B**) are paired for three fossil samples. The difference in pit shape between samples 1 and 3 compared to sample 2 is due to variation in the primary beam between different analytical session days, April 10, 2015 and November 11, 2014, respectively.

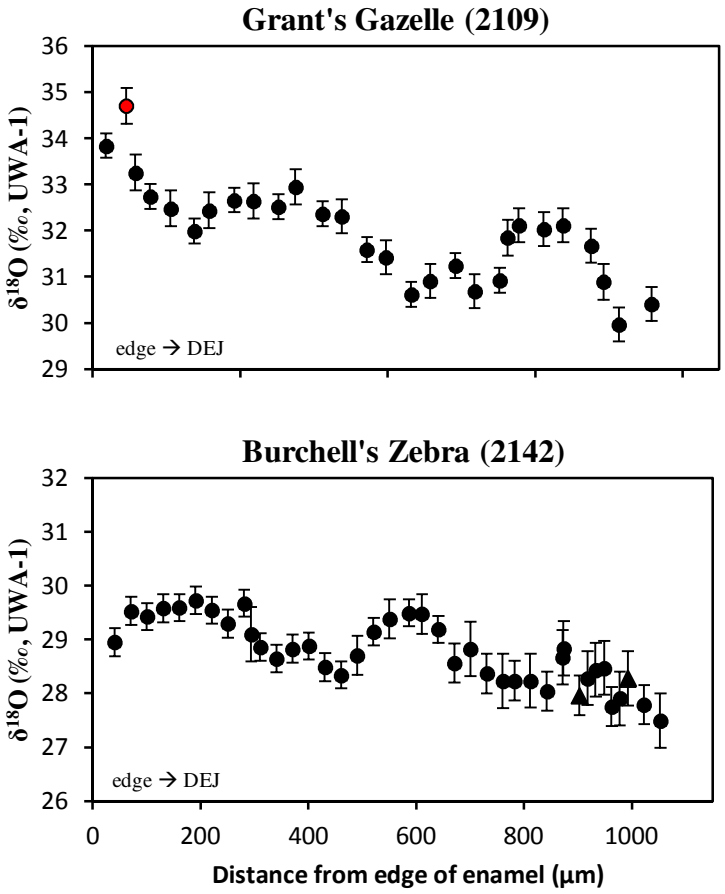

Figure 3.7: Plot of modern fauna SIMS $\delta^{18}O$ transect. The two modern samples track what appear to be changes in the $\delta^{18}O$ (with 2SD error bars) similar to sinusoidal patterns of precipitation. There is no evidence of diagenesis identified by CLFM fluorescence. Each transect line plots all SIMS analyses including, biogenic (filled in symbols) and non-biogenic values. Values were determined to be non-biogenic if the pit was irregular (determined by SEM; triangle symbol), or the relative yield analysis was an outlier (determined statistically per analytical session; red symbols).

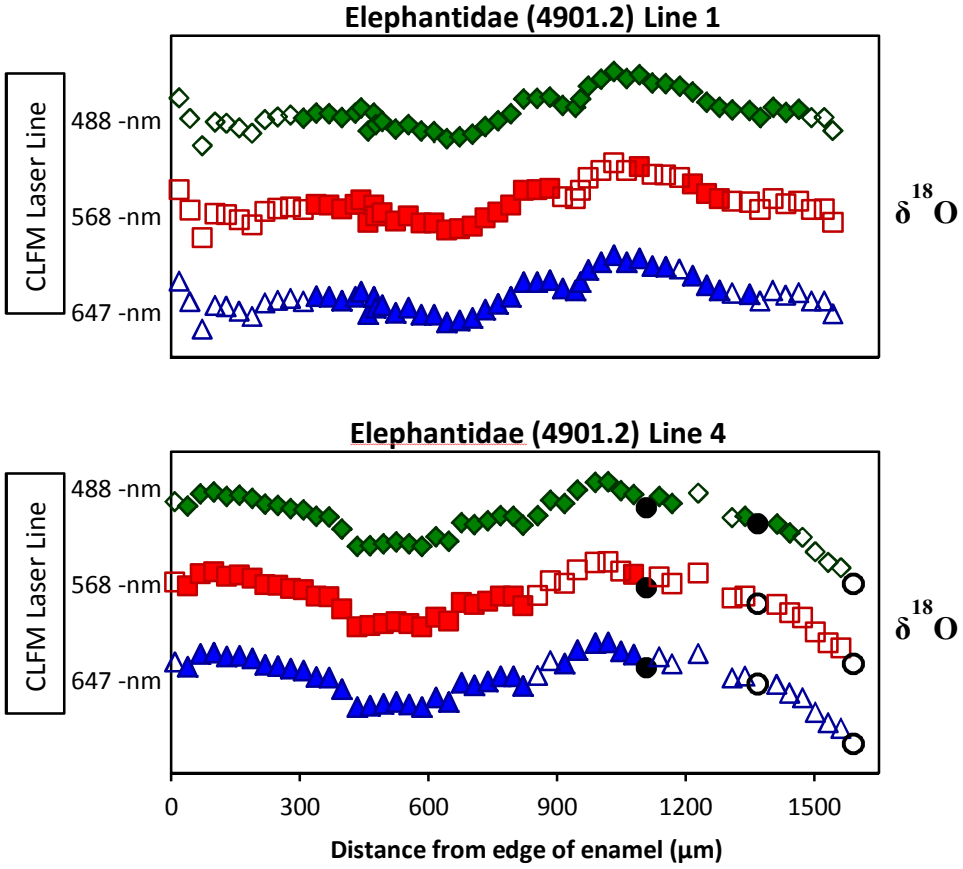

Figure 3.8: Comparison of fluorophores in SIMS transect for Elephantidae. Elephantidae (4901.2) transect lines of relative $\delta^{18}O$ values for the three laser lines produced by CLFM: green (488-nm), red (568-nm), and far-red (647-nm) fluorophores. After processing the images with Image-J software to add thresholds at a brightness of 85, 210, and 50 for the green, red, and far-red fluorophores, respectively, the open-symbols in each line represent where a SIMS pit analysis was in the fluoresced zone. The filled-symbols are SIMS pit analyses in enamel that is not suspected of diagenetic alteration. The circle-symbols are SIMS analyses that had a relative yield that was an outlier for the analytical session and is removed from the dataset.

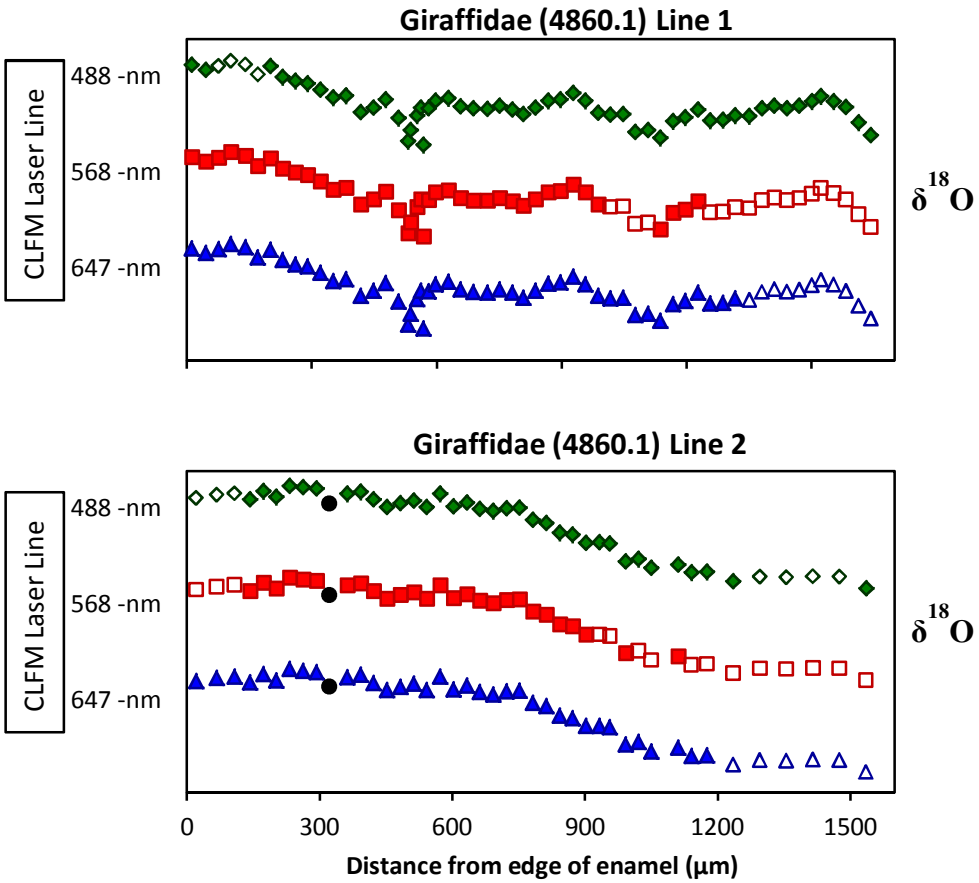

Figure 3.9: Comparison of fluorophores in SIMS transect for Giraffidae. Giraffidae (4860.1) transect lines of relative $\delta^{18}O$ values for the three laser lines produced by CLFM: green (488-nm), red (568-nm), and far-red (647-nm) fluorophores. After processing the images with Image-J software to add thresholds at a brightness of 85, 210, and 50 for the green, red, and far-red fluorophores, respectively, the open-symbols in each line represent where a SIMS pit analysis was in the fluoresced zone. The filled-symbols are SIMS pit analyses in enamel that is not suspected of diagenetic alteration. The circle-symbols are SIMS analyses that had a relative yield that was an outlier for the analytical session and is removed from the dataset.

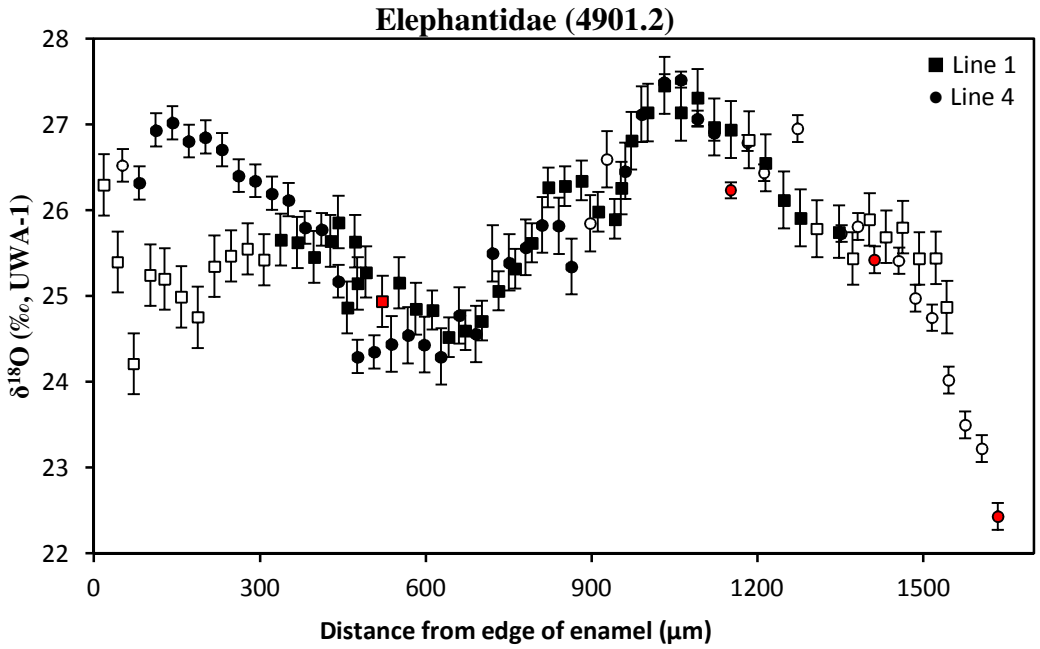

Figure 3.10: Plot of Elephantidae SIMS (4901.2) $\delta^{18}O$ transect. The Elephantidae (4901.2) sample line transect lines recorded a similar pattern of $\delta^{18}O$ (with 2SD error bars) values for the unaltered region of enamel. In the suspected altered zones identified by fluorescence, the best fit line characterizing the diagenetically altered zones, which did not follow the expected overlapping pattern of $\delta^{18}O$ values, was when the CLFM far-red fluorophores was used. Each transect line plots all SIMS analyses including, biogenic (filled in symbols) and non-biogenic values. Values were determined to be non-biogenic if they were suspected to be diagenetically altered (determined by the presence of CLFM far-far-red fluorophores; open symbols), the pit was irregular (determined by SEM; triangle symbol), and /or the relative yield analysis was an outlier (determined statistically per analytical session; red symbols).

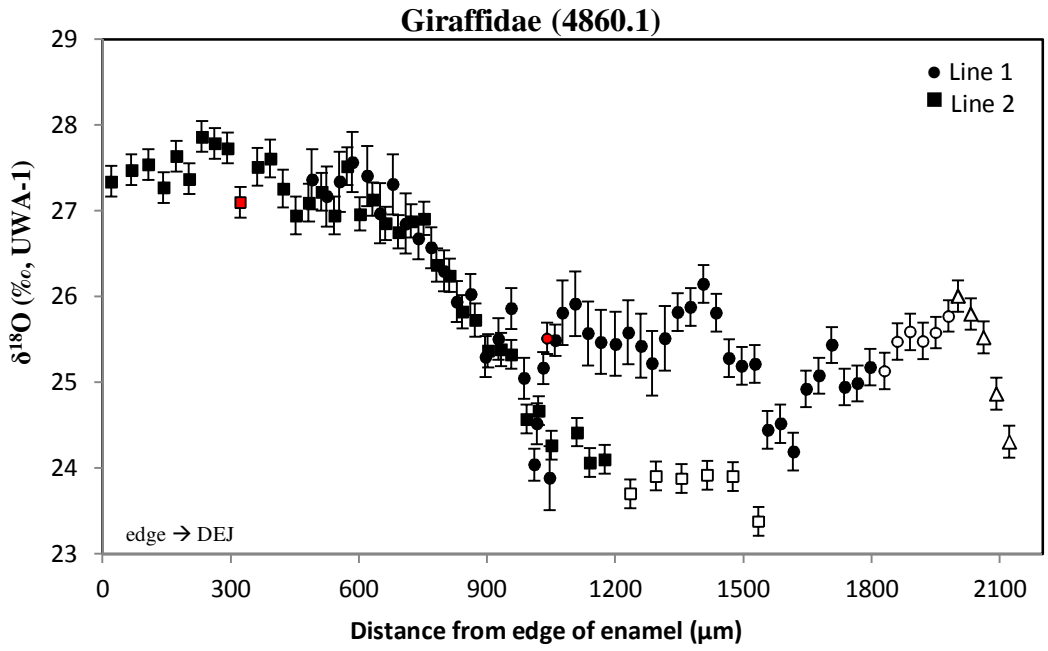

Figure 3.11: Plot of Giraffidae (4860.1) SIMS $\delta^{18}O$ transect. The Giraffidae (4860.1) sample line transect lines recorded a similar pattern of $\delta^{18}O$ (with 2SD error bars) values for the unaltered region of enamel. In the suspected altered zones identified by fluorescence, the best fit line characterizing the diagenetically altered zones, which did not follow the expected overlapping pattern of $\delta^{18}O$ values, was when the CLFM far-red fluorophores was used. Each transect line plots all SIMS analyses including, biogenic (filled in symbols) and non-biogenic values. Values were determined to be non-biogenic if they were suspected to be diagenetically altered (determined by the presence of CLFM far-far-red fluorophores; open symbols), the pit was irregular (determined by SEM; triangle symbol), and /or the relative yield analysis was an outlier (determined statistically per analytical session; red symbols).

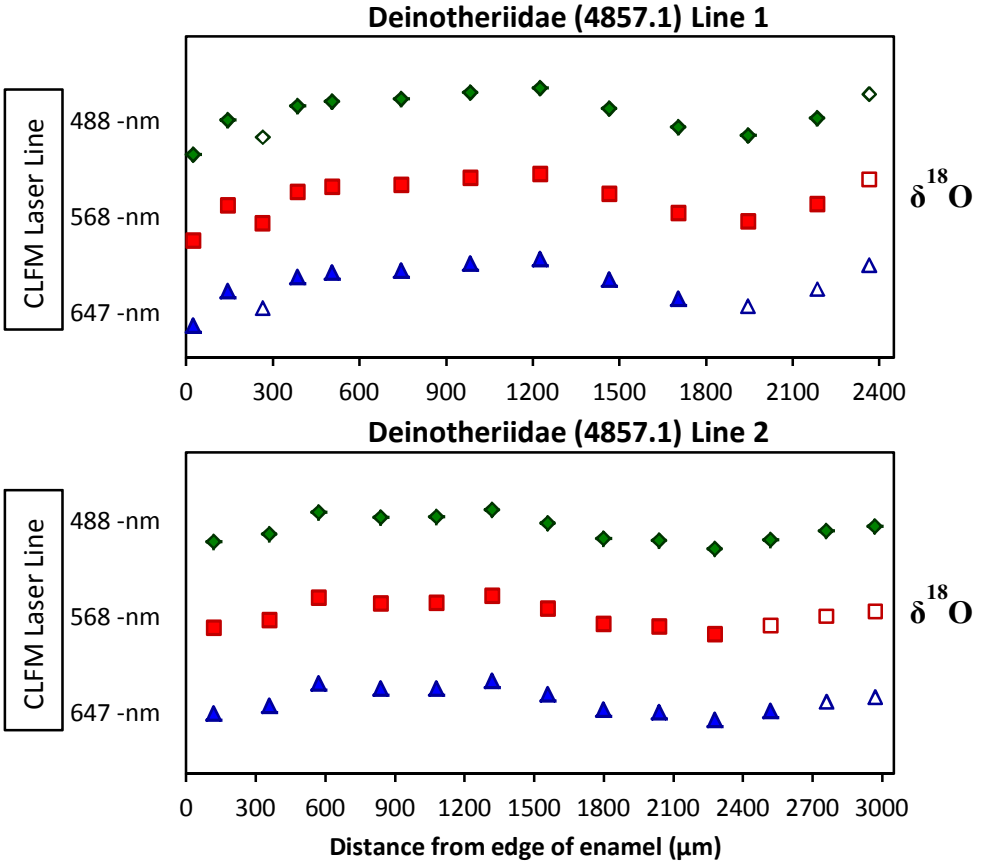

Figure 3.12: Comparison of fluorophores in SIMS transect for Deinotheriidae. Deinotheriidae (4857.1) transect lines of relative $\delta^{18}O$ values for the three laser lines produced by CLFM: green (488-nm), red (568-nm), and far-red (647-nm) fluorophores. After processing the images with Image-J software to add thresholds at a brightness of 85, 210, and 50 for the green, red, and far-red fluorophores, respectively, the open-symbols in each line represent where a SIMS pit analysis was in the fluoresced zone. The filled-symbols are SIMS pit analyses in enamel that is not suspected of diagenetic alteration.

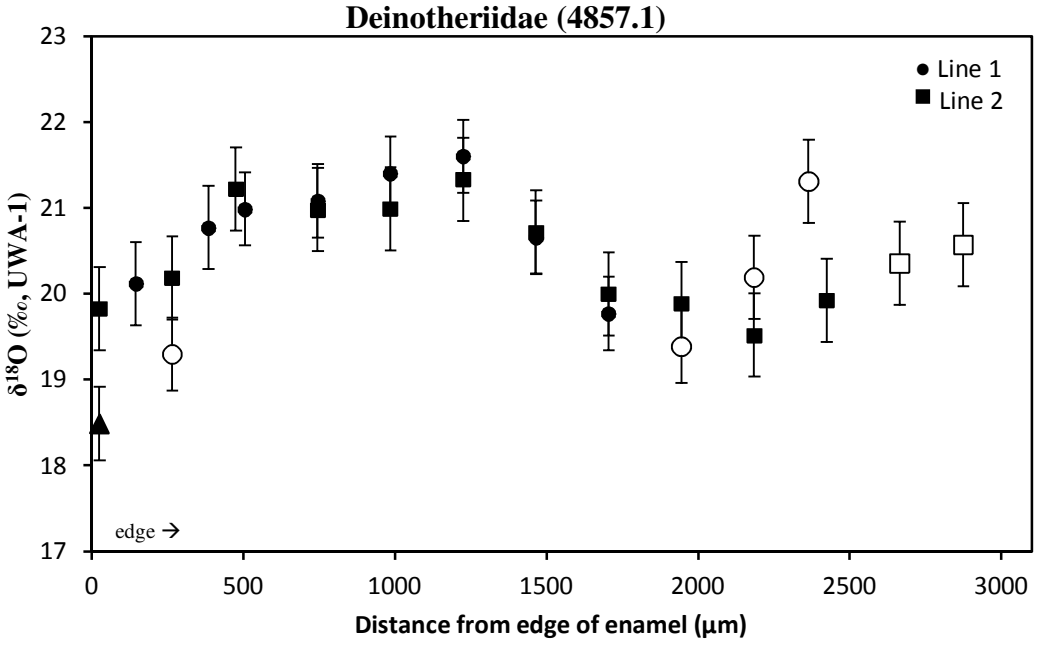

Figure 3.13: Plot of Deinotheriidae (4857.1) SIMS $\delta^{18}O$ transect. The Deinotheriidae (4857.1) sample line transect lines recorded a similar pattern of $\delta^{18}O$ (with 2SD error bars) values for the unaltered region of enamel. In the suspected altered zones identified by fluorescence, the best fit line characterizing the diagenetically altered zones, which did not follow the expected overlapping pattern of $\delta^{18}O$ values, was when the CLFM far-red fluorophores was used. Each transect line plots all SIMS analyses including, biogenic (filled symbols) and non-biogenic values. Values were determined to be non-biogenic if they were suspected to be diagenetically altered (determined by the presence of CLFM far-red fluorophores; open symbols) and/or the pit was irregular (determined by SEM; triangle symbol).

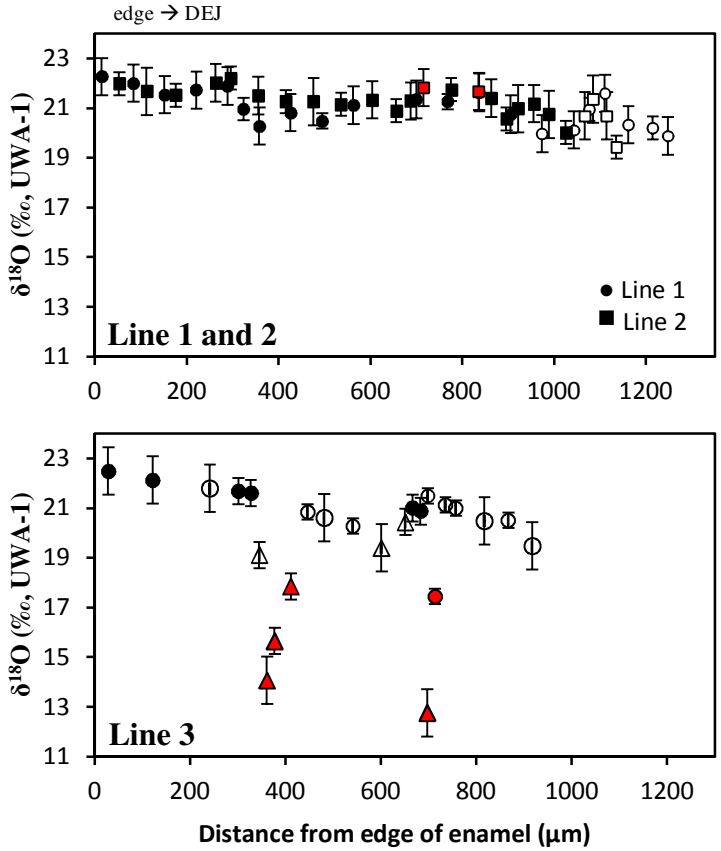

Figure 3.14: Plot of Giraffidae (4859b3) SIMS $\delta^{18}O$ transect. The Giraffidae (4859b3) had two transects (Line 1 and 2) through enamel with fluorescence only near the DEJ. However, Line 3 presented a different pattern of $\delta^{18}O$ through a highly fluoresced zone with values altered by as much as 10‰ in two areas with non-fluoresced defects (See Figure 3.x). Each transect line plots all SIMS analyses (with 2SD error bars) including, biogenic (filled in symbols) and non-biogenic values. Values were determined to be non-biogenic if they were suspected to be diagenetically altered (determined by the presence of CLFM far-red fluorophores; open symbols), the pit was irregular (determined by SEM; triangle symbol), and /or the relative yield analysis was an outlier (determined statistically per analytical session; red symbols).

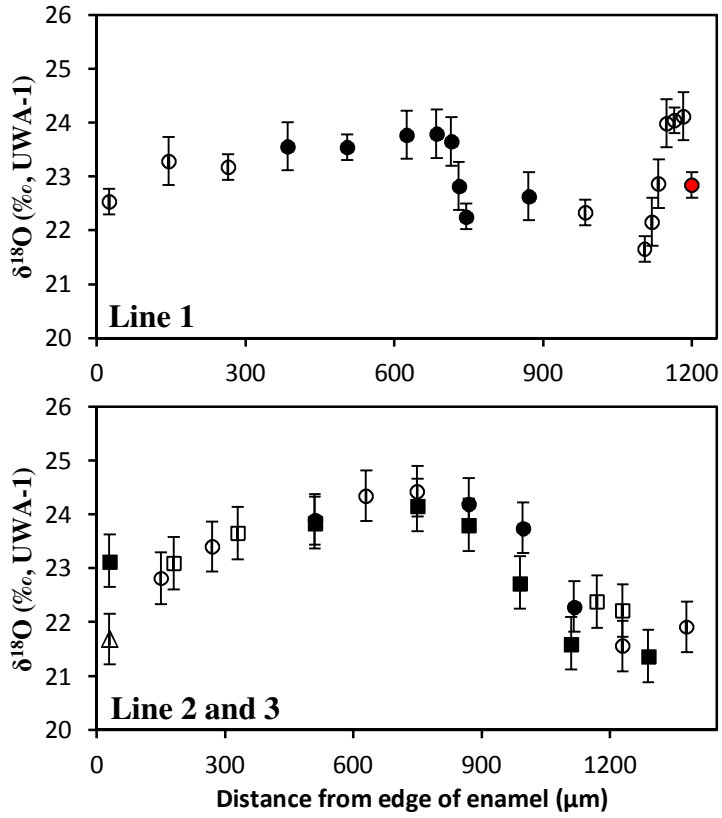

Figure 3.15: Plot of Elephantidae (4908a3) SIMS $\delta^{18}O$ transect. The Elephantidae (4908a3) presented a unique example of a different pattern of $\delta^{18}O$ (Line 1) that did not overlap with the other sample line transects (Line 2 and 3). Each transect line plots all SIMS analyses (with 2SD error bars) including, biogenic (filled in symbols) and non-biogenic values. Values were determined to be non-biogenic if they were suspected to be diagenetically altered (determined by the presence of CLFM far-red fluorophores; open symbols), the pit was irregular (determined by SEM; triangle symbol), and /or the relative yield analysis was an outlier (determined statistically per analytical session; red symbols).

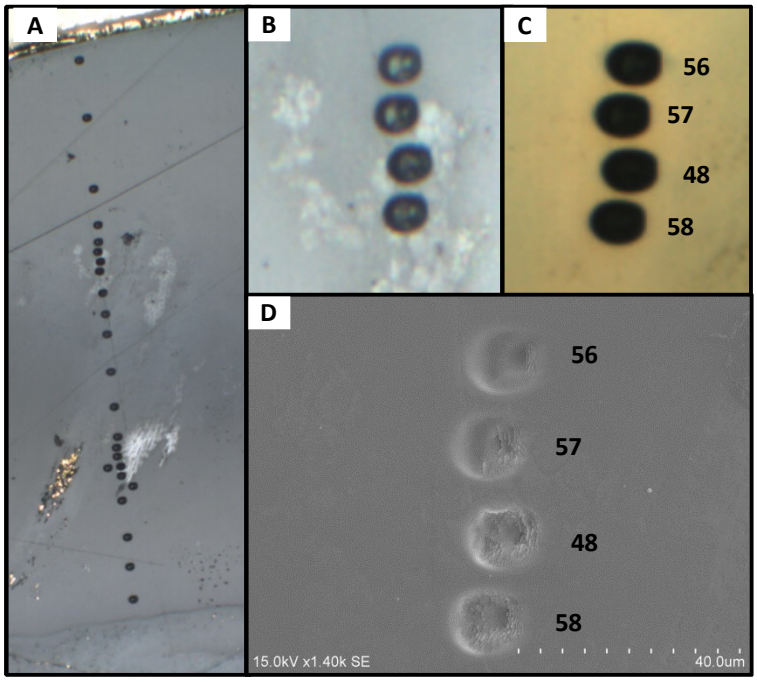

Figure 3.16: Images of unique enamel inclusion in Giraffidae (4859b3) Line 3. The Giraffidae Line 3 had SIMS pits placed in a non-fluoresced region, but appeared to be affected by diagenesis. (**A**) A transmitted light image of Line 3 post-SIMS analysis after the gold coat has been removed. It appears the line transect bisects two areas in the enamel that have been altered. (**B**) A close-up of one of the altered areas of enamel. (**C**) Same four spots (pit numbers 56, 57, 48, and 58) with the gold coat, the altered area is not visible. (**D**) SEM image of the same four spots indicating that pits 57, 48, and 58 were irregular, while pit 56 not in the altered zone is a regular SIMS pit.

Table 3.1. Comparison of SIMS $\delta^{18}O$ biogenic range compared to non-biogenic range

			$\delta^{18}O$ (‰, PDB), only biogenic values					$\delta^{18}O$ (‰, PDB), all values					Range
Sample	**Family**	**Line**	**N**	**Mean**	**Max**	**Min**	**Range**	**N**	**Mean**	**Max**	**Min**	**Range**	**Difference**
2142	Modern Zebra	1	38	28.79	29.72	27.42	2.24	40	28.75	29.72	27.49	2.24	0.00
2109	Modern Gazelle	1	27	31.87	33.84	29.96	3.87	28	31.97	34.7	29.96	4.74	0.87
4857.1	Deinotheriidae	1	8	20.80	21.60	19.77	1.83	13	20.39	21.60	18.48	3.12	1.29
4857.1	Deinotheriidae	2	11	20.42	21.33	19.52	1.82	13	20.42	21.33	19.52	1.82	0.00
4901.2	Elephantidae	1	36	25.83	27.46	24.52	2.94	56	25.69	27.46	24.21	3.25	0.31
4901.2	Elephantidae	4	33	25.88	27.52	24.29	3.23	50	25.69	27.52	22.43	5.09	1.86
4908a3	Elephantidae	1	8	23.25	23.79	22.25	1.54	19	23.1	24.12	21.65	2.47	0.93
4908a3	Elephantidae	2	4	23.54	24.21	22.29	1.92	11	23.11	24.42	21.55	2.87	0.95
4908a3	Elephantidae	3	7	22.95	24.17	21.37	2.80	11	22.91	24.17	21.37	2.80	0.00
4860.1	Giraffidae	1	47	25.19	27.07	23.38	3.68	59	25.13	27.07	23.38	3.68	0.00
4860.1	Giraffidae	2	36	26.00	27.36	23.57	3.80	43	25.63	27.36	22.88	4.48	0.68
4859b3	Giraffidae	1	14	21.28	22.26	20.27	1.99	21	20.99	22.26	19.87	2.39	0.40
4859b3	Giraffidae	2	19	21.29	22.20	20.01	2.19	25	21.21	22.20	19.41	2.79	0.60
4859b3	Giraffidae	3	6	21.62	22.48	20.86	1.62	24	19.75	22.48	12.75	9.73	8.11

Chapter 3 Appendix: Raw data of $\delta^{18}O$ measurements of apatites by SIMS (Cameca 1280)

Analysis #	Sample	Line #	Diagenesis* SEM GR	Diagenesis* CLFM RD	Diagenesis* CLFM FRD	Bias (α) A	$\delta^{18}O_{RAW}$‰ B	±2 SE C	$\delta^{18}O_{COR}$‰ D	±2 SD E	Distance from edge of enamel (µm)
Sample: 2142 (Modern Zebra) with UWA-1 (fluorapatite standard).											
UWA-1 (used as bracketing standard; $\delta^{18}O$ = 12.70‰)											
20150406@9	UWA-1 Grain 1 (G1)						23.588	0.261			
20150406@10	UWA-1 G1						23.402	0.271			
20150406@11	UWA-1 G1						23.610	0.269			
20150406@12	UWA-1 G1						23.590	0.234			
Average and ±2 SD							**23.548**	**0.195**			
Enamel											
20150406@13	2142-001	1					39.993	0.246	28.95	0.26	41
20150406@14	2142-002	1					40.577	0.250	29.53	0.26	71
20150406@15	2142-003	1					40.626	0.298	29.58	0.26	131
20150406@16	2142-004	1					40.776	0.280	29.72	0.26	191
20150406@17	2142-005	1					40.339	0.265	29.29	0.26	251
20150406@18	2142-006	1					39.899	0.240	28.86	0.26	311
20150406@19	2142-007	1					39.865	0.235	28.82	0.26	371
20150406@20	2142-008	1					39.521	0.288	28.48	0.26	431
UWA-1											
20150406@21	UWA-1 G1						23.628	0.230			
20150406@22	UWA-1 G1; Cs res 179-181						23.680	0.308			
20150406@23	UWA-1 G1						23.339	0.207			
20150406@24	UWA-1 G1						23.710	0.192			
Average and ±2 SD							**23.589**	**0.340**			
Bracket: Average and ±2 SD						**1.0107**	**23.568**	**0.261**			
Enamel											

Analysis #	Sample	Line #	Diagenesis*				Bias (α)	$\delta^{18}O_{RAW}$‰	±2 SE	$\delta^{18}O_{COR}$‰	±2 SD	Distance from edge
			SEM	CLFM								
				GR	RD	FRD	A	B	C	D	E	of enamel (µm)
20150406@25	2142-009	1						39.840	0.330	28.70	0.36	491
20150406@26	2142-010	1						40.530	0.225	29.38	0.36	551
20150406@27	2142-011	1						40.621	0.246	29.47	0.36	611
20150406@28	2142-012	1						39.703	0.320	28.56	0.36	671
20150406@29	2142-013	1						39.502	0.274	28.36	0.36	731
20150406@30	2142-014	1						39.369	0.231	28.23	0.36	783
20150406@31	2142-015	1						39.173	0.216	28.04	0.36	843
20150406@32	2142-016	1	**SEM**					39.091	0.202	27.96	0.36	903
20150406@33	2142-017	1						38.886	0.247	27.75	0.36	963
20150406@34	2142-018	1						38.921	0.244	27.79	0.36	1023
UWA-1												
20150406@35	UWA-1 G1							23.847	0.257			
20150406@36	UWA-1 G1							23.910	0.329			
20150406@37	UWA-1 G1							23.507	0.263			
20150406@38	UWA-1 G1							23.733	0.200			
Average and ±2 SD								**23.749**	**0.355**			
Bracket: Average and ±2 SD							**1.0108**	**23.669**	**0.364**			
UWA-1												
20150406@75	UWA-1 G1							23.875	0.198			
20150406@76	UWA-1 G1							23.619	0.312			
20150406@77	UWA-1 G1							23.773	0.180			
20150406@78	UWA-1 G1							23.760	0.299			
Average and ±2 SD								**23.757**	**0.211**			
Enamel												
20150406@79	2142-019	1						40.682	0.263	29.42	0.25	101
20150406@80	2142-020	1						40.850	0.271	29.59	0.25	161
20150406@81	2142-021	1						40.802	0.213	29.54	0.25	221

Analysis #	Sample	Line #	Diagenesis*				Bias (α)	$\delta^{18}O_{RAW}$‰	±2 SE	$\delta^{18}O_{COR}$‰	±2 SD	Distance from edge
			SEM	CLFM								
				GR	RD	FRD	A	B	C	D	E	of enamel (µm)
20150406@82	2142-022	1						40.930	0.305	29.67	0.25	281
20150406@83	2142-023	1						39.892	0.328	28.64	0.25	341
20150406@84	2142-024	1						40.129	0.262	28.88	0.25	401
20150406@85	2142-025	1						39.582	0.296	28.34	0.25	461
20150406@86	2142-026	1						40.398	0.189	29.14	0.25	521
20150406@87	2142-027	1						40.750	0.314	29.49	0.25	587
20150406@88	2142-028	1						40.439	0.246	29.18	0.25	641
UWA-1												
20150406@89	UWA-1 G1							23.619	0.225			
20150406@90	UWA-1 G1							23.696	0.211			
20150406@91	UWA-1 G1							23.930	0.245			
20150406@92	UWA-1 G1							23.923	0.220			
Average and ±2 SD								**23.792**	**0.317**			
Bracket: Average and ±2 SD							**1.0109**	**23.774**	**0.252**			
Enamel												
20150406@93	2142-029	1						39.969	0.299	28.82	0.50	701
20150406@94	2142-030	1						39.368	0.181	28.23	0.50	761
20150406@95	2142-031	1						39.370	0.340	28.23	0.50	812
20150406@96	2142-032	1						39.811	0.174	28.67	0.50	872
20150406@97	2142-033	1						39.575	0.265	28.43	0.50	933
20150406@98	2142-034	1	**SEM**					39.414	0.264	28.27	0.50	993
20150406@99	2142-035	1						38.620	0.317	27.49	0.50	1053
20150406@100	2142-036	1						39.977	0.247	28.83	0.50	874
20150406@101	2142-037	1						40.246	0.267	29.10	0.50	294
20150406@102	2142-038	1						39.612	0.277	28.47	0.50	949
20150406@103	2142-039	1						39.419	0.192	28.28	0.50	918
20150406@104	2142-040	1						39.037	0.220	27.90	0.50	978

Analysis #	Sample	Line #	Diagenesis* SEM	CLFM		Bias (α)	$\delta^{18}O_{RAW}$‰	±2 SE	$\delta^{18}O_{COR}$‰	±2 SD	Distance from edge
				GR	RD FRD	A	B	C	D	E	of enamel (µm)
UWA-1											
20150406@105	UWA-1 G1						23.743	0.221			
20150406@106	UWA-1 G1						23.860	0.286			
20150406@107	UWA-1 G1						23.310	0.231			
20150406@108	UWA-1 G1						23.300	0.192			
Average and ±2 SD							**23.553**	**0.581**			
Bracket: Average and ±2 SD						**1.0108**	**23.673**	**0.503**			
Sample: 2109 (Modern Grant's Gazelle) with UWA-1.											
UWA-1											
20150406@35	UWA-1 G1						23.847	0.257			
20150406@36	UWA-1 G1						23.910	0.329			
20150406@37	UWA-1 G1						23.507	0.263			
20150406@38	UWA-1 G1						23.733	0.200			
Average and ±2 SD							**23.749**	**0.355**			
Enamel											
20150406@39	2109-001	1					45.110	0.230	33.84	0.27	18
20150406@40	2109-002	1					44.000	0.207	32.74	0.27	78
20150406@41	2109-003	1					43.234	0.256	31.98	0.27	138
20150406@42	2109-004	1					43.918	0.277	32.66	0.27	192
20150406@43	2109-005	1					43.769	0.168	32.51	0.27	252
20150406@44	2109-006	1					43.620	0.228	32.36	0.27	312
20150406@45	2109-007	1					42.831	0.197	31.58	0.27	372
20150406@46	2109-008	1					41.848	0.226	30.61	0.27	432
20150406@47	2109-009	1					42.483	0.168	31.24	0.27	492
20150406@48	2109-010	1					42.158	0.170	30.92	0.27	552
UWA-1											
20150406@49	UWA-1 G1						23.678	0.285			

Analysis #	Sample	Line #	Diagenesis* SEM	Diagenesis* CLFM			Bias (α)	$\delta^{18}O_{RAW}$‰	±2 SE	$\delta^{18}O_{COR}$‰	±2 SD	Distance from edge
				GR	RD	FRD	A	B	C	D	E	of enamel (µm)
20150406@50	UWA-1 G1							23.638	0.268			
20150406@51	UWA-1 G1							23.757	0.260			
20150406@52	UWA-1 G1; Cs res 181-182							23.870	0.190			
Average and ±2 SD								**23.736**	**0.204**			
Bracket: Average and ±2 SD							**1.0109**	**23.743**	**0.268**			
Enamel												
20150406@53	2109-011	1						43.129	0.281	32.02	0.37	612
20150406@54	2109-012	1						42.763	0.221	31.66	0.37	676
20150406@55	2109-013	1						41.492	0.224	30.40	0.37	758
20150406@56	2109-014	1						41.048	0.223	29.96	0.37	714
20150406@57	2109-015	1						43.219	0.227	32.11	0.37	638
20150406@58	2109-016	1						43.217	0.214	32.11	0.37	578
20150406@59	2109-017	1						41.773	0.253	30.68	0.37	518
20150406@60	2109-018	1						41.997	0.278	30.90	0.37	458
20150406@61	2109-019	1						42.522	0.282	31.42	0.37	398
20150406@62	2109-020	1						43.415	0.228	32.31	0.37	338
UWA-1												
20150406@63	UWA-1 G1							23.403	0.221			
20150406@64	UWA-1 G1							23.461	0.161			
20150406@65	UWA-1 G1							23.334	0.222			
20150406@66	UWA-1 G1							23.648	0.221			
Average and ±2 SD								**23.462**	**0.269**			
Bracket: Average and ±2 SD							**1.0108**	**23.599**	**0.367**			
Enamel												
20150406@67	2109-021	1						44.069	0.194	32.94	0.39	275
20150406@68	2109-022	1						43.760	0.233	32.64	0.39	218
20150406@69	2109-023	1						43.558	0.248	32.44	0.39	158

Analysis #	Sample	Line #	Diagenesis* SEM	CLFM GR	CLFM RD	CLFM FRD	Bias (α) A	$\delta^{18}O_{RAW}$‰ B	±2 SE C	$\delta^{18}O_{COR}$‰ D	±2 SD E	Distance from edge of enamel (µm)
20150406@70	2109-024	1						43.600	0.242	32.48	0.39	106
20150406@71	2109-025	1						~~45.850~~	~~9.792~~	~~34.70~~	~~0.39~~	46
20150406@72	2109-026	1						44.383	0.271	33.25	0.39	58
20150406@73	2109-027	1						42.960	0.221	31.84	0.39	563
20150406@74	2109-028	1						41.992	0.317	30.89	0.39	693
UWA-1												
20150406@75	UWA-1 G1							23.875	0.198			
20150406@76	UWA-1 G1							23.619	0.312			
20150406@77	UWA-1 G1							23.773	0.180			
20150406@78	UWA-1 G1							23.760	0.299			
Average and ±2 SD								**23.757**	**0.211**			
Bracket: Average and ±2 SD							**1.0108**	**23.609**	**0.387**			
Sample: 4859b3 (Giraffidae) with UWA-1.												
UWA-1												
20150406@535	UWA-1 Grain 5 (G5)							20.893	0.273			
20150406@536	UWA-1 Grain 6 (G6)							20.714	0.258			
20150406@537	UWA-1 G6							21.150	0.227			
20150406@538	UWA-1 G6							20.921	0.191			
Average and ±2 SD								**20.920**	**0.358**			
Enamel												
20150406@539	4859b3-001	1		**x**	**x**	**x**		28.237	0.252	19.87	0.76	1248
20150406@540	4859b3-002	1		**x**	**x**	**x**		29.965	0.235	21.58	0.76	1111
20150406@541	4859b3-003	1			**x**	**x**		28.332	0.190	19.96	0.76	974
20150406@542	4859b3-004	1						30.001	0.194	21.62	0.76	837
20150406@543	4859b3-005	1						29.720	0.239	21.34	0.76	700
20150406@544	4859b3-006	1						29.483	0.203	21.10	0.76	563
20150406@545	4859b3-007	1						29.186	0.220	20.81	0.76	426

Analysis #	Sample	Line #	Diagenesis* SEM	CLFM GR	CLFM RD	CLFM FRD	Bias (α) A	$\delta^{18}O_{RAW}$‰ B	±2 SE C	$\delta^{18}O_{COR}$‰ D	±2 SD E	Distance from edge of enamel (µm)
20150406@546	4859b3-008	1						30.265	0.233	21.88	0.76	289
UWA-1												
20150406@547	UWA-1 G6							21.783	0.204			
20150406@548	UWA-1 G6							20.942	0.251			
20150406@549	UWA-1 G6							21.177	0.182			
20150406@550	UWA-1 G6							20.521	0.218			
Average and ±2 SD								**21.106**	**1.054**			
Bracket: Average and ±2 SD							**1.0082**	**21.013**	**0.755**			
Enamel												
20150406@551	4859b3-009	1						29.934	0.264	21.53	0.75	152
20150406@552	4859b3-010	1		x	x			30.668	0.254	22.26	0.75	15
20150406@553	4859b3-011	1						30.403	0.298	21.99	0.75	84
20150406@554	4859b3-012	1						28.661	0.211	20.27	0.75	358
20150406@555	4859b3-013	1						30.125	0.229	21.72	0.75	221
20150406@556	4859b3-014	1			x			29.147	0.248	20.75	0.75	906
20150406@557	4859b3-015	1			x	x		28.498	0.283	20.10	0.75	1043
20150406@558	4859b3-016	1		x	x	x		28.707	0.247	20.31	0.75	1162
UWA-1												
20150406@559	UWA-1 G6							21.105	0.250			
20150406@560	UWA-1 G6							20.677	0.181			
20150406@561	UWA-1 G6							21.028	0.224			
20150406@562	UWA-1 G6							21.025	0.180			
Average and ±2 SD								**20.959**	**0.383**			
Bracket: Average and ±2 SD							**1.0082**	**21.032**	**0.750**			
Enamel												
20150406@563	4859b3-017	1			x	x		29.099	0.191	20.94	0.46	1077

Analysis #	Sample	Line #	Diagenesis* SEM	CLFM GR	CLFM RD	CLFM FRD	Bias (α) A	$\delta^{18}O_{RAW}$‰ B	±2 SE C	$\delta^{18}O_{COR}$‰ D	±2 SD E	Distance from edge of enamel (µm)
20150406@564	4859b3-018	1		x	x	x		28.340	0.276	20.19	0.46	1215
20150406@565	4859b3-019	1						29.112	0.197	20.95	0.46	324
20150406@566	4859b3-020	2			x			30.145	0.198	21.98	0.46	23
20150406@567	4859b3-021	2		x	x	x		27.561	0.237	19.41	0.46	1106
20150406@568	4859b3-022	2		x				28.159	0.234	20.01	0.46	996
20150406@569	4859b3-023	2		x				28.717	0.248	20.56	0.46	866
20150406@570	4859b3-024	2		x				29.897	0.296	21.73	0.46	746
20150406@571	4859b3-025	2						29.046	0.201	20.89	0.46	626
20150406@572	4859b3-026	2						29.295	0.229	21.13	0.46	506
20150406@573	4859b3-027	2						29.414	0.232	21.25	0.46	386
20150406@574	4859b3-028	2						30.369	0.237	22.20	0.46	266
20150406@575	4859b3-029	2						29.681	0.188	21.52	0.46	146
UWA-1												
20150406@576	UWA-1 G6							20.547	0.184			
20150406@577	UWA-1 G6							20.813	0.202			
20150406@578	UWA-1 G6							20.603	0.263			
20150406@579	UWA-1 G6							20.550	0.264			
Average and ±2 SD								**20.628**	**0.252**			
Bracket: Average and ±2 SD							**1.0080**	**20.794**	**0.463**			
Enamel												
20150406@580	4859b3-030	2						30.356	0.230	22.01	0.75	233
20150406@581	4859b3-031	2						29.839	0.256	21.50	0.75	326
20150406@582	4859b3-032	2						29.667	0.258	21.33	0.75	574
20150406@583	4859b3-033	2						~~30.161~~	~~0.297~~	~~21.82~~	~~0.75~~	686
20150406@584	4859b3-034	2		x				~~29.998~~	~~0.267~~	~~21.65~~	~~0.75~~	806
20150406@585	4859b3-035	2		x				29.731	0.336	21.39	0.75	833
20150406@586	4859b3-036	2						29.620	0.238	21.28	0.75	658
20150406@587	4859b3-037	2		x				29.508	0.275	21.17	0.75	926

Analysis #	Sample	Line #	Diagenesis*				Bias (α)	$\delta^{18}O_{RAW}$‰	±2 SE	$\delta^{18}O_{COR}$‰	±2 SD	Distance from edge of enamel (µm)
			SEM	CLFM								
				GR	RD	FRD	A	B	C	D	E	
UWA-1												
20150406@588	UWA-1 G6							21.339	0.237			
20150406@589	UWA-1 G6							21.349	0.234			
20150406@590	UWA-1 G6							21.325	0.259			
20150406@591	UWA-1 G6							21.240	0.182			
Average and ±2 SD								**21.313**	**0.100**			
Bracket: Average and ±2 SD							**1.0082**	**20.971**	**0.753**			
Enamel												
20150406@592	4859b3-038	2						29.914	0.159	21.67	0.95	83
20150406@593	4859b3-039	2		x				28.975	0.246	20.74	0.95	959
20150406@594	4859b3-040	2		x				29.210	0.280	20.97	0.95	892
20150406@595	4859b3-041	2		x		x		29.596	0.348	21.35	0.95	1055
20150406@596	4859b3-042	2		x		x		28.907	0.249	20.67	0.95	1037
20150406@597	4859b3-043	2		x		x		28.907	0.264	20.67	0.95	1085
20150406@598	4859b3-044	2						29.489	0.220	21.25	0.95	446
20150406@599	4859b3-045	3		x				30.728	0.230	22.48	0.95	28
20150406@600	4859b3-046	3						30.365	0.256	22.12	0.95	121
20150406@601	4859b3-047	3		x		x		30.024	0.203	21.78	0.95	241
20150406@602	4859b3-048	3	SEM					~~22.245~~	~~0.263~~	~~14.06~~	~~0.95~~	361
20150406@603	4859b3-049	3				x		28.831	0.257	20.60	0.95	481
20150406@604	4859b3-050	3	SEM					27.619	0.183	19.39	0.95	601
20150406@605	4859b3-051	3	SEM					~~20.923~~	~~0.223~~	~~12.75~~	~~0.95~~	697
20150406@606	4859b3-052	3		x	x	x		28.720	0.254	20.49	0.95	817
20150406@607	4859b3-053	3		x	x	x		27.689	0.261	19.46	0.95	917
UWA-1												
20150406@608	UWA-1 G6							20.486	0.242			
20150406@609	UWA-1 G6							20.296	0.213			

Analysis #	Sample	Line #	Diagenesis*				Bias (α)	$\delta^{18}O_{RAW}$‰	±2 SE	$\delta^{18}O_{COR}$‰	±2 SD	Distance from edge
			SEM	CLFM								
				GR	RD	FRD	A	B	C	D	E	of enamel (µm)
20150406@610	UWA-1 G6							20.459	0.152			
20150406@611	UWA-1 G6							20.477	0.244			
Average and ±2 SD								**20.430**	**0.179**			
Bracket: Average and ±2 SD							**1.0081**	**20.871**	**0.954**			
Enamel												
20150406@612	4859b3-054	3		x				29.696	0.237	21.68	0.53	301
20150406@613	4859b3-055	3	**SEM**			x		~~25.826~~	~~0.307~~	~~17.84~~	~~0.53~~	411
20150406@614	4859b3-056	3						29.620	0.215	21.60	0.53	327
20150406@615	4859b3-057	3	**SEM**					27.102	0.175	19.10	0.53	345
20150406@616	4859b3-058	3	**SEM**					~~23.609~~	~~0.187~~	~~15.64~~	~~0.53~~	377
20150406@617	4859b3-059	3	**SEM**					28.435	0.264	20.43	0.53	651
20150406@618	4859b3-060	3						29.003	0.178	20.99	0.53	666
20150406@619	4859b3-061	3						28.873	0.254	20.86	0.53	683
UWA-1												
20150406@620	UWA-1 G6							20.809	0.212			
20150406@621	UWA-1 G6							21.045	0.274			
20150406@622	UWA-1 G6							20.955	0.235			
20150406@623	UWA-1 G6							20.647	0.174			
Average and ±2 SD								**20.864**	**0.349**			
Bracket: Average and ±2 SD							**1.0078**	**20.647**	**0.531**			
Enamel												
20150406@624	4859b3-062	3		x	x	x		29.160	0.177	21.00	0.31	757
20150406@625	4859b3-063	3		x				~~25.566~~	~~0.248~~	~~17.43~~	~~0.31~~	713
20150406@626	4859b3-064	3		x	x	x		29.280	0.221	21.12	0.31	735
20150406@627	4859b3-065	3		x	x	x		29.658	0.267	21.49	0.31	698
20150406@628	4859b3-066	3				x		29.005	0.231	20.84	0.31	446
20150406@629	4859b3-067	3		x	x	x		28.663	0.240	20.50	0.31	867

Analysis #	Sample	Line #	Diagenesis* SEM	CLFM		Bias (α)	$\delta^{18}O_{RAW}$‰	±2 SE	$\delta^{18}O_{COR}$‰	±2 SD	Distance from edge
				GR	RD FRD	A	B	C	D	E	of enamel (µm)
20150406@630	4859b3-068	3			x		28.421	0.267	20.26	0.31	541
20150406@631	4859b3-069	1					29.416	0.201	21.25	0.31	768
20150406@632	4859b3-070	1					28.629	0.234	20.47	0.31	495
UWA-1											
20150406@633	UWA-1 G6						20.758	0.334			
20150406@634	UWA-1 G6; Cs res 189-190						20.689	0.220			
20150406@635	UWA-1 G6						20.869	0.177			
20150406@636	UWA-1 G6						20.596	0.191			
Average and ±2 SD							**20.728**	**0.230**			
Bracket: Average and ±2 SD						**1.0078**	**20.647**	**0.531**			
Sample: 4860.1 (Giraffidae) with UWA-1.											
UWA-1											
20141110@10	UWA-1 G2						18.825	0.431			
20141110@11	UWA-1 G3						19.130	0.351			
20141110@12	UWA-1 G4						18.753	0.429			
20141110@13	UWA-1 G2						18.848	0.334			
20141110@14	UWA-1 G2						18.551	0.329			
Average and ±2 SD							**18.821**	**0.417**			
Enamel											
20141110@15	4860.1-001	1					33.090	0.381	26.87	0.35	11
20141110@16	4860.1-002	1					32.891	0.422	26.67	0.35	45
20141110@17	4860.1-003	1		x			33.063	0.359	26.84	0.35	75
20141110@18	4860.1-004	1		x			33.292	0.375	27.07	0.35	105
20141110@19	4860.1-005	1		x			33.131	0.453	26.91	0.35	140
20141110@20	4860.1-006	1		x			32.692	0.427	26.47	0.35	170
20141110@21	4860.1-007	1					33.033	0.475	26.81	0.35	200
20141110@22	4860.1-008	1					32.572	0.468	26.35	0.35	230

Analysis #	Sample	Line #	Diagenesis* SEM	CLFM		Bias (α)	$\delta^{18}O_{RAW}$‰	±2 SE	$\delta^{18}O_{COR}$‰	±2 SD	Distance from edge of enamel (µm)
				GR	RD FRD	A	B	C	D	E	
UWA-1											
20141110@23	UWA-1 G2						18.876	0.445			
20141110@24	UWA-1 G2						18.893	0.422			
20141110@25	UWA-1 G2						18.647	0.365			
20141110@26	UWA-1 G2						19.010	0.445			
Average and ±2 SD							**18.857**	**0.304**			
Bracket: Average and ±2 SD						**1.0061**	**18.837**	**0.350**			
Enamel											
20141110@27	4860.1-009	1					32.421	0.467	26.18	0.24	260
20141110@28	4860.1-010	1					32.315	0.514	26.07	0.24	290
20141110@29	4860.1-011	1					32.044	0.429	25.80	0.24	320
20141110@30	4860.1-012	1					31.684	0.551	25.44	0.24	350
20141110@31	4860.1-013	1					31.768	0.488	25.53	0.24	382
20141110@32	4860.1-014	1					31.038	0.406	24.80	0.24	417
20141110@33	4860.1-015	1					31.246	0.577	25.01	0.24	447
20141110@34	4860.1-016	1					31.602	0.454	25.36	0.24	477
20141110@35	4860.1-017	1					30.784	0.806	24.55	0.24	507
20141110@36	4860.1-018	1					30.253	0.500	24.02	0.24	537
UWA-1											
20141110@37	UWA-1 G2						18.999	0.345			
20141110@38	UWA-1 G2						18.905	0.366			
20141110@39	UWA-1 G2						18.799	0.381			
20141110@40	UWA-1 G2						18.780	0.499			
Average and ±2 SD							**18.871**	**0.203**			
Bracket: Average and ±2 SD						**1.0061**	**18.864**	**0.240**			
Enamel											

Analysis #	Sample	Line #	Diagenesis* SEM	CLFM		Bias (α)	$\delta^{18}O_{RAW}$‰	±2 SE	$\delta^{18}O_{COR}$‰	±2 SD	Distance from edge
				GR	RD FRD	A	B	C	D	E	of enamel (µm)
20141110@41	4860.1-019	1					29.564	0.628	23.38	0.37	567
20141110@42	4860.1-020	1					31.503	0.566	25.31	0.37	597
20141110@43	4860.1-021	1					31.609	0.450	25.42	0.37	627
20141110@44	4860.1-022	1					31.261	0.414	25.07	0.37	657
20141110@45	4860.1-023	1					31.160	0.462	24.97	0.37	687
20141110@46	4860.1-024	1					31.138	0.472	24.95	0.37	721
20141110@47	4860.1-025	1					31.273	0.407	25.08	0.37	751
20141110@48	4860.1-026	1					31.117	0.431	24.93	0.37	781
20141110@49	4860.1-027	1					30.910	0.520	24.72	0.37	807
20141110@50	4860.1-028	1					31.203	0.461	25.01	0.37	837
UWA-1											
20141110@51	UWA-1 G2						19.078	0.510			
20141110@52	UWA-1 G2						18.831	0.368			
20141110@53	UWA-1 G2						18.624	0.494			
20141110@54	UWA-1 G2; Cs res 135-136						18.506	0.449			
Average and ±2 SD							**18.760**	**0.502**			
Bracket: Average and ±2 SD						**1.0060**	**18.815**	**0.374**			
UWA-1											
20141110@56	UWA-1 G2						18.866	0.368			
20141110@57	UWA-1 G2						18.619	0.467			
20141110@58	UWA-1 G2						18.661	0.387			
20141110@59	UWA-1 G2						18.824	0.353			
Average and ±2 SD							**18.743**	**0.242**			
Enamel											
20141110@60	4860.1-029	1					31.481	0.481	25.32	0.22	867
20141110@61	4860.1-030	1					31.544	0.504	25.38	0.22	897
20141110@62	4860.1-031	1					31.811	0.478	25.65	0.22	927

Analysis #	Sample	Line #	Diagenesis* SEM	CLFM		Bias (α)	$\delta^{18}O_{RAW}$‰	±2 SE	$\delta^{18}O_{COR}$‰	±2 SD	Distance from edge
				GR	RD FRD	A	B	C	D	E	of enamel (µm)
20141110@63	4860.1-032	1					31.473	0.477	25.31	0.22	957
20141110@64	4860.1-033	1					30.945	0.403	24.79	0.22	987
20141110@65	4860.1-034	1					30.849	0.460	24.69	0.22	1017
20141110@66	4860.1-035	1			x		30.877	0.475	24.72	0.22	1047
20141110@67	4860.1-036	1			x		30.101	0.465	23.95	0.22	1077
20141110@68	4860.1-037	1			x		30.173	0.415	24.02	0.22	1107
20141110@69	4860.1-038	1					29.847	0.391	23.69	0.22	1137
UWA-1											
20141110@70	UWA-1 G2						18.823	0.444			
20141110@71	UWA-1 G2						18.833	0.389			
20141110@72	UWA-1 G2						18.947	0.394			
20141110@73	UWA-1 G2; Cs res 136-137						18.721	0.422			
Average and ±2 SD							**18.831**	**0.185**			
Bracket: Average and ±2 SD						**1.0060**	**18.787**	**0.220**			
UWA-1											
20141110@75	UWA-1 G2						18.654	0.381			
20141110@76	UWA-1 G2						18.764	0.376			
20141110@77	UWA-1 G2						18.573	0.377			
20141110@78	UWA-1 G2						18.812	0.446			
Average and ±2 SD							**18.701**	**0.216**			
Enamel											
20141110@79	4860.1-039	1					30.543	0.402	24.42	0.21	1167
20141110@80	4860.1-040	1					30.698	0.454	24.58	0.21	1197
20141110@81	4860.1-041	1					31.059	0.495	24.94	0.21	1227
20141110@82	4860.1-042	1			x		30.567	0.432	24.45	0.21	1257
20141110@83	4860.1-043	1			x		30.608	0.540	24.49	0.21	1287
20141110@84	4860.1-044	1			x		30.797	0.446	24.68	0.21	1317

Analysis #	Sample	Line #	Diagenesis*			Bias (α)	$\delta^{18}O_{RAW}$‰	±2 SE	$\delta^{18}O_{COR}$‰	±2 SD	Distance from edge
			SEM	CLFM							
				GR	RD FRD	A	B	C	D	E	of enamel (µm)
20141110@85	4860.1-045	1			x x		30.754	0.407	24.63	0.21	1351
20141110@86	4860.1-046	1			x x		31.098	0.438	24.98	0.21	1381
20141110@87	4860.1-047	1			x x		31.213	0.355	25.09	0.21	1411
20141110@88	4860.1-048	1			x x		31.105	0.441	24.98	0.21	1441
UWA-1											
20141110@89	UWA-1 G2						18.816	0.439			
20141110@90	UWA-1 G2						18.770	0.389			
20141110@91	UWA-1 G2						18.909	0.338			
20141110@92	UWA-1 G2						18.692	0.426			
Average and ±2 SD							**18.797**	**0.181**			
Bracket: Average and ±2 SD						**1.0060**	**18.749**	**0.211**			
Enamel											
20141110@93	4860.1-049	1			x x		31.200	0.517	25.08	0.18	1471
20141110@94	4860.1-050	1			x x		31.394	0.481	25.27	0.18	1501
20141110@95	4860.1-051	1	**SEM**		x x		31.628	0.456	25.51	0.18	1523
20141110@96	4860.1-052	1	**SEM**		x x		31.419	0.392	25.30	0.18	1553
20141110@97	4860.1-053	1	**SEM**		x x		31.143	0.489	25.02	0.18	1583
20141110@98	4860.1-054	1	**SEM**		x x		30.482	0.544	24.37	0.18	1613
20141110@99	4860.1-055	1	**SEM**		x x		29.921	0.440	23.81	0.18	1643
20141110@100	4860.1-056	1					31.132	0.497	25.01	0.18	561
20141110@101	4860.1-057	1					29.651	0.480	23.54	0.18	531
20141110@102	4860.1-058	1					30.784	0.441	24.67	0.18	552
20141110@103	4860.1-059	1					31.110	0.729	24.99	0.18	580
UWA-1											
20141110@104	UWA-1 G2						18.718	0.407			
20141110@105	UWA-1 G2						18.777	0.451			
20141110@106	UWA-1 G2						18.630	0.408			

Analysis #	Sample	Line #	Diagenesis* SEM	CLFM GR	CLFM RD	CLFM FRD	Bias (α) A	$\delta^{18}O_{RAW}$‰ B	±2 SE C	$\delta^{18}O_{COR}$‰ D	±2 SD E	Distance from edge of enamel (µm)
20141110@107	UWA-1 G2							18.648	0.448			
Average and ±2 SD								**18.693**	**0.135**			
Bracket: Average and ±2 SD							**1.0060**	**18.745**	**0.185**			
UWA-1												
20141110@548	UWA-1 G2							20.279	0.379			
20141110@549	UWA-1 G2							20.299	0.307			
20141110@550	UWA-1 G2							20.387	0.312			
20141110@551	UWA-1 G2							20.296	0.247			
Average and ±2 SD								**20.315**	**0.097**			
Enamel												
20141110@552	4860.1-060	2		**x**	**x**			34.502	0.397	26.84	0.18	20
20141110@553	4860.1-061	2		**x**	**x**			34.640	0.384	26.98	0.18	67
20141110@554	4860.1-062	2		**x**	**x**			34.703	0.306	27.04	0.18	107
20141110@555	4860.1-063	2						34.431	0.280	26.77	0.18	142
20141110@556	4860.1-064	2						34.801	0.365	27.14	0.18	172
20141110@557	4860.1-065	2						34.534	0.268	26.87	0.18	202
20141110@558	4860.1-066	2						35.028	0.341	27.36	0.18	232
20141110@559	4860.1-067	2						34.949	0.356	27.29	0.18	262
20141110@560	4860.1-068	2						34.893	0.400	27.23	0.18	292
20141110@561	4860.1-069	2						~~34.258~~	~~0.303~~	~~26.60~~	~~0.18~~	322
UWA-1												
20141110@562	UWA-1 G2							20.287	0.299			
20141110@563	UWA-1 G2							20.094	0.279			
20141110@564	UWA-1 G2							20.202	0.277			
20141110@565	UWA-1 G2							20.185	0.309			
Average and ±2 SD								**20.192**	**0.158**			
Bracket: Average and ±2 SD							**1.0075**	**20.254**	**0.179**			

Analysis #	Sample	Line #	Diagenesis* SEM	Diagenesis* CLFM			Bias (α)	$\delta^{18}O_{RAW}$‰	±2 SE	$\delta^{18}O_{COR}$‰	±2 SD	Distance from edge of enamel (µm)
				GR	RD	FRD	A	B	C	D	E	
Enamel												
20141110@566	4860.1-070	2						34.703	0.340	27.01	0.22	362
20141110@567	4860.1-071	2						34.797	0.250	27.11	0.22	392
20141110@568	4860.1-072	2						34.449	0.440	26.76	0.22	422
20141110@569	4860.1-073	2						34.128	0.351	26.44	0.22	452
20141110@570	4860.1-074	2						34.278	0.261	26.59	0.22	482
20141110@571	4860.1-075	2						34.411	0.292	26.72	0.22	512
20141110@572	4860.1-076	2						34.130	0.444	26.45	0.22	542
20141110@573	4860.1-077	2						34.709	0.307	27.02	0.22	572
UWA-1												
20141110@574	UWA-1 G2							20.333	0.299			
20141110@575	UWA-1 G2							20.369	0.338			
20141110@576	UWA-1 G2							20.393	0.283			
20141110@577	UWA-1 G2; Cs res 154-152							20.386	0.312			
Average and ±2 SD								**20.370**	**0.054**			
Bracket: Average and ±2 SD							**1.0075**	**20.281**	**0.220**			
UWA-1												
20141110@579	UWA-1 G2							20.630	0.354			
20141110@580	UWA-1 G2							20.588	0.300			
20141110@581	UWA-1 G2							20.352	0.278			
20141110@582	UWA-1 G2							20.506	0.258			
Average and ±2 SD								**20.519**	**0.245**			
Enamel												
20141110@583	4860.1-078	2						34.360	0.302	26.46	0.19	602
20141110@584	4860.1-079	2						34.533	0.405	26.63	0.19	632
20141110@585	4860.1-080	2						34.252	0.370	26.36	0.19	662

Analysis #	Sample	Line #	Diagenesis*			Bias (α)	$\delta^{18}O_{RAW}$‰	±2 SE	$\delta^{18}O_{COR}$‰	±2 SD	Distance from edge
			SEM	CLFM							
				GR	RD FRD						
						A	B	C	D	E	of enamel (µm)
20141110@586	4860.1-081	2					34.152	0.334	26.26	0.19	692
20141110@587	4860.1-082	2					34.279	0.424	26.38	0.19	722
20141110@588	4860.1-083	2					34.307	0.312	26.41	0.19	752
20141110@589	4860.1-084	2					33.765	0.360	25.87	0.19	782
20141110@590	4860.1-085	2					33.640	0.423	25.75	0.19	812
20141110@591	4860.1-086	2					33.215	0.386	25.33	0.19	842
20141110@592	4860.1-087	2					33.116	0.389	25.23	0.19	872
20141110@593	4860.1-088	2					32.755	0.386	24.87	0.19	902
20141110@594	4860.1-089	2			x		32.772	0.337	24.89	0.19	932
UWA-1											
20141110@595	UWA-1 G2						20.563	0.348			
20141110@596	UWA-1 G2						20.448	0.322			
20141110@597	UWA-1 G2						20.451	0.321			
20141110@598	UWA-1 G2						20.397	0.247			
Average and ±2 SD							**20.465**	**0.140**			
Bracket: Average and ±2 SD						**1.0077**	**20.492**	**0.194**			
Enamel											
20141110@599	4860.1-090	2					31.866	0.325	24.07	0.17	992
20141110@600	4860.1-091	2			x		31.560	0.412	23.77	0.17	1050
20141110@601	4860.1-092	2					31.714	0.354	23.92	0.17	1110
20141110@602	4860.1-093	2			x		31.393	0.340	23.60	0.17	1175
20141110@603	4860.1-094	2			x	x	30.990	0.347	23.20	0.17	1235
20141110@604	4860.1-095	2		x	x	x	31.196	0.302	23.41	0.17	1295
20141110@605	4860.1-096	2		x	x	x	31.170	0.263	23.38	0.17	1355
20141110@606	4860.1-097	2		x	x	x	31.209	0.365	23.42	0.17	1415
20141110@607	4860.1-098	2		x	x	x	31.194	0.366	23.40	0.17	1475
20141110@608	4860.1-099	2			x	x	30.666	0.277	22.88	0.17	1535
20141110@609	4860.1-100	2			x		32.627	0.316	24.83	0.17	956

Analysis #	Sample	Line #	Diagenesis* SEM	CLFM		Bias (α)	$\delta^{18}O_{RAW}$‰	±2 SE	$\delta^{18}O_{COR}$‰	±2 SD	Distance from edge
				GR	RD FRD	A	B	C	D	E	of enamel (µm)
20141110@610	4860.1-101	2			x		31.966	0.329	24.17	0.17	1020
20141110@611	4860.1-102	2			x		31.360	0.377	23.57	0.17	1140
UWA-1											
20141110@612	UWA-1 G2						20.340	0.311			
20141110@613	UWA-1 G2						20.350	0.348			
20141110@614	UWA-1 G2						20.292	0.359			
20141110@615	UWA-1 G2						20.420	0.306			
Average and ±2 SD							**20.351**	**0.106**			
Bracket: Average and ±2 SD						**1.0076**	**20.408**	**0.168**			
Sample: 4901.2 (Elephantidae) with UWA-1.											
UWA-1											
20141110@155	UWA-1 G2						18.617	0.386			
20141110@156	UWA-1 G3						18.718	0.461			
20141110@157	UWA-1 G4						18.877	0.372			
20141110@158	UWA-1 G1						18.828	0.388			
Average and ±2 SD							**18.760**	**0.232**			
Enamel											
20141110@159	4901.2-001	1		x	x x		32.555	0.495	26.29	0.36	18
20141110@160	4901.2-002	1		x	x x		31.650	0.400	25.39	0.36	43
20141110@161	4901.2-003	1		x	x x		30.457	0.438	24.21	0.36	72
20141110@162	4901.2-004	1		x	x x		31.498	0.363	25.24	0.36	102
20141110@163	4901.2-005	1		x	x x		31.449	0.359	25.20	0.36	128
20141110@164	4901.2-006	1		x	x x		31.240	0.471	24.99	0.36	158
20141110@165	4901.2-007	1		x	x x		31.003	0.372	24.75	0.36	188
20141110@166	4901.2-008	1		x	x x		31.598	0.428	25.34	0.36	218
UWA-1											

Analysis #	Sample	Line #	Diagenesis* SEM	CLFM GR	CLFM RD	CLFM FRD	Bias (α) A	$\delta^{18}O_{RAW}$‰ B	±2 SE C	$\delta^{18}O_{COR}$‰ D	±2 SD E	Distance from edge of enamel (µm)
20141110@167	UWA-1 G1							19.187	0.361			
20141110@168	UWA-1 G1							19.031	0.431			
20141110@169	UWA-1 G1							18.818	0.375			
20141110@170	UWA-1 G3							18.946	0.332			
Average and ±2 SD								**18.996**	**0.310**			
Bracket: Average and ±2 SD							**1.0061**	**18.878**	**0.357**			
Enamel												
20141110@171	4901.2-009	1		**x**	**x**	**x**		31.748	0.469	25.47	0.30	248
20141110@172	4901.2-010	1		**x**	**x**	**x**		31.828	0.464	25.55	0.30	278
20141110@173	4901.2-011	1			**x**	**x**		31.699	0.455	25.42	0.30	308
20141110@174	4901.2-012	1						31.938	0.431	25.66	0.30	338
20141110@175	4901.2-013	1						31.906	0.375	25.62	0.30	368
20141110@176	4901.2-014	1						31.734	0.433	25.45	0.30	398
20141110@177	4901.2-015	1						31.922	0.380	25.64	0.30	428
20141110@178	4901.2-016	1						31.141	0.443	24.86	0.30	458
20141110@179	4901.2-017	1						31.556	0.475	25.28	0.30	492
20141110@180	4901.2-018	1						31.214	0.491	24.94	0.30	522
20141110@181	4901.2-019	1						31.432	0.410	25.15	0.30	552
20141110@182	4901.2-020	1						31.126	0.369	24.85	0.30	582
UWA-1												
20141110@183	UWA-1 G1							18.896	0.453			
20141110@184	UWA-1 G1							18.796	0.433			
20141110@185	UWA-1 G1							18.719	0.325			
20141110@186	UWA-1 G1							18.828	0.355			
Average and ±2 SD								**18.810**	**0.147**			
Bracket: Average and ±2 SD							**1.0061**	**18.903**	**0.300**			
Enamel												

Analysis #	Sample	Line #	Diagenesis* SEM	CLFM		Bias (α)	$\delta^{18}O_{RAW}$‰	±2 SE	$\delta^{18}O_{COR}$‰	±2 SD	Distance from edge
				GR	RD FRD	A	B	C	D	E	of enamel (µm)
20141110@187	4901.2-021	1					31.083	0.341	24.83	0.23	612
20141110@188	4901.2-022	1					30.767	0.466	24.52	0.23	642
20141110@189	4901.2-023	1					30.847	0.521	24.60	0.23	672
20141110@190	4901.2-024	1					30.958	0.385	24.71	0.23	702
20141110@191	4901.2-025	1					31.309	0.355	25.06	0.23	732
20141110@192	4901.2-026	1					31.568	0.385	25.32	0.23	762
20141110@193	4901.2-027	1					31.872	0.432	25.62	0.23	792
20141110@194	4901.2-028	1					32.522	0.413	26.26	0.23	822
20141110@195	4901.2-029	1					32.538	0.403	26.28	0.23	852
20141110@196	4901.2-030	1					32.601	0.431	26.34	0.23	882
20141110@197	4901.2-031	1			x		32.236	0.423	25.98	0.23	912
20141110@198	4901.2-032	1			x		32.153	0.464	25.90	0.23	942
UWA-1											
20141110@199	UWA-1 G1						19.111	0.406			
20141110@200	UWA-1 G1						18.930	0.378			
20141110@201	UWA-1 G1						18.872	0.422			
20141110@202	UWA-1 G1; Cs res 144-145						18.846	0.378			
Average and ±2 SD							**18.940**	**0.239**			
Bracket: Average and ±2 SD						**1.0061**	**18.875**	**0.230**			
UWA-1											
20141110@204	UWA-1 G1						19.028	0.349			
20141110@205	UWA-1 G1						18.735	0.382			
20141110@206	UWA-1 G1						18.705	0.429			
20141110@207	UWA-1 G1						19.010	0.378			
Average and ±2 SD							**18.870**	**0.346**			
Enamel											
20141110@208	4901.2-033	1			x		33.173	0.537	26.81	0.33	972

Analysis #	Sample	Line #	Diagenesis* SEM	CLFM		Bias (α)	$\delta^{18}O_{RAW}$‰	±2 SE	$\delta^{18}O_{COR}$‰	±2 SD	Distance from edge
				GR	RD FRD	A	B	C	D	E	of enamel (µm)
20141110@209	4901.2-034	1			x		33.503	0.414	27.14	0.33	1002
20141110@210	4901.2-035	1			x		33.824	0.462	27.46	0.33	1032
20141110@211	4901.2-036	1			x		33.507	0.420	27.14	0.33	1062
20141110@212	4901.2-037	1					33.679	0.383	27.31	0.33	1092
20141110@213	4901.2-038	1			x		33.331	0.350	26.97	0.33	1122
20141110@214	4901.2-039	1			x		33.306	0.381	26.94	0.33	1152
20141110@215	4901.2-040	1			x	x	33.182	0.410	26.82	0.33	1185
20141110@216	4901.2-041	1					32.915	0.318	26.55	0.33	1215
20141110@217	4901.2-042	1					32.478	0.419	26.12	0.33	1248
20141110@218	4901.2-043	1					32.266	0.378	25.91	0.33	1278
20141110@219	4901.2-044	1			x	x	32.140	0.523	25.78	0.33	1308
UWA-1											
20141110@220	UWA-1 G1						19.111	0.405			
20141110@221	UWA-1 G1						19.031	0.412			
20141110@222	UWA-1 G1						19.032	0.455			
20141110@223	UWA-1 G1; Cs res 145-146						19.161	0.366			
Average and ±2 SD							**19.084**	**0.127**			
Bracket: Average and ±2 SD						**1.0062**	**18.977**	**0.333**			
UWA-1											
20141110@226	UWA-1 G1						18.927	0.380			
20141110@227	UWA-1 G1						18.840	0.400			
20141110@228	UWA-1 G1						18.756	0.429			
20141110@229	UWA-1 G1						18.692	0.350			
Average and ±2 SD							**18.804**	**0.204**			
Enamel											
20141110@230	4901.2-045	1			x		31.999	0.373	25.75	0.31	1348
20141110@231	4901.2-046	1			x	x	31.686	0.470	25.44	0.31	1373

Analysis #	Sample	Line #	Diagenesis* SEM	CLFM GR	CLFM RD	CLFM FRD	Bias (α) A	$\delta^{18}O_{RAW}$‰ B	±2 SE C	$\delta^{18}O_{COR}$‰ D	±2 SD E	Distance from edge of enamel (µm)
20141110@232	4901.2-047	1			x	x		32.143	0.342	25.89	0.31	1403
20141110@233	4901.2-048	1			x	x		31.938	0.394	25.69	0.31	1433
20141110@234	4901.2-049	1			x	x		32.051	0.345	25.80	0.31	1463
20141110@235	4901.2-050	1		x	x	x		31.684	0.397	25.43	0.31	1493
20141110@236	4901.2-051	1		x	x	x		31.690	0.446	25.44	0.31	1523
20141110@237	4901.2-052	1		x	x	x		31.113	0.477	24.87	0.31	1543
20141110@238	4901.2-053	1			x			32.512	0.363	26.26	0.31	954
20141110@239	4901.2-054	1						32.112	0.397	25.86	0.31	442
20141110@240	4901.2-055	1						31.394	0.351	25.15	0.31	477
20141110@241	4901.2-056	1						31.887	0.430	25.64	0.31	472
UWA-1												
20141110@242	UWA-1 G1							19.030	0.415			
20141110@243	UWA-1 G1							18.811	0.445			
20141110@244	UWA-1 G1							18.777	0.329			
20141110@245	UWA-1 G1							19.148	0.411			
Average and ±2 SD								**18.942**	**0.355**			
Bracket: Average and ±2 SD							**1.0061**	**18.873**	**0.306**			
UWA-1												
20141110@268	UWA-1 G1							18.858	0.364			
20141110@269	UWA-1 G1							18.758	0.355			
20141110@270	UWA-1 G1							19.003	0.436			
20141110@271	UWA-1 G1							18.983	0.392			
Average and ±2 SD								**18.901**	**0.229**			
Enamel												
20141110@272	4901.2-074	4		x	x	x		32.814	0.425	26.52	0.19	8
20141110@273	4901.2-075	4						32.608	0.265	26.32	0.19	38
20141110@274	4901.2-076	4						33.229	0.430	26.93	0.19	68

Analysis #	Sample	Line #	Diagenesis* SEM	CLFM		Bias (α)	$\delta^{18}O_{RAW}$‰	±2 SE	$\delta^{18}O_{COR}$‰	±2 SD	Distance from edge
				GR	RD FRD	A	B	C	D	E	of enamel (µm)
20141110@275	4901.2-077	4					33.316	0.389	27.02	0.19	98
20141110@276	4901.2-078	4					33.099	0.339	26.80	0.19	128
20141110@277	4901.2-079	4					33.147	0.367	26.85	0.19	158
20141110@278	4901.2-080	4					32.999	0.420	26.70	0.19	188
20141110@279	4901.2-081	4					32.695	0.462	26.40	0.19	218
20141110@280	4901.2-082	4					32.635	0.379	26.34	0.19	248
20141110@281	4901.2-083	4					32.487	0.440	26.20	0.19	278
20141110@282	4901.2-084	4					32.412	0.369	26.12	0.19	308
20141110@283	4901.2-085	4					32.087	0.349	25.80	0.19	338
20141110@284	4901.2-086	4					32.063	0.420	25.77	0.19	368
20141110@285	4901.2-087	4					31.455	0.444	25.17	0.19	398
20141110@286	4901.2-088	4					30.571	0.477	24.29	0.19	433
20141110@287	4901.2-089	4					30.627	0.405	24.35	0.19	463

UWA-1

20141110@288	UWA-1 G1		18.839	0.350
20141110@289	UWA-1 G1		19.037	0.439
20141110@290	UWA-1 G1		18.938	0.439
20141110@291	UWA-1 G1; Cs res 147-148		18.852	0.461
Average and ±2 SD			**18.917**	**0.183**
Bracket: Average and ±2 SD		**1.0061**	**18.909**	**0.193**

UWA-1

20141110@293	UWA-1 G3		19.122	0.480
20141110@294	UWA-1 G3		18.739	0.382
20141110@295	UWA-1 G3		18.890	0.435
20141110@296	UWA-1 G3		18.844	0.421
Average and ±2 SD			**18.899**	**0.323**

Enamel

Analysis #	Sample	Line #	Diagenesis*			Bias (α)	$\delta^{18}O_{RAW}$‰	±2 SE	$\delta^{18}O_{COR}$‰	±2 SD	Distance from edge
			SEM	CLFM							
				GR	RD FRD						
						A	B	C	D	E	of enamel (µm)
20141110@297	4901.2-089 B	4					30.687	0.457	24.44	0.33	494
20141110@298	4901.2-090	4					30.791	0.382	24.54	0.33	524
20141110@299	4901.2-091	4					30.680	0.441	24.43	0.33	554
20141110@300	4901.2-092	4					30.541	0.508	24.29	0.33	584
20141110@301	4901.2-093	4					31.023	0.356	24.77	0.33	617
20141110@302	4901.2-094	4					30.805	0.528	24.56	0.33	647
20141110@303	4901.2-095	4					31.751	0.390	25.50	0.33	677
20141110@304	4901.2-096	4					31.644	0.429	25.39	0.33	707
20141110@305	4901.2-097	4					31.820	0.413	25.56	0.33	737
20141110@306	4901.2-098	4					32.084	0.391	25.83	0.33	767
20141110@307	4901.2-099	4					32.075	0.517	25.82	0.33	797
20141110@308	4901.2-100	4					31.595	0.455	25.34	0.33	820
20141110@309	4901.2-101	4		x	x		32.102	0.414	25.85	0.33	854
20141110@310	4901.2-102	4		x	x		32.854	0.375	26.59	0.33	884
20141110@311	4901.2-103	4		x			32.716	0.459	26.46	0.33	917
20141110@312	4901.2-104	4		x			33.384	0.409	27.12	0.33	947
UWA-1											
20141110@313	UWA-1 G3						18.822	0.415			
20141110@314	UWA-1 G3						18.794	0.435			
20141110@315	UWA-1 G3						18.683	0.420			
20141110@316	UWA-1 G3						19.120	0.434			
Average and ±2 SD							**18.855**	**0.373**			
Bracket: Average and ±2 SD						**1.0061**	**18.877**	**0.327**			
UWA-1											
20141110@503	UWA-1 G3						20.150	0.291			
20141110@504	UWA-1 G3						20.021	0.355			
20141110@505	UWA-1 G3						19.999	0.236			
20141110@506	UWA-1 G3						20.047	0.317			

Analysis #	Sample	Line #	Diagenesis* SEM	CLFM GR	CLFM RD	CLFM FRD	Bias (α) A	$\delta^{18}O_{RAW}$‰ B	±2 SE C	$\delta^{18}O_{COR}$‰ D	±2 SD E	Distance from edge of enamel (µm)
Average and ±2 SD								**20.054**	**0.134**			
Enamel												
20141110@507	4901.2-105	4			x			34.946	0.398	27.49	0.09	988
20141110@508	4901.2-106	4			x			34.977	0.313	27.52	0.09	1018
20141110@509	4901.2-107	4			x			34.519	0.278	27.07	0.09	1048
20141110@510	4901.2-108	4						34.353	0.360	26.90	0.09	1078
20141110@511	4901.2-109	4						~~33.679~~	~~0.605~~	~~26.23~~	~~0.09~~	1108
20141110@512	4901.2-110	4			x	x		34.235	0.311	26.78	0.09	1138
20141110@513	4901.2-111	4			x	x		33.883	0.345	26.43	0.09	1168
20141110@514	4901.2-112	4		x	x	x		33.169	0.441	25.73	0.09	1308
UWA-1												
20141110@515	UWA-1 G3							20.011	0.274			
20141110@516	UWA-1 G3							20.036	0.323			
20141110@517	UWA-1 G3							20.054	0.328			
20141110@518	UWA-1 G3							20.074	0.320			
Average and ±2 SD								**20.044**	**0.054**			
Bracket: Average and ±2 SD							**1.0073**	**20.049**	**0.095**			
Enamel												
20141110@519	4901.2-113	4			x	x		33.256	0.356	25.81	0.16	1338
20141110@520	4901.2-114	4			x	x		~~32.866~~	~~0.244~~	~~25.42~~	~~0.16~~	1368
20141110@521	4901.2-115	4			x	x		32.854	0.355	25.41	0.16	1412
20141110@522	4901.2-116	4			x	x		32.415	0.312	24.97	0.16	1442
20141110@523	4901.2-117	4		x	x	x		32.185	0.310	24.75	0.16	1472
20141110@524	4901.2-118	4		x	x	x		31.452	0.378	24.02	0.16	1502
20141110@525	4901.2-119	4		x	x	x		30.924	0.320	23.49	0.16	1532
20141110@526	4901.2-120	4		x	x	x		30.649	0.363	23.22	0.16	1562
20141110@527	4901.2-121	4		x	x	x		~~29.853~~	~~0.344~~	~~22.43~~	~~0.16~~	1591

Analysis #	Sample	Line #	Diagenesis* SEM	CLFM GR	CLFM RD	CLFM FRD	Bias (α) A	$\delta^{18}O_{RAW}$‰ B	±2 SE C	$\delta^{18}O_{COR}$‰ D	±2 SD E	Distance from edge of enamel (µm)
20141110@528	4901.2-122	4		x	x	x		34.407	0.327	26.95	0.16	1229
UWA-1												
20141110@529	UWA-1 G3							20.141	0.261			
20141110@530	UWA-1 G3							20.179	0.404			
20141110@531	UWA-1 G3							19.958	0.392			
20141110@532	UWA-1 G3							19.966	0.343			
Average and ±2 SD								**20.061**	**0.231**			
Bracket: Average and ±2 SD							**1.0073**	**20.052**	**0.156**			
Sample: 4908a3 (Elephantidae) with UWA-1.												
UWA-1												
20150406@638	UWA-1 G1							20.589	0.182			
20150406@639	UWA-1 G2							20.467	0.220			
20150406@640	UWA-1 G2							20.476	0.192			
20150406@641	UWA-1 G2							20.597	0.231			
Average and ±2 SD								**20.532**	**0.141**			
Enamel												
20150406@642	4908a3-001	1		x	x	x		30.519	0.234	22.53	0.24	25
20150406@643	4908a3-002	1			x	x		31.157	0.209	23.17	0.24	265
20150406@644	4908a3-003	1						31.538	0.219	23.55	0.24	505
20150406@645	4908a3-004	1						30.235	0.257	22.25	0.24	745
20150406@646	4908a3-005	1			x	x		30.310	0.191	22.33	0.24	985
20150406@647	4908a3-006	1			x	x		32.037	0.256	24.04	0.24	1165
20150406@648	4908a3-007	1		x	x	x		29.627	0.275	21.65	0.24	1105
20150406@649	4908a3-008	1			x	x		~~30.821~~	~~0.244~~	~~22.83~~	~~0.24~~	1200
UWA-1												
20150406@650	UWA-1 G2							20.704	0.236			

Analysis #	Sample	Line #	Diagenesis*				Bias (α)	$\delta^{18}O_{RAW}$‰	±2 SE	$\delta^{18}O_{COR}$‰	±2 SD	Distance from edge
			SEM	CLFM								
				GR	RD	FRD	A	B	C	D	E	of enamel (µm)
20150406@651	UWA-1 G2							20.530	0.241			
20150406@652	UWA-1 G2							20.697	0.180			
20150406@653	UWA-1 G2							20.805	0.254			
Average and ±2 SD								**20.684**	**0.228**			
Bracket: Average and ±2 SD							**1.0078**	**20.608**	**0.239**			
Enamel												
20150406@654	4908a3-009	1			**x**	**x**		32.141	0.275	24.12	0.45	1183
20150406@655	4908a3-010	1			**x**	**x**		32.010	0.237	23.99	0.45	1149
20150406@656	4908a3-011	1			**x**	**x**		30.880	0.247	22.86	0.45	1133
20150406@657	4908a3-012	1			**x**	**x**		30.162	0.295	22.15	0.45	1120
20150406@658	4908a3-013	1						30.645	0.269	22.63	0.45	871
20150406@659	4908a3-014	1						31.794	0.327	23.77	0.45	625
20150406@660	4908a3-015	1						31.815	0.243	23.79	0.45	685
20150406@661	4908a3-016	1						31.671	0.302	23.65	0.45	715
20150406@662	4908a3-017	1						30.838	0.261	22.82	0.45	730
20150406@663	4908a3-018	1						31.576	0.247	23.55	0.45	385
20150406@664	4908a3-019	1			**x**	**x**		31.301	0.225	23.28	0.45	145
UWA-1												
20150406@665	UWA-1 G2							20.306	0.182			
20150406@666	UWA-1 G2							20.349	0.275			
20150406@667	UWA-1 G2; Cs res 190-191							20.751	0.267			
20150406@668	UWA-1 G2							20.950	0.233			
Average and ±2 SD								**20.589**	**0.626**			
Bracket: Average and ±2 SD							**1.0078**	**20.637**	**0.448**			
Enamel												
20150406@669	4908a3-020	2	**SEM**	**x**	**x**	**x**		29.670	0.310	21.68	0.47	30
20150406@670	4908a3-021	2			**x**	**x**		31.400	0.242	23.40	0.47	270

Analysis #	Sample	Line #	Diagenesis* SEM	CLFM GR	CLFM RD	CLFM FRD	Bias (α) A	$\delta^{18}O_{RAW}$‰ B	±2 SE C	$\delta^{18}O_{COR}$‰ D	±2 SD E	Distance from edge of enamel (µm)
20150406@671	4908a3-022	2			x	x		32.434	0.226	24.42	0.47	750
20150406@672	4908a3-023	2			x	x		29.537	0.234	21.55	0.47	1230
20150406@673	4908a3-024	2		x	x	x		29.896	0.206	21.91	0.47	1380
20150406@674	4908a3-025	2						31.752	0.226	23.75	0.47	997
20150406@675	4908a3-026	2						30.280	0.191	22.29	0.47	1117
20150406@676	4908a3-027	2						31.912	0.227	23.91	0.47	510
20150406@677	4908a3-028	2				x		32.352	0.190	24.34	0.47	630
20150406@678	4908a3-029	2						32.214	0.369	24.21	0.47	870
UWA-1												
20150406@679	UWA-1 G2							~~21.363~~	~~0.234~~			
20150406@680	UWA-1 G2							20.569	0.295			
20150406@681	UWA-1 G2							20.790	0.217			
20150406@682	UWA-1 G2							20.618	0.191			
Average and ±2 SD								**20.659**	**0.232**			
Bracket: Average and ±2 SD							**1.0078**	**20.619**	**0.469**			
Enamel												
20150406@683	4908a3-030	3		x	x			31.235	0.219	23.13	0.49	30
20150406@684	4908a3-031	3						31.951	0.195	23.84	0.49	510
20150406@685	4908a3-032	3						30.825	0.313	22.73	0.49	990
20150406@686	4908a3-033	3			x	x		30.305	0.223	22.21	0.49	1230
20150406@687	4908a3-034	3						32.278	0.388	24.17	0.49	750
20150406@688	4908a3-035	3		x	x	x		31.749	0.281	23.64	0.49	330
20150406@689	4908a3-036	3						31.911	0.240	23.80	0.49	870
20150406@690	4908a3-037	3			x			29.456	0.134	21.37	0.49	1290
20150406@691	4908a3-038	3		x	x			29.687	0.246	21.60	0.49	1110
20150406@692	4908a3-039	3		x	x	x		30.470	0.262	22.37	0.49	1170
20150406@693	4908a3-040	3		x	x	x		31.187	0.244	23.09	0.49	180
20150406@694	4908a3-041	2		x	x	x		30.907	0.176	22.81	0.49	150

Analysis #	Sample	Line #	Diagenesis* SEM	CLFM GR	CLFM RD	CLFM FRD	Bias (α) A	$\delta^{18}O_{RAW}$‰ B	±2 SE C	$\delta^{18}O_{COR}$‰ D	±2 SD E	Distance from edge of enamel (µm)
UWA-1												
20150406@695	UWA-1 G2							21.223	0.233			
20150406@696	UWA-1 G2							20.508	0.257			
20150406@697	UWA-1 G2							20.580	0.351			
20150406@698	UWA-1 G2							20.742	0.275			
Average and ±2 SD								**20.763**	**0.643**			
Bracket: Average and ±2 SD							**1.0079**	**20.719**	**0.487**			
Sample: 4857.1 (Deinotheriidae) with UWA-1.												
UWA-1												
20150406@495	UWA-1 G2							23.685	0.202			
20150406@496	UWA-1 G3							23.984	0.266			
20150406@497	UWA-1 G1							23.833	0.237			
20150406@498	UWA-1 G1							23.788	0.251			
Average and ±2 SD								**23.823**	**0.248**			
Enamel												
20150406@499	4857.1-001	1	**SEM**					29.701	0.215	18.48	0.43	25
20150406@500	4857.1-002	1		**x**		**x**		30.520	0.182	19.29	0.43	265
20150406@501	4857.1-003	1						32.231	0.291	20.99	0.43	505
20150406@502	4857.1-004	1						32.326	0.295	21.08	0.43	745
20150406@503	4857.1-005	1						32.651	0.286	21.40	0.43	985
20150406@504	4857.1-006	1						32.851	0.275	21.60	0.43	1225
20150406@505	4857.1-007	1						31.894	0.368	20.65	0.43	1465
20150406@506	4857.1-008	1						30.997	0.229	19.77	0.43	1705
20150406@507	4857.1-009	1				**x**		30.610	0.257	19.38	0.43	1945
UWA-1												
20150406@508	UWA-1 G1							23.889	0.280			

Analysis #	Sample	Line #	Diagenesis* SEM	CLFM GR	CLFM RD	CLFM FRD	Bias (α) A	$\delta^{18}O_{RAW}$‰ B	±2 SE C	$\delta^{18}O_{COR}$‰ D	±2 SD E	Distance from edge of enamel (µm)
20150406@509	UWA-1 G1							23.518	0.225			
20150406@510	UWA-1 G1							24.247	0.230			
20150406@511	UWA-1 G1							23.877	0.217			
Average and ±2 SD								**23.883**	**0.595**			
Bracket: Average and ±2 SD							**1.0110**	**23.853**	**0.427**			
Enamel												
20150406@512	4857.1-010	1				**x**		31.554	0.239	20.19	0.49	2185
20150406@513	4857.1-011	1		**x**	**x**	**x**		32.688	0.294	21.31	0.49	2365
20150406@514	4857.1-012	1						32.140	0.177	20.77	0.49	385
20150406@515	4857.1-013	1						31.482	0.221	20.12	0.49	145
20150406@516	4857.1-014	2						31.188	0.258	19.83	0.49	120
20150406@517	4857.1-015	2						31.548	0.336	20.18	0.49	360
20150406@518	4857.1-016	2						32.352	0.237	20.98	0.49	840
20150406@519	4857.1-017	2						32.711	0.224	21.33	0.49	1320
20150406@520	4857.1-018	2						31.360	0.273	20.00	0.49	1800
20150406@521	4857.1-019	2						30.875	0.275	19.52	0.49	2280
20150406@522	4857.1-020	2			**x**	**x**		31.719	0.247	20.35	0.49	2760
20150406@523	4857.1-021	2			**x**	**x**		31.938	0.291	20.57	0.49	2970
20150406@524	4857.1-022	2			**x**			31.284	0.274	19.92	0.49	2520
20150406@525	4857.1-023	2						31.247	0.211	19.88	0.49	2040
20150406@526	4857.1-024	2						32.088	0.244	20.72	0.49	1560
20150406@527	4857.1-025	2						32.363	0.179	20.99	0.49	1080
20150406@528	4857.1-026	2						32.600	0.176	21.22	0.49	570
UWA-1												
20150406@529	UWA-1 G2							24.081	0.238			
20150406@530	UWA-1 G2							24.132	0.206			
20150406@531	UWA-1 G2							24.234	0.180			
20150406@532	UWA-1 G2							23.878	0.156			

Analysis #	Sample	Line #	Diagenesis*				Bias (α)	$\delta^{18}O_{RAW}$‰	±2 SE	$\delta^{18}O_{COR}$‰	±2 SD	Distance from edge of enamel (µm)
			SEM	CLFM								
				GR	RD	FRD	A	B	C	D	E	
Average and ±2 SD								**24.081**	**0.299**			
Bracket: Average and ±2 SD							**1.0111**	**23.982**	**0.485**			

A: Insturmental bias, which is calculated as $\alpha = (1+\delta^{18}O_{RAW}/1000)/(1+\delta^{18}O_{STD}/1000)$

B: SIMS raw measured $^{18}O/^{16}O$ ratios, converted to delta notation

C: Internal error of a single analysis (per analysis n = 20)

D: Corrected $\delta^{18}O$, corrected for instrumental bias (based on UWA-1 standard)

E: Standard deviation for individual sample within a standard bracket

Strickthrough text indicates samples considered outliers due to relative yield analysis (statistically determined as Tukey Outliers)

* SEM indicate pits not included in the diagenesis analysis due to irregular pits

References

Armstrong W. 1963. The presence of ultra violet absorbing material and its relation to fluorescence "quenching" effects in carious dentine. Archives of Oral Biology 8(2):223-231.

Aubert M, Williams IS, Boljkovac K, Moffat I, Moncel M-H, Dufour E, and Grün R. 2012. In situ oxygen isotope micro-analysis of faunal material and human teeth using a SHRIMP II: a new tool for palaeo-ecology and archaeology. Journal of Archaeological Science 39(10):3184-3194.

Beasley MM, Martinez A, Simons D, and Bartelink EJ. 2013. Paleodietary analysis of a San Francisco Bay Area shellmond: stable carbon and nitrogen analysis of late Holocene humans from the Ellis Landing site (CA-CCO-295). Journal of Archaeological Science 40:2084-2094.

Blumenthal SA, Cerling TE, Chritz KL, Bromage TG, Kozdon R, and Valley JW. 2014. Stable isotope time-series in mammalian teeth: in situ $\delta^{18}O$ from the innermost enamel layer. Geochimica et Cosmochimica Acta 124:223-236.

Bobe R. 2011. Fossil Mammals and Paleoenvironments in the Omo-Turkana Basin. Evolutionary Anthropology: Issues, News, and Reviews 20(6):254-263.

Boyde A, Fortelius M, Lester K, and Martin L. 1988. Basis of the structure and development of mammalian enamel as seen by scanning electron microscopy. Scanning Microscopy 2:1479-1490.

Brown FH, and McDougall I. 2011. Geochronology of the Turkana depression of northern Kenya and southern Ethiopia. Evolutionary Anthropology: Issues, News, and Reviews 20(6):217-227.

Bryant JD, Koch PL, Froelich PN, Showers WJ, and Genna BJ. 1996. Oxygen isotope partitioning between phosphate and carbonate in mammalian apatite. Geochimica et Cosmochimica Acta 60(24):5145-5148.

Buchalla W. 2005. Comparative fluorescence spectroscopy shows differences in noncavitated enamel lesions. Caries Research 39(2):150-156.

Cerling TE, Manthi FK, Mbua EN, Leakey LN, Leakey MG, Leakey RE, Brown FH, Grine FE, Hart JA, and Kaleme P. 2013. Stable isotope-based diet reconstructions of Turkana Basin hominins. Proceedings of the National Academy of Sciences 110(26):10501-10506.

Coble PG. 1996. Characterization of marine and terrestrial DOM in seawater using excitation-emission matrix spectroscopy. Marine Chemistry 51(4):325-346.

Dean M. 1987. Growth layers and incremental markings in hard tissues; a review of the literature and some preliminary observations about enamel structure in *Paranthropus boisei*. Journal of Human Evolution 16(2):157-172.

DeNiro M, and Epstein S. 1976. You are what you eat (plus a few per mil): the carbon isotope cycle in food chains. Program Abstracts Geological Society of America Annual Meeting 8:834-835.

DeNiro MJ, and Epstein S. 1978. Influence of Diet on Distribution of Carbon Isotopes in Animals. Geochimica et Cosmochimica Acta 42(5):495-506.

DeNiro MJ, and Epstein S. 1981. Influence of Diet on the Distribution of Nitrogen Isotopes in Animals. Geochimica et Cosmochimica Acta 45(3):341-351.

Duschner H, Gotz H, Walker R, and Lussi A. 2000. Erosion of dental enamel visualized by confocal laser microscopy. In: Addy M, Embery G, Edgar W, and Orchardson R, editors. Tooth Wear and Sensitivity. London: Martin Dunitz. p 67-73.

Feibel CS. 2011. A geological history of the Turkana Basin. Evolutionary Anthropology: Issues, News, and Reviews 20(6):206-216.

Foley R. 1993. The influence of seasonality on hominid evolution. In: Ulijaszek S, and Strickland S, editors. Seasonality and Human Ecology. Cambridge: Cambridge University Press. p 17-37.

Fricke HC, and O'Neil JR. 1996. Inter-and intra-tooth variation in the oxygen isotope composition of mammalian tooth enamel phosphate: implications for palaeoclimatological and palaeobiological research. Palaeogeography, Palaeoclimatology, Palaeoecology 126(1):91-99.

Garcia-Herraiz A, Leiva-Garcia R, Sailvestre F, and Garcia-Anton J. 2012. Applications of Confocal Laser Scanning Microscopy in Dentistry: Study of the changes of the post-extraction sites. In: Mendez-Vilas A, editor. Current Microscopy Contributions to Advances in Science and Technology. Badajoz: Formatex. p 569-581.

Garvie-Lok SJ, Varney TL, and Katzenberg MA. 2004. Preparation of Bone Carbonate for Stable Isotope Analysis: The Effects of Treatment Time and Acid Concentration. Journal of Archaeological Science 31(6):763-776.

Glasser J, and Fonda GR. 1938. The fluorescence of double salts of calcium phosphate. Journal of the American Chemical Society 60(3):722-722.

Götz H, Duschner H, White DJ, and Klukowska MA. 2007. Effects of elevated hydrogen peroxide ‘strip’bleaching on surface and subsurface enamel including subsurface histomorphology, micro-chemical composition and fluorescence changes. Journal of Dentistry 35(6):457-466.

Gustafson G, and Gustafson A. 1967. Microanatomy and histochemistry of enamel. In: Miles A, editor. The Structural and Chemical Organization of Teeth. New York: Academic Press. p 75-134.

Haas H, and Banewicz J. 1980. Radiocarbon dating of bone apatite using thermal release of CO^2. Radiocarbon 22(2):537-544.

Hall J, Hefferren J, and Olsen N. 1970. Study of Fluorescent Characteristics of Extracted Human Teeth by use of a Clinical Fluorometer. Journal of Dental Research 49:1431.

Hartles R, and Leaver A. 1953. The fluorescence of teeth under ultraviolet irradiation. Biochemical Journal 54(4):632.

Hedges REM, Lee-Thorp J, and Tuross N. 1995. Is tooth enamel carbonate a suitable material for radiocarbon dating? Radiocarbon 37(2):417-429.

Hefferren JJ, Cooley RO, Hall JB, Olsen NH, and Lyon HW. 1971. Use of ultraviolet illumination in oral diagnosis. The Journal of the American Dental Association 82(6):1353-1360.

Hillson S. 2005. Teeth, Second Editon. Cambridge: Cambridge University Press.

Horibe H, Katsura S, Fujimori K, and Yamada M. 1974. Multiple distribution of the fluorescence in human teeth. Acta Histochemica et Cytochemica 7(4):334-341.

Iacumin P, Bocherens H, Mariotti A, and Longinelli A. 1996. An isotopic palaeoenvironmental study of human skeletal remains from the Nile Valley. Palaeogeography Palaeoclimatology Palaeoecology 126(1-2):15-30.

Jacques L, Ogle N, Moussa I, Kalin R, Vignaud P, Brunet M, and Bocherens H. 2008. Implications of diagenesis for the isotopic analysis of Upper Miocene large mammalian herbivore tooth enamel from Chad. Palaeogeography, Palaeoclimatology, Palaeoecology 266(3):200-210.

Kellner C, and Schoeninger M. 2007. A Simple Carbon Isotope Model for Reconstructing Prehistoric Human Diet. American Journal of Physical Anthropology 133:1112-1127.

Kingston JD. 2005. Orbital controls on seasonality. Cambridge Studies In Biologocal and Evolutionary Anthropology 1(44):519-542.

Kita N, Huberty J, Kozdon R, Beard B, and Valley J. 2011. High-precision SIMS oxygen, sulfur and iron stable isotope analyses of geological materials: accuracy, surface topography and crystal orientation. Surface and Interface Analysis 43(1-2):427-431.

Kita NT, Ushikubo T, Fu B, and Valley JW. 2009. High precision SIMS oxygen isotope analysis and the effect of sample topography. Chemical Geology 264(1):43-57.

Koch PL, Tuross N, and Fogel ML. 1997. The Effects of Sample Treatment and Diagenesis on the Isotopic Integrity of Carbonate in Biogenic Hydroxylapatite. Journal of Archaeological Science 24(5):417-429.

Koenig K, Hibst R, Meyer H, Flemming G, and Schneckenburger H. 1993. Laser induced auto-fluorescence of carious regions of human teeth and caries-involved bacteria. Proceedings of SPIE, Dental Applications of Lasers 2080:170-180.

Kohn MJ, Schoeninger MJ, and Barker WW. 1999. Altered states: Effects of diagenesis on fossil tooth chemistry. Geochimica et Cosmochimica Acta 63(18):2737-2747.

Kohn MJ, Schoeninger MJ, and Valley JW. 1998. Variability in oxygen isotope compositions of herbivore teeth: reflections of seasonality or developmental physiology? Chemical Geology 152(1-2):97-112.

Kolodny Y, Bar-Matthews M, Ayalon A, and McKeegan KD. 2003. A high spatial resolution $\delta^{18}O$ profile of a speleothem using an ion-microprobe. Chemical Geology 197(1):21-28.

Kolodny Y, Luz B, and Navon O. 1983. Oxygen isotope variations in phosphate of biogenic apatites, I. Fish bone apatite - rechecking the rules of the game. Earth and Planetary Science Letters 64:398-404.

Krueger HW. 1991. Exchange of Carbon with Biological Apatite. Journal of Archaeological Science 18(3):355-361.

Lambert JB, Weydert JM, Williams SR, and Buikstra JE. 1990. Comparison of Methods for the Removal of Diagenetic Material in Buried Bone. Journal of Archaeological Science 17(4):453-468.

Leakey MG, Feibel CS, McDougall I, and Walker A. 1995. New four-million-year-old hominid species from Kanapoi and Allia Bay, Kenya. Nature 376(6541):565-571.

Leakey MG, Feibel CS, McDougall I, Ward C, and Walker A. 1998. New specimens and confirmation of an early age for *Australopithecus anamensis*. Nature 393(6680):62-66.

Lee-Thorp J. 2002. Two decades of progress towards understanding fossilization processes and isotopic signals in calcified tissue minerals. Archaeometry 44:435-446.

Lee-Thorp J, Likius A, Mackaye HT, Vignaud P, Sponheimer M, and Brunet M. 2012. Isotopic evidence for an early shift to C_4 resources by Pliocene hominins in Chad. Proceedings of the National Academy of Sciences 109(50):20369-20372.

Lee-Thorp J, and Sponheimer M. 2003a. Three Case Studies Used to Reassess the Reliability of Fossil Bone and Enamel Isotope Signals for Paleodietary Studies. Journal of Anthropological Archaeology 22(3):208-216.

Lee-Thorp J, and van der Merwe NJ. 1987. Carbon isotope analysis of fossil bone apatite. South African Journal of Science 83:712-713.

Lee-Thorp JA. 2000. Preservation of biogenic carbon isotopic signals in Plio-Pleistocene bone and tooth mineral. In: Ambrose SH, and Katzenberg MA, editors. Biogeochemical Approaches to Paleodietary Analysis. New York: Kluwer Academic/Plenum Publishers. p 89-115.

Lee-Thorp JA, and Sponheimer M. 2003b. Three case studies used to reassess the reliability of fossil bone and enamel isotope signals for paleodietary studies. Journal of Anthropological Archaeology 22:298-216.

Lee-Thorp JA, and van der Merwe NJ. 1991. Aspects of the chemistry of modern and fossil biological apatites. J Archaeol Sci 18(3):343-354.

LeGeros R, and Tung M. 1983. Chemical stability of carbonate-and fluoride-containing apatites. Caries Research 17(5):419-429.

LeGeros RZ. 1981. Apatites in biological systems. Progress in Crystal Growth and Characterization 4(1):1-45.

LeGeros RZ, LeGeros JP, Trautz OR, and Shirra WP. 1971. Conversion of monetite, $CaHPO_4$, to apatites: effect of carbonate on the crystallinity and the morphology of the apatite crystallites. Advances in X-ray Analysis 14:57-66.

Levin NE, Haile-Selassie Y, Frost SR, and Saylor BZ. 2015. Dietary change among hominins and cercopithecids in Ethiopia during the early Pliocene. Proceedings of the National Academy of Sciences 112(40):12304-12309.

Longinelli A. 1966. Ratios of Oxygen-18 : Oxygen-16 in Phosphate and Carbonate from Living and Fossil Marine Organisms. Nature 211(5052):923-927.

Longinelli A. 1984. Oxygen isotopes in mammal bone phosphate: A new tool for paleohydrological and paleoclimatological research? Geochimica et Cosmochimica Acta 48:385-390.

Longinelli A, and Nuti S. 1973. Oxygen isotope measurements of phosphate from fish teeth and bones. Earth and Planetary Science Letters 20:337-340.

Mancewicz SA, and Hoerman K. 1964. Characteristics of insoluble protein of tooth and bone—I Fluorescence of some acidic hydrolytic fragments. Archives of Oral Biology 9(5):535IN535-544.

McConnell G, Girkin J, Ameer-Beg S, Barber P, Vojnovic B, Ng T, Banerjee A, Watson T, and Cook R. 2007. Time-correlated single-photon counting fluorescence lifetime confocal imaging of decayed and sound dental structures with a white-light supercontinuum source. Journal of Microscopy 225(2):126-136.

McGarry SF, and Baker A. 2000. Organic acid fluorescence: applications to speleothem palaeoenvironmental reconstruction. Quaternary Science Reviews 19(11):1087-1101.

Moore J. 1996. Savanna chimpanzees, referential models and the last common ancestor. In: McGrew WC, Marchant LF, and Nishida T, editors. Great Ape Societies. Cambridge: Cambridge University Press. p 275-292.

Moreno E, Kresak M, and Zahradnik R. 1977. Physicochemical aspects of fluoride-apatite systems relevant to the study of dental caries. Caries Research 11(Suppl. 1):142-171.

Nelson BK, Deniro MJ, Schoeninger MJ, Depaolo DJ, and Hare PE. 1986. Effects of Diagenesis on Strontium, Carbon, Nitrogen and Oxygen Concentration and Isotopic Composition of Bone. Geochimica et Cosmochimica Acta 50(9):1941-1949.

Nelson SV. 2005. Paleoseasonality inferred from equid teeth and intra-tooth isotopic variability. Palaeogeography, Palaeoclimatology, Palaeoecology 222(1):122-144.

Nielsen-Marsh CM, and Hedges REM. 2000a. Patterns of Diagenesis in Bone I: The Effects of Site Environments. Journal of Archaeological Science 27:1139-1150.

Nielsen-Marsh CM, and Hedges REM. 2000b. Patterns of Diagenesis in Bone II: Effects of Acetic Acid Treatment and the Removal of Diagenetic CO^2_3-. Journal of Archaeological Science 27:1151-1159.

Orland IJ, Bar-Matthews M, Kita NT, Ayalon A, Matthews A, and Valley JW. 2009. Climate deterioration in the Eastern Mediterranean as revealed by ion microprobe analysis of a speleothem that grew from 2.2 to 0.9 ka in Soreq Cave, Israel. Quaternary Research 71(1):27-35.

Potts R. 1998. Environmental hypotheses of hominin evolution. American Journal of Physical Anthropology 107(s27):93-136.

Reed KE, and Fish JL. 2005. Tropical and temperate seasonal influences on human evolution. In: Brockman D, and Van Schaik C, editors. Seasonality in primates: studies of living and extinct human and non-human primates. Cambridge: Cambridge University Press. p 489-518.

Scherer M, and Seitz H. 1980. Rare-earth element distribution in Holocene and Pleistocene corals and their redistribution during diagenesis. Chemical Geology 28:279-289.

Schoeninger MJ, and Deniro MJ. 1982a. Carbon Isotope Ratios of Apatite from Fossil Bone Cannot Be Used to Reconstruct Diets of Animals. Nature 297(5867):577-578.

Schoeninger MJ, and Deniro MJ. 1982b. Diagenetic Effects on Stable Isotope Ratios in Bone Apatite and Collagen. American Journal of Physical Anthropology 57(2):225-225.

Schoeninger MJ, and Deniro MJ. 1983. Carbon Isotope Ratios of Bone Apatite and Animal Diet Reconstruction - Reply. Nature 301(5896):178-178.

Schoeninger MJ, Hallin K, Reeser H, Valley JW, and Fournelle J. 2003. Isotopic alteration of mammalian tooth enamel. International Journal of Osteoarchaeology 13(1-2):11-19.

Senesi N, Miano TM, Provenzano MR, and Brunetti G. 1991. Characterization, differentiation, and classification of humic substances by fluorescence spectroscopy. Soil Science 152(4):259-271.

Sillen A. 1986. Biogenic and diagenetic Sr/Ca in Plio-Pleistocene fossils of the Omo Shangura Formation. Paleobiology 12:311-323.

Sillen A. 1989. Diagenesis of the inorgainc phase of cortical bone. In: Price TD, editor. The Chemistry of Prehistoric Human Bone. London: Cambridge University Press. p 211-229.

Sillen A, and LeGeros R. 1991. Solubility Profiles of Synthetic Apatites and of Modern and Fossil Bones. Journal of Archaeological Science 18(3):385-397.

Sillen A, Sealy JC, and van der Merwe NJ. 1989. Chemistry and Paleodietary Research: No More Easy Answers. American Antiquity 54(3):504-512.

Spitzer D, and Ten Bosch J. 1976. The total luminescence of bovine and human dental enamel. Calcified Tissue Research 20(1):201-208.

Sponheimer M, and Lee-Thorp JA. 1999. Alteration of enamel carbonate environments during fossilization. Journal of Archaeological Science 26(2):143-150.

Sullivan CH, and Krueger HW. 1981. Carbon Isotope Analysis of Separate Chemical Phases in Modern and Fossil Bone. Nature 292(5821):333-335.

Sullivan CH, and Krueger HW. 1983. Carbon Isotope Ratios of Bone Apatite and Animal Diet Reconstruction. Nature 301(5896):177-177.

Surovell T. 2000. Radiocarbon dating of bone apatite by step heating. Geoarchaeology 15(6):591-608.

Tafforeau P, Bentaleb I, Jaeger J-J, and Martin C. 2007. Nature of laminations and mineralization in rhinoceros enamel using histology and X-ray synchrotron microtomography: potential implications for palaeoenvironmental isotopic studies. Palaeogeography, Palaeoclimatology, Palaeoecology 246(2):206-227.

Taubinsky I, Alexandrov M, Koz'ma SY, and Chernyi V. 2000. Prospects for applying fluorescence spectroscopy to diagnose the hard tissues of a tooth. Critical Reviews in Biomedical Engineering 28(5&6):137-144.

Treble P, Schmitt AK, Edwards R, McKeegan KD, Harrison T, Grove M, Cheng H, and Wang Y. 2007. High resolution Secondary Ionisation Mass Spectrometry (SIMS) $\delta^{18}O$ analyses of Hulu Cave speleothem at the time of Heinrich Event 1. Chemical Geology 238(3):197-212.

Valeur B, and Berberan-Santos MN. 2012. Molecular fluorescence: principles and applications. Germany: John Wiley & Sons.

Valley JW, Kinny PD, Schulze DJ, and Spicuzza MJ. 1998. Zircon megacrysts from kimberlite: oxygen isotope variability among mantle melts. Contributions to Mineralogy and Petrology 133(1-2):1-11.

Valley JW, and Kita NT. 2009. *In situ* oxygen isotope geochemistry by ion microprobe. Secondary Ion Mass Spectrometry in the Earth Sciences (MAC Short Course) Canada: Mineralogical Association of Canada. p 19-63.

van der Merwe NJ, and Vogel JC. 1978. ^{13}C Content of Human Collagen as a Measure of Prehistoric Diet in Woodland North America. Nature 276:815-816.

Vogel JC, and van der Merwe NJ. 1977. Isotopic Evidence for Early Maize Cultivation in New York State. American Antiquity 42:238-242.

Wang Y, and Cerling TE. 1994. A Model of Fossil Tooth and Bone Diagenesis - Implications for Paleodiet Reconstruction from Stable Isotopes. Palaeogeography Palaeoclimatology Palaeoecology 107(3-4):281-289.

Weidel BC, Ushikubo T, Carpenter SR, Kita NT, Cole JJ, Kitchell JF, Pace ML, and Valley JW. 2007. Diary of a bluegill (*Lepomis macrochirus*): daily $\delta^{13}C$ and $\delta^{18}O$ records in otoliths by ion microprobe. Canadian Journal of Fisheries and Aquatic Sciences 64(12):1641-1645.

White TD, Ambrose SH, Suwa G, Su DF, DeGusta D, Bernor RL, Boisserie J-R, Brunet M, Delson E, Frost S et al. . 2009. Macrovertebrate Paleontology and the Pliocene Habitat of *Ardipithecus ramidus*. Science 326(5949):67-93.

Wood B, and Leakey M. 2011. The Omo-Turkana Basin Fossil Hominins and Their Contribution to Our Understanding of Human Evolution in Africa. Evolutionary Anthropology: Issues, News, and Reviews 20(6):264-292.

Wright LE, and Schwarcz HP. 1996. Infrared and Isotopic Evidence for Diagenesis of Bone Apatite at Dos Pilas, Guatemala: Palaeodietary Implications. Journal of Archaeological Science 23(6):933-944.

Yoder C, and Bartelink EJ. 2010. Effects of different sample preparation methods of stable carbon and oxygen isotope values of bone apatite: A comparison of two treatment protocols. Archaeometry 52(1):115-130.

Yuretich RF. 1979. Modern sediments and sedimentary processes in Lake Rudolf (Lake Turkana) eastern Rift Valley, Kenya. Sedimentology 26(3):313-331.

Zazzo A. 2014. Bone and enamel carbonate diagenesis: a radiocarbon prospective. Palaeogeography, Palaeoclimatology, Palaeoecology 416:168-178.

Zazzo A, Lecuyer C, and Mariotti A. 2004. Experimentally-controlled carbon and oxygen isotope exchange between bioapatites and water under inorganic and microbially-mediated conditions. Geochimica et Cosmochimica Acta 68(1):1-12.

CHAPTER 4: SEASONALITY AND ADAPTIVE FLEXIBILITY IN EARLY HOMININS AT ALLIA BAY, KENYA 3.97 MA

Introduction

The environment has long been thought to have played a significant role in human evolution because fluctuations in climate would affect resource availability, such that expanding grasslands would result in different selective pressures acting on early hominins than on the last common ape-human ancestor (deMenocal 2011; Isbell and Young 1996). Foley (1995) explained this as the environment of evolutionary adaptedness linking, for example, the expanding grassland to the origins of bipedalism. However, the initiation of the expanding grasslands in East Africa at 8 to 6 Ma (Cerling et al. 1997) predates the emergence of the *Australopithecus* genus, which is associated with obligate bipedal locomotion (Grine et al. 2006). It seems that the major shift towards a more arid environment occurred later in the Pliocene at around 3.2 Ma and the major changes in faunal turnover occurred 3.0 to 2.0 Ma, which is more than one million years after the first appearance datum (FAD) of *Australopithecus* (Behrensmeyer et al. 1997; deMenocal 1995; deMenocal 2004; Grine et al. 2006; Reed 1997; Vrba et al. 1995; Vrba 1988). Based on faunal assemblage data, it has been suggested that *Australopithecus* inhabited relatively more wooded regions and that *Homo* was the first in our lineage to exploit completely open habitats; if true, then the opening of habitats possibly contributed to the demise rather than the success of the earliest hominins (Bobe and Behrensmeyer 2004; Reed 1997). Additionally, the discovery of *Ardipithecus ramidus* (4.4 Ma) as the earliest facultative biped, which inhabited open woodlands not expanding savanna grasslands (White et al. 2009; see Cerling et al 2010 for alternative interpretation), now leaves the types of environments and ecological niches inhabited by our earliest facultative and, subsequently, obligate bipedal ancestors open to question.

In extant nonhuman primates, seasonal patterns of aridity, day length, temperature, and food availability greatly impact reproduction, social life, life history patterns, and behavioral

ecology (Brockman and van Schaik 2005). Seasonality has been implicated as a key factor in the evolution of humans as well (Foley 1993; Kingston 2005; Moore 1996; Nelson 2005; Potts 1998a; Reed and Fish 2005). Reed and Fish (2005) suggest that some early *Australopithecus* and *Paranthropus* species may have switched their foraging effort to underground storage organs (USOs) during longer dry seasons because in response to drought, some plants will store energy (higher caloric value) in USOs instead of producing leaves, shoots, and fruits (Archibold 1995). Therefore, it is critical to determine the full range of variability in the patterns of rainfall at specific fossil localities in order to better understand the ecology and habitat in regions where bipedalism was successful. Recent studies reviewed by Kingston (2007) highlight that short-term ecological changes (e.g., shifts in seasonal precipitation) might match or even exceed the influence of long-term changes on evolution; assuming this is correct, then it is no longer reasonable to frame human evolution within long-term global or regional trends, but instead the focus must be on smaller, more local sites and time scales.

Paleoenvironmental reconstructions in East Africa often rely on surface-collected fossil fauna that combine multiple temporal and geographically dispersed components that are not *in situ*. Therefore, hypotheses that attempt to explain human evolution in the context of environmental and ecological change focus on large regions and long geologic time scales (thousands to millions of years) (Grine 1986; Hewes 1961; Hunt 1994; Isbell and Young 1996; Kingdon 2003; Kingston 2007; Rayner et al. 1993). This framework lacks the temporal-spatial resolution to develop solid causal links between evolution and the environment (Kingston 2007). Traditional bulk isotopic analysis of tooth enamel distinguishes open from closed ($\delta^{13}C$) and arid from humid ($\delta^{18}O$) habitats of individual animals, but at too large a scale (i.e., aggregates multiple years) to explain the adaptive flexibility of early hominins to ecological variables like seasonality. Recent work has suggested that environmental conditions vary across a wide range of time scales (Potts 2012), including intra-annual seasons. Traditional bulk serial isotopic sampling along the

growth axis of larger mammal teeth can aggregate long time periods depending of the tooth size and duration of enamel formation, such sampling requires the destruction of much of a single tooth or multiple teeth for smaller mammals. Unfortunately, much of the enamel material available for destructive isotopic analysis from fossil localities is fragmented material not complete teeth or tooth rows and it is difficult to serial sample fragments using traditional bulk methods for evaluating seasonal patterns of $\delta^{18}O$. This study is the first to apply secondary ion mass spectrometry (SIMS) analysis to fossil fauna enamel fragments from a hominin locality to generate $\delta^{18}O$ seasonal patterns recorded in enamel at an intra-annual time scale (during the duration of enamel deposition of an individual animal). The high-resolution sampling capability of SIMS, with analysis spots 10 µm *in situ* (Valley and Kita 2009), provide a new scale of analysis for paleoenvironment reconstructions to address questions about seasonality and hominin evolution. The technique is especially well suited to the site of interest because the material consists of enamel fragments rather than whole teeth.

In the Omo-Turkana Basin, three sites have remains of *Australopithecus anamensis*, the earliest confirmed obligate hominin bipedal species. This hominin species has been recovered in association with Giraffidae, Elephantidae, Deinotheriidae, Hippopotamidae, Suidae, Equidae, and Bovidae (Leakey et al. 1995; Leakey et al. 1998), which suggests some form of mosaic habitat (Behrensmeyer and Reed 2013). At the site of Allia Bay, Kenya (3.97±0.03 Ma), the fossil fauna come from a single excavation locality (site 261-1) with good temporal resolution on the eastern shore of Lake Turkana in the Koobi Fora Region (Leakey et al. 1995; Leakey et al. 1998; Wood and Leakey 2011). A phylogenetic analysis supports the idea that the *Au. anamensis* specimens found at Allia Bay represent part of an anagenetically evolving lineage, that was a sudden transition from *Ardipithecus* and later gave rise to *Au. afarensis* (Haile-Selassie et al. 2010; Kimbel et al. 2006; White et al. 2006). Kimbel et al. (2006) suggest that each site-sample captures a different point along the evolutionary trajectory of early hominins. Therefore, teasing apart the

specifics of habitat type at the time of *Au. anamensis* is particularly important in order to understand the relationship between environment and the origins of obligate bipedalism.

Some researchers have suggested that the Turkana Basin has been a continuous arid environment over the past 4Ma (Cerling et al. 2015; Passey et al. 2010). Yet, traditional bulk $\delta^{13}C$ and $\delta^{18}O$ ratios of fossil fauna enamel suggest a very different environment compared to the modern Koobi Fora region (Schoeninger et al. 2003). Stable carbon isotope ratios from the fauna indicate a more mesic environment with more tree cover than today indicating that *Au. anamensis* could have had access to open woodland habitat rather than the open grass-brushland that exists in the region today (see Chapter 2 for discussion). Four paleosol samples from Allia Bay also have $\delta^{13}C$ values indicative of significant woody cover (>40%) (Levin et al. 2011). These results suggest a habitat similar to that put forth by White et al. (2009) for *Ardipithecus* and, as a consequence, the early occurrence of facultative and obligate bipedalism occurred in a woodland mosaic habitat that varied widely in the moisture availability but had significant canopy cover with patches of open space rather than an arid savanna grassland with few trees on the paleolandscape (suggested by Cerling et al. 2010). It also supports the hypothesis that selection for bipedalism in early hominins originated in an environment similar to modern Miombo woodlands (Moore 1996), which are wetter than the modern day arid Koobi Fora region.

Several studies have suggested that there is an increase in seasonality in the Late Miocene and early Pliocene, which would increase habitat diversity (Foley 1994; Kingston 2007; Macho et al. 2003). While traditional bulk $\delta^{13}C$ and $\delta^{18}O$ analysis of fossil enamel provide an overall average of habitat type, much of the detail required to test for seasonality is not possible because of the inherent difficulties in obtaining $\delta^{18}O$ values unaffected by diagenetic alteration (see chapter 3 for details). In order to test the idea of how marked seasonality changes at the origins of *Australopithecus* could have impacted the origins of the genus and morphological features such as bipedalism, we need higher-resolution sampling methods within individual teeth to avoid areas

in enamel affected by diagenesis to ensure biogenic values are obtained to understand the pattern of seasonal rainfall.

The SIMS technique generates such high-resolution $\delta^{18}O$ values recorded during enamel deposition that allow us to assess seasonal patterns in rainfall. At tropical latitudes (areas with limited fluctuations in temperature), the relationship between rainfall and $\delta^{18}O$ values indicate seasonal precipitation amount and duration can result in major shifts in vegetation within open habitats (i.e., savannas) but have limited impact to vegetation in forest ecosystems (Dansgaard 1964; Nelson 2005; Nelson 2007; Payne and Wilson 1999). Today, local temperatures have little intra-annual fluctuation, as expected in regions close to the equator, and the area is open and arid adjacent to Lake Turkana with one rainy season, which is recorded as lower enamel $\delta^{18}O$ values (Kohn et al. 1998, Meteorological Office 1983). Oxygen isotope ratios from enamel of non-drinking species (e.g., giraffes) track changes in relative humidity, while water-dependent species (e.g., hippos) track variation in meteoric water values, which correlate with precipitation amount in equatorial Africa (Kohn 1996; Kohn et al. 1996; Levin et al. 2006; Rozanski et al. 1992). An increase in seasonality, aridification (suggested by higher $\delta^{18}O$ values), and amount/duration of rainfall would favor more open habitats over closed forest habitats, so it is critical to reconstruct the paleoenvironments of early hominin sites at high-resolution scales of analyses to evaluate the interplay between habitat and human evolution.

Hominin evolution and paleoenvironment reconstructions

Many hypotheses about bipedalism, commonly associated with the origins of the hominin lineage, invoke a changing environment with an increase in savanna habitats and a loss of continuous tree cover (Feibel 1997; Grine 1986; Kingdon 2003; Potts 1998a; Vrba et al. 1995). Such hypotheses emphasize various selective forces as contributors to bipedal evolution, including efficiency in traveling terrestrially in an open environment where food resources are

widely distributed (Isbell and Young 1996; Niemitz 2010), the freeing of hands to gather and collect resources (Hewes 1961; Hunt 1994), and advantages of thermoregulation (Wheeler 1991). Variably characterized as hot/dry open landscapes (e.g. Cerling et al. 2010) or woodland landscapes interspersed with open grasslands and variable rainfall (e.g. Moore 1996), savanna habitats feature prominently in explanations for the origins of bipedalism. The Savanna Hypothesis posits that the last common ancestor of apes and humans inhabited forests and that hominin bipedalism is an adaptive response to expanding grassland savanna habitats (Bartholomew and Birdsell 1953; Dart 1925; Domínguez-Rodrigo 2014; Laporte and Zihlman 1983; Niemitz 2010). Alternatively, the Forest Hypothesis (Rayner et al. 1993), claims that the early stages of bipedal evolution occurred in more closed habitats, where scavenging opportunities would have been ideal (Blumenschine et al. 1987) and a terrestrial feeding posture would have been advantageous (Hunt 1994).

More recent interpretations of early hominin environments and the origins of bipedal locomotion, however, acknowledge the variation in environmental data and invoke terms such as mixed, mosaic, or fluctuating habitats (Kingston 2007; Kingston and Harrison 2007; Leakey et al. 2001; Potts 1996; Potts 1998b; Potts 2013). One of these, the Shifting Heterogeneity Model (Kingston 2007), highlights the complexity of early hominin habitats and argues that in response to variation of paleoprecipitation the patterns of environmental heterogeneity shifted, causing fluctuations in animal and plant communities over periods of tens of thousands of years (Kingston 2007). These periods of fluctuation would have occurred within the evolutionary history of a single hominin species, requiring flexibility to cope with changing habitats. Fluctuations in plant and animal species composition would result in dispersal of hominins into potentially novel or isolated ecosystems that created variable selective pressures, possibly favoring bipedal locomotion (Kingston 2007).

Studies of modern plant communities have shown that shifts in the timing of plant activities (i.e., growth seasons) are finely tuned to the seasonal shifts in precipitation and temperature, which in turn can be linked to shifts in global climate (Cleland et al. 2007). Plant phenology assesses the influence of seasonality on the periodic life cycles in plants. Recent research suggests that within tropical ecosystems, phenology is less sensitive to temperature and photoperiod changes, and more closely correlated with seasonal shifts in precipitation (Payne and Wilson 1999; Reich 1995; Walther et al. 2002). Assuming modern plant phenology can be used as analogues for past plant communities, paleoanthropologists should use datasets that reflect high-resolution, short-term time intervals in localities that contain hominin fossil material.

Mosaic habitats and *Au. anamensis*

Currently, *Au. anamensis* has been recovered at three fossil sites in the Omo-Turkana Basin (Allia Bay, Kanapoi, and Fejej) and possibly four sites in the Afar Rift of Ethiopia (Aramis, Asa Issie, Woranso-Mille and Galili). The hominin remains at Galili and Woranso-Mille are attributed to *Au. anamensis* by some authors, while others suggest further analysis is needed to confirm their species identification, but both localities will be included in this discussion of mosaic habitats (Behrensmeyer and Reed 2013; Ward 2014). If Kimbel et al. (2006) is correct that each site-sample captures a different point along the evolutionary trajectory of early hominins, then it is important to understand each paleoenvironment of the other six *Au. anamensis* fossil localities to understand the adaptive flexibility of the species. All seven sites have been generally described as mosaic habitats, but variation in canopy cover and moisture regimes (i.e., wet versus dry sites) highlight the idea that *Au. anamensis* was adaptively flexible in a variety of environments and does not appear to be confined to a specific ecological niche. However, within each mosaic habitat the patterns of seasonal rainfall are unknown and are a

critical variable to understand the shifting biomass availability (i.e., resources available to early hominins) on the paleolandscape.

- *Kanapoi, Kenya (4.17-4.07 Ma)(Leakey et al. 1995; Leakey et al. 1998)*: The paleoenvironment at Kanapoi is determined to be an arid to semi-arid climate with seasonal moisture in a mosaic of gallery forest to closed woodland opening into open grassland patches (Harris and Leakey 2003; Bobe 2011; Geraads et al. 2013; Wynn 2000). Paleosol data indicate a seasonal climate regime with paleoprecipitation estimated at approximately 620 ± 100 mm/year (1SD; Wynn 2004). Bobe (2011) suggests that Kanapoi was relatively dry and open based on the faunal assemblage and the patterns of cercopithecines to colobines at the site (3:1 ratio). A similar ratio of cercopithecines to colobines has been recovered at Allia Bay (Jablonski and Leakey 2008), but the bulk isotopic enamel fossil ungulate data suggests a mesic open woodland environment (see discussion Chapter 2).
- *Fejej, Ethiopia (4.18-4.00 Ma) (Kappelman et al. 1996; Van Couvering 2000; Ward 2014):* At Fejej, the paleoecology has not been published in detail but the fauna used to date the site indicate browsing (*Nyanzachoerus*) and grazing (*Hipparion* and Gompotheriidae) species were present in what was likely a mosaic habitat that was well-watered to accommodate Hippopotamidae and Crocodilia (Asfaw et al. 1991).
- *Asa Issie and Aramis, Ethiopia (4.2-4.1 Ma) (White et al. 2006):* Asa Issie and Aramis have been characterized as a woodland context with relatively few open habitat species present (White et al. 2006). Over half of the fossil taxa recovered at Asa Issie are tragelaphins and colobines, which indicate an environment with significant woodland or edge environments, whereas open habitat species like reduncins and alcelaphins are absent (White et al. 2006). At Asa Issie, the colobines outnumber the cercopithecines by approximately 6:1 and Aramis paleosol isotope data indicate a humid climate with only

25-35% C_4-grasses present on the landscape (White et al. 2006). The combination of woodland habit and edge environments opening into patches of savanna grassland indicated by the taxon list from the Asa Issie localities and the Aramis locality 14 paleosol isotope data at suggests that this mosaic habitat of *Au. anamensis* was likely much more densely covered compared to Allia Bay. The Allia Bay bovid bulk $\delta^{13}C$ carbon data indicates that there were pure C_4 grazers present, so some open ecological niches would have been present to sustain them.

- *Woranso-Mille, Ethiopia (3.8-3.57 Ma) (Haile-Selassie et al. 2010):* At Woranso-Mille in the Central Afar region, a very different mosaic habitat distribution can be interpreted compared to the nearby Asa Issie and Aramis localities. The identifiable fossil mammal assemblage at Woranso-Mille is dominated by cercopithecids and while colobines are present in the assemblage they are relatively rare (Frost et al. 2014; Haile-Selassie et al. 2007). This indicates the presence of tree-cover on the landscape but the dominate primate species is the terrestrial-grazing species, *Theropithecus oswaldi darti*, requiring a greater amount of open habitat in the region (Frost et al. 2014; Haile-Selassie et al. 2007). Similar to Asa Issie, the tragelaphines dominate the bovid species signaling a high degree of woodland habitat presence and woodland fringe dwelling species like aepycerotini are also present (Geraads et al. 2009; Haile-Selassie et al. 2007). However, unlike Asa Issie and Aramis, at Woranso-Mille reduncins and alcelaphins are rare but present indicating there are open areas of grassland savannas (Geraads et al. 2009; Haile-Selassie et al. 2007). Haile-Selassie et al. (2010) describes the mosaic habitat at Woranso-Mille as a riverine gallery forest that extends into woodland and grassland. Oxygen isotope data from fossil fauna indicate that the site is a wetter environment based on the relationship between aridity and the offset in $\delta^{18}O$ for giraffids and hippopotamids (Levin et al. 2015).

The faunal assemblage suggests it was possibly a wetter more open mosaic habitat compared to Allia Bay.

- *Galili (4.5-3.5 Ma) (Kullmer et al. 2008):* At Galili, the fossil fauna species indicate open woodland to bushland conditions and is described as having "major closed-wet habitats" (Kullmer et al. 2008). However, Galili is additionally described as having an environment similar to Kanapoi, which has an arid to semi-arid climate (Kullmer et al. 2008). The Galili fauna consists of grazing proboscideans and reduncins requiring open grasslands, but browsing rhinos, tragelaphins, and giraffe would also require significant tree-cover and woodlands (Behrensmeyer and Reed 2013).

The seven sites that have yielded *Au. anamensis* fossils all point to the species occupying a habitat defined as a mosaic of closed woodland to open grassland paleoenvironments. Wynn (2000) accurately notes that *Au. anamensis* thrived in a variety of mixed ecological settings. But is it possible that *Au. anamensis* preferred a particular habitat not because of the mosaic nature of the woodland/grasslands composition but because of the seasonal rainfall in a region which impacts resource availability? *Au. anamensis* fossils are most abundant at drier fossil localities (Kanapoi) compared to more humid regions (Allia Bay, Aramis, Asa Issie, and Woranso-Mille). Biomass availability in open dry habitats is more greatly impacted by patterns of seasonal rainfall compared to closed forested regions, so *Au. anamensis* might have preferred regions with access to open areas with seasonally available resources. Or is this a taphonomic bias? At Hadar, localities with *Au. afarensis* occurring at similar time intervals are most abundant in drier regions (Campisano and Feibel 2008). While it is clear that *Au. anamensis* could survive in a variety of ecosystems from wetter closed woodlands with patches of open grassland to drier woodland and shrubland regions, the abundance of *Au. anamensis* recovered at the more arid localities suggests a preference for that habitat that continued as the preferable habitat of *Au. afarensis*. It is critical to investigate the variation in seasonal rainfall patterns at each of these early hominin localities to

understand the role of seasonality in the origins of *Australopithecus.* While addressing that question is beyond the scope of this paper, by investigating the variation in seasonal patterns of rainfall at Allia Bay we can better understand the necessary adaptive flexibility of *Au. anamensis* at a single local site.

In more forested ecosystems, if seasonal precipitation has less impact to the vegetation, then early hominins might have more competition for resources with strict closed-habitat species in these more mesic refugium. If resource competition in mesic refugium is a selective pressure, then the adaptive flexibility in a species, like *Au. anamensis*, would be beneficial for exploitation of resources in more open arid habitats where seasonal precipitation changes can result in major shifts in vegetation. The key to the success of *Au. anamensis* across a variety of ecosystems is that the species could thrive under highly variable conditions within the wide definition of a "mosaic" habitat. It is possible that the drier open fossil localities were more impacted by duration and regularity of seasonal rains resulting in these regions being the preferred but not the sole habitat of *Au. anamensis*. If Drapeau et al. (2014) is correct about mesic environments not being favored by early hominins, then it is possible that seasonal rains, which impact the available biomass are critical to understanding the dispersal of our early bipedal ancestors.

East Africa paleoclimate

Climate change occurs because of a complex system that is characterized by fluctuations of environmental patterns driven, in part, by orbital forcing (effects due to change in Earth's orbit) (Bennett 1990; deMenocal 1995; deMenocal 2004; Hays et al. 1976; Hughen et al. 2004; Kingston 2005; Kingston 2007; Pokras and Mix 1987) and tectonic uplift (effects due to reorganization of atmospheric circulation) (Sepulchre et al. 2006).The changes in the Earth's orbit (i.e., Milankovitch cycles that occur in varying cycles of 20-400 ka) alter the amount of solar radiation by season and latitude resulting in profound impacts on precipitation patterns (Bennett

1990; Kingston 2005). There are few datasets from the terrestrial ecosystem concerning how regional biospheres respond to orbital cycles, but it is assumed that patterns in East Africa of precipitation and seasonality result in fluctuations of vegetation (Kingston 2005; Stanley 1995).

Changes in the eastern African topography during the past 8-2 Ma led to reorganization of atmospheric circulation, altering aridification and resulting in paleoenvironmental changes due to the massive uplift and creation of the East African Rift System (Sepulchre et al. 2006). Topography affects moisture transport in the spatial patterns and amounts of rainfall on a regional scale, which in turns shifts vegetation distribution across a landscape (Sepulchre et al. 2006). Although the data on terrestrial ecosystems are limited, the pollen assemblage indices highlight the effects that these climatic orbital-oscillations and tectonic uplifts can have on plant communities (Bonnefille and Mohammed 1994; Elenga et al. 1994). Paleo-datasets (i.e., pollen and charcoal) suggest that during short-term climatic variability, vegetation communities respond by reshuffling the relative distribution of different plants rather than whole-scale extinctions or speciation events (Kingston and Hill 2005). However, the linkage between global, regional, and local climate and environment change is still poorly understood because of the high environmental variability across the African continent (Lee-Thorp et al. 2007; Sponheimer and Lee-Thorp 2014). As environments changed through time, early hominins would have to cope with the altered spatial distribution of resources in the surrounding landscape as shifting precipitation patterns affected plant and animal distribution.

A number of proxy methods exist for detecting seasonal precipitation patterns in ecosystems. Paleoprecipitation, specifically mean annual precipitation, can be estimated from the measured depth to the top of a soil's calcic horizon (Retallack 1994; Retallack 2005) and has been applied to 33 paleosols of the composite Turkana Basin record (Wynn 2004). Paleoprecipitation reconstructions from paleosols demonstrate that aridification has covaried with vegetation over the past 4 Ma in East Africa (Retallack 1994; Retallack 2000; Wynn 2000; Wynn

2004). Certain intervals in the Turkana Basin, however, are not represented in the sequence (4-3.6 Ma, 3.4-2.5 Ma, and 2.2-1.9 Ma) because of the presence of noncalcic soils, which cannot be assessed during non-seasonal to mildly seasonal periods of precipitation or when mean annual precipitation is greater than 1,000mm (Wynn 2004). The material from Allia Bay (3.97 Ma) represents a period that has not been characterized by paleosols and reflects a time bracketed by relatively wet time periods (mean rainfall >550±130 mm/year) compared to later more arid intervals (mean rainfall 370±140 mm/year, 1.65-1.4Ma) (Wynn 2004). The presence of noncalcic soils at 4-3.6 Ma suggest that when *Au. anamensis* occupied Allia Bay, the site experienced either little seasonal precipitation or had mean annual precipitation values greater than 1,000mm.

Stable oxygen isotopes and precipitation

In the absence of calcic soils at Allia Bay 3.97 Ma, another promising method for detecting seasonal precipitation patterns is the use of stable oxygen isotope values of biological carbonates and phosphates in shell, bone, and teeth (Abell et al. 1996; Fricke et al. 1998; Gadbury et al. 2000; Koch et al. 1989; Luz and Kolodny 1985; Sharp and Cerling 1998; Sponheimer and Lee-Thorp 1999; Tojo and Ohno 1999). The $^{18}O/^{16}O$ ratio, expressed as $\delta^{18}O$, varies in meteoric water due to differences in mean annual precipitation, ambient temperature, distance from the sea, altitude, and humidity (Dansgaard 1964; Luz et al. 1984; Poage and Chamberlain 2001; Rozanski et al. 1993; Sponheimer and Lee-Thorp 2014; Yurtsever and Gat 1981). Stable oxygen isotope ratios ($\delta^{18}O$) in biogenic apatites (e.g. tooth enamel or bone apatite) (Longinelli 1984; Luz and Kolodny 1985; Luz et al. 1984) serve as proxies for prevailing climatic conditions (i.e., annual rainfall, seasonality, and aridity) (Fricke et al. 1998; Hallin et al. 2012; Harris and Cerling 2002; Harris et al. 2008; Souron et al. 2012; Vogel 1983).

The $\delta^{18}O$ values in the phosphate and carbonate fraction of enamel ($\delta^{18}O_{en}$) vary with the values in body water, which is mainly controlled by the isotopic composition of ingested water

obtained by drinking or from food (Luz et al. 1984; Podlesak et al. 2008; Sponheimer and Lee-Thorp 1999) and has been shown to strongly correlate with the $\delta^{18}O$ signal of local precipitation ($\delta^{18}O_{ppt}$) (Podlesak et al. 2008). The $\delta^{18}O_{ppt}$ values vary seasonally near the equator due to the amount of rainfall (Dongmann et al. 1974; Flanagan and Ehleringer 1991; Gat 1980; Rozanski et al. 1992). Specifically in Kenya, seasonal changes in the $\delta^{18}O_{ppt}$ values appear to be due to the 'Amount Effect' (an important relationship between precipitation/humidity, temperature, and $\delta^{18}O$) (Dansgaard 1964; Rozanski et al. 1993; Rozanski et al. 1996; Verschuren et al. 2009; Verschuren et al. 2000). The Amount Effect is experienced when temperatures rise (above ~20°C) and there is significant precipitation and/or high humidity resulting in the ^{18}O abundance in meteoric water to decrease (Rozanski et al. 1993). So as animals drink or consume leaf water, seasonal fluctuations of the isotopic composition of ingested water are recorded in enamel (Balasse 2002; Balasse et al. 2002; Balasse et al. 2003; Kohn et al. 1998). Mammals that lived over a wide range of climatic conditions will have intra-tooth $\delta^{18}O_{en}$ values that track both seasonal and mean annual differences of $\delta^{18}O_{ppt}$ values (Fricke et al. 1998; Hoefs 2009).

In equatorial Africa, seasonal variation in precipitation has been identified through $\delta^{18}O$ values in tooth enamel of modern fauna (Kohn et al. 1998). In the tropics, seasonal changes in $\delta^{18}O_{ppt}$ values result in generally lower $\delta^{18}O_{en}$ values with greater amount of rainfall (wet season), while higher $\delta^{18}O_{en}$ values indicate lower amounts of rainfall (dry season) (Balasse et al. 2003; Kohn and Welker 2005; Rozanski et al. 1992).Levin et al. (2006) used bulk enamel samples to show that East African mammals with varying water dependency can track precipitation (obligate drinking animals) and relative humidity (non-obligate drinking animals). One complication is when large mammals that drink mainly from a drinking source that is itself evaporated (e.g., lakes), then their drinking water would also be enriched in ^{18}O relative to local meteoric water (Craig 1961). Cerling et al. (2008) demonstrated this effect difference between river-dwelling hippos (lower $\delta^{18}O_{en}$ values) versus lake-dwelling hippos (higher $\delta^{18}O_{en}$ values) in the Turkana

Basin. While modern Lake Turkana has been shown to be well mixed and isotope values are not subject to evaporative effects, the samples for this project represent a fluvial period when drinking surface water from a paleolake was not available.

It has been established that serially sampling tooth enamel by micro-drilling a series of horizontal bands from the tip of the cusp (occlusal surface) to the neck of the crown (CEJ) will track intra-tooth patterns of isotopes to obtain the record of regular seasonal cycles established during enamel maturation (Balasse 2002; Balasse 2003; Zazzo et al. 2005; Zazzo et al. 2012). Serially sampling enamel to evaluate intra-tooth isotope variation result in values and patterns that can be used to interpret habitat, dietary change, rainfall patterns, and variation in birth season experienced by animals (Balasse 2003; Hallin et al. 2012). Serial sampling enamel from multiple teeth within a single mandible for extant gazelles in Kenya demonstrates that the $\delta^{18}O$ values vary in association with rainfall values such that the recorded greater seasonality in Nairobi's rainfall associates with greater fluctuations (larger amplitude difference = $\Delta^{18}O_{max\text{-}min}$) than at Lake Turkana (see Table 4.1; Kohn et al. 1998). Known patterns of modern seasonal climates can be used as a model for past precipitation patterns because distinct isotopic patterns vary on an annual basis (e.g., modern modeled intra-annual enamel variation for Nairobi (two rainy seasons; $\Delta^{18}O_{en}$ = 4.3‰) compared Lake Turkana (one rainy season; $\Delta^{18}O_{en}$ = 2.5‰; Kohn et al. 1998).

To monitor seasonality or reconstruct climate changes with confidence, it is necessary to assess intra- and inter-tooth isotopic variation with high temporal resolution sampling strategies. Samples from the same individual of zebra and gazelle indicate that intra-tooth sampling records more variation compared to inter-tooth serial sampling, but this depends on tooth type (i.e., third molars record the most variation) (see Table 4.1; Kohn et al. 1998). However, this is only true when climates have relatively constant annual temperatures throughout the year (like equatorial Africa), because regions with greater temperature fluctuations will influence $\delta^{18}O_{ppt}$ (McCrea 1950). Intra- and inter-tooth comparison of herbivores from South Africa (Balasse et al. 2002)

and Iran (Bocherens et al. 2001), two regions with great temperature fluctuations, show greater variation when multiple teeth are sampled from an individual.

However, sampling methods have been questioned on the likelihood that the serial sections are not truly isolating discrete amounts of time (Balasse 2002; Passey and Cerling 2002). Despite the coarseness of the sampling procedure, seasonal change has been observed but there is admixture of multiple enamel deposition layers that are averaged within a single sample so that weeks to months of time (depending on rate of enamel maturation) are aggregated (Balasse 2003; Passey and Cerling 2002; Passey et al. 2005). There might also be a dampening or averaging to the input isotope values because of the change in growth rate along the growth axis of the tooth resulting in a diminished tracking of any Amount Effect recorded in the enamel (Higgins and MacFadden 2004). For whole teeth, with a slow enamel growth rate (i.e., Elephantidae molar plates can take 10 years to form; Dirks et al. 2012) or a large enough high-crown, traditional bulk isotopic serial sampling of a single large mammal tooth or multiple consecutive teeth from a single smaller mammal would record intra or inter-annual variation in $\delta^{18}O_{ppt}$. However, tooth fragments rather than whole teeth are often recovered at fossil localities and are the material available for destructive analysis. The SIMS high-resolution sampling (analysis spots 10 μm) allows application of serial sampling of $\delta^{18}O_{en}$ values across enamel fragments to generate patterns otherwise not recoverable by traditional bulk sampling methods. The high-resolution $\delta^{18}O_{en}$ values of fossil fauna from Allia Bay generated by this study would be independent of and complementary to other methods of paleoclimate reconstruction. By comparing species of obligate drinkers (proxy for precipitation) and non-drinkers (proxy for relative humidity), the $\delta^{18}O_{en}$ in animals with different behaviors and physiologies can record different parameters of the same ecosystem (Levin et al. 2006).

Temporal resolution of enamel sampling

Tooth enamel in mammals takes a variable amount of time to develop, representing months to more than a year in a progressive and discontinuous process (Balasse 2002; Balasse 2003; Bromage 1989; Engel and Hilding 1983; Fukuhara 1959; Hillson 1992; Moss-Salentijn et al. 1997; Suga 1982; Suga 1983; Tafforeau et al. 2007; Weinmann et al. 1942; Zazzo et al. 2005; Zazzo et al. 2012). Enamel formation is a complex process that is still not fully understood, but it is accepted that there are two principle phases during enamel maturation consisting of a secretion of an enamel matrix by ameloblast cells followed by the maturation of the matrix (Hillson 2005; Reith and Butcher 1967; Robinson et al. 1978; Suga 1983). The $\delta^{13}C$ values in bovine enamel fed known diets with a change from C_3 to C_4 foods resulted in two distinct mineralization gradients that progress vertically (occlusal surface to CEJ) and horizontally (DEJ to outer enamel) (Zazzo et al. 2005; Zazzo et al. 2012).

During the enamel secretion process there is cyclic variation that leads to the formation of incremental features, such as cross-striations, Retzius lines (brown striae of Retzius), and laminations that remain visible in enamel (Boyde et al. 1988; Dean 1987; Gustafson and Gustafson 1967; Tafforeau et al. 2007). The Retzius lines correspond to long-period cycles of successive positions of ameloblast movement as secretion activity occurs at regular periods (Boyde 1976; Dean 1987; Gustafson and Gustafson 1967). The non-cuspal parts of the Retzius lines that reach the outer surface of the tooth correspond to external rings known as perikymata (Hillson 2005). Laminations are regularly spaced features parallel to the Retzius lines that represent isochrons of enamel deposition (Hillson 2005; Tafforeau et al. 2007). In rhinoceros, humans, and probably most middle- and large-sized herbivorous mammals, laminations and cross-striations are equivalent daily features in enamel (FitzGerald 1998; Tafforeau et al. 2007).

To evaluate seasonal variability of $\delta^{18}O_{en}$ values it is imperative to understand enamel deposition growth rates to determine the period of time represented by the high-resolution

intratooth $\delta^{18}O_{en}$ values generated by SIMS analysis. The sampling transect distance within enamel corresponds to a particular period of time that records the duration of a particular source $\delta^{18}O$ signal expected to change between wet and dry seasons (Kohn et al. 1998; Uno et al. 2013). Unfortunately, data on enamel deposition of modern fauna is limited and usually reports deposition rates along the growth axis (i.e., enamel extension rates from occlusal surface to CEJ) (Dirks et al. 2012; Kierdorf et al. 2012; Passey et al. 2005; Tafforeau et al. 2007; Uno et al. 2013), not the growth rate of enamel thickening (growth perpendicular to the DEJ). The initial work using SIMS on fossil enamel fragments to evaluate diagenesis serial sampled transects of $\delta^{18}O_{en}$ values perpendicular to the DEJ, so the enamel thickness growth rate is necessary to evaluate the period of seasonal fluctuations recorded in enamel (see Chapter 3).

Recent work on Elephantidae (*Mammuthus columbi*) and Mammutidae (*Mammut americanum*) calculated enamel thickness growth rates (X) using the distance between cross striations (d) and the angle between enamel prisms and the DEJ in the occlusal direction (I) to determine a daily growth rate (Metcalfe and Longstaffe 2012; Metcalfe and Longstaffe 2014; Shellis 1984).

$$X = d(\sin I)$$

Shellis (1984) noted that the angle I changed along the growth axis of the tooth with a more acute angle near the occlusal surface increasing towards the cervical margin. For Mammutidae this impacts daily thickness growth rates which are higher near the occlusal surface (3.7-4.6 µm/day) compared to a slower growth rate near the cervical margin (1.8-3.0 µm/day) (Metcalfe and Longstaffe 2014). From published values of large herbivore mammals, daily enamel thickness growth rates can be calculated for Elephantidae (2.2-4.1 µm/day) (Metcalfe and Longstaffe 2012) and Equidae (3.1-4.1 µm/day) (Hoppe et al. 2004). It has been noted that growth rates vary with sex, age, tooth type, and location within the cusp (Kierdorf et al. 2012; Shellis 1984; Tafforeau et al. 2007; Uno et al. 2013), and for the Allia Bay fossil samples none of these variable are known.

Although there is variation in growth rates, to our knowledge the current known rates are less than 5 µm/day, so for the purpose of this study the duration of time represented by transect lengths will be estimated based on a minimum (1.8 µm) and maximum (4.6 µm) daily enamel thickness growth rate.

High-resolution $\delta^{18}O_{en}$ values generated by SIMS

Recent studies in geochemistry and cosmochemistry have used a large radius secondary ionization mass spectrometer (SIMS) technique to evaluate high-resolution patterns of zoned isotope differences of light stable isotopes (i.e., $\delta^{18}O$, $\delta^{13}C$) in a variety of minerals (i.e., oxides, silicates, carbonates) (Valley et al. 1998a). SIMS techniques use far less sample material compared with techniques that analyze conventional acid-digestion of mechanically shaved/drilled powdered samples with measurement by CO^2-gas source mass spectrometry (Kita et al. 2009; Valley and Kita 2009). When sequential measurements are made along the growth axis of materials with chronological depositional growth (i.e., otoliths and speleothems), a spatial resolution of approximately 10-15 µm is routinely achievable for detecting zoned isotopic differences even for samples of uncertain homogeneity (Kolodny et al. 2003; Orland et al. 2009; Treble et al. 2007; Valley et al. 1998b; Weidel et al. 2007). For speleothems, previous paleoclimate studies have shown that this approach yielded at least yearly (Kolodny et al. 2003) or sub-annual resolution (Treble et al. 2007), depending on growth rate. Similarly, otolith studies have shown that with a spatial resolution of approximately10-15µm, spot sample analyses can represent a few days of time during periods of rapid growth or a few weeks of growth during slower periods of growth (Weidel et al. 2007).

For enamel, intra-tooth micro-drilling studies have a resolution of about nine samples per centimeter along the growth axis of a tooth (Balasse et al. 2012; Hoppe et al. 2004; Zazzo et al. 2012). Laser ablation techniques improve the resolution of $\delta^{18}O_{en}$ values by sampling from an area about 100 µm wide plus halosr extending outward 100-200 µm so that days to weeks are

aggregated (Balasse 2003; Sharp and Cerling 1998). Neither of these methods can approach the spatial resolution achieved by SIMS, as these other techniques must aggregate a sample area that is many times wider in cross-section than the increments representing differing growth periods. The result is an averaging of the stable isotope ratios generated from multiple growth increments. With the SIMS spot analysis capability of approximately 10 µm and estimated daily enamel thickness growth rates <5 µm, it is possible that SIMS analysis only aggregates 2 days of enamel deposition.

Two modern ungulate species (Burchell's zebra and Grant's gazelle) have been analyzed with SIMS at a resolution of an analysis pit every 30µm from the outer edge of the enamel transversely to the DEJ and result in more variation ($\Delta^{18}O$) compared to inter-tooth sampling of the same individual (Table 4.1). Crown formation time is unknown for zebra's but similar tall-crowned (i.e., hypsodont) species exhibit tooth formation over several months to years (i.e., M3 of *Equus* takes 3 years) (Higgins and MacFadden 2004; Hoppe et al. 2004). The distance of the zebra SIMS transect (1012 µm) likely represents 8.2 to 10.9 months of time and exhibits greater variation compared to the third molar intra-tooth analysis of the same species collected the same year in Koobi Fora, which suggests that SIMS likely exceeds the variation recorded in traditional intra-tooth sampling along the growth axis. Gazelle (*Gazelle granti)* molar crown formation times (CFT) have been reported to be as short as 4 months based on isotopes (Kohn et al. 1998) or as long as 2.9 years based on enamel cross-striation counts (Macho and Williamson 2002). This discrepancy in gazelle CFT is possibly explained by high enamel apposition rates that might lead to misidentification of daily incremental lines which would result in an overestimation of CFT (Kierdorf et al. 2012), such as the results reported for medium sized African bovids of CFT greater than 1000 days (Macho and Williamson 2002). The gazelle SIMS transect is 740 µm and using the most conservative daily enamel thickness growth rates could represent 6-13.7 months, however the high enamel apposition rates of other medium-bodied ungulates (sheep and goats;

Kierforf et al. 2012) would suggest that the SIMS transect represents a duration of time on the lower end of the estimate. The SIMS transect of the gazelle M3 recorded more than six time the amount of variation across a transect compared to the traditional inter-tooth bulk sampling of M2 and M3 (Table 4.1).

Paleoprecipitation predictions

It is imperative to estimate the period of time represented by fossil enamel fragments in order to evaluate seasonal variability of $\delta^{18}O_{en}$ values generated by SIMS analysis. Previous SIMS analysis of modern enamel using the conservative daily enamel thickness estimates indicate fluctuations in $\delta^{18}O_{en}$ patterns similar to expected seasonally shifting sinusoidal curves across enamel transects that represent time periods of months to a year depending on the thickness of the enamel. This proof of concept is the basis for applying the SIMS method to fossil samples at Allia Bay for paleoenvironment reconstruction (Chapter 3 this dissertation). The SIMS generated serial samples of $\delta^{18}O_{en}$ values used for reconstructing paleoenvironmental shifts at Allia Bay will either show no evidence of change across the enamel fragment or some evidence of seasonal fluctuation in $\delta^{18}O$ values. There are two possible reasons for no evidence of seasonal change. Either the source of $\delta^{18}O$ is constant throughout the duration of enamel deposition, or the period of enamel deposition represented by the sample did not occur during a period of seasonal fluctuation, so no shift was recorded during enamel development. If no shift in $\delta^{18}O$ values is observed, then the dimensions of the enamel fragment will be used to estimate the period of stasis in the environment to assess the possible duration of dry or wet seasons. If seasonal fluctuations in $\delta^{18}O$ values are observed across enamel transects, then modern environmental analogs in equatorial East Africa will be used to make seasonality predictions. It has been modeled that areas with one rainy season experience a decreased amplitude difference in $\delta^{18}O$ values recorded within an individual compared to regions with multiple rainy seasons (Kohn et al. 1998). The possible predicted outcomes are not intended to imply that the number of rainy seasons alone corresponds

to a given environment, but it is the expectation that in conjunction with bulk $\delta^{13}C$ values the high-resolution $\delta^{18}O_{en}$ values generated in this study will clarify the seasonal environment at Allia Bay. This study provides an independent and complementary line of evidence to augment previous paleoenvironment reconstructions for Allia Bay by identifying seasonal rainfall patterns at a new scale of analysis for a fossil locality where fauna are thought to have experienced seasonal stress based on histological analysis of enamel thin sections (Macho et al. 2003).

Materials and methods

Fossil sample

This study examines a total of 12 fossil fauna enamel fragments from Allia Bay representing seven families: Bovidae (n = 1), Deinotheriidae (n = 2), Elephantidae (n = 2), Equidae (n = 1), Giraffidae (n = 2), Hippopotamidae (n = 3), and Suidae (n = 2). Traditional bulk $\delta^{18}O_{en}$ and $\delta^{13}C_{en}$ analysis of each sample was previously conducted to determine the diet of each individual to ensure the sample represented browsers, mixed C_3/C_4 feeders, and grazers (Table 4.1). Modern analogs of these seven families indicate that the majority of the sample were obligate drinkers (hippos, suids, equids, deinotheres, and elephants) whose $\delta^{18}O_{en}$ values should correlate with the oxygen stable isotope composition of precipitation ($\delta^{18}O_{ppt}$). Modern bovid species can be either obligate or non-obligate drinkers(Dorst and Dandelot 1970; Estes 1991), but because the single bovid sample is a grazer ($\delta^{13}C$ = -0.3‰) it is likely that it was an obligate drinker. The two giraffid samples can not be identified as either *Giraffa* or *Sivatherium*, but previous $\delta^{18}O_{en}$ values from Aramis indicate a reliance on obtaining water from enriched leaf water by both genera (White et al. 2009). Therefore, the $\delta^{18}O_{en}$ values in both giraffids, non-obligate drinkers, should track relative humidity.

Despite the constraints of taxonomic identification, the use of material from a single-excavation with deposition limited to approximately 60 ka of time ensures that relatively high-

temporal resolution data will be generated. In hominin evolution 60 ka is a short window of time, but it is a significant temporal period in terms of characterizing shifting seasonality patterns (Maslin and Trauth 2009; Trauth et al. 2007). There is no way to know when each fossil tooth was mineralizing during the 60 ka of time represented at Allia Bay, but we assume that each enamel fragment represents no more than a single year of time (i.e., estimates based on daily enamel thickness growth rates across transect distances). It is possible that each fossil tooth represents a different temporal period of time within the 60 ka deposit at Allia Bay (i.e., 24 different years). This means that the amount of variation in the $\delta^{18}O_{en}$ patterns of drinking species can be used to test the consistency of the habitat within the 60 ka occupation of the site. If multiple patterns are observed among the teeth, then there were likely multiple environments across the landscape experiencing different seasonal precipitation patterns during the 60 ka).

Sample preparation, confocal laser fluorescent microscopy (CLFM)

Each fossil fragment was bisected in a longitudinal direction (occlusal surface to root tip) and mounted, along with 4-6 grains of UWA-1 (fluorapatite standard; $\delta^{18}O = 12.70‰$, VSMOW), in polished 2.5-cm-diameter epoxy plugs. To minimize instrumental bias associated with sample position, the region of interest for SIMS analysis was placed within 5mm of the center of the plug (Kita et al. 2009; Treble et al. 2007). Confocal laser fluorescent microscopy (CLFM) was subsequently completed at the Keck Bioimaging Laboratory at UW-Madison using a Bio-Rad MRC-1024 scanning confocal microscope operated with a 40-mW three laser line imaging system. Each sample was imaged by the 488-nm (green fluorophores), 568-nm (red fluorophores), and 647-nm (far-red fluorophores) laser lines to detect potential diagenetically altered regions. Images of enamel fluorescence were collected and processed with Image-J software to add a threshold of 85, 210, and 50 for the green, red, and far-red fluorophores, respectively, to distinguish the likely diagenetically altered areas from unaltered areas during data analysis (see discussion in Chapter 3).

Secondary ion mass spectrometry (SIMS)

Oxygen isotope data were acquired at the UW-Madison WiscSIMS Laboratory using a CAMECA ims-1280 high resolution, large radius multicollector ion microprobe using a ~1.9 nA primary beam of $^{133}Cs^{+}$ focused to approximately 12 to 13-µm beam-spot size (Kita et al. 2011; Kita et al. 2009; Valley and Kita 2009). The primary beam sputtered a ~2-µm-deep pit in the enamel for analyses of the secondary oxygen ions. Charging of the sample surface was compensated by a gold coat on the epoxy mount, which was applied following cleaning in deionized water and ethyl alcohol.

A total of 661 oxygen analyses were made of the 12 fossil samples in transverse transects across the enamel fragments spaced 30 to 240-µm apart (spot size varied between different analytical sessions; see Appendix 4.1). Throughout the analytical sessions, 4-5 consecutive measurements of UWA-1 fluorapatite standard were analyzed before and after every 8-16 sample analyses for determination of the standard deviation of each sample analysis (Appendix 4.1). The ion microprobe instrumental mass fractionation factor (IMF = $\delta^{18}O_{measured}$ - $\delta^{18}O_{VSMOW}$) in fluorapatite is calculated from each bracketing set of UWA-1 measurements and was typically 1.01‰. The precision of a set of bracketing standard analyses, on average equals to 0.33‰ (2 standard deviations, SD; Appendix 4.1), was used to estimate the spot-to-spot reproducibility of the enamel sample analyses. The 2SD for each bracket is the best estimate of the analytical uncertainty of individual sample analyses.

A typical secondary $^{16}O^{-}$ ion intensity was $2.4x10^{9}$ cps. The mass resolving power was 2200 and the $^{18}O^{-}$ and $^{16}O^{-}$ions were simultaneously collected by two Faraday Cup detectors in the multicollection system. Each analysis lasted approximately 4 min, including a pre-sputtering burn through the gold coat (10 s), an automatic recentering of secondary ions in the field aperture (~60 s), and 20 cycles of 4-s integrations of oxygen ions for isotopic measurements (80 s). Detailed

analytical conditions of the WiscSIMS system are described by previous workers (Kita et al. 2011; Kita et al. 2009).

It is important to note that the δ18O values generated from this analysis are not confidently tied to the VSMOW scale because of the range of acid-digestion δ18O values accepted for the UWA-1 fluorapatite standard. The UWA-1 standard is a geological fluorapatite, while enamel is a biological hydroxyapatite ($Ca_{10}(PO_4)_6(OH)_2$) with possible ion substitutions of fluoride, chloride, or carbonate. Matrix differences between fluorapatite to hydroxyapatite prohibit accurate correction of enamel to VSMOW. The SIMS primary beam sputters all the oxygen ions contained within an analysis pit, which includes PO_4, CO_3 and OH, in the enamel and we assume a fractionation occurs for "bulk oxygen ions" versus the oxygen analyzed by traditional bulk enamel carbonate methods. Additionally, phosphates are more complex systems than carbonates and there is no nationally recognized standard for tooth enamel phosphate, meaning that results need to be compared with others from the site to obtain relative differences (Aubert et al. 2012; Bryant et al. 1996; Fricke and O'Neil 1996; Iacumin et al. 1996; Zazzo et al. 2004). All sample $\delta^{18}O$ values generated in this study are corrected to the UWA-1 standard and the relative variability between values is the focus of the following interpretations. Until a uniform biological apatite standard is found for SIMS analyses, interpretations of $\delta^{18}O$ values should not be related to bulk carbonate stable isotopic absolute $\delta^{18}O$ values. However, internal $\delta^{18}O$ patterns within a single tooth and the $\delta^{18}O$ differences between individuals in this study are the focus of the subsequent paleoenvironment discussion. All $\delta^{18}O$ values and figures reported in this study are relative to UWA-1 ($\delta^{18}O = 12.7‰$).

SIMS pit quality evaluation and assessment of diagenesis

To ensure only reliable biogenic $\delta^{18}O$ values are used for reconstructing the seasonal precipitation patterns at Allia Bay three sample quality checks were employed to each sample pit analysis: scanning electron microscope (SEM) pit imaging, relative yield analysis, and CLFM

analysis. After oxygen isotope analysis at WiscSIMS, every analysis pit (standards and samples) were examined with SEM to ensure each analysis pit was a uniform "regular" pit with reliable $\delta^{18}O$ generated. Pits that are classified as "irregular" were eliminated from paleoenvironmental analyses because irregular pit margins might alter $\delta^{18}O$ values due to an irregularity with the primary beam or a diagenetic inclusion in the enamel (see Chapter 3 for a more detailed discussion). A total of 28 pits were excluded based on the SEM sample quality check.

To check the performance of the primary beam (i.e., the efficiency of the beam sputtering oxygen ions) during an analysis session, the oxygen ion yield for each analysis was analyzed as a relative yield throughout an entire analytical session. The relative yield of each sample is compared to the average yield of the bracketing standards and based on the Tukey definition of an outlier, all samples with relative yields outside the accepted range were excluded. A total of 20 pits were excluded based on the relative yield analysis sample quality check.

Finally, post-SIMS analysis CLFM imaging of each sample transect was conducted following the same pre-SIMS CLFM protocol to ensure pits were placed in enamel not diagenetically altered. Sample pits placed within the fluoresced regions of the far-red fluorophores CLFM image were excluded from the paleoenvironment analysis (see Chapter 3 for further discussion). A total of 136 pits were excluded because of suspected diagenetic alteration. Some of the sample pits analyzed were determined as generating non-biogenic $\delta^{18}O$ values based on multiple sample quality checks, so out of a 661 enamel sample analyses a total of 503 was used for the Allia Bay paleoenvironment reconstruction.

Results and Discussion

Table 4.2 and 4.3 present the summarized SIMS generated data for each enamel fragment (Table 4.2) and each transect line (Table 4.3) (all raw data in Chapter 4 Appendix). Each family is discussed below in relation to the ecological signal or important finding from the sample that

contributes to the overall seasonal paleoenvironment at Allia Bay. Based on the range of published values for ungulate daily lamination enamel deposition in the transverse direction, Table 4.3 presents a minimum (4.6 µm) and maximum (1.8 µm) daily enamel thickness growth rate to estimate the period of time that a single SIMS transect represents (a conservative estimate of the number of months is calculated based on the minimum growth rate value). However, temporal estimates will be used cautiously as calculating time by using incremental features in enamel can lead to erroneous interpretations as other authors have cautioned (Kierdorf et al. 2012; Passey and Cerling 2002; Tafforeau et al. 2007; Zazzo et al. 2012). As this is the first study to analyze fossil enamel with SIMS and the $\delta^{18}O$ values generated don't correlate to bulk $\delta^{18}O$ values, all interpretations are made relative to the internal patterns of a single sample and comparisons across samples by comparing $\delta^{18}O_{SIMS}$ values and SIMS generated $\Delta^{18}O$ differences. Therefore, "wetter" compared to "drier" periods are seasonal fluctuations relative to changes in the patterns recorded in the enamel.

Variation in $\delta^{18}O$ across a tooth

Transverse transects across enamel were analyzed to investigate seasonal variation because SIMS pits were placed along the vertical growth axis (not reported in this study) for three samples (bovid, suid, and deinothere) and greater variation in $\delta^{18}O$ values was found in the transverse direction. It is possible that due to tooth curvature, hypothesized schematics of enamel maturation, and the small spot size of SIMS analyses, that sampling in a transect along the growth axis in large herbivores does not capture the greatest amount of variation because one could sample in a similar enamel deposition layer (Passey and Cerling 2002; Zazzo et al. 2012). Blumenthal et al. (2014) was successful in recording $\delta^{18}O$ variation by sampling extant woodrats along the growth axis near the dentine, however when SIMS is applied to fossil samples the enamel near the dentine is most often diagenetically altered and should be avoided (see discussion in Chapter 3). Additionally, the SIMS sample analysis viewing capability for large enamel

samples makes it hard to determine sample location during an analytical session when sampling in the vertical growth axis direction of large mammal teeth, so greater confidence of sample location is achieved by sampling in the horizontal direction to avoid diagenetically altered zones.

This is does not mean that there is not variation in the pattern of $\delta^{18}O$ values in transverse transects placed along the vertical growth axis, which is exemplified by the Bovidae specimen (4877) (Figure 4.1). A total of five parallel transverse transects were analyzed in the 4877 enamel fragment to better understand the relationship between enamel mineralization and the duration of enamel maturation using $\delta^{18}O$ as a proxy (not discussed in this paper). Each line transect represents possibly 7-8 months of time (it could be a shorter period if Kierdorf et al. (2012) is correct about high enamel apposition rates of medium-sized bovids), with some periods of enamel mineralization overlapping between transects during the development of the entire tooth. It is significant to note that the $\Delta^{18}O$ increases when values from an entire tooth are averaged compared to a single line transect (Table 4.2 and 4.3). This is due to a greater amount of time represented in enamel deposition when multiple transects are plotted within a tooth. The greater $\Delta^{18}O$ across the tooth compared to a single transect line is highlighted by the example of specimen 4877 with an overall $\Delta^{18}O$ of 2.65‰ compared to a range of per-line $\Delta^{18}O$ values of 0.91 to 2.18‰. In this sample, it indicates that while the tooth was forming the overall $\delta^{18}O_{source}$ fluctuated more than during the formation of the enamel represented in a single line transect. As most of the teeth in this study are represented by a single line transect or two lines that overlap in the timing of enamel deposition, the paleoseasonality recorded by these samples is a conservative estimate.

Based on the size of the Bovidae specimen, the individual was likely a smaller-medium sized bovid with a tooth formation time of approximately a year or so. The combined five transects encompass at minimum a year of time and exhibit a $\Delta^{18}O$ of 2.65‰ for the entire tooth, which is approximately the amount of $\Delta^{18}O$ modeled for gazelles from the modern Lake Turkana

region (one rainy season; $\Delta^{18}O_{en}$ = 2.5‰; Kohn et al. 1998). However, none of the transect lines signal dramatic fluctuations, but rather gradual seasonal shifts (Figure 4.1). The mean $\delta^{18}O_{SIMS}$ of the enamel fragment (21.58‰) indicates that 4877 was occupying Allia Bay during a wetter seasonal period compared to other samples (Table 4.2).

Establishing the baseline of the $\delta^{18}O$ ecosystem: Hippopotamidae

Hippos are often the most ^{18}O-depleted mammals in ecosystems and often reliable proxies for the source water and local vegetation because they are a water-dependent species with a preference for feeding along lake and river shores, if evaporative effects are accounted for (Cerling et al. 2008; Harris et al. 2008). However, recent work on modern fauna from the Koobi Fora region on the eastern edge of Lake Turkana show that the mean $\delta^{18}O_{bulk}$ values for suids (warthogs) is depleted by 1‰ compared to modern hippos (Chapter 2 this dissertation). This modern analog of the Turkana Basin ecosystem suggests that both hippos and suids represent the most depleted $\delta^{18}O_{en}$ values in an ecosystem and act as excellent paleoenvironmental monitors of the available $\delta^{18}O_{source}$ values because of their reliance on access to water. The overall patterns of the $\delta^{18}O$ in the three hippo samples are very stable and exhibit the least amount of variation for any sample in the dataset (Table 4.2, Figure 4.2). Two of the hippo samples (4892.1 and 4891.1) have complete transects sampled from the edge of the enamel to the DEJ representing at minimum 11-15 months, while 4891.2 is a partial transect representing at minimum approximately 4.5 months. There appears to be two distinct mean values at ~17 and 23‰ for the three samples suggesting either 1) two different species of Hippopomatidae occupying different ecological niches at Allia Bay and/or 2) a distinct difference in the $\delta^{18}O_{source}$ reflected by a 6‰ shift in the hippo enamel.

Besides the primates, no complete faunal assemblage analysis has been published for Allia Bay, so limited information is known about the distinct species present. Macho et al. (2003) analyzed the stress lines in enamel of two specimens identified as *Hexaprotodon protaphibius*

and *Hippopotamus* sp. suggesting both taxa were present. However, recent work has concluded that the Turkana Basin hippos formerly classified as *Hexaprotodon* are more closely related to the extant *Hippopotamus* genus (Boisserie 2005). Under the original classification *Hexaprotodon* where considered more terrestrial browsers compared to the aquatic grazer, *Hippopotamus* (Coryndon 1978). This means that at Allia Bay in the lower part of the Koobi Fora Formation the common hippo, aff. *Hippopotamus* cf. *H. protamphibius* and a larger *Hippopotamus* species have been recovered at Allia Bay (Harris et al. 2008). Modern isotopic data of the common hippo suggest it is an opportunistic rather than an obligate grazer (Boisserie et al. 2005). The Allia Bay fossil hippos conform to this expectation with a large range $\delta^{13}C_{bulk}$ values (-11.7 to -1.1‰) and the three hippos selected for SIMS analysis span the range of values ($\delta^{13}C_{bulk}$: -11.7, -4.2, and -2.0; Chapter 2 data).

The combined $\delta^{13}C_{bulk}$ and $\delta^{18}O_{SIMS}$ values suggest a wide range of feeding ecologies for Hippopotamidae at Allia Bay. Browsers have the expected higher $\delta^{18}O$ combined with lower $\delta^{13}C$ values and grazers have lower $\delta^{18}O$ combined with higher $\delta^{13}C$ values. In addition, there are a number of mixed feeders (i.e., C_3 and C_4). This might indicate one species with a wide feeding ecology range. Alternatively, the two previously identified species of *Hippopotamus* (Harris et al. 2008) had different but overlapping dietary adaptations: one with an emphasis on browse with some individuals feeding on mixed browse and graze, and the second with an emphasis on graze with some mixed-feeding individuals.

The ~6‰ difference between the Hippopotamidaes also highlights the importance of generating high-resolution serial samples in the $\delta^{18}O$ enamel record because the bulk sample difference between the Hippopotamidaes is only 3‰ (Table 4.2). This means that the SIMS method was able to capture a greater amount of variation between samples compared to what is generated by traditional bulk samples, which can result in different interpretations about the paleoenvironment.

Browser $\delta^{18}O$ paleoseasonality signal: Gradual change under stable and fluctuating conditions

The browser samples (excluding the browsing Hippopotamidae) are represented by two Giraffidaes, a Deinotheriidae, and two Elephantidaes (the C_3-dominate mixed feeding Elephantidae is included with the browsers). Generally the browsers exhibit two patterns: periods of more stable wet environments and periods of more marked seasonal shifts between wet and dry seasons recorded during the overall driest periods recorded in this study. It is possible that seasonal rainfall fluctuations at Allia Bay were greatest when the climate was overall drier, causing more marked seasonality. All the patterns recorded for browsers (even the extreme fluctuations) do not exhibit abrupt shifts (defined as no overlap between the 2SD error bar for pits ~30µm apart) in the $\delta^{18}O$ values, possibly due to 1) the paleoenvironment or 2) the growth rate of the enamel of animals with large body size and concurrent averaging to the input isotopic signal during enamel maturation.

The Giraffidae samples represent the only non-obligate drinkers in the fossil sample and have $\delta^{18}O$ enamel values that correlate to the relative humidity of the paleoenvironment. The two Giraffidae specimens represent two distinct patterns of seasonal relative humidity signals at Allia Bay (Figure 4.3). With the most conservative enamel growth rate, the two parallel overlapping transects of Giraffidae 4860.1 (Figure 4.3A) represent about 13 months of recorded $\delta^{18}O$ values (distance 1776 µm), so at minimum the pattern is approximately a single annual cycle. From the outer edge of the enamel, there is a prolonged arid period (~4.8 months) that gradually decreases by almost 4‰ over ~2.7 months to a more humid phase that rebounds by an increase of ~2‰ to a moderately dry phase in ~3 weeks. The moderately dry phase lasts for ~2 months before returning to a short humid phase (decrease by ~2‰) over a period of gradual decline of ~1,5 months. This suggests that the enamel recorded the possible tail-end of a drought because the prolonged higher $\delta^{18}O$ values are some of the highest recorded from the SIMS analysis in this study. The arid period was followed by sporadic short successive periods of humidity. The second Giraffidae

sample (4859b3) represents at minimum ~7.3 months, so an entire annual cycle is not recorded in the enamel (Figure 4.3B). However, the sample records less variation during the enamel deposition ($\Delta^{18}O = 2.47‰$) with the highest recorded value at the outer edge of the enamel and the lowest value at the DEJ indicating a gradual shift from the arid to humid phase. There are no drastic drops in the relative humidity over the 7 month period and has a relatively constant climate compared to the fluctuations recorded every couple months in Giraffidae 4860.1. Giraffidae 4859b3 occupied Allia Bay during a more stable humid climate regime ($\delta^{18}O_{SIMS} = 21.34‰$) compared to Giraffidae 4860.1 ($\delta^{18}O_{SIMS} = 25.54‰$), in fact there is more than 1‰ difference between the lowest $\delta^{18}O_{SIMS}$ value of 4860.1 and the highest recorded value in 4859b3.

Similar to the giraffids, the three Procoscidaes exhibit two different patterns depending on if the individual inhabited Allia Bay when it was well-watered compared to possible drought conditions (Figure 4.4). Elephantidae 4901.2 records a continuous sinusoidal pattern for $\delta^{18}O$ with the high values indicating a dry season and the low values indicating the wet season over a minimum of 9.2 months. The distance between the peaks of the two recorded dry seasons is 920 µm (possibly a duration of 6.6 months between dry seasons). At the peak of the dry season, there is a gradual shift to the wet season by a decrease of 2.73‰ in ~3.5 months followed by an increase of 3.17‰ in ~3.1 months. Elephantidae (4908a3) had enamel formed during a wetter phase of Allia Bay ($\delta^{18}O_{SIMS} = 23.20‰$) compared to 4901.2 ($\delta^{18}O_{SIMS} = 25.85‰$), and while there is no overlap in values the highest and lowest values recorded in each sample were only 0.08‰ different. Elephantidae 4908a3 similarly records ~9.1 months of time, but only records one dry season peak. The estimated time between the peak of the dry season and the corresponding decrease of 2.84‰ to the lowest recorded value is ~3 months, which is a similar pattern recorded by 4901.2. However, prior to the driest peak for 4908a3, there is ~6 months of a relatively stable climate ($\Delta^{18}O = 1.08‰$), suggesting that during overall wetter periods the climate is more stable for prolonged periods of time. Despite the differences in the patterns

between the two Elephantidae samples, it is possible that for a period of time during the 60ka occupation of Allia Bay the durations of the seasons were similar from year to year (evidenced by the similar 3 month shift from dry to wet periods), but the amount of rain varied. This is similar to what we see in modern environments with seasonal duration being more stable than the amount of rainfall.

The Deinotheriidae (4857.1) showed a similar pattern of gradual variation as Elephantidae (4908a3), but over a longer period of time (~17.4 months) with even lower $\delta^{18}O$ values ($\delta^{18}O_{SIMS}$ = 20.58‰) (Figure 4.4). The "driest" value recorded by 4857.1 is equivalent to the "wettest" period recorded by the Elephantidae, 21.60±0.43‰ and 21.37±0.49‰, respectively. The distance between the dry and wet peak values is 960µm representing a minimum of ~7 months, which is about twice as long as what is documented in the Elephantidaes, and 4857.1 has a lower overall $\Delta^{18}O$ (2.08‰) compared to the Elephantidae samples. This is further support that during the wettest period recorded at Allia Bay, there was little seasonal difference in rainfall and there was a more constant $\delta^{18}O_{source}$ available.

Grazer $\delta^{18}O$ paleoseasonality signal: Possible abrupt shifts within relatively stable conditions

Although the grazing Bovidae (previously discussed) does not exhibit an abrupt shift in the environment, the grazing Suidae (4883) and the C_4-dominant mixed feeding Equidae and Suidae (4879.2) each show evidence of an abrupt shift in $\delta^{18}O_{SIMS}$ values. Abrupt shifts occurred within all three samples at varying lengths and possibly have behavioral explanations. Overall the Equidae (4858a4) documents a gradual change in the $\delta^{18}O$ values over a minimum of 6.5 months (Figure 4.5). However, in the middle of the dry peak there is an abrupt decrease in the $\delta^{18}O$ values over a distance of 90µm. A conservative estimate of the duration of this shift is a period of 20 days (using the 4.6µm enamel growth rate) when the $\Delta^{18}O$ is 1.21‰. This could be a true documentation of a brief intense rain, or since behaviorally equids are known to migrate during

droughts this decrease in $\delta^{18}O$ values may reflect movement of the individual on the paleolandscape as it accessed a different water source for a few weeks.

Both suid samples record at a minimum 10.5 and 11.8 months of time representing almost a complete annual cycle of rainfall. Similar to the equid, the grazing Suidae (4883) shows an abrupt shift of 1.13‰ over a short period of time, signaling the start of a drier period that continues for ~7 months until another sudden shift to a wetter period occurs, recorded as a decrease of 1.09‰ (Figure 4.6). The other suid (4879.2) has a similar possible ~1‰ shift recorded in the enamel but it is not distinct and only lasts for ~2.4 months (Figure 4.6). It is possible that the difference in the abrupt shifts recorded for the two suids is due to the dietary ecology of each individual. The grazer (4883) has a prolonged distinct shift recorded, while the C_4-dominant mixed feeder might be selectively buffering against shifts in the moisture regime by moving between C_3 and C_4 environments.

Overall the suids record two of the most stable "dry" periods from this data set for Allia Bay. While the Giraffidae (4860.1) and Elephantidae (4901.2) record the highest $\delta^{18}O$ values, 27.36±0.18‰ and 27.36±0.18‰, respectively, both individuals also document gradual shifts to wet periods with a decrease in $\delta^{18}O$ values by more than 3‰. There are no such shifts to a significantly wetter period documented by either of the suids, with overall $\Delta^{18}O$ of 1.75 and 2.15‰ over almost an entire annual cycle (10.5 and 11.8 months, respectively). Further support of the suids recording prolonged dry seasons is that in the modern Koobi Fora region, the suids (*Phacochoerus* sp.) exhibit the lowest mean $\delta^{18}O_{bulk}$ values, even lower than the hippos. Modern suids exhibit depleted $\delta^{18}O_{bulk}$ values by 5-6‰ compared to modern Koobi Fora Bovidae and Equidae (see Table 2.2). However, the SIMS generated means for the Bovidae (21.58‰) and Equidae (23.39‰) are lower compared to the mean Suidae values (25.59 and 24.94‰). If the offset between the species is maintained in the past, then the bovid and equid samples occupied Allia Bay during a wetter period compared to the suids.

Paleoseasonality at Allia Bay

The range in duration of the time represented by enamel transects is from 4.5 to 17.4 months (based on conservative estimates). Therefore, variation in the seasonal rainfall patterns at Allia Bay can be discussed in terms of differences between seasons (shorter duration recorded in enamel) and intra-annual variation (~12 months of time recorded in enamel). The high-resolution $\delta^{18}O$ serial samples generated by SIMS for the seven faunal families at Allia Bay indicate that there were 1) periods when the local environment had a stable moisture regime (i.e., $\Delta^{18}O <$ 2.20‰ like the intra-annual stability over 10.5 to 14.7 months recorded in Hippopotamidaes and Suidaes), and 2) periods of more extreme aridity resulting in greater marked seasonality intra-annually (i.e, $\Delta^{18}O > 3.20$‰ like the patterns of Giraffidae 4860.1 and Elephantidae 4901.2 recorded over 12.9 and 9.2 months, respectively). It is possibly that if the Elephantidae sample recorded a full intra-annual period (an additional 3 months), then it would have a $\Delta^{18}O > 4$‰ similar to the Giraffidae sample. It is interesting to note that the SIMS data from the modern gazelle, which is a non-obligate drinker similar to the Giraffidaes, has a $\Delta^{18}O$ of 3.87‰ (likely represents ~6 months) and the highest mean (31.87‰) of any of the large mammals studied with SIMS. The two modern Koobi Fora SIMS samples do record higher $\delta^{18}O_{en}$ values compared to any of the fossil Allia Bay samples, supporting the bulk $\delta^{18}O_{en}$ findings that Allia Bay was overall wetter compared to the modern Koobi Fora environment. The gazelle pattern of $\delta^{18}O_{en}$ values suggests that the time tracked by the SIMS transect records the transition from a drier period to the wetter period (highest value at outer edge of enamel and lowest value near the DEJ in a continuous declining pattern; see Chapter 3). This is further evidence that non-obligate drinkers during the drier time periods will record larger $\Delta^{18}O$ across enamel transects representing single seasons transitions (modern gazelle) or intra-annual shifts (fossil giraffid) depending on the length of time analyzed.

Of the twelve fossil samples in this study, only two (16.7%) of them indicated marked seasonality within an intra-annual period, while the other ten (83.3%) samples represented periods of relative stability with mildly seasonal rainfall $\delta^{18}O_{en}$ shifts during the wetter periods. This likely explains why noncalcic soils formed at Allia Bay that result from non-seasonal to mildly seasonal periods of precipitation (periods of paleoprecipitation stasis) or when mean annual precipitation (MAP) is greater than 1,000mm (suggested by the $\delta^{18}O_{bulk}$ data relative to Kanapoi which has an estimated MAP of 620 ± 100 mm/year; Wynn 2004). However, variation in the mean values between the mildly seasonal periods suggest a shift in the baseline values of the source water over the 60ka period of occupation at Allia Bay.

If suids and hippos occupying the same habitat are assumed to record the lowest values of $\delta^{18}O$ in an ecosystem at a particular time period (i.e., acting as the baseline value for large mammals as they do in the modern Koobi Fora ecosystem), then the difference in suid and hippo values can be interpreted as representing at least two distinct period of stability in the paleoenvironment with a shift of ~6-8‰ (baseline $\delta^{18}O_{en}$ at ~17 and ~23-25‰), while maintaining a similar magnitude of $\Delta^{18}O$. The hippos SIMS transects maintain a similar seasonal pattern for all three hippos, but reflect an offset of ~6‰. Shifts of $\delta^{18}O_{en}$ values, while maintaining similar seasonal annual patterns have been observed in other species by traditional serial sampling methods of single moalrs (Hipparionini, Nelson 2005) and multiple teeth (gazelle and goats; Hallin et al. 2012). From 10 to 6.3 Ma in the Siwaliks of Pakistan, Hipparioninis recorded similar patterns of $\delta^{18}O_{en}$ values but shifted by an overall ~6‰, with shifts of ~4‰ occurring over short time periods (i.e., higher values by ~4‰ between 9.7-9.3 Ma, reverting back to lower values by ~4‰ between 8.7-8.5 Ma; Nelson 2005). On a shorter timescale, gazelles compared between Amud Cave (53-70ka) and modern Israel maintain similar seasonal patterns but exhibit a shift in mean $\delta^{18}O_{en}$ values of 3‰ (Hallin et al. 2012). The shifts between the $\delta^{18}O_{en}$ values have been interpreted as transitions between closed and open habitats accompanied by

differences in rainfall, but with the seasonal cycle being maintained as the amplitude does not change (Hallin et al. 2012; Nelson 2005). At Allia Bay, the SIMS data can be interpreted as recording at minimum a shift between two different baseline values documented by the hippos and suids at 16-17‰ and 23-25‰ when the general pattern of the seasonal cycle recorded was similar but the amount of rainfall changed between a wetter and drier phase.

Kingston (2007) correctly observes that resolving terrestrial seasonality at the level of weeks has eluded researchers interested in accessing paleoseasonality in East Africa at hominin localities. The SIMS spot size provides a new scale of analysis to characterize seasonality at the necessary scale to make inferences about the association of an increase in seasonality with increasing aridity. The samples from this study suggest that at Allia Bay there is evidence of increased marked seasonal rainfall intra-annual fluctuations that occur during the driest periods recorded at the site. The marked seasonality during drier periods at Allia Bay would have differentially impacted the animals and vegetation in the ecosystem because depending on dispersal thresholds the different mammalian families would respond by moving across the paleolandscape as vegetation resources shifted during varied seasonal rainfall regimes. With multiple patterns of paleoprecipitation recorded in this dataset, it lends support to the Shifting Heterogeneity Model (Kingston 2007), because the *Au. anamensis* ecosystem would have shifted significantly over a period of tens of thousands of years suggested by the 6-8‰ baseline $\delta^{18}O_{en}$ values documented in the hippos and suids. As rainfall patterns fluctuated, animal and plant communities were impacted and the early hominins would have required adaptive flexibility to cope with the changing habitat.

However, evidence of species longevity patterns for early hominins do not indicate that hominins are uniquely resilient to environmental changes relative to other mammals (Kingston 2007). For large herbivore mammals, this is supported by the SIMS dataset at Allia Bay because individuals within a single family (i.e., Giraffidae and Elephantidaes) were adaptively flexible

between periods of greater stability and periods with more marked seasonality. Until further species identification analysis is conducted at Allia Bay, it is unclear if this flexibility is within species inhabiting the site or families. The differences recorded between individuals of the same family have implications for the adaptive flexibility of a species over longer periods of time during the Pliocene at Allia Bay.

Conclusion

The new high-resolution Allia Bay fossil fauna isotope data presented in this study highlights need for early hominins to be adaptively flexible in an ever changing paleoenvironment. It appears that *Au. anamensis* could thrive in a variety of mosaic habitats with varied moisture regimes: prolonged periods of stable wetter environments and marked fluctuating seasonality with increasingly drier phases at Allia Bay. At the origins of the *Australopithecus* genus, early hominins were not likely ecological niche specialists, but adaptively flexible. It is possible that facultative bipedalism coincided with the initial C_4 grassland expansion occurring 7-4.4 Ma, but that those earlier hominins were still restricted to woodland and edge ecotones. Then the selective pressures associated with increasing variable seasonality patterns impacting the biomass resource availability on the landscape might have been the driving force resulting in the origins of the obligate bipedal genus, *Australopithecus,* when the climate was still relatively wet in local ecological niches like Allia Bay. Then as aridification increased through time, the further opening of woodland environments resulted in the origins of *Homo* (Bobe and Behrensmeyer 2004; Reed 1997). We have demonstrated the variation in seasonality recorded for a single *Au. anamensis* fossil locality from the high-resolution isotope data generated from faunal enamel samples recovered from a short temporal period of 60ka. This is a first step at applying SIMS high-resolution methods for documenting seasonality at early hominin sites.

Acknowledgements

This chapter is currently being prepared for submission for publication of the material with co-authors Margaret J. Schoeninger, Ian Orland and John Valley. The dissertation author was the primary investigator and author of this material.

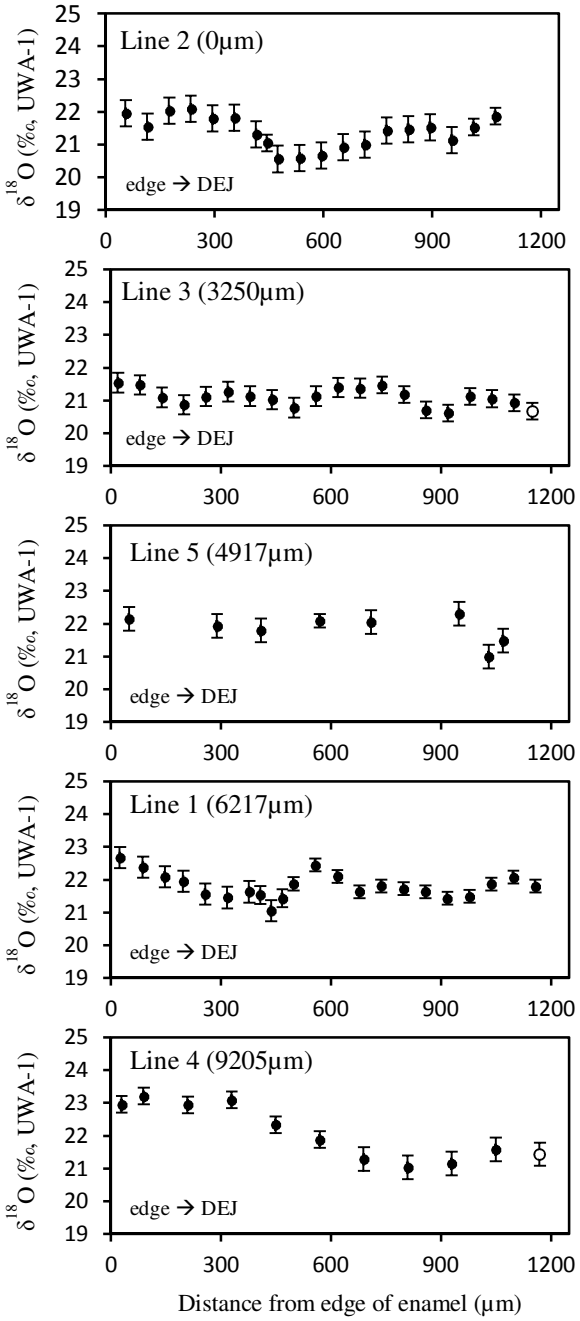

Figure 4.1: Plot of Bovidae (4877) SIMS $\delta^{18}O$ transects. Comparison of the intra-tooth SIMS transect of $\delta^{18}O$ (with 2SD error bars) for 5 line transects from the outer enamel layer to the DEJ along the growth axis (measurements relative to Line 2 – near occlusal surface) of a grazing Bovidae. Each transect line plots all SIMS analyses including, biogenic (filled in symbols) and unreliable values. Values were determined to be unreliable and excluded from the paleoenvironment reconstruction if they were suspected to be diagenetically altered (determined by the presence of CLFM far-red fluorophores; open symbols).

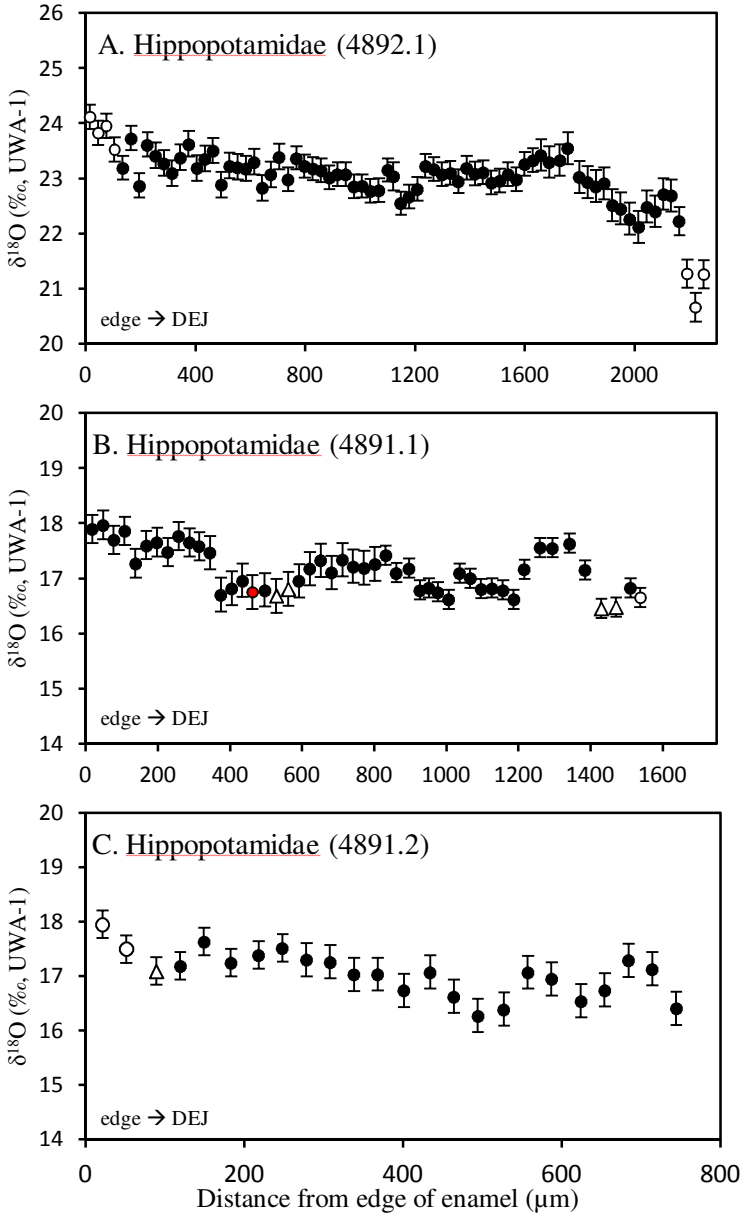

Figure 4.2: Plot of three Hippopotamidae SIMS $\delta^{18}O$ transects. Comparison of the intra-tooth SIMS transect of $\delta^{18}O$ (with 2SD error bars) variation recorded from the outer enamel layer to the DEJ for a browsing hippo (**A**) and two C_4-dominate mixed feeder hippos (**B, C**). Each transect line plots all SIMS analyses including, biogenic (black circles) circles) and unreliable values. Values were determined to be unreliable and excluded from the paleoenvironment reconstruction if they were suspected to be diagenetically altered (determined by the presence of CLFM far-red fluorophores; open symbols), the pit was irregular (determined by SEM; triangle symbol), and /or the relative yield analysis was an outlier (determined statistically per analytical session; red symbols).

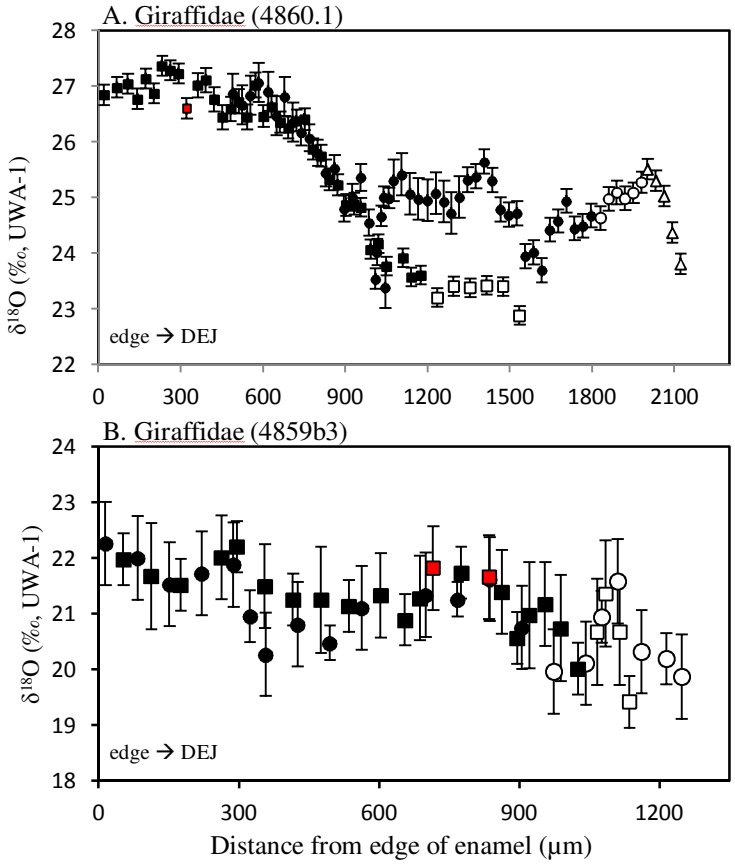

Figure 4.3: Plot of two Giraffidae SIMS $\delta^{18}O$ transects. Comparison of the intra-tooth SIMS transect of $\delta^{18}O$ (with 2SD error bars) variation recorded from the outer enamel layer to the DEJ for two browsing Giraffidaes. Each transect line plots all SIMS analyses including, biogenic (filled in symbols) and unreliable values. Values were determined to be unreliable and excluded from the paleoenvironment reconstruction if they were suspected to be diagenetically altered (determined by the presence of CLFM far-red fluorophores; open symbols), the pit was irregular (determined by SEM; triangle symbol), and /or the relative yield analysis was an outlier (determined statistically per analytical session; red symbols).

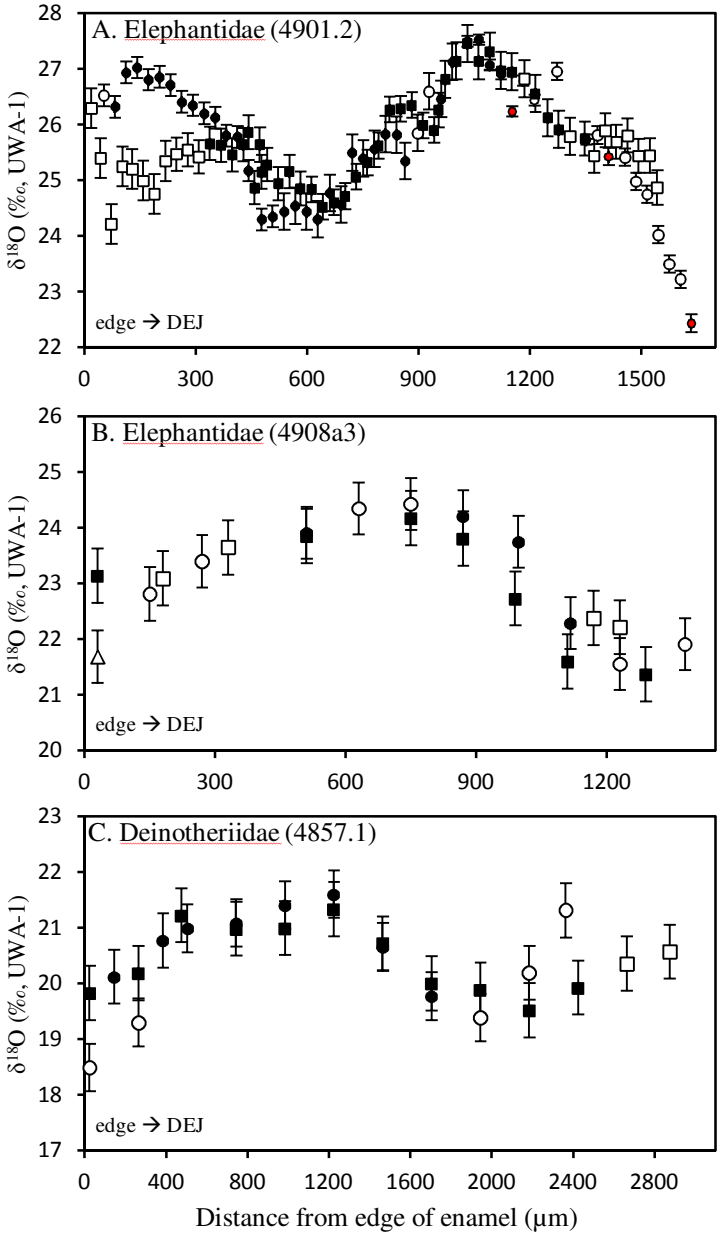

Figure 4.4: Plot of three Proboscidaes SIMS $\delta^{18}O$ transects. Comparison of the intra-tooth SIMS transect of $\delta^{18}O$ (with 2SD error bars) variation recorded from the outer enamel layer to the DEJ for two browsing proboscidaes (**A, C**) and a mixed C_3/C_4 feeder (**B**). Each transect line plots all SIMS analyses including, biogenic (filled in symbols) and unreliable values. Values were determined to be unreliable and excluded from the paleoenvironment reconstruction if they were suspected to be diagenetically altered (determined by the presence of CLFM far-red fluorophores; open symbols), the pit was irregular (determined by SEM; triangle symbol), and /or the relative yield analysis was an outlier (determined statistically per analytical session; red symbols).

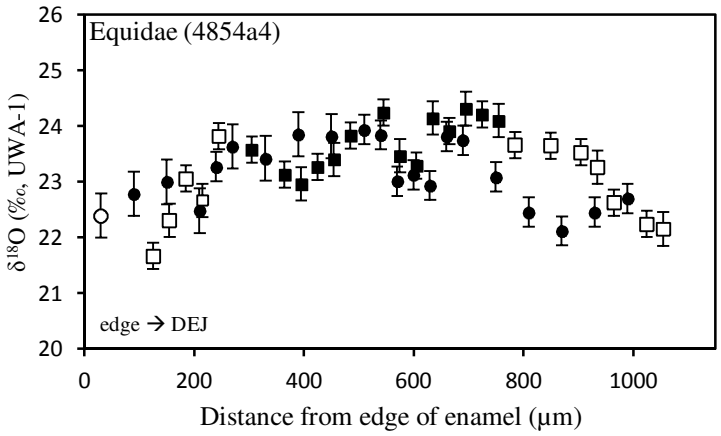

Figure 4.5: Plot of Equidae (4854a4) SIMS $\delta^{18}O$ transects. Comparison of the intra-tooth SIMS transect of $\delta^{18}O$ (with 2SD error bars) variation recorded from the outer enamel layer to the DEJ for an Equidae. Each transect line plots all SIMS analyses including, biogenic (black circles) and unreliable values. Values were determined to be unreliable and excluded from the paleoenvironment reconstruction if they were suspected to be diagenetically altered (determined by the presence of CLFM far-red fluorophores; open symbols).

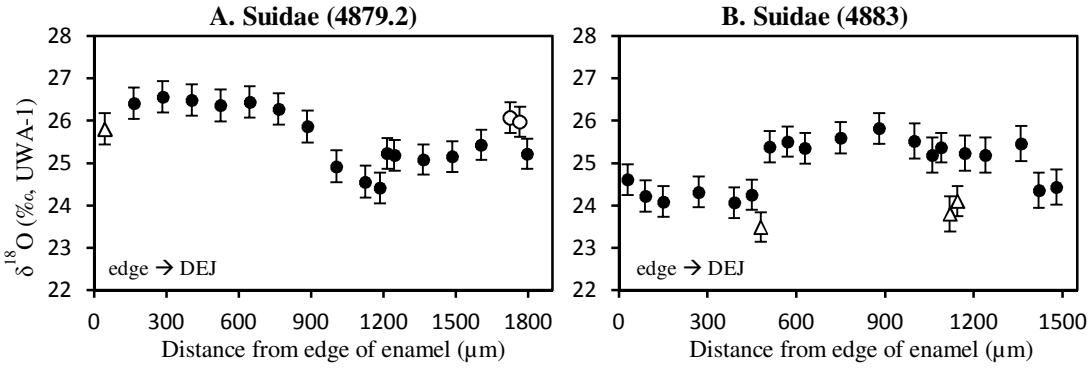

Figure 4.6: Plot of two Suidae SIMS $\delta^{18}O$ transects. Comparison of the intra-tooth SIMS transect of $\delta^{18}O$ (with 2SD error bars) variation recorded from the outer enamel layer to the DEJ for a mixed C_3/C_4 feeding suid (**A**) and a grazing suid (**B**). Each transect line plots all SIMS analyses including, biogenic (black circles) and unreliable values. Values were determined to be unreliable and excluded from the paleoenvironment reconstruction if they were suspected to be diagenetically altered (determined by the presence of CLFM far-red fluorophores; open symbols) and/or the pit was irregular (determined by SEM; triangle symbol).

Table 4.1: Comparison of variation in $\Delta^{18}O$ recorded by different serial sampling methods of modern herbivores in Kenya

Location	Rainfall (peak)	Species	Sample #	Teeth	N	$\Delta^{18}O$
Inter-tooth Variation (all teeth from a single individual)						
Koobi Fora	One (April)	Grant's Gazelle[a]	MS 2109	P3, P4, M2, M3	9	2.2
Koobi Fora	One (April)	Topi[b]	MS 2484	P4, M3	2	2.8
Koobi Fora	One (April)	Dikdik[b]	MS 2278	I1, P2, P4, M1, M3	9	2.0
Koobi Fora	One (April)	Burchell's Zebra[b]	MS 2142	M2, M3	4	0.6
Koobi Fora	One (April)	Burchell's Zebra[b]	MS 2306	M2, M3	4	0.4
Nairobi	Two (April, November)	Gazelle[a]	G-1	P3, P4, M1, M2, M3	17	3.2
Nairobi	Two (April, November)	Gazelle[a]	G-2	P2, P3, M1, M2, M3	18	2.3
Intra-tooth Variation (multiple horizontal samples from a single tooth along growth axis)						
Koobi Fora	One (April)	Burchell's Zebra[a]	MS 2306	M3	12	1.4
Nairobi	Two (April, November)	Gazelle[a]	G-2	M3	14	3.0
Nairobi	Two (April, November)	Gazelle[a]	G-2	M1	6	0.3
Nairobi	Two (April, November)	Gazelle[a]	G-2	M2	14	1.7
Enkorika	Two (May, November)	Goat[c]	Goat-1	M2R	15	3.8
Intra-tooth Variation (SIMS sampling transects from outer edge of enamel to DEJ)						
Koobi Fora	One (April)	Burchell's Zebra[d]	MS 2142	M3	38	2.24
Koobi Fora	One (April)	Grant's Gazelle[d]	MS 2109	M3	27	3.87

[a]Kohn et al. 1998

[b]Kohn et al 1996

[c]Balasse 2003

[d]Chapter 3 this dissertation

Table 4.2: Summary data for Allia Bay fossil samples.

Sample	Family	# of Transects	SIMS pits (n)	biogenic SIMS pits (n)	$\delta^{13}C$‰ (bulk)	$\delta^{18}O$‰ (bulk)	$\delta^{18}O_{SIMS}$‰ (mean)[a]	$\Delta^{18}O_{SIMS}$‰ (amplitude dif)[a]	Duration (months)[b]
4877	Bovidae	5	80	78	-0.3	29.3	21.58	2.65	>12
4857.1	Deinotheriidae	2	26	19	-13.1	29.8	20.58	2.08	17.4
4901.2	Elephantidae	2	106	69	-12.6	33.5	25.85	3.23	9.2
4908a3	Elephantidae	3	41	19	-7.4	30.3	23.20	2.84	9.1
4854a4	Equidae	2	47	34	-4.9	30.7	23.39	2.20	6.5
4860.1	Giraffidae	2	102	83	-15.5	33.9	25.54	4.16	12.9
4859b3	Giraffidae	3	70	39	-14.0	29.8	21.34	2.47	7.3
4892.1	Hippopotamidae	1	75	68	-11.7	29.8	23.03	1.61	14.7
4891.1	Hippopotamidae	1	49	43	-4.2	26.8	17.24	1.35	10.6
4891.2	Hippopotamidae	1	24	21	-2.0	26.8	16.98	1.36	4.5
4879.2	Suidae	1	19	16	-2.1	32.8	25.59	2.15	11.8
4883	Suidae	1	22	19	-1.0	33.0	24.94	1.75	10.5

[a]Only the biogenic SIMS pits were used to calculate the mean and amplitude difference

[b]Duration of the $\Delta^{18}O$ estimated based on daily enamel thickness growth rates for combined parallel lines (see calculation Table 4.3)

Table 4.3: Temporal resolution of line transects for Allia Bay fossil samples.

Sample	Family	Line	SIMS pits (n)	biogenic SIMS pits (n)	Distance (edge-DEJ) (µm)	Min days* (4.6 µm)	Max days* (1.8 µm)	Conservative estimate (months)	$\delta^{18}O_{SIMS}$‰ (mean)	$\Delta^{18}O_{SIMS}$‰ (amplitude difference)
4877	Bovidae	1	22	22	1133	246	629	8.2	21.79	1.62
4877	Bovidae	2	19	19	1020	222	567	7.4	21.38	1.53
4877	Bovidae	3	20	19	1080	235	600	7.8	21.11	0.91
4877	Bovidae	4	11	10	1020	222	567	7.4	22.14	2.18
4877	Bovidae	5	8	8	1020	222	567	7.4	21.84	1.31
4857.1	Deinotheriidae	1	13	8	1560	339	867	11.3	20.80	1.83
4857.1	Deinotheriidae	2	13	11	2400	522	1333	17.4	20.42	1.82
4901.2	Elephantidae	1	56	36	1010	220	561	7.3	25.83	2.94
4901.2	Elephantidae	4	50	33	1040	226	578	7.5	25.88	3.23
4908a3	Elephantidae	1	19	8	486	106	270	3.5	23.75	1.54
4908a3	Elephantidae	2	11	4	607	132	337	4.4	23.54	1.92
4908a3	Elephantidae	3	11	7	1260	274	700	9.1	22.95	2.80
4854a4	Equidae	1	21	20	900	196	500	6.5	23.17	1.82
4854a4	Equidae	2	26	14	450	98	250	3.3	23.70	1.35
4860.1	Giraffidae	1	59	47	1306	284	726	9.5	25.19	3.68
4860.1	Giraffidae	2	43	36	1155	251	642	8.4	26.00	3.80
4859b3	Giraffidae	1	21	14	891	194	495	6.5	21.28	1.99
4859b3	Giraffidae	2	25	19	973	212	541	7.1	21.29	2.19
4859b3	Giraffidae	3	24	6	655	142	364	4.7	21.62	1.62
4892.1	Hippopotamidae	1	75	68	2029	441	1127	14.7	23.03	1.61
4891.1	Hippopotamidae	1	49	38	1463	318	813	10.6	17.24	1.35
4891.2	Hippopotamidae	1	24	21	625	136	347	4.5	16.98	1.36

Table 4.3: Temporal resolution of line transects for Allia Bay fossil samples. (continued)

Sample	Family	Line	SIMS pits (n)	biogenic SIMS pits (n)	Distance (edge-DEJ) (µm)	Min days* (4.6 µm)	Max days* (1.8 µm)	Conservative estimate (months)	$\delta^{18}O_{SIMS}‰$ (mean)	$\Delta^{18}O_{SIMS}‰$ (amplitude difference)
4879.2	Suidae	1	19	16	1630	354	906	11.8	25.59	2.15
4883	Suidae	1	22	19	1450	315	806	10.5	24.94	1.75

*enamel thickness growth rates (x) estimated as: x = d(sin I) (where d = distance between cross striations and I = angle between enamel prisms and the DEJ) (Metcalfe and Longstaffe 2014)

Chapter 4 Appendix: Raw data of $\delta^{18}O$ measurements of apatites by SIMS (Cameca 1280)

Analysis #	Sample	Line #	Diagenesis* SEM	Diagenesis* CLFM			Bias (α)	$\delta^{18}O_{RAW}$‰	±2 SE	$\delta^{18}O_{COR}$‰	±2 SD	Distance from edge of enamel (μm)
				GR	RD	FRD	A	B	C	D	E	
Sample: 4859b3 (Giraffidae) with UWA-1.												
UWA-1												
20150406@535	UWA-1 Grain 5 (G5)							20.893	0.273			
20150406@536	UWA-1 Grain 6 (G6)							20.714	0.258			
20150406@537	UWA-1 G6							21.150	0.227			
20150406@538	UWA-1 G6							20.921	0.191			
Average and ±2 SD								**20.920**	**0.358**			
Enamel												
20150406@539	4859b3-001	1		**x**	**x**	**x**		28.237	0.252	19.87	0.76	1248
20150406@540	4859b3-002	1		**x**	**x**	**x**		29.965	0.235	21.58	0.76	1111
20150406@541	4859b3-003	1			**x**	**x**		28.332	0.190	19.96	0.76	974
20150406@542	4859b3-004	1						30.001	0.194	21.62	0.76	837
20150406@543	4859b3-005	1						29.720	0.239	21.34	0.76	700
20150406@544	4859b3-006	1						29.483	0.203	21.10	0.76	563
20150406@545	4859b3-007	1						29.186	0.220	20.81	0.76	426
20150406@546	4859b3-008	1						30.265	0.233	21.88	0.76	289
UWA-1												
20150406@547	UWA-1 G6							21.783	0.204			
20150406@548	UWA-1 G6							20.942	0.251			
20150406@549	UWA-1 G6							21.177	0.182			
20150406@550	UWA-1 G6							20.521	0.218			
Average and ±2 SD								**21.106**	**1.054**			
Bracket: Average and ±2 SD							**1.0082**	**21.013**	**0.755**			
Enamel												
20150406@551	4859b3-009	1						29.934	0.264	21.53	0.75	152

Analysis #	Sample	Line #	Diagenesis*			Bias (α)	$\delta^{18}O_{RAW}$‰	±2 SE	$\delta^{18}O_{COR}$‰	±2 SD	Distance from edge of enamel (µm)
			SEM	CLFM							
			GR	RD	FRD	A	B	C	D	E	
20150406@552	4859b3-010	1	x	x			30.668	0.254	22.26	0.75	15
20150406@553	4859b3-011	1					30.403	0.298	21.99	0.75	84
20150406@554	4859b3-012	1					28.661	0.211	20.27	0.75	358
20150406@555	4859b3-013	1					30.125	0.229	21.72	0.75	221
20150406@556	4859b3-014	1		x			29.147	0.248	20.75	0.75	906
20150406@557	4859b3-015	1		x	x		28.498	0.283	20.10	0.75	1043
20150406@558	4859b3-016	1	x	x	x		28.707	0.247	20.31	0.75	1162
UWA-1											
20150406@559	UWA-1 G6						21.105	0.250			
20150406@560	UWA-1 G6						20.677	0.181			
20150406@561	UWA-1 G6						21.028	0.224			
20150406@562	UWA-1 G6						21.025	0.180			
Average and ±2 SD							**20.959**	**0.383**			
Bracket: Average and ±2 SD						**1.0082**	**21.032**	**0.750**			
Enamel											
20150406@563	4859b3-017	1		x	x		29.099	0.191	20.94	0.46	1077
20150406@564	4859b3-018	1	x	x	x		28.340	0.276	20.19	0.46	1215
20150406@565	4859b3-019	1					29.112	0.197	20.95	0.46	324
20150406@566	4859b3-020	2		x			30.145	0.198	21.98	0.46	23
20150406@567	4859b3-021	2	x	x	x		27.561	0.237	19.41	0.46	1106
20150406@568	4859b3-022	2	x				28.159	0.234	20.01	0.46	996
20150406@569	4859b3-023	2	x				28.717	0.248	20.56	0.46	866
20150406@570	4859b3-024	2	x				29.897	0.296	21.73	0.46	746
20150406@571	4859b3-025	2					29.046	0.201	20.89	0.46	626
20150406@572	4859b3-026	2					29.295	0.229	21.13	0.46	506
20150406@573	4859b3-027	2					29.414	0.232	21.25	0.46	386
20150406@574	4859b3-028	2					30.369	0.237	22.20	0.46	266
20150406@575	4859b3-029	2					29.681	0.188	21.52	0.46	146

Analysis #	Sample	Line #	Diagenesis* SEM	CLFM		Bias (α)	$\delta^{18}O_{RAW}$‰	±2 SE	$\delta^{18}O_{COR}$‰	±2 SD	Distance from edge of enamel (µm)
				GR	RD FRD	A	B	C	D	E	
UWA-1											
20150406@576	UWA-1 G6						20.547	0.184			
20150406@577	UWA-1 G6						20.813	0.202			
20150406@578	UWA-1 G6						20.603	0.263			
20150406@579	UWA-1 G6						20.550	0.264			
Average and ±2 SD							**20.628**	**0.252**			
Bracket: Average and ±2 SD						**1.0080**	**20.794**	**0.463**			
Enamel											
20150406@580	4859b3-030	2					30.356	0.230	22.01	0.75	233
20150406@581	4859b3-031	2					29.839	0.256	21.50	0.75	326
20150406@582	4859b3-032	2					29.667	0.258	21.33	0.75	574
20150406@583	4859b3-033	2					~~30.161~~	~~0.297~~	~~21.82~~	~~0.75~~	686
20150406@584	4859b3-034	2		**x**			~~29.998~~	~~0.267~~	~~21.65~~	~~0.75~~	806
20150406@585	4859b3-035	2		**x**			29.731	0.336	21.39	0.75	833
20150406@586	4859b3-036	2					29.620	0.238	21.28	0.75	658
20150406@587	4859b3-037	2		**x**			29.508	0.275	21.17	0.75	926
UWA-1											
20150406@588	UWA-1 G6						21.339	0.237			
20150406@589	UWA-1 G6						21.349	0.234			
20150406@590	UWA-1 G6						21.325	0.259			
20150406@591	UWA-1 G6						21.240	0.182			
Average and ±2 SD							**21.313**	**0.100**			
Bracket: Average and ±2 SD						**1.0082**	**20.971**	**0.753**			
Enamel											
20150406@592	4859b3-038	2					29.914	0.159	21.67	0.95	83
20150406@593	4859b3-039	2		**x**			28.975	0.246	20.74	0.95	959

Analysis #	Sample	Line #	Diagenesis*				Bias (α)	$\delta^{18}O_{RAW}$‰	±2 SE	$\delta^{18}O_{COR}$‰	±2 SD	Distance from edge
			SEM	CLFM								
				GR	RD	FRD	A	B	C	D	E	of enamel (µm)
20150406@594	4859b3-040	2		x				29.210	0.280	20.97	0.95	892
20150406@595	4859b3-041	2		x		x		29.596	0.348	21.35	0.95	1055
20150406@596	4859b3-042	2		x		x		28.907	0.249	20.67	0.95	1037
20150406@597	4859b3-043	2		x		x		28.907	0.264	20.67	0.95	1085
20150406@598	4859b3-044	2						29.489	0.220	21.25	0.95	446
20150406@599	4859b3-045	3		x				30.728	0.230	22.48	0.95	28
20150406@600	4859b3-046	3						30.365	0.256	22.12	0.95	121
20150406@601	4859b3-047	3		x		x		30.024	0.203	21.78	0.95	241
20150406@602	4859b3-048	3	SEM					~~22.245~~	~~0.263~~	~~14.06~~	~~0.95~~	361
20150406@603	4859b3-049	3				x		28.831	0.257	20.60	0.95	481
20150406@604	4859b3-050	3	SEM					27.619	0.183	19.39	0.95	601
20150406@605	4859b3-051	3	SEM					~~20.923~~	~~0.223~~	~~12.75~~	~~0.95~~	697
20150406@606	4859b3-052	3		x	x	x		28.720	0.254	20.49	0.95	817
20150406@607	4859b3-053	3		x	x	x		27.689	0.261	19.46	0.95	917
UWA-1												
20150406@608	UWA-1 G6							20.486	0.242			
20150406@609	UWA-1 G6							20.296	0.213			
20150406@610	UWA-1 G6							20.459	0.152			
20150406@611	UWA-1 G6							20.477	0.244			
Average and ±2 SD								**20.430**	**0.179**			
Bracket: Average and ±2 SD							**1.0081**	**20.871**	**0.954**			
Enamel												
20150406@612	4859b3-054	3		x				29.696	0.237	21.68	0.53	301
20150406@613	4859b3-055	3	SEM			x		~~25.826~~	~~0.307~~	~~17.84~~	~~0.53~~	411
20150406@614	4859b3-056	3						29.620	0.215	21.60	0.53	327
20150406@615	4859b3-057	3	SEM					27.102	0.175	19.10	0.53	345
20150406@616	4859b3-058	3	SEM					~~23.609~~	~~0.187~~	~~15.64~~	~~0.53~~	377
20150406@617	4859b3-059	3	SEM					28.435	0.264	20.43	0.53	651

Analysis #	Sample	Line #	Diagenesis* SEM	CLFM GR	CLFM RD	CLFM FRD	Bias (α) A	$\delta^{18}O_{RAW}$‰ B	±2 SE C	$\delta^{18}O_{COR}$‰ D	±2 SD E	Distance from edge of enamel (µm)
20150406@618	4859b3-060	3						29.003	0.178	20.99	0.53	666
20150406@619	4859b3-061	3						28.873	0.254	20.86	0.53	683
UWA-1												
20150406@620	UWA-1 G6							20.809	0.212			
20150406@621	UWA-1 G6							21.045	0.274			
20150406@622	UWA-1 G6							20.955	0.235			
20150406@623	UWA-1 G6							20.647	0.174			
Average and ±2 SD								**20.864**	**0.349**			
Bracket: Average and ±2 SD							**1.0078**	**20.647**	**0.531**			
Enamel												
20150406@624	4859b3-062	3		**x**	**x**	**x**		29.160	0.177	21.00	0.31	757
20150406@625	4859b3-063	3		**x**				~~25.566~~	~~0.248~~	~~17.43~~	~~0.31~~	713
20150406@626	4859b3-064	3		**x**	**x**	**x**		29.280	0.221	21.12	0.31	735
20150406@627	4859b3-065	3		**x**	**x**	**x**		29.658	0.267	21.49	0.31	698
20150406@628	4859b3-066	3				**x**		29.005	0.231	20.84	0.31	446
20150406@629	4859b3-067	3		**x**	**x**	**x**		28.663	0.240	20.50	0.31	867
20150406@630	4859b3-068	3				**x**		28.421	0.267	20.26	0.31	541
20150406@631	4859b3-069	1						29.416	0.201	21.25	0.31	768
20150406@632	4859b3-070	1						28.629	0.234	20.47	0.31	495
UWA-1												
20150406@633	UWA-1 G6							20.758	0.334			
20150406@634	UWA-1 G6; Cs res 189-190							20.689	0.220			
20150406@635	UWA-1 G6							20.869	0.177			
20150406@636	UWA-1 G6							20.596	0.191			
Average and ±2 SD								**20.728**	**0.230**			
Bracket: Average and ±2 SD							**1.0078**	**20.647**	**0.531**			

Analysis #	Sample	Line #	Diagenesis* SEM	CLFM GR	CLFM RD	CLFM FRD	Bias (α) A	$\delta^{18}O_{RAW}$‰ B	±2 SE C	$\delta^{18}O_{COR}$‰ D	±2 SD E	Distance from edge of enamel (µm)
Sample: 4860.1 (Giraffidae) with UWA-1.												
UWA-1												
20141110@10	UWA-1 G2							18.825	0.431			
20141110@11	UWA-1 G3							19.130	0.351			
20141110@12	UWA-1 G4							18.753	0.429			
20141110@13	UWA-1 G2							18.848	0.334			
20141110@14	UWA-1 G2							18.551	0.329			
Average and ±2 SD								**18.821**	**0.417**			
Enamel												
20141110@15	4860.1-001	1						33.090	0.381	26.87	0.35	11
20141110@16	4860.1-002	1						32.891	0.422	26.67	0.35	45
20141110@17	4860.1-003	1		**x**				33.063	0.359	26.84	0.35	75
20141110@18	4860.1-004	1		**x**				33.292	0.375	27.07	0.35	105
20141110@19	4860.1-005	1		**x**				33.131	0.453	26.91	0.35	140
20141110@20	4860.1-006	1		**x**				32.692	0.427	26.47	0.35	170
20141110@21	4860.1-007	1						33.033	0.475	26.81	0.35	200
20141110@22	4860.1-008	1						32.572	0.468	26.35	0.35	230
UWA-1												
20141110@23	UWA-1 G2							18.876	0.445			
20141110@24	UWA-1 G2							18.893	0.422			
20141110@25	UWA-1 G2							18.647	0.365			
20141110@26	UWA-1 G2							19.010	0.445			
Average and ±2 SD								**18.857**	**0.304**			
Bracket: Average and ±2 SD							**1.0061**	**18.837**	**0.350**			
Enamel												
20141110@27	4860.1-009	1						32.421	0.467	26.18	0.24	260
20141110@28	4860.1-010	1						32.315	0.514	26.07	0.24	290

Analysis #	Sample	Line #	Diagenesis* SEM	Diagenesis* CLFM			Bias (α)	$\delta^{18}O_{RAW}$‰	±2 SE	$\delta^{18}O_{COR}$‰	±2 SD	Distance from edge
				GR	RD	FRD	A	B	C	D	E	of enamel (µm)
20141110@29	4860.1-011	1						32.044	0.429	25.80	0.24	320
20141110@30	4860.1-012	1						31.684	0.551	25.44	0.24	350
20141110@31	4860.1-013	1						31.768	0.488	25.53	0.24	382
20141110@32	4860.1-014	1						31.038	0.406	24.80	0.24	417
20141110@33	4860.1-015	1						31.246	0.577	25.01	0.24	447
20141110@34	4860.1-016	1						31.602	0.454	25.36	0.24	477
20141110@35	4860.1-017	1						30.784	0.806	24.55	0.24	507
20141110@36	4860.1-018	1						30.253	0.500	24.02	0.24	537
UWA-1												
20141110@37	UWA-1 G2							18.999	0.345			
20141110@38	UWA-1 G2							18.905	0.366			
20141110@39	UWA-1 G2							18.799	0.381			
20141110@40	UWA-1 G2							18.780	0.499			
Average and ±2 SD								**18.871**	**0.203**			
Bracket: Average and ±2 SD							**1.0061**	**18.864**	**0.240**			
Enamel												
20141110@41	4860.1-019	1						29.564	0.628	23.38	0.37	567
20141110@42	4860.1-020	1						31.503	0.566	25.31	0.37	597
20141110@43	4860.1-021	1						31.609	0.450	25.42	0.37	627
20141110@44	4860.1-022	1						31.261	0.414	25.07	0.37	657
20141110@45	4860.1-023	1						31.160	0.462	24.97	0.37	687
20141110@46	4860.1-024	1						31.138	0.472	24.95	0.37	721
20141110@47	4860.1-025	1						31.273	0.407	25.08	0.37	751
20141110@48	4860.1-026	1						31.117	0.431	24.93	0.37	781
20141110@49	4860.1-027	1						30.910	0.520	24.72	0.37	807
20141110@50	4860.1-028	1						31.203	0.461	25.01	0.37	837

UWA-1

Analysis #	Sample	Line #	Diagenesis* SEM	CLFM GR	CLFM RD	CLFM FRD	Bias (α) A	$\delta^{18}O_{RAW}$‰ B	±2 SE C	$\delta^{18}O_{COR}$‰ D	±2 SD E	Distance from edge of enamel (µm)
20141110@51	UWA-1 G2							19.078	0.510			
20141110@52	UWA-1 G2							18.831	0.368			
20141110@53	UWA-1 G2							18.624	0.494			
20141110@54	UWA-1 G2; Cs res 135-136							18.506	0.449			
Average and ±2 SD								**18.760**	**0.502**			
Bracket: Average and ±2 SD							**1.0060**	**18.815**	**0.374**			
UWA-1												
20141110@56	UWA-1 G2							18.866	0.368			
20141110@57	UWA-1 G2							18.619	0.467			
20141110@58	UWA-1 G2							18.661	0.387			
20141110@59	UWA-1 G2							18.824	0.353			
Average and ±2 SD								**18.743**	**0.242**			
Enamel												
20141110@60	4860.1-029	1						31.481	0.481	25.32	0.22	867
20141110@61	4860.1-030	1						31.544	0.504	25.38	0.22	897
20141110@62	4860.1-031	1						31.811	0.478	25.65	0.22	927
20141110@63	4860.1-032	1						31.473	0.477	25.31	0.22	957
20141110@64	4860.1-033	1						30.945	0.403	24.79	0.22	987
20141110@65	4860.1-034	1						30.849	0.460	24.69	0.22	1017
20141110@66	4860.1-035	1			x			30.877	0.475	24.72	0.22	1047
20141110@67	4860.1-036	1			x			30.101	0.465	23.95	0.22	1077
20141110@68	4860.1-037	1			x			30.173	0.415	24.02	0.22	1107
20141110@69	4860.1-038	1						29.847	0.391	23.69	0.22	1137
UWA-1												
20141110@70	UWA-1 G2							18.823	0.444			
20141110@71	UWA-1 G2							18.833	0.389			
20141110@72	UWA-1 G2							18.947	0.394			

Analysis #	Sample	Line #	Diagenesis* SEM	CLFM GR	CLFM RD	CLFM FRD	Bias (α) A	$\delta^{18}O_{RAW}$‰ B	±2 SE C	$\delta^{18}O_{COR}$‰ D	±2 SD E	Distance from edge of enamel (µm)
20141110@73	UWA-1 G2; Cs res 136-137							18.721	0.422			
Average and ±2 SD								**18.831**	**0.185**			
Bracket: Average and ±2 SD							**1.0060**	**18.787**	**0.220**			
UWA-1												
20141110@75	UWA-1 G2							18.654	0.381			
20141110@76	UWA-1 G2							18.764	0.376			
20141110@77	UWA-1 G2							18.573	0.377			
20141110@78	UWA-1 G2							18.812	0.446			
Average and ±2 SD								**18.701**	**0.216**			
Enamel												
20141110@79	4860.1-039	1						30.543	0.402	24.42	0.21	1167
20141110@80	4860.1-040	1						30.698	0.454	24.58	0.21	1197
20141110@81	4860.1-041	1						31.059	0.495	24.94	0.21	1227
20141110@82	4860.1-042	1			**x**			30.567	0.432	24.45	0.21	1257
20141110@83	4860.1-043	1			**x**			30.608	0.540	24.49	0.21	1287
20141110@84	4860.1-044	1			**x**			30.797	0.446	24.68	0.21	1317
20141110@85	4860.1-045	1			**x**	**x**		30.754	0.407	24.63	0.21	1351
20141110@86	4860.1-046	1			**x**	**x**		31.098	0.438	24.98	0.21	1381
20141110@87	4860.1-047	1			**x**	**x**		31.213	0.355	25.09	0.21	1411
20141110@88	4860.1-048	1			**x**	**x**		31.105	0.441	24.98	0.21	1441
UWA-1												
20141110@89	UWA-1 G2							18.816	0.439			
20141110@90	UWA-1 G2							18.770	0.389			
20141110@91	UWA-1 G2							18.909	0.338			
20141110@92	UWA-1 G2							18.692	0.426			
Average and ±2 SD								**18.797**	**0.181**			
Bracket: Average and ±2 SD							**1.0060**	**18.749**	**0.211**			

Analysis #	Sample	Line #	Diagenesis*				Bias (α)	$\delta^{18}O_{RAW}$‰	±2 SE	$\delta^{18}O_{COR}$‰	±2 SD	Distance from edge of enamel (µm)
			SEM	CLFM								
				GR	RD	FRD	A	B	C	D	E	
Enamel												
20141110@93	4860.1-049	1			x	x		31.200	0.517	25.08	0.18	1471
20141110@94	4860.1-050	1			x	x		31.394	0.481	25.27	0.18	1501
20141110@95	4860.1-051	1	**SEM**		x	x		31.628	0.456	25.51	0.18	1523
20141110@96	4860.1-052	1	**SEM**		x	x		31.419	0.392	25.30	0.18	1553
20141110@97	4860.1-053	1	**SEM**		x	x		31.143	0.489	25.02	0.18	1583
20141110@98	4860.1-054	1	**SEM**		x	x		30.482	0.544	24.37	0.18	1613
20141110@99	4860.1-055	1	**SEM**		x	x		29.921	0.440	23.81	0.18	1643
20141110@100	4860.1-056	1						31.132	0.497	25.01	0.18	561
20141110@101	4860.1-057	1						29.651	0.480	23.54	0.18	531
20141110@102	4860.1-058	1						30.784	0.441	24.67	0.18	552
20141110@103	4860.1-059	1						31.110	0.729	24.99	0.18	580
UWA-1												
20141110@104	UWA-1 G2							18.718	0.407			
20141110@105	UWA-1 G2							18.777	0.451			
20141110@106	UWA-1 G2							18.630	0.408			
20141110@107	UWA-1 G2							18.648	0.448			
Average and ±2 SD								**18.693**	**0.135**			
Bracket: Average and ±2 SD							**1.0060**	**18.745**	**0.185**			
UWA-1												
20141110@548	UWA-1 G2							20.279	0.379			
20141110@549	UWA-1 G2							20.299	0.307			
20141110@550	UWA-1 G2							20.387	0.312			
20141110@551	UWA-1 G2							20.296	0.247			
Average and ±2 SD								**20.315**	**0.097**			
Enamel												

Analysis #	Sample	Line #	Diagenesis* SEM	CLFM		Bias (α)	$\delta^{18}O_{RAW}$‰	±2 SE	$\delta^{18}O_{COR}$‰	±2 SD	Distance from edge
				GR	RD FRD	A	B	C	D	E	of enamel (µm)
20141110@552	4860.1-060	2		x	x		34.502	0.397	26.84	0.18	20
20141110@553	4860.1-061	2		x	x		34.640	0.384	26.98	0.18	67
20141110@554	4860.1-062	2		x	x		34.703	0.306	27.04	0.18	107
20141110@555	4860.1-063	2					34.431	0.280	26.77	0.18	142
20141110@556	4860.1-064	2					34.801	0.365	27.14	0.18	172
20141110@557	4860.1-065	2					34.534	0.268	26.87	0.18	202
20141110@558	4860.1-066	2					35.028	0.341	27.36	0.18	232
20141110@559	4860.1-067	2					34.949	0.356	27.29	0.18	262
20141110@560	4860.1-068	2					34.893	0.400	27.23	0.18	292
20141110@561	4860.1-069	2					~~34.258~~	~~0.303~~	~~26.60~~	~~0.18~~	322
UWA-1											
20141110@562	UWA-1 G2						20.287	0.299			
20141110@563	UWA-1 G2						20.094	0.279			
20141110@564	UWA-1 G2						20.202	0.277			
20141110@565	UWA-1 G2						20.185	0.309			
Average and ±2 SD							**20.192**	**0.158**			
Bracket: Average and ±2 SD						**1.0075**	**20.254**	**0.179**			
Enamel											
20141110@566	4860.1-070	2					34.703	0.340	27.01	0.22	362
20141110@567	4860.1-071	2					34.797	0.250	27.11	0.22	392
20141110@568	4860.1-072	2					34.449	0.440	26.76	0.22	422
20141110@569	4860.1-073	2					34.128	0.351	26.44	0.22	452
20141110@570	4860.1-074	2					34.278	0.261	26.59	0.22	482
20141110@571	4860.1-075	2					34.411	0.292	26.72	0.22	512
20141110@572	4860.1-076	2					34.130	0.444	26.45	0.22	542
20141110@573	4860.1-077	2					34.709	0.307	27.02	0.22	572

UWA-1

Analysis #	Sample	Line #	Diagenesis* SEM	Diagenesis* CLFM			Bias (α)	$\delta^{18}O_{RAW}$‰	±2 SE	$\delta^{18}O_{COR}$‰	±2 SD	Distance from edge
				GR	RD	FRD	A	B	C	D	E	of enamel (µm)
20141110@574	UWA-1 G2							20.333	0.299			
20141110@575	UWA-1 G2							20.369	0.338			
20141110@576	UWA-1 G2							20.393	0.283			
20141110@577	UWA-1 G2; Cs res 154-152							20.386	0.312			
Average and ±2 SD								**20.370**	**0.054**			
Bracket: Average and ±2 SD							**1.0075**	**20.281**	**0.220**			
UWA-1												
20141110@579	UWA-1 G2							20.630	0.354			
20141110@580	UWA-1 G2							20.588	0.300			
20141110@581	UWA-1 G2							20.352	0.278			
20141110@582	UWA-1 G2							20.506	0.258			
Average and ±2 SD								**20.519**	**0.245**			
Enamel												
20141110@583	4860.1-078	2						34.360	0.302	26.46	0.19	602
20141110@584	4860.1-079	2						34.533	0.405	26.63	0.19	632
20141110@585	4860.1-080	2						34.252	0.370	26.36	0.19	662
20141110@586	4860.1-081	2						34.152	0.334	26.26	0.19	692
20141110@587	4860.1-082	2						34.279	0.424	26.38	0.19	722
20141110@588	4860.1-083	2						34.307	0.312	26.41	0.19	752
20141110@589	4860.1-084	2						33.765	0.360	25.87	0.19	782
20141110@590	4860.1-085	2						33.640	0.423	25.75	0.19	812
20141110@591	4860.1-086	2						33.215	0.386	25.33	0.19	842
20141110@592	4860.1-087	2						33.116	0.389	25.23	0.19	872
20141110@593	4860.1-088	2						32.755	0.386	24.87	0.19	902
20141110@594	4860.1-089	2		**x**				32.772	0.337	24.89	0.19	932
UWA-1												
20141110@595	UWA-1 G2							20.563	0.348			

Analysis #	Sample	Line #	Diagenesis* SEM	CLFM GR	CLFM RD	CLFM FRD	Bias (α) A	$\delta^{18}O_{RAW}$‰ B	±2 SE C	$\delta^{18}O_{COR}$‰ D	±2 SD E	Distance from edge of enamel (µm)
20141110@596	UWA-1 G2							20.448	0.322			
20141110@597	UWA-1 G2							20.451	0.321			
20141110@598	UWA-1 G2							20.397	0.247			
Average and ±2 SD								**20.465**	**0.140**			
Bracket: Average and ±2 SD							**1.0077**	**20.492**	**0.194**			
Enamel												
20141110@599	4860.1-090	2						31.866	0.325	24.07	0.17	992
20141110@600	4860.1-091	2			x			31.560	0.412	23.77	0.17	1050
20141110@601	4860.1-092	2						31.714	0.354	23.92	0.17	1110
20141110@602	4860.1-093	2			x			31.393	0.340	23.60	0.17	1175
20141110@603	4860.1-094	2			x	x		30.990	0.347	23.20	0.17	1235
20141110@604	4860.1-095	2		x	x	x		31.196	0.302	23.41	0.17	1295
20141110@605	4860.1-096	2		x	x	x		31.170	0.263	23.38	0.17	1355
20141110@606	4860.1-097	2		x	x	x		31.209	0.365	23.42	0.17	1415
20141110@607	4860.1-098	2		x	x	x		31.194	0.366	23.40	0.17	1475
20141110@608	4860.1-099	2			x	x		30.666	0.277	22.88	0.17	1535
20141110@609	4860.1-100	2			x			32.627	0.316	24.83	0.17	956
20141110@610	4860.1-101	2			x			31.966	0.329	24.17	0.17	1020
20141110@611	4860.1-102	2			x			31.360	0.377	23.57	0.17	1140
UWA-1												
20141110@612	UWA-1 G2							20.340	0.311			
20141110@613	UWA-1 G2							20.350	0.348			
20141110@614	UWA-1 G2							20.292	0.359			
20141110@615	UWA-1 G2							20.420	0.306			
Average and ±2 SD								**20.351**	**0.106**			
Bracket: Average and ±2 SD							**1.0076**	**20.408**	**0.168**			

Sample: 4901.2 (Elephantidae) with UWA-1.

Analysis #	Sample	Line #	Diagenesis* SEM	CLFM GR	CLFM RD	CLFM FRD	Bias (α) A	$\delta^{18}O_{RAW}$‰ B	±2 SE C	$\delta^{18}O_{COR}$‰ D	±2 SD E	Distance from edge of enamel (µm)
UWA-1												
20141110@155	UWA-1 G2							18.617	0.386			
20141110@156	UWA-1 G3							18.718	0.461			
20141110@157	UWA-1 G4							18.877	0.372			
20141110@158	UWA-1 G1							18.828	0.388			
Average and ±2 SD								**18.760**	**0.232**			
Enamel												
20141110@159	4901.2-001	1		x	x	x		32.555	0.495	26.29	0.36	18
20141110@160	4901.2-002	1		x	x	x		31.650	0.400	25.39	0.36	43
20141110@161	4901.2-003	1		x	x	x		30.457	0.438	24.21	0.36	72
20141110@162	4901.2-004	1		x	x	x		31.498	0.363	25.24	0.36	102
20141110@163	4901.2-005	1		x	x	x		31.449	0.359	25.20	0.36	128
20141110@164	4901.2-006	1		x	x	x		31.240	0.471	24.99	0.36	158
20141110@165	4901.2-007	1		x	x	x		31.003	0.372	24.75	0.36	188
20141110@166	4901.2-008	1		x	x	x		31.598	0.428	25.34	0.36	218
UWA-1												
20141110@167	UWA-1 G1							19.187	0.361			
20141110@168	UWA-1 G1							19.031	0.431			
20141110@169	UWA-1 G1							18.818	0.375			
20141110@170	UWA-1 G3							18.946	0.332			
Average and ±2 SD								**18.996**	**0.310**			
Bracket: Average and ±2 SD							**1.0061**	**18.878**	**0.357**			
Enamel												
20141110@171	4901.2-009	1		x	x	x		31.748	0.469	25.47	0.30	248
20141110@172	4901.2-010	1		x	x	x		31.828	0.464	25.55	0.30	278
20141110@173	4901.2-011	1			x	x		31.699	0.455	25.42	0.30	308
20141110@174	4901.2-012	1						31.938	0.431	25.66	0.30	338

Analysis #	Sample	Line #	Diagenesis* SEM	CLFM		Bias (α)	$\delta^{18}O_{RAW}$‰	±2 SE	$\delta^{18}O_{COR}$‰	±2 SD	Distance from edge
				GR	RD FRD	A	B	C	D	E	of enamel (µm)
20141110@175	4901.2-013	1					31.906	0.375	25.62	0.30	368
20141110@176	4901.2-014	1					31.734	0.433	25.45	0.30	398
20141110@177	4901.2-015	1					31.922	0.380	25.64	0.30	428
20141110@178	4901.2-016	1					31.141	0.443	24.86	0.30	458
20141110@179	4901.2-017	1					31.556	0.475	25.28	0.30	492
20141110@180	4901.2-018	1					31.214	0.491	24.94	0.30	522
20141110@181	4901.2-019	1					31.432	0.410	25.15	0.30	552
20141110@182	4901.2-020	1					31.126	0.369	24.85	0.30	582
UWA-1											
20141110@183	UWA-1 G1						18.896	0.453			
20141110@184	UWA-1 G1						18.796	0.433			
20141110@185	UWA-1 G1						18.719	0.325			
20141110@186	UWA-1 G1						18.828	0.355			
Average and ±2 SD							**18.810**	**0.147**			
Bracket: Average and ±2 SD						**1.0061**	**18.903**	**0.300**			
Enamel											
20141110@187	4901.2-021	1					31.083	0.341	24.83	0.23	612
20141110@188	4901.2-022	1					30.767	0.466	24.52	0.23	642
20141110@189	4901.2-023	1					30.847	0.521	24.60	0.23	672
20141110@190	4901.2-024	1					30.958	0.385	24.71	0.23	702
20141110@191	4901.2-025	1					31.309	0.355	25.06	0.23	732
20141110@192	4901.2-026	1					31.568	0.385	25.32	0.23	762
20141110@193	4901.2-027	1					31.872	0.432	25.62	0.23	792
20141110@194	4901.2-028	1					32.522	0.413	26.26	0.23	822
20141110@195	4901.2-029	1					32.538	0.403	26.28	0.23	852
20141110@196	4901.2-030	1					32.601	0.431	26.34	0.23	882
20141110@197	4901.2-031	1			x		32.236	0.423	25.98	0.23	912
20141110@198	4901.2-032	1			x		32.153	0.464	25.90	0.23	942

Analysis #	Sample	Line #	Diagenesis* SEM	CLFM GR	CLFM RD	CLFM FRD	Bias (α) A	$\delta^{18}O_{RAW}$‰ B	±2 SE C	$\delta^{18}O_{COR}$‰ D	±2 SD E	Distance from edge of enamel (µm)
UWA-1												
20141110@199	UWA-1 G1							19.111	0.406			
20141110@200	UWA-1 G1							18.930	0.378			
20141110@201	UWA-1 G1							18.872	0.422			
20141110@202	UWA-1 G1; Cs res 144-145							18.846	0.378			
Average and ±2 SD								**18.940**	**0.239**			
Bracket: Average and ±2 SD							**1.0061**	**18.875**	**0.230**			
UWA-1												
20141110@204	UWA-1 G1							19.028	0.349			
20141110@205	UWA-1 G1							18.735	0.382			
20141110@206	UWA-1 G1							18.705	0.429			
20141110@207	UWA-1 G1							19.010	0.378			
Average and ±2 SD								**18.870**	**0.346**			
Enamel												
20141110@208	4901.2-033	1			**x**			33.173	0.537	26.81	0.33	972
20141110@209	4901.2-034	1			**x**			33.503	0.414	27.14	0.33	1002
20141110@210	4901.2-035	1			**x**			33.824	0.462	27.46	0.33	1032
20141110@211	4901.2-036	1			**x**			33.507	0.420	27.14	0.33	1062
20141110@212	4901.2-037	1						33.679	0.383	27.31	0.33	1092
20141110@213	4901.2-038	1			**x**			33.331	0.350	26.97	0.33	1122
20141110@214	4901.2-039	1			**x**			33.306	0.381	26.94	0.33	1152
20141110@215	4901.2-040	1			**x**	**x**		33.182	0.410	26.82	0.33	1185
20141110@216	4901.2-041	1						32.915	0.318	26.55	0.33	1215
20141110@217	4901.2-042	1						32.478	0.419	26.12	0.33	1248
20141110@218	4901.2-043	1						32.266	0.378	25.91	0.33	1278
20141110@219	4901.2-044	1			**x**	**x**		32.140	0.523	25.78	0.33	1308

Analysis #	Sample	Line #	Diagenesis*				Bias (α)	$\delta^{18}O_{RAW}$‰	±2 SE	$\delta^{18}O_{COR}$‰	±2 SD	Distance from edge of enamel (µm)
			SEM	CLFM								
				GR	RD	FRD	A	B	C	D	E	
UWA-1												
20141110@220	UWA-1 G1							19.111	0.405			
20141110@221	UWA-1 G1							19.031	0.412			
20141110@222	UWA-1 G1							19.032	0.455			
20141110@223	UWA-1 G1; Cs res 145-146							19.161	0.366			
Average and ±2 SD								**19.084**	**0.127**			
Bracket: Average and ±2 SD							**1.0062**	**18.977**	**0.333**			
UWA-1												
20141110@226	UWA-1 G1							18.927	0.380			
20141110@227	UWA-1 G1							18.840	0.400			
20141110@228	UWA-1 G1							18.756	0.429			
20141110@229	UWA-1 G1							18.692	0.350			
Average and ±2 SD								**18.804**	**0.204**			
Enamel												
20141110@230	4901.2-045	1			x			31.999	0.373	25.75	0.31	1348
20141110@231	4901.2-046	1			x	x		31.686	0.470	25.44	0.31	1373
20141110@232	4901.2-047	1			x	x		32.143	0.342	25.89	0.31	1403
20141110@233	4901.2-048	1			x	x		31.938	0.394	25.69	0.31	1433
20141110@234	4901.2-049	1			x	x		32.051	0.345	25.80	0.31	1463
20141110@235	4901.2-050	1		x	x	x		31.684	0.397	25.43	0.31	1493
20141110@236	4901.2-051	1		x	x	x		31.690	0.446	25.44	0.31	1523
20141110@237	4901.2-052	1		x	x	x		31.113	0.477	24.87	0.31	1543
20141110@238	4901.2-053	1			x			32.512	0.363	26.26	0.31	954
20141110@239	4901.2-054	1						32.112	0.397	25.86	0.31	442
20141110@240	4901.2-055	1						31.394	0.351	25.15	0.31	477
20141110@241	4901.2-056	1						31.887	0.430	25.64	0.31	472

UWA-1

Analysis #	Sample	Line #	Diagenesis* SEM	CLFM GR	CLFM RD	CLFM FRD	Bias (α) A	$\delta^{18}O_{RAW}$‰ B	±2 SE C	$\delta^{18}O_{COR}$‰ D	±2 SD E	Distance from edge of enamel (µm)
20141110@242	UWA-1 G1							19.030	0.415			
20141110@243	UWA-1 G1							18.811	0.445			
20141110@244	UWA-1 G1							18.777	0.329			
20141110@245	UWA-1 G1							19.148	0.411			
Average and ±2 SD								**18.942**	**0.355**			
Bracket: Average and ±2 SD							**1.0061**	**18.873**	**0.306**			
UWA-1												
20141110@268	UWA-1 G1							18.858	0.364			
20141110@269	UWA-1 G1							18.758	0.355			
20141110@270	UWA-1 G1							19.003	0.436			
20141110@271	UWA-1 G1							18.983	0.392			
Average and ±2 SD								**18.901**	**0.229**			
Enamel												
20141110@272	4901.2-074	4		x	x	x		32.814	0.425	26.52	0.19	8
20141110@273	4901.2-075	4						32.608	0.265	26.32	0.19	38
20141110@274	4901.2-076	4						33.229	0.430	26.93	0.19	68
20141110@275	4901.2-077	4						33.316	0.389	27.02	0.19	98
20141110@276	4901.2-078	4						33.099	0.339	26.80	0.19	128
20141110@277	4901.2-079	4						33.147	0.367	26.85	0.19	158
20141110@278	4901.2-080	4						32.999	0.420	26.70	0.19	188
20141110@279	4901.2-081	4						32.695	0.462	26.40	0.19	218
20141110@280	4901.2-082	4						32.635	0.379	26.34	0.19	248
20141110@281	4901.2-083	4						32.487	0.440	26.20	0.19	278
20141110@282	4901.2-084	4						32.412	0.369	26.12	0.19	308
20141110@283	4901.2-085	4						32.087	0.349	25.80	0.19	338
20141110@284	4901.2-086	4						32.063	0.420	25.77	0.19	368
20141110@285	4901.2-087	4						31.455	0.444	25.17	0.19	398
20141110@286	4901.2-088	4						30.571	0.477	24.29	0.19	433

Analysis #	Sample	Line #	Diagenesis* SEM	Diagenesis* CLFM			Bias (α)	$\delta^{18}O_{RAW}$‰	±2 SE	$\delta^{18}O_{COR}$‰	±2 SD	Distance from edge of enamel (µm)
				GR	RD	FRD	A	B	C	D	E	
20141110@287	4901.2-089	4						30.627	0.405	24.35	0.19	463
UWA-1												
20141110@288	UWA-1 G1							18.839	0.350			
20141110@289	UWA-1 G1							19.037	0.439			
20141110@290	UWA-1 G1							18.938	0.439			
20141110@291	UWA-1 G1; Cs res 147-148							18.852	0.461			
Average and ±2 SD								**18.917**	**0.183**			
Bracket: Average and ±2 SD							**1.0061**	**18.909**	**0.193**			
UWA-1												
20141110@293	UWA-1 G3							19.122	0.480			
20141110@294	UWA-1 G3							18.739	0.382			
20141110@295	UWA-1 G3							18.890	0.435			
20141110@296	UWA-1 G3							18.844	0.421			
Average and ±2 SD								**18.899**	**0.323**			
Enamel												
20141110@297	4901.2-089 B	4						30.687	0.457	24.44	0.33	494
20141110@298	4901.2-090	4						30.791	0.382	24.54	0.33	524
20141110@299	4901.2-091	4						30.680	0.441	24.43	0.33	554
20141110@300	4901.2-092	4						30.541	0.508	24.29	0.33	584
20141110@301	4901.2-093	4						31.023	0.356	24.77	0.33	617
20141110@302	4901.2-094	4						30.805	0.528	24.56	0.33	647
20141110@303	4901.2-095	4						31.751	0.390	25.50	0.33	677
20141110@304	4901.2-096	4						31.644	0.429	25.39	0.33	707
20141110@305	4901.2-097	4						31.820	0.413	25.56	0.33	737
20141110@306	4901.2-098	4						32.084	0.391	25.83	0.33	767
20141110@307	4901.2-099	4						32.075	0.517	25.82	0.33	797
20141110@308	4901.2-100	4						31.595	0.455	25.34	0.33	820

Analysis #	Sample	Line #	Diagenesis*			Bias (α)	$\delta^{18}O_{RAW}$‰	±2 SE	$\delta^{18}O_{COR}$‰	±2 SD	Distance from edge of enamel (µm)
			SEM	CLFM							
				GR	RD	FRD	A	B	C	D	E	
20141110@309	4901.2-101	4			x	x		32.102	0.414	25.85	0.33	854
20141110@310	4901.2-102	4			x	x		32.854	0.375	26.59	0.33	884
20141110@311	4901.2-103	4			x			32.716	0.459	26.46	0.33	917
20141110@312	4901.2-104	4			x			33.384	0.409	27.12	0.33	947
UWA-1												
20141110@313	UWA-1 G3							18.822	0.415			
20141110@314	UWA-1 G3							18.794	0.435			
20141110@315	UWA-1 G3							18.683	0.420			
20141110@316	UWA-1 G3							19.120	0.434			
Average and ±2 SD								**18.855**	**0.373**			
Bracket: Average and ±2 SD							**1.0061**	**18.877**	**0.327**			
UWA-1												
20141110@503	UWA-1 G3							20.150	0.291			
20141110@504	UWA-1 G3							20.021	0.355			
20141110@505	UWA-1 G3							19.999	0.236			
20141110@506	UWA-1 G3							20.047	0.317			
Average and ±2 SD								**20.054**	**0.134**			
Enamel												
20141110@507	4901.2-105	4			x			34.946	0.398	27.49	0.09	988
20141110@508	4901.2-106	4			x			34.977	0.313	27.52	0.09	1018
20141110@509	4901.2-107	4			x			34.519	0.278	27.07	0.09	1048
20141110@510	4901.2-108	4						34.353	0.360	26.90	0.09	1078
20141110@511	4901.2-109	4						~~33.679~~	~~0.605~~	~~26.23~~	~~0.09~~	1108
20141110@512	4901.2-110	4			x	x		34.235	0.311	26.78	0.09	1138
20141110@513	4901.2-111	4			x	x		33.883	0.345	26.43	0.09	1168
20141110@514	4901.2-112	4		x	x	x		33.169	0.441	25.73	0.09	1308

Analysis #	Sample	Line #	Diagenesis* SEM	CLFM GR	CLFM RD	CLFM FRD	Bias (α) A	$\delta^{18}O_{RAW}$‰ B	±2 SE C	$\delta^{18}O_{COR}$‰ D	±2 SD E	Distance from edge of enamel (µm)
UWA-1												
20141110@515	UWA-1 G3							20.011	0.274			
20141110@516	UWA-1 G3							20.036	0.323			
20141110@517	UWA-1 G3							20.054	0.328			
20141110@518	UWA-1 G3							20.074	0.320			
Average and ±2 SD								**20.044**	**0.054**			
Bracket: Average and ±2 SD							**1.0073**	**20.049**	**0.095**			
Enamel												
20141110@519	4901.2-113	4			**x**	**x**		33.256	0.356	25.81	0.16	1338
20141110@520	4901.2-114	4			**x**	**x**		~~32.866~~	~~0.244~~	~~25.42~~	~~0.16~~	1368
20141110@521	4901.2-115	4			**x**	**x**		32.854	0.355	25.41	0.16	1412
20141110@522	4901.2-116	4			**x**	**x**		32.415	0.312	24.97	0.16	1442
20141110@523	4901.2-117	4		**x**	**x**	**x**		32.185	0.310	24.75	0.16	1472
20141110@524	4901.2-118	4		**x**	**x**	**x**		31.452	0.378	24.02	0.16	1502
20141110@525	4901.2-119	4		**x**	**x**	**x**		30.924	0.320	23.49	0.16	1532
20141110@526	4901.2-120	4		**x**	**x**	**x**		30.649	0.363	23.22	0.16	1562
20141110@527	4901.2-121	4		**x**	**x**	**x**		~~29.853~~	~~0.344~~	~~22.43~~	~~0.16~~	1591
20141110@528	4901.2-122	4		**x**	**x**	**x**		34.407	0.327	26.95	0.16	1229
UWA-1												
20141110@529	UWA-1 G3							20.141	0.261			
20141110@530	UWA-1 G3							20.179	0.404			
20141110@531	UWA-1 G3							19.958	0.392			
20141110@532	UWA-1 G3							19.966	0.343			
Average and ±2 SD								**20.061**	**0.231**			
Bracket: Average and ±2 SD							**1.0073**	**20.052**	**0.156**			
Sample: 4908a3 (Elephantidae) with UWA-1.												
UWA-1												

Analysis #	Sample	Line #	Diagenesis* SEM	CLFM GR	CLFM RD	CLFM FRD	Bias (α) A	$\delta^{18}O_{RAW}$‰ B	±2 SE C	$\delta^{18}O_{COR}$‰ D	±2 SD E	Distance from edge of enamel (µm)
20150406@638	UWA-1 G1							20.589	0.182			
20150406@639	UWA-1 G2							20.467	0.220			
20150406@640	UWA-1 G2							20.476	0.192			
20150406@641	UWA-1 G2							20.597	0.231			
Average and ±2 SD								**20.532**	**0.141**			
Enamel												
20150406@642	4908a3-001	1		x	x	x		30.519	0.234	22.53	0.24	25
20150406@643	4908a3-002	1			x	x		31.157	0.209	23.17	0.24	265
20150406@644	4908a3-003	1						31.538	0.219	23.55	0.24	505
20150406@645	4908a3-004	1						30.235	0.257	22.25	0.24	745
20150406@646	4908a3-005	1			x	x		30.310	0.191	22.33	0.24	985
20150406@647	4908a3-006	1			x	x		32.037	0.256	24.04	0.24	1165
20150406@648	4908a3-007	1		x	x	x		29.627	0.275	21.65	0.24	1105
20150406@649	4908a3-008	1			x	x		~~30.821~~	~~0.244~~	~~22.83~~	~~0.24~~	1200
UWA-1												
20150406@650	UWA-1 G2							20.704	0.236			
20150406@651	UWA-1 G2							20.530	0.241			
20150406@652	UWA-1 G2							20.697	0.180			
20150406@653	UWA-1 G2							20.805	0.254			
Average and ±2 SD								**20.684**	**0.228**			
Bracket: Average and ±2 SD							**1.0078**	**20.608**	**0.239**			
Enamel												
20150406@654	4908a3-009	1			x	x		32.141	0.275	24.12	0.45	1183
20150406@655	4908a3-010	1			x	x		32.010	0.237	23.99	0.45	1149
20150406@656	4908a3-011	1			x	x		30.880	0.247	22.86	0.45	1133
20150406@657	4908a3-012	1			x	x		30.162	0.295	22.15	0.45	1120
20150406@658	4908a3-013	1						30.645	0.269	22.63	0.45	871

Analysis #	Sample	Line #	Diagenesis*				Bias (α)	$\delta^{18}O_{RAW}$‰	±2 SE	$\delta^{18}O_{COR}$‰	±2 SD	Distance from edge
			SEM	CLFM								
				GR	RD	FRD	A	B	C	D	E	of enamel (µm)
20150406@659	4908a3-014	1						31.794	0.327	23.77	0.45	625
20150406@660	4908a3-015	1						31.815	0.243	23.79	0.45	685
20150406@661	4908a3-016	1						31.671	0.302	23.65	0.45	715
20150406@662	4908a3-017	1						30.838	0.261	22.82	0.45	730
20150406@663	4908a3-018	1						31.576	0.247	23.55	0.45	385
20150406@664	4908a3-019	1			x	x		31.301	0.225	23.28	0.45	145
UWA-1												
20150406@665	UWA-1 G2							20.306	0.182			
20150406@666	UWA-1 G2							20.349	0.275			
20150406@667	UWA-1 G2; Cs res 190-191							20.751	0.267			
20150406@668	UWA-1 G2							20.950	0.233			
Average and ±2 SD								**20.589**	**0.626**			
Bracket: Average and ±2 SD							**1.0078**	**20.637**	**0.448**			
Enamel												
20150406@669	4908a3-020	2	**SEM**	x	x	x		29.670	0.310	21.68	0.47	30
20150406@670	4908a3-021	2			x	x		31.400	0.242	23.40	0.47	270
20150406@671	4908a3-022	2			x	x		32.434	0.226	24.42	0.47	750
20150406@672	4908a3-023	2			x	x		29.537	0.234	21.55	0.47	1230
20150406@673	4908a3-024	2		x	x	x		29.896	0.206	21.91	0.47	1380
20150406@674	4908a3-025	2						31.752	0.226	23.75	0.47	997
20150406@675	4908a3-026	2						30.280	0.191	22.29	0.47	1117
20150406@676	4908a3-027	2						31.912	0.227	23.91	0.47	510
20150406@677	4908a3-028	2				x		32.352	0.190	24.34	0.47	630
20150406@678	4908a3-029	2						32.214	0.369	24.21	0.47	870
UWA-1												
20150406@679	UWA-1 G2							~~21.363~~	~~0.234~~			
20150406@680	UWA-1 G2							20.569	0.295			

Analysis #	Sample	Line #	Diagenesis* SEM	CLFM GR	CLFM RD	CLFM FRD	Bias (α) A	$\delta^{18}O_{RAW}$‰ B	±2 SE C	$\delta^{18}O_{COR}$‰ D	±2 SD E	Distance from edge of enamel (µm)
20150406@681	UWA-1 G2							20.790	0.217			
20150406@682	UWA-1 G2							20.618	0.191			
Average and ±2 SD								**20.659**	**0.232**			
Bracket: Average and ±2 SD							**1.0078**	**20.619**	**0.469**			
Enamel												
20150406@683	4908a3-030	3		x	x			31.235	0.219	23.13	0.49	30
20150406@684	4908a3-031	3						31.951	0.195	23.84	0.49	510
20150406@685	4908a3-032	3						30.825	0.313	22.73	0.49	990
20150406@686	4908a3-033	3			x	x		30.305	0.223	22.21	0.49	1230
20150406@687	4908a3-034	3						32.278	0.388	24.17	0.49	750
20150406@688	4908a3-035	3		x	x	x		31.749	0.281	23.64	0.49	330
20150406@689	4908a3-036	3						31.911	0.240	23.80	0.49	870
20150406@690	4908a3-037	3			x			29.456	0.134	21.37	0.49	1290
20150406@691	4908a3-038	3		x	x			29.687	0.246	21.60	0.49	1110
20150406@692	4908a3-039	3		x	x	x		30.470	0.262	22.37	0.49	1170
20150406@693	4908a3-040	3		x	x	x		31.187	0.244	23.09	0.49	180
20150406@694	4908a3-041	2		x	x	x		30.907	0.176	22.81	0.49	150
UWA-1												
20150406@695	UWA-1 G2							21.223	0.233			
20150406@696	UWA-1 G2							20.508	0.257			
20150406@697	UWA-1 G2							20.580	0.351			
20150406@698	UWA-1 G2							20.742	0.275			
Average and ±2 SD								**20.763**	**0.643**			
Bracket: Average and ±2 SD							**1.0079**	**20.719**	**0.487**			
Sample: 4857.1 (Deinotheriidae) with UWA-1.												
UWA-1												
20150406@495	UWA-1 G2							23.685	0.202			

Analysis #	Sample	Line #	Diagenesis*				Bias (α)	$\delta^{18}O_{RAW}$‰	±2 SE	$\delta^{18}O_{COR}$‰	±2 SD	Distance from edge
			SEM	CLFM								
				GR	RD	FRD	A	B	C	D	E	of enamel (µm)
20150406@496	UWA-1 G3							23.984	0.266			
20150406@497	UWA-1 G1							23.833	0.237			
20150406@498	UWA-1 G1							23.788	0.251			
Average and ±2 SD								**23.823**	**0.248**			
Enamel												
20150406@499	4857.1-001	1	**SEM**					29.701	0.215	18.48	0.43	25
20150406@500	4857.1-002	1		**x**		**x**		30.520	0.182	19.29	0.43	265
20150406@501	4857.1-003	1						32.231	0.291	20.99	0.43	505
20150406@502	4857.1-004	1						32.326	0.295	21.08	0.43	745
20150406@503	4857.1-005	1						32.651	0.286	21.40	0.43	985
20150406@504	4857.1-006	1						32.851	0.275	21.60	0.43	1225
20150406@505	4857.1-007	1						31.894	0.368	20.65	0.43	1465
20150406@506	4857.1-008	1						30.997	0.229	19.77	0.43	1705
20150406@507	4857.1-009	1				**x**		30.610	0.257	19.38	0.43	1945
UWA-1												
20150406@508	UWA-1 G1							23.889	0.280			
20150406@509	UWA-1 G1							23.518	0.225			
20150406@510	UWA-1 G1							24.247	0.230			
20150406@511	UWA-1 G1							23.877	0.217			
Average and ±2 SD								**23.883**	**0.595**			
Bracket: Average and ±2 SD							**1.0110**	**23.853**	**0.427**			
Enamel												
20150406@512	4857.1-010	1				**x**		31.554	0.239	20.19	0.49	2185
20150406@513	4857.1-011	1		**x**	**x**	**x**		32.688	0.294	21.31	0.49	2365
20150406@514	4857.1-012	1						32.140	0.177	20.77	0.49	385
20150406@515	4857.1-013	1						31.482	0.221	20.12	0.49	145
20150406@516	4857.1-014	2						31.188	0.258	19.83	0.49	120

Analysis #	Sample	Line #	Diagenesis* SEM	CLFM GR	CLFM RD	CLFM FRD	Bias (α) A	$\delta^{18}O_{RAW}$‰ B	±2 SE C	$\delta^{18}O_{COR}$‰ D	±2 SD E	Distance from edge of enamel (µm)
20150406@517	4857.1-015	2						31.548	0.336	20.18	0.49	360
20150406@518	4857.1-016	2						32.352	0.237	20.98	0.49	840
20150406@519	4857.1-017	2						32.711	0.224	21.33	0.49	1320
20150406@520	4857.1-018	2						31.360	0.273	20.00	0.49	1800
20150406@521	4857.1-019	2						30.875	0.275	19.52	0.49	2280
20150406@522	4857.1-020	2			x	x		31.719	0.247	20.35	0.49	2760
20150406@523	4857.1-021	2			x	x		31.938	0.291	20.57	0.49	2970
20150406@524	4857.1-022	2			x			31.284	0.274	19.92	0.49	2520
20150406@525	4857.1-023	2						31.247	0.211	19.88	0.49	2040
20150406@526	4857.1-024	2						32.088	0.244	20.72	0.49	1560
20150406@527	4857.1-025	2						32.363	0.179	20.99	0.49	1080
20150406@528	4857.1-026	2						32.600	0.176	21.22	0.49	570

UWA-1

20150406@529	UWA-1 G2							24.081	0.238			
20150406@530	UWA-1 G2							24.132	0.206			
20150406@531	UWA-1 G2							24.234	0.180			
20150406@532	UWA-1 G2							23.878	0.156			
Average and ±2 SD								**24.081**	**0.299**			
Bracket: Average and ±2 SD							**1.0111**	**23.982**	**0.485**			

Sample: 4892.1 (Hippopotamidae) with UWA-1.

UWA-1

20141110@323	UWA-1 Grain 1 (G1)							19.085	0.380			
20141110@324	UWA-1 Grain 2 (G2)							19.194	0.399			
20141110@325	UWA-1 Grain 3 (G3)							19.040	0.260			
20141110@326	UWA-1 Grain 4 (G4)							19.093	0.471			
Average and ±2 SD								**19.103**	**0.130**			

Enamel

Analysis #	Sample	Line #	Diagenesis* SEM	CLFM GR	CLFM RD	CLFM FRD	Bias (α) A	$\delta^{18}O_{RAW}$‰ B	±2 SE C	$\delta^{18}O_{COR}$‰ D	±2 SD E	Distance from edge of enamel (µm)
20141110@327	4892.1-001	1		x	x	x		30.580	0.351	24.11	0.22	15
20141110@328	4892.1-002	1		x	x	x		30.292	0.344	23.82	0.22	45
20141110@329	4892.1-003	1		x	x	x		30.414	0.460	23.94	0.22	75
20141110@330	4892.1-004	1		x	x	x		29.988	0.403	23.52	0.22	105
20141110@331	4892.1-005	1		x	x			29.653	0.476	23.19	0.22	135
20141110@332	4892.1-006	1		x	x			30.192	0.347	23.72	0.22	165
20141110@333	4892.1-007	1		x	x			29.330	0.431	22.87	0.22	195
20141110@334	4892.1-008	1		x				30.075	0.361	23.61	0.22	225
UWA-1												
20141110@335	UWA-1 G4							18.872	0.437			
20141110@336	UWA-1 G4							19.224	0.344			
20141110@337	UWA-1 G4							19.160	0.476			
20141110@338	UWA-1 G4; Cs res 149-150							19.121	0.328			
Average and ±2 SD								**19.094**	**0.308**			
Bracket: Average and ±2 SD							**1.0063**	**19.099**	**0.219**			
UWA-1												
20141110@340	UWA-1 G4							19.178	0.378			
20141110@341	UWA-1 G4							18.867	0.313			
20141110@342	UWA-1 G4							19.037	0.334			
20141110@343	UWA-1 G4							18.967	0.322			
Average and ±2 SD								**19.012**	**0.261**			
Enamel												
20141110@344	4892.1-009	1		x				29.833	0.476	23.41	0.23	255
20141110@345	4892.1-010	1		x	x			29.693	0.478	23.27	0.23	285
20141110@346	4892.1-011	1		x	x			29.517	0.339	23.09	0.23	315
20141110@347	4892.1-012	1		x				29.802	0.420	23.38	0.23	345
20141110@348	4892.1-013	1		x	x			30.043	0.346	23.62	0.23	375

Analysis #	Sample	Line #	Diagenesis* SEM	Diagenesis* CLFM			Bias (α)	$\delta^{18}O_{RAW}$‰	±2 SE	$\delta^{18}O_{COR}$‰	±2 SD	Distance from edge
				GR	RD	FRD	A	B	C	D	E	of enamel (µm)
20141110@349	4892.1-014	1		x				29.610	0.358	23.19	0.23	405
20141110@350	4892.1-015	1		x				29.775	0.412	23.35	0.23	435
20141110@351	4892.1-016	1						29.926	0.332	23.50	0.23	464
20141110@352	4892.1-017	1						29.302	0.463	22.88	0.23	494
20141110@353	4892.1-018	1		x				29.648	0.455	23.22	0.23	524
20141110@354	4892.1-019	1						29.628	0.394	23.20	0.23	554
20141110@355	4892.1-020	1						29.599	0.413	23.18	0.23	584
20141110@356	4892.1-021	1						29.719	0.322	23.30	0.23	614
20141110@357	4892.1-022	1						29.246	0.486	22.83	0.23	644
20141110@358	4892.1-023	1						29.491	0.409	23.07	0.23	675
20141110@359	4892.1-024	1						29.814	0.347	23.39	0.23	705
UWA-1												
20141110@360	UWA-1 G4							19.125	0.418			
20141110@361	UWA-1 G4							19.001	0.304			
20141110@362	UWA-1 G4							19.062	0.339			
20141110@363	UWA-1 G4							19.221	0.331			
Average and ±2 SD								**19.102**	**0.188**			
Bracket: Average and ±2 SD							**1.0063**	**19.057**	**0.232**			
UWA-1												
20141110@369	UWA-1 G4							19.282	0.379			
20141110@370	UWA-1 G4							19.191	0.408			
20141110@371	UWA-1 G4							19.174	0.393			
20141110@372	UWA-1 G4							19.069	0.393			
Average and ±2 SD								**19.179**	**0.175**			
Enamel												
20141110@373	4892.1-025	1						29.576	0.398	22.98	0.21	738
20141110@374	4892.1-026	1						29.968	0.412	23.37	0.21	768

Analysis #	Sample	Line #	Diagenesis* SEM	Diagenesis* CLFM			Bias (α)	$\delta^{18}O_{RAW}$‰	±2 SE	$\delta^{18}O_{COR}$‰	±2 SD	Distance from edge of enamel (µm)
				GR	RD	FRD	A	B	C	D	E	
20141110@375	4892.1-027	1						29.819	0.391	23.22	0.21	798
20141110@376	4892.1-028	1						29.771	0.392	23.17	0.21	828
20141110@377	4892.1-029	1						29.739	0.386	23.14	0.21	858
20141110@378	4892.1-030	1						29.611	0.443	23.01	0.21	888
20141110@379	4892.1-031	1						29.671	0.405	23.07	0.21	918
20141110@380	4892.1-032	1						29.669	0.332	23.07	0.21	948
20141110@381	4892.1-033	1						29.450	0.432	22.85	0.21	978
20141110@382	4892.1-034	1						29.456	0.471	22.86	0.21	1008
20141110@383	4892.1-035	1						29.368	0.410	22.77	0.21	1038
20141110@384	4892.1-036	1						29.381	0.402	22.78	0.21	1068
20141110@385	4892.1-037	1						29.747	0.380	23.15	0.21	1101
20141110@386	4892.1-038	1						29.142	0.379	22.55	0.21	1149
UWA-1												
20141110@387	UWA-1 G4							19.152	0.346			
20141110@388	UWA-1 G4							19.322	0.364			
20141110@389	UWA-1 G4							19.402	0.362			
20141110@390	UWA-1 G4							19.267	0.353			
Average and ±2 SD								**19.286**	**0.210**			
Bracket: Average and ±2 SD							**1.0065**	**19.232**	**0.212**			
Enamel												
20141110@391	4892.1-039	1						29.364	0.291	22.66	0.22	1179
20141110@392	4892.1-040	1						29.509	0.372	22.80	0.22	1209
20141110@393	4892.1-041	1						29.930	0.421	23.22	0.22	1239
20141110@394	4892.1-042	1						29.869	0.416	23.16	0.22	1269
20141110@395	4892.1-043	1						29.773	0.399	23.07	0.22	1299
20141110@396	4892.1-044	1						29.800	0.389	23.09	0.22	1329
20141110@397	4892.1-045	1						29.652	0.398	22.95	0.22	1359
20141110@398	4892.1-046	1						29.890	0.457	23.18	0.22	1389

Analysis #	Sample	Line #	Diagenesis* SEM	CLFM GR	CLFM RD	CLFM FRD	Bias (α) A	$\delta^{18}O_{RAW}$‰ B	±2 SE C	$\delta^{18}O_{COR}$‰ D	±2 SD E	Distance from edge of enamel (µm)
20141110@399	4892.1-047	1						29.787	0.389	23.08	0.22	1419
20141110@400	4892.1-048	1						29.810	0.292	23.10	0.22	1449
20141110@401	4892.1-049	1						29.627	0.379	22.92	0.22	1479
20141110@402	4892.1-050	1						29.662	0.397	22.96	0.22	1509
20141110@403	4892.1-051	1						29.777	0.377	23.07	0.22	1539
20141110@404	4892.1-052	1						29.683	0.400	22.98	0.22	1570
20141110@405	4892.1-053	1						29.967	0.441	23.26	0.22	1600
20141110@406	4892.1-054	1						30.034	0.394	23.33	0.22	1630
UWA-1												
20141110@407	UWA-1 G4							19.452	0.287			
20141110@408	UWA-1 G4							19.381	0.342			
20141110@409	UWA-1 G4							19.466	0.374			
20141110@410	UWA-1 G4							19.262	0.371			
Average and ±2 SD								**19.390**	**0.186**			
Bracket: Average and ±2 SD							**1.0066**	**19.338**	**0.215**			
Enamel												
20141110@411	4892.1-055	1						30.082	0.363	23.42	0.29	1660
20141110@412	4892.1-056	1						29.957	0.385	23.29	0.29	1690
20141110@413	4892.1-057	1						29.990	0.355	23.33	0.29	1728
20141110@414	4892.1-058	1						30.207	0.476	23.54	0.29	1758
20141110@415	4892.1-059	1						29.685	0.391	23.02	0.29	1800
20141110@416	4892.1-060	1						29.590	0.456	22.93	0.29	1830
20141110@417	4892.1-061	1		**x**		**x**		29.517	0.413	22.86	0.29	1860
20141110@418	4892.1-062	1		**x**		**x**		29.566	0.361	22.91	0.29	1890
20141110@419	4892.1-063	1		**x**		**x**		29.171	0.437	22.51	0.29	1920
20141110@420	4892.1-064	1		**x**		**x**		29.109	0.396	22.45	0.29	1950
20141110@421	4892.1-065	1		**x**		**x**		28.922	0.414	22.27	0.29	1983
20141110@422	4892.1-066	1		**x**		**x**		28.772	0.431	22.12	0.29	2016

Analysis #	Sample	Line #	Diagenesis* SEM	CLFM			Bias (α)	$\delta^{18}O_{RAW}$‰	±2 SE	$\delta^{18}O_{COR}$‰	±2 SD	Distance from edge
				GR	RD	FRD	A	B	C	D	E	of enamel (µm)
20141110@423	4892.1-067	1		x	x			29.141	0.395	22.48	0.29	2046
20141110@424	4892.1-068	1		x	x			29.058	0.354	22.40	0.29	2076
20141110@425	4892.1-069	1		x	x			29.370	0.353	22.71	0.29	2106
20141110@426	4892.1-070	1		x	x			29.345	0.364	22.69	0.29	2135
UWA-1												
20141110@427	UWA-1 G4							19.089	0.329			
20141110@428	UWA-1 G4							19.336	0.303			
20141110@429	UWA-1 G4							19.270	0.421			
20141110@430	UWA-1 G4							19.100	0.303			
Average and ±2 SD								**19.199**	**0.247**			
Bracket: Average and ±2 SD							**1.0065**	**19.295**	**0.288**			
Enamel												
20141110@431	4892.1-071	1		x	x			28.775	0.449	22.22	0.26	2164
20141110@432	4892.1-072	1		x	x	x		27.815	0.381	21.27	0.26	2193
20141110@433	4892.1-073	1		x	x	x		27.201	0.382	20.66	0.26	2223
20141110@434	4892.1-074	1		x	x	x		27.802	0.316	21.25	0.26	2253
20141110@435	4892.1-075	1						29.591	0.391	23.03	0.26	1122
UWA-1												
20141110@447	UWA-1 G4							18.964	0.411			
20141110@448	UWA-1 G4							19.262	0.390			
20141110@449	UWA-1 G4							19.211	0.318			
20141110@450	UWA-1 G4							19.308	0.359			
Average and ±2 SD								**19.186**	**0.307**			
Bracket: Average and ±2 SD							**1.0064**	**19.193**	**0.258**			

Sample: 4891.1 (Hippopotamidae) with UWA-1.

UWA-1

Analysis #	Sample	Line #	Diagenesis* SEM	CLFM GR	CLFM RD	CLFM FRD	Bias (α) A	$\delta^{18}O_{RAW}$‰ B	±2 SE C	$\delta^{18}O_{COR}$‰ D	±2 SD E	Distance from edge of enamel (µm)
20141110@427	UWA-1 G4							19.089	0.329			
20141110@428	UWA-1 G4							19.336	0.303			
20141110@429	UWA-1 G4							19.270	0.421			
20141110@430	UWA-1 G4							19.100	0.303			
Average and ±2 SD								**19.199**	**0.247**			
Enamel												
20141110@436	4891.1-001	1						24.417	0.346	17.89	0.26	18
20141110@437	4891.1-002	1						24.491	0.357	17.96	0.26	48
20141110@438	4891.1-003	1						24.219	0.485	17.69	0.26	78
20141110@439	4891.1-004	1						24.382	0.391	17.86	0.26	108
20141110@440	4891.1-005	1						23.789	0.357	17.27	0.26	138
20141110@441	4891.1-006	1						24.122	0.337	17.60	0.26	168
20141110@442	4891.1-007	1						24.173	0.291	17.65	0.26	198
20141110@443	4891.1-008	1						23.995	0.291	17.47	0.26	228
20141110@444	4891.1-009	1						24.288	0.362	17.76	0.26	258
20141110@445	4891.1-010	1						24.172	0.366	17.65	0.26	288
20141110@446	4891.1-011	1						24.100	0.347	17.58	0.26	315
UWA-1												
20141110@447	UWA-1 G4							18.964	0.411			
20141110@448	UWA-1 G4							19.262	0.390			
20141110@449	UWA-1 G4							19.211	0.318			
20141110@450	UWA-1 G4							19.308	0.359			
Average and ±2 SD								**19.186**	**0.307**			
Bracket: Average and ±2 SD							**1.0064**	**19.193**	**0.258**			
Enamel												
20141110@451	4891.1-012	1						24.076	0.330	17.46	0.30	345
20141110@452	4891.1-013	1						23.307	0.358	16.70	0.30	375

Analysis #	Sample	Line #	Diagenesis* SEM	Diagenesis* CLFM GR	Diagenesis* CLFM RD	Diagenesis* CLFM FRD	Bias (α) A	$\delta^{18}O_{RAW}$‰ B	±2 SE C	$\delta^{18}O_{COR}$‰ D	±2 SD E	Distance from edge of enamel (µm)
20141110@453	4891.1-014	1						23.427	0.426	16.82	0.30	405
20141110@454	4891.1-015	1						23.571	0.308	16.96	0.30	435
20141110@455	4891.1-016	1						~~23.357~~	~~0.413~~	~~16.75~~	~~0.30~~	462
20141110@456	4891.1-017	1						23.397	0.348	16.79	0.30	497
20141110@457	4891.1-018	1	**SEM**					23.286	0.399	16.68	0.30	529
20141110@458	4891.1-019	1	**SEM**					23.412	0.408	16.80	0.30	562
20141110@459	4891.1-020	1						23.562	0.440	16.95	0.30	592
20141110@460	4891.1-021	1						23.784	0.448	17.17	0.30	622
20141110@461	4891.1-022	1						23.937	0.432	17.32	0.30	652
20141110@462	4891.1-023	1						23.714	0.409	17.10	0.30	682
20141110@463	4891.1-024	1						23.948	0.443	17.33	0.30	712
20141110@464	4891.1-025	1						23.827	0.429	17.21	0.30	742
20141110@465	4891.1-026	1						23.802	0.454	17.19	0.30	772
20141110@466	4891.1-027	1						23.869	0.366	17.26	0.30	802
UWA-1												
20141110@467	UWA-1 G4							19.288	0.325			
20141110@468	UWA-1 G4							19.379	0.362			
20141110@469	UWA-1 G4							19.384	0.389			
20141110@470	UWA-1 G4							19.469	0.421			
Average and ±2 SD								**19.380**	**0.148**			
Bracket: Average and ±2 SD							**1.0065**	**19.283**	**0.304**			
Enamel												
20141110@471	4891.1-028	1						24.098	0.467	17.41	0.17	832
20141110@472	4891.1-029	1						23.779	0.354	17.10	0.17	862
20141110@473	4891.1-030	1						23.860	0.424	17.18	0.17	897
20141110@474	4891.1-031	1						23.467	0.387	16.79	0.17	927
20141110@475	4891.1-032	1						23.506	0.451	16.83	0.17	952
20141110@476	4891.1-033	1						23.430	0.436	16.75	0.17	977

Analysis #	Sample	Line #	Diagenesis*				Bias (α)	$\delta^{18}O_{RAW}$‰	±2 SE	$\delta^{18}O_{COR}$‰	±2 SD	Distance from edge
			SEM	CLFM								
				GR	RD	FRD	A	B	C	D	E	of enamel (µm)
20141110@477	4891.1-034	1						23.297	0.454	16.62	0.17	1007
20141110@478	4891.1-035	1						23.771	0.430	17.09	0.17	1037
20141110@479	4891.1-036	1						23.679	0.306	17.00	0.17	1067
20141110@480	4891.1-037	1						23.490	0.351	16.81	0.17	1097
20141110@481	4891.1-038	1						23.502	0.439	16.82	0.17	1127
20141110@482	4891.1-039	1						23.467	0.379	16.79	0.17	1157
20141110@483	4891.1-040	1						23.294	0.427	16.62	0.17	1187
20141110@484	4891.1-041	1						23.841	0.393	17.16	0.17	1217
20141110@485	4891.1-042	1						24.238	0.398	17.55	0.17	1260
20141110@486	4891.1-043	1						24.234	0.351	17.55	0.17	1295
20141110@487	4891.1-044	1						24.314	0.434	17.63	0.17	1342
20141110@488	4891.1-045	1		x				23.833	0.410	17.15	0.17	1385
20141110@489	4891.1-046	1	SEM	x				23.125	0.481	16.45	0.17	1430
20141110@490	4891.1-047	1	SEM	x				23.154	0.439	16.48	0.17	1471
20141110@491	4891.1-048	1		x				23.506	0.392	16.83	0.17	1511
20141110@492	4891.1-049	1		x	x			23.327	0.401	16.65	0.17	1538
UWA-1												
20141110@493	UWA-1 G4							19.241	0.331			
20141110@494	UWA-1 G4							19.242	0.386			
20141110@495	UWA-1 G4							19.375	0.305			
20141110@496	UWA-1 G4							19.444	0.348			
Average and ±2 SD								**19.326**	**0.202**			
Bracket: Average and ±2 SD							**1.0066**	**19.353**	**0.174**			
Sample: 4891.2 (Hippopotamidae) with UWA-1.												
UWA-1												
20141110@113	UWA-1 G1							18.149	0.448			
20141110@114	UWA-1 G1							18.304	0.337			
20141110@115	UWA-1 G1							18.329	0.320			

Analysis #	Sample	Line #	Diagenesis* SEM	CLFM GR	CLFM RD	CLFM FRD	Bias (α) A	$\delta^{18}O_{RAW}$‰ B	±2 SE C	$\delta^{18}O_{COR}$‰ D	±2 SD E	Distance from edge of enamel (µm)
20141110@116	UWA-1 G1							18.444	0.375			
Average and ±2 SD								**18.307**	**0.243**			
Enamel												
20141110@117	4891.2-001	1		x	x	x		23.643	0.402	17.94	0.25	21
20141110@118	4891.2-002	1		x	x	x		23.189	0.434	17.49	0.25	51
20141110@119	4891.2-003	1	SEM	x				22.777	0.378	17.08	0.25	89
20141110@120	4891.2-004	1		x				22.879	0.430	17.18	0.25	119
20141110@121	4891.2-005	1		x				23.322	0.403	17.62	0.25	149
20141110@122	4891.2-006	1		x				22.932	0.434	17.24	0.25	183
20141110@123	4891.2-007	1		x				23.076	0.429	17.38	0.25	218
20141110@124	4891.2-008	1		x				23.211	0.484	17.51	0.25	248
UWA-1												
20141110@125	UWA-1 G1							18.558	0.358			
20141110@126	UWA-1 G1							18.409	0.351			
20141110@127	UWA-1 G1							18.305	0.401			
20141110@128	UWA-1 G1; CS res 138-139							18.474	0.393			
Average and ±2 SD								**18.437**	**0.214**			
Bracket: Average and ±2 SD							**1.0056**	**18.372**	**0.253**			
UWA-1												
20141110@129	UWA-1 G1							18.707	0.398			
20141110@130	UWA-1 G1							18.607	0.408			
20141110@131	UWA-1 G1							18.421	0.470			
20141110@132	UWA-1 G1							18.458	0.350			
Average and ±2 SD								**18.548**	**0.266**			
Enamel												
20141110@133	4891.2-009	1		x				23.164	0.483	17.30	0.31	278

Analysis #	Sample	Line #	Diagenesis* SEM	CLFM			Bias (α)	$\delta^{18}O_{RAW}$‰	±2 SE	$\delta^{18}O_{COR}$‰	±2 SD	Distance from edge
				GR	RD	FRD	A	B	C	D	E	of enamel (µm)
20141110@134	4891.2-010	1		x				23.119	0.401	17.25	0.31	308
20141110@135	4891.2-011	1						22.887	0.364	17.02	0.31	338
20141110@136	4891.2-012	1						22.893	0.404	17.03	0.31	368
20141110@137	4891.2-013	1						22.594	0.431	16.73	0.31	401
20141110@138	4891.2-014	1						22.930	0.545	17.06	0.31	434
20141110@139	4891.2-015	1						22.481	0.436	16.62	0.31	464
20141110@140	4891.2-016	1						22.124	0.439	16.26	0.31	494
20141110@141	4891.2-017	1						22.246	0.534	16.38	0.31	527
20141110@142	4891.2-018	1						22.928	0.408	17.06	0.31	557
20141110@143	4891.2-019	1						22.809	0.505	16.94	0.31	587
20141110@144	4891.2-020	1						22.397	0.432	16.53	0.31	624
20141110@145	4891.2-021	1						22.598	0.448	16.73	0.31	654
20141110@146	4891.2-022	1						23.150	0.517	17.28	0.31	684
20141110@147	4891.2-023	1						22.989	0.492	17.12	0.31	714
20141110@148	4891.2-024	1						22.260	0.467	16.40	0.31	744
UWA-1												
20141110@149	UWA-1 G1							18.424	0.375			
20141110@150	UWA-1 G1							18.329	0.412			
20141110@151	UWA-1 G1							18.625	0.371			
20141110@152	UWA-1 G1							18.752	0.415			
Average and ±2 SD								**18.533**	**0.383**			
Bracket: Average and ±2 SD							**1.0058**	**18.540**	**0.306**			
Sample: 4854a4 (Equidae) with UWA-1.												
UWA-1												
20150406@111	UWA-1 G1							23.674	0.210			
20150406@112	UWA-1 G1							23.903	0.222			
20150406@113	UWA-1 G1							23.570	0.245			
20150406@114	UWA-1 G1							23.753	0.265			

Analysis #	Sample	Line #	Diagenesis* SEM	CLFM GR	CLFM RD	CLFM FRD	Bias (α) A	$\delta^{18}O_{RAW}$‰ B	±2 SE C	$\delta^{18}O_{COR}$‰ D	±2 SD E	Distance from edge of enamel (µm)
Average and ±2 SD								**23.725**	**0.281**			
Enamel												
20150406@115	4854a4-001	1		x	x	x		33.378	0.187	22.39	0.40	30
20150406@116	4854a4-002	1		x	x			33.773	0.252	22.78	0.40	90
20150406@117	4854a4-003	1		x				33.991	0.333	22.99	0.40	150
20150406@118	4854a4-004	1						33.470	0.259	22.48	0.40	210
20150406@119	4854a4-005	1						34.634	0.229	23.63	0.40	270
20150406@120	4854a4-006	1		x				34.419	0.260	23.42	0.40	330
20150406@121	4854a4-007	1						34.854	0.257	23.85	0.40	390
20150406@122	4854a4-008	1						34.820	0.244	23.81	0.40	450
UWA-1												
20150406@123	UWA-1 G1							23.654	0.304			
20150406@124	UWA-1 G1							23.454	0.198			
20150406@125	UWA-1 G1							23.296	0.260			
20150406@126	UWA-1 G1							23.390	0.202			
Average and ±2 SD								**23.449**	**0.303**			
Bracket: Average and ±2 SD							**1.0108**	**23.587**	**0.401**			
Enamel												
20150406@127	4854a4-009	1						34.815	0.254	23.93	0.26	510
20150406@128	4854a4-010	1						33.880	0.322	23.00	0.26	570
20150406@129	4854a4-011	1						33.804	0.253	22.93	0.26	630
20150406@130	4854a4-012	1		x				34.624	0.249	23.74	0.26	690
20150406@131	4854a4-013	1		x				33.958	0.259	23.08	0.26	750
20150406@132	4854a4-014	1		x	x			33.321	0.203	22.45	0.26	810
20150406@133	4854a4-015	1		x	x			32.978	0.235	22.11	0.26	870
20150406@134	4854a4-016	1		x	x			33.318	0.199	22.45	0.26	930
20150406@135	4854a4-017	1		x	x			33.569	0.186	22.70	0.26	990

Analysis #	Sample	Line #	Diagenesis*			Bias (α)	$\delta^{18}O_{RAW}$‰	±2 SE	$\delta^{18}O_{COR}$‰	±2 SD	Distance from edge of enamel (µm)
			SEM	CLFM							
				GR	RD FRD	A	B	C	D	E	
20150406@136	4854a4-018	1		x			34.695	0.236	23.81	0.26	660
20150406@137	4854a4-019	1					33.996	0.253	23.12	0.26	600
20150406@138	4854a4-020	1					34.721	0.248	23.84	0.26	540
20150406@139	4854a4-021	1					34.145	0.265	23.27	0.26	240
UWA-1											
20150406@140	UWA-1 G1						23.339	0.185			
20150406@141	UWA-1 G1						23.524	0.268			
20150406@142	UWA-1 G1						23.430	0.178			
20150406@143	UWA-1 G1						23.640	0.171			
Average and ±2 SD							**23.483**	**0.258**			
Bracket: Average and ±2 SD						**1.0106**	**23.466**	**0.263**			
Enamel											
20150406@144	4854a4-022	2		x	x x		32.572	0.166	21.66	0.24	45
20150406@145	4854a4-023	2		x	x x		33.976	0.228	23.05	0.24	105
20150406@146	4854a4-024	2		x	x		34.748	0.202	23.81	0.24	165
20150406@147	4854a4-025	2			x		34.502	0.236	23.57	0.24	225
20150406@148	4854a4-026	2					34.051	0.194	23.12	0.24	285
20150406@149	4854a4-027	2		x			34.192	0.265	23.26	0.24	345
20150406@150	4854a4-028	2		x	x		34.760	0.248	23.83	0.24	405
20150406@151	4854a4-029	2		x	x		35.180	0.235	24.24	0.24	465
20150406@152	4854a4-030	2					34.209	0.317	23.28	0.24	525
20150406@153	4854a4-031	2		x			34.840	0.226	23.91	0.24	585
20150406@154	4854a4-032	2		x	x		35.141	0.209	24.20	0.24	645
20150406@155	4854a4-033	2		x	x x		34.588	0.300	23.66	0.24	705
20150406@156	4854a4-034	2		x	x x		34.577	0.234	23.64	0.24	770
20150406@157	4854a4-035	2		x	x x		34.452	0.252	23.52	0.24	825
20150406@158	4854a4-036	2		x	x x		33.542	0.221	22.62	0.24	885
20150406@159	4854a4-037	2		x	x x		33.155	0.242	22.24	0.24	945

Analysis #	Sample	Line #	Diagenesis* SEM	CLFM GR	CLFM RD	CLFM FRD	Bias (α) A	$\delta^{18}O_{RAW}$‰ B	±2 SE C	$\delta^{18}O_{COR}$‰ D	±2 SD E	Distance from edge of enamel (µm)
UWA-1												
20150406@160	UWA-1 G1							23.550	0.201			
20150406@161	UWA-1 G1							23.640	0.201			
20150406@162	UWA-1 G1							23.613	0.212			
20150406@163	UWA-1 G1							23.385	0.248			
Average and ±2 SD								**23.547**	**0.229**			
Bracket: Average and ±2 SD							**1.0107**	**23.515**	**0.236**			
Enamel												
20150406@164	4854a4-038	2		**x**	**x**	**x**		33.139	0.233	22.30	0.30	75
20150406@165	4854a4-039	2		**x**	**x**	**x**		33.504	0.209	22.66	0.30	135
20150406@166	4854a4-040	2		**x**				34.312	0.214	23.46	0.30	495
20150406@167	4854a4-041	2		**x**	**x**			34.993	0.188	24.14	0.30	555
20150406@168	4854a4-042	2		**x**	**x**			34.947	0.253	24.09	0.30	675
20150406@169	4854a4-043	2		**x**	**x**	**x**		34.105	0.153	23.26	0.30	855
20150406@170	4854a4-044	2		**x**	**x**	**x**		32.983	0.253	22.15	0.30	975
20150406@171	4854a4-045	2		**x**	**x**			35.166	0.313	24.31	0.30	615
20150406@172	4854a4-046	2			**x**			34.247	0.257	23.40	0.30	375
20150406@173	4854a4-047	2		**x**				33.800	0.204	22.96	0.30	315
UWA-1												
20150406@174	UWA-1 G1							23.424	0.171			
20150406@175	UWA-1 G1							23.342	0.208			
20150406@176	UWA-1 G1							23.252	0.215			
20150406@177	UWA-1 G1							23.277	0.140			
Average and ±2 SD								**23.324**	**0.154**			
Bracket: Average and ±2 SD							**1.0106**	**23.435**	**0.299**			

Sample: 4877 (Bovidae) with UWA-1.

Analysis #	Sample	Line #	Diagenesis* SEM	CLFM GR	CLFM RD	CLFM FRD	Bias (α) A	$\delta^{18}O_{RAW}$‰ B	±2 SE C	$\delta^{18}O_{COR}$‰ D	±2 SD E	Distance from edge of enamel (µm)
UWA-1												
20150406@179	UWA-1 G2							23.875	0.251			
20150406@180	UWA-1 G3							23.664	0.168			
20150406@181	UWA-1 G1							23.560	0.269			
20150406@182	UWA-1 G1							23.934	0.174			
Average and ±2 SD								**23.758**	**0.352**			
Enamel												
20150406@183	4877-001	1						33.767	0.215	22.67	0.32	25
20150406@184	4877-002	1						33.461	0.236	22.37	0.32	88
20150406@185	4877-003	1		x				33.168	0.291	22.08	0.32	148
20150406@186	4877-004	1						33.028	0.237	21.94	0.32	198
20150406@187	4877-005	1						32.638	0.264	21.56	0.32	258
20150406@188	4877-006	1			x			32.527	0.232	21.45	0.32	318
20150406@189	4877-007	1		x	x			32.705	0.252	21.62	0.32	378
20150406@190	4877-008	1		x				32.130	0.201	21.05	0.32	438
UWA-1												
20150406@191	UWA-1 G1							23.437	0.277			
20150406@192	UWA-1 G1							23.611	0.184			
20150406@193	UWA-1 G1							23.730	0.252			
20150406@194	UWA-1 G1							23.677	0.176			
Average and ±2 SD								**23.614**	**0.255**			
Bracket: Average and ±2 SD							**1.0108**	**23.686**	**0.324**			
Enamel												
20150406@195	4877-009	1			x			32.903	0.258	21.86	0.20	498
20150406@196	4877-010	1			x			33.485	0.253	22.44	0.20	558
20150406@197	4877-011	1						33.132	0.284	22.09	0.20	618
20150406@198	4877-012	1						32.66	0.223	21.62	0.20	678

Analysis #	Sample	Line #	Diagenesis* SEM	CLFM		Bias (α)	$\delta^{18}O_{RAW}$‰	±2 SE	$\delta^{18}O_{COR}$‰	±2 SD	Distance from edge
				GR	RD FRD	A	B	C	D	E	of enamel (µm)
20150406@199	4877-013	1			x		32.843	0.213	21.80	0.20	738
20150406@200	4877-014	1			x		32.753	0.238	21.72	0.20	798
20150406@201	4877-015	1					32.666	0.25	21.63	0.20	858
20150406@202	4877-016	1					32.453	0.229	21.42	0.20	918
20150406@203	4877-017	1					32.516	0.226	21.48	0.20	978
20150406@204	4877-018	1		x			32.899	0.212	21.86	0.20	1038
20150406@205	4877-019	1		x	x		33.103	0.198	22.06	0.20	1098
20150406@206	4877-020	1		x	x		32.828	0.241	21.79	0.20	1158
UWA-1											
20150406@207	UWA-1 G1						23.627	0.215			
20150406@208	UWA-1 G1						23.680	0.247			
20150406@209	UWA-1 G1						23.604	0.272			
20150406@210	UWA-1 G1						23.753	0.205			
Average and ±2 SD							**23.666**	**0.132**			
Bracket: Average and ±2 SD						**1.0108**	**23.640**	**0.196**			
Enamel											
20150406@211	4877-021	1					32.382	0.266	21.42	0.28	468
20150406@212	4877-022	1					32.483	0.252	21.52	0.28	408
UWA-1											
20150406@213	UWA-1 G1; Cs res 181-182						23.361	0.229			
20150406@214	UWA-1 G1						23.523	0.293			
20150406@215	UWA-1 G1						23.588	0.247			
20150406@216	UWA-1 G1						23.376	0.244			
Average and ±2 SD							**23.462**	**0.223**			
Bracket: Average and ±2 SD						**1.0107**	**23.564**	**0.276**			
Enamel											

Analysis #	Sample	Line #	Diagenesis* SEM	Diagenesis* CLFM			Bias (α)	$\delta^{18}O_{RAW}$‰	±2 SE	$\delta^{18}O_{COR}$‰	±2 SD	Distance from edge of enamel (µm)
				GR	RD	FRD	A	B	C	D	E	
20150406@227	4877-033	5						32.880	0.265	22.07	0.21	570
UWA-1												
20150406@233	UWA-1 G1							23.379	0.171			
20150406@234	UWA-1 G1							23.364	0.212			
20150406@235	UWA-1 G1							23.408	0.232			
20150406@236	UWA-1 G1							23.259	0.204			
Average and ±2 SD								**23.353**	**0.130**			
Bracket: Average and ±2 SD							**1.0106**	**23.407**	**0.205**			
UWA-1												
20150406@253	UWA-1 G1							23.598	0.234			
20150406@254	UWA-1 G1							23.432	0.240			
20150406@255	UWA-1 G1							23.612	0.175			
20150406@256	UWA-1 G1							23.352	0.203			
Average and ±2 SD								**23.499**	**0.255**			
Enamel												
20150406@257	4877-055	2		**x**				33.007	0.209	21.95	0.40	55
20150406@258	4877-056	2						32.584	0.279	21.53	0.40	115
20150406@259	4877-057	2						33.089	0.239	22.03	0.40	175
20150406@260	4877-058	2						33.137	0.248	22.08	0.40	235
20150406@261	4877-059	2						32.842	0.240	21.79	0.40	295
20150406@262	4877-060	2						32.857	0.178	21.80	0.40	355
20150406@263	4877-061	2						32.353	0.208	21.31	0.40	415
20150406@264	4877-062	2						31.590	0.264	20.55	0.40	475
20150406@265	4877-063	2						31.612	0.227	20.57	0.40	535
20150406@266	4877-064	2						31.691	0.268	20.65	0.40	595
20150406@267	4877-065	2						31.949	0.196	20.91	0.40	655
20150406@268	4877-066	2						32.042	0.270	21.00	0.40	715

Analysis #	Sample	Line #	Diagenesis* SEM	CLFM			Bias (α)	$\delta^{18}O_{RAW}$‰	±2 SE	$\delta^{18}O_{COR}$‰	±2 SD	Distance from edge
				GR	RD	FRD	A	B	C	D	E	of enamel (µm)
20150406@269	4877-067	2						32.478	0.179	21.43	0.40	775
20150406@270	4877-068	2			x			32.502	0.244	21.45	0.40	835
20150406@271	4877-069	2			x			32.574	0.225	21.52	0.40	895
20150406@272	4877-070	2						32.181	0.270	21.14	0.40	955
UWA-1												
20150406@273	UWA-1 G1							23.751	0.254			
20150406@274	UWA-1 G1							23.847	0.231			
20150406@275	UWA-1 G1							23.694	0.233			
20150406@276	UWA-1 G1							23.950	0.235			
Average and ±2 SD								**23.811**	**0.225**			
Bracket: Average and ±2 SD							**1.0108**	**23.655**	**0.401**			
Enamel												
20150406@277	4877-071	2						32.706	0.211	21.52	0.26	1015
20150406@278	4877-072	2		x	x			33.038	0.226	21.85	0.26	1075
20150406@279	4877-073	2						32.221	0.250	21.04	0.26	445
UWA-1												
20150406@293	UWA-1 G1							23.690	0.169			
20150406@294	UWA-1 G1							23.966	0.237			
20150406@295	UWA-1 G1							23.779	0.230			
20150406@296	UWA-1 G1							23.605	0.233			
Average and ±2 SD								**23.760**	**0.309**			
Bracket: Average and ±2 SD							**1.0109**	**23.785**	**0.256**			
Enamel												
20150406@297	4877-087	3		x				32.614	0.270	21.53	0.30	20
20150406@298	4877-088	3		x				32.554	0.209	21.47	0.30	80
20150406@299	4877-089	3						32.167	0.235	21.08	0.30	140

Analysis #	Sample	Line #	Diagenesis* SEM	CLFM GR	CLFM RD	CLFM FRD	Bias (α) A	$\delta^{18}O_{RAW}$‰ B	±2 SE C	$\delta^{18}O_{COR}$‰ D	±2 SD E	Distance from edge of enamel (µm)
20150406@300	4877-090	3						31.941	0.245	20.86	0.30	200
20150406@301	4877-091	3						32.196	0.218	21.11	0.30	260
20150406@302	4877-092	3		x				32.345	0.224	21.26	0.30	320
20150406@303	4877-093	3		x	x			32.205	0.290	21.12	0.30	380
20150406@304	4877-094	3						32.100	0.224	21.02	0.30	440
20150406@305	4877-095	3		x				31.853	0.262	20.77	0.30	500
20150406@306	4877-096	3		x				32.212	0.220	21.13	0.30	560
20150406@307	4877-097	3						32.475	0.268	21.39	0.30	620
20150406@308	4877-098	3		x				32.452	0.212	21.37	0.30	680
UWA-1												
20150406@309	UWA-1 G1							23.525	0.248			
20150406@310	UWA-1 G1; Cs res 182-183							23.648	0.208			
20150406@311	UWA-1 G1							23.527	0.207			
20150406@312	UWA-1 G1							23.790	0.204			
Average and ±2 SD								**23.623**	**0.251**			
Bracket: Average and ±2 SD							**1.0109**	**23.691**	**0.299**			
Enamel												
20150406@313	4877-099	3		x				32.459	0.224	21.46	0.25	740
20150406@314	4877-100	3		x				32.177	0.266	21.18	0.25	800
20150406@315	4877-101	3		x				31.694	0.188	20.70	0.25	860
20150406@316	4877-102	3			x			31.607	0.217	20.61	0.25	920
20150406@317	4877-103	3			x			32.117	0.292	21.12	0.25	980
20150406@318	4877-104	3		x	x			32.043	0.202	21.05	0.25	1040
20150406@319	4877-105	3		x	x			31.921	0.222	20.93	0.25	1100
20150406@320	4877-106	3		x	x	x		31.652	0.239	20.66	0.25	1150
20150406@324	4877-110	4		x				33.960	0.184	22.94	0.25	30
20150406@325	4877-111	4		x				34.219	0.247	23.20	0.25	90
20150406@326	4877-112	4						33.949	0.346	22.93	0.25	210

Analysis #	Sample	Line #	Diagenesis* SEM	CLFM			Bias (α)	$\delta^{18}O_{RAW}$‰	±2 SE	$\delta^{18}O_{COR}$‰	±2 SD	Distance from edge
				GR	RD	FRD	A	B	C	D	E	of enamel (µm)
20150406@327	4877-113	4		x	x			34.101	0.230	23.08	0.25	330
20150406@328	4877-114	4			x			33.340	0.262	22.33	0.25	450
20150406@329	4877-115	4						32.877	0.252	21.87	0.25	570
UWA-1												
20150406@330	UWA-1 G1							23.637	0.198			
20150406@331	UWA-1 G1							23.729	0.175			
20150406@332	UWA-1 G1							23.615	0.190			
20150406@333	UWA-1 G1							23.386	0.205			
Average and ±2 SD								**23.592**	**0.292**			
Bracket: Average and ±2 SD							**1.0108**	**23.607**	**0.254**			
Enamel												
20150406@334	4877-116	4		x	x			32.153	0.240	21.28	0.36	690
20150406@335	4877-117	4			x			31.886	0.321	21.02	0.36	810
20150406@336	4877-118	4			x			32.004	0.227	21.14	0.36	930
20150406@337	4877-119	4			x			32.438	0.197	21.57	0.36	1050
20150406@338	4877-120	4		x	x	x		32.296	0.243	21.43	0.36	1170
20150406@343	4877-125	5						33.024	0.200	22.15	0.36	50
20150406@344	4877-126	5						32.796	0.291	21.92	0.36	290
20150406@345	4877-127	5						32.660	0.325	21.79	0.36	410
20150406@346	4877-128	5						32.926	0.243	22.05	0.36	710
20150406@347	4877-129	5						33.176	0.188	22.30	0.36	950
20150406@348	4877-130	5		x	x			31.850	0.224	20.99	0.36	1031
20150406@349	4877-131	5		x	x			32.350	0.213	21.48	0.36	1070
UWA-1												
20150406@354	UWA-1 G1							23.550	0.245			
20150406@355	UWA-1 G1							23.383	0.173			
20150406@356	UWA-1 G1							23.268	0.267			

Analysis #	Sample	Line #	Diagenesis* SEM	CLFM GR	CLFM RD	CLFM FRD	Bias (α) A	$\delta^{18}O_{RAW}$‰ B	±2 SE C	$\delta^{18}O_{COR}$‰ D	±2 SD E	Distance from edge of enamel (µm)
20150406@357	UWA-1 G1							23.246	0.274			
Average and ±2 SD								**23.362**	**0.278**			
Bracket: Average and ±2 SD							**1.0106**	**23.477**	**0.361**			
Sample: 4879.2 (Suidae) with UWA-1.												
UWA-1												
20150406@441	UWA-1 G1							24.222	0.189			
20150406@442	UWA-1 G1							23.918	0.271			
20150406@443	UWA-1 G1							24.140	0.211			
20150406@444	UWA-1 G1							24.478	0.184			
Average and ±2 SD								**24.190**	**0.463**			
Enamel												
20150406@445	4879.2-001	1	**SEM**	**x**	**x**	**x**		37.438	0.287	25.80	0.37	45
20150406@446	4879.2-002	1						38.051	0.238	26.41	0.37	165
20150406@447	4879.2-003	1						38.202	0.246	26.56	0.37	285
20150406@448	4879.2-004	1						38.128	0.229	26.48	0.37	405
20150406@449	4879.2-005	1						37.999	0.273	26.35	0.37	525
20150406@450	4879.2-006	1						38.081	0.292	26.44	0.37	645
20150406@451	4879.2-007	1						37.912	0.267	26.27	0.37	765
20150406@452	4879.2-008	1						37.495	0.242	25.86	0.37	885
20150406@453	4879.2-009	1						36.545	0.268	24.92	0.37	1005
20150406@454	4879.2-010	1						36.179	0.283	24.55	0.37	1125
UWA-1												
20150406@455	UWA-1 G1							24.379	0.239			
20150406@456	UWA-1 G1							24.030	0.220			
20150406@457	UWA-1 G1							24.067	0.245			
20150406@458	UWA-1 G1							24.283	0.233			
Average and ±2 SD								**24.190**	**0.337**			

Analysis #	Sample	Line #	Diagenesis*				Bias (α)	$\delta^{18}O_{RAW}$‰	±2 SE	$\delta^{18}O_{COR}$‰	±2 SD	Distance from edge of enamel (µm)
			SEM	CLFM								
				GR	RD	FRD	A	B	C	D	E	
Bracket: Average and ±2 SD							**1.0113**	**24.190**	**0.375**			
Enamel												
20150406@459	4879.2-011	1		x				36.873	0.263	25.18	0.36	1245
20150406@460	4879.2-012	1						36.769	0.170	25.08	0.36	1365
20150406@461	4879.2-013	1						36.841	0.258	25.15	0.36	1485
20150406@462	4879.2-014	1						37.119	0.258	25.42	0.36	1605
20150406@463	4879.2-015	1		x	x	x		37.766	0.320	26.06	0.36	1725
20150406@464	4879.2-016	1						36.908	0.316	25.21	0.36	1795
20150406@473	4879.2-025	1		x	x	x		37.671	0.228	25.97	0.36	1765
20150406@474	4879.2-026	1						36.092	0.254	24.41	0.36	1185
20150406@475	4879.2-027	1		x				36.918	0.237	25.22	0.36	1215
UWA-1												
20150406@476	UWA-1 G1							24.574	0.219			
20150406@477	UWA-1 G1							24.344	0.209			
20150406@478	UWA-1 G1							24.159	0.227			
20150406@479	UWA-1 G1							24.183	0.256			
Average and ±2 SD								**24.315**	**0.382**			
Bracket: Average and ±2 SD							**1.0114**	**24.252**	**0.359**			
Sample: 4883 (Suidae) with UWA-1.												
UWA-1												
20150406@359	UWA-1 Grain 2 (G2)							23.853	0.255			
20150406@360	UWA-1 Grain 3 (G3)							23.759	0.186			
20150406@361	UWA-1 G1							23.642	0.268			
20150406@362	UWA-1 G1; Cs res 182-183							24.029	0.205			
20150406@363	UWA-1 G1							23.589	0.234			
Average and ±2 SD								**23.774**	**0.351**			

Analysis #	Sample	Line #	Diagenesis* SEM	CLFM GR	CLFM RD	CLFM FRD	Bias (α) A	$\delta^{18}O_{RAW}$‰ B	±2 SE C	$\delta^{18}O_{COR}$‰ D	±2 SD E	Distance from edge of enamel (µm)
Enamel												
20150406@364	4883-001	1		x	x			35.820	0.227	24.61	0.36	30
20150406@365	4883-002	1						35.427	0.184	24.22	0.36	90
20150406@366	4883-003	1						35.294	0.267	24.09	0.36	150
20150406@367	4883-004	1		x	x			35.520	0.305	24.31	0.36	270
20150406@368	4883-005	1			x			35.267	0.246	24.06	0.36	390
20150406@369	4883-006	1						36.599	0.187	25.38	0.36	510
20150406@370	4883-007	1						36.568	0.266	25.35	0.36	630
20150406@371	4883-008	1						36.813	0.247	25.59	0.36	750
20150406@372	4883-009	1			x			37.039	0.210	25.81	0.36	880
UWA-1												
20150406@373	UWA-1 G1							24.050	0.319			
20150406@374	UWA-1 G1; Cs res 183-185							~~24.323~~	~~0.326~~			
20150406@375	UWA-1 G1							~~24.326~~	~~0.203~~			
20150406@376	UWA-1 G1; Cs res 185-186							23.592	0.242			
20150406@377	UWA-1 G1							23.752	0.241			
Average and ±2 SD								**23.798**	**0.465**			
Bracket: Average and ±2 SD							**1.0109**	**23.783**	**0.364**			
Enamel												
20150406@378	4883-010	1			x			36.758	0.209	25.52	0.42	1000
20150406@379	4883-011	1	**SEM**		x			35.019	0.257	23.80	0.42	1120
20150406@380	4883-012	1						36.420	0.172	25.18	0.42	1240
20150406@381	4883-013	1						36.696	0.343	25.45	0.42	1360
20150406@382	4883-014	1						35.661	0.261	24.43	0.42	1480
20150406@383	4883-015	1			x			35.587	0.308	24.36	0.42	1420
20150406@384	4883-016	1			x			36.470	0.255	25.23	0.42	1170
20150406@385	4883-017	1			x			36.427	0.275	25.19	0.42	1060

Analysis #	Sample	Line #	Diagenesis*				Bias (α)	$\delta^{18}O_{RAW}$‰	±2 SE	$\delta^{18}O_{COR}$‰	±2 SD	Distance from edge
			SEM	CLFM								
				GR	RD	FRD	A	B	C	D	E	of enamel (µm)
UWA-1												
20150406@386	UWA-1 G1							23.526	0.246			
20150406@387	UWA-1 G1							24.078	0.234			
20150406@388	UWA-1 G1							23.804	0.319			
20150406@389	UWA-1 G1							23.814	0.229			
Average and ±2 SD								**23.806**	**0.451**			
Bracket: Average and ±2 SD							**1.0110**	**23.802**	**0.417**			
Enamel												
20150406@390	4883-018	1						35.474	0.248	24.25	0.35	450
20150406@391	4883-019	1	**SEM**					34.700	0.205	23.48	0.35	480
20150406@392	4883-020	1			**x**			36.734	0.252	25.50	0.35	570
20150406@393	4883-021	1			**x**			36.594	0.194	25.36	0.35	1090
20150406@394	4883-022	1	**SEM**		**x**			35.318	0.203	24.10	0.35	1145
UWA-1												
20150406@395	UWA-1 G1							23.964	0.314			
20150406@396	UWA-1 G1							23.690	0.290			
20150406@397	UWA-1 G1; Cs res 186-187							23.648	0.230			
20150406@398	UWA-1 G1; Cs res 187-188							23.854	0.214			
Average and ±2 SD								**23.789**	**0.293**			
Bracket: Average and ±2 SD							**1.0110**	**23.797**	**0.353**			

A: Insturmental bias, which is calculated as $\alpha = (1+\delta^{18}O_{RAW}/1000)/(1+\delta^{18}O_{STD}/1000)$

B: SIMS raw measured $^{18}O/^{16}O$ ratios, converted to delta notation

C: Internal error of a single analysis (per analysis n = 20)

D: Corrected $\delta^{18}O$, corrected for instrumental bias (based on UWA-1 standard)

E: Standard deviation for individual sample within a standard bracket

Strickthrough text indicates samples considered outliers due to relative yield analysis (statistically determined as Tukey Outliers)

Analysis #	Sample	Line #	Diagenesis*				Bias (α)	$\delta^{18}O_{RAW}$‰	±2 SE	$\delta^{18}O_{COR}$‰	±2 SD	Distance from edge of enamel (µm)
			SEM	CLFM								
				GR	RD	FRD	A	B	C	D	E	

* SEM & CLFM (FRD) indicate pits not included in the paleoenvironment analysis due to irregular pits (SEM) and/or altered by diagenesis (CLFM)

References

Abell PI, Amegashitsi L, and Ochumba PB. 1996. The shells of *Etheria elliptica* as recorders of seasonality at Lake Victoria. Palaeogeography, Palaeoclimatology, Palaeoecology 119(3):215-219.

Archibold O. 1995. Ecology of Wild Vegetation. London: Chapman and Hill.

Balasse M. 2002. Reconstructing dietary and environmental history from enamel isotopic analysis: Time resolution of intra-tooth sequential sampling. International Journal of Osteoarchaeology 12(3):155-165.

Balasse M. 2003. Potential biases in sampling design and interpretation of intra-tooth isotope analysis. International Journal of Osteoarchaeology 13(1-2):3-10.

Balasse M, Ambrose SH, Smith AB, and Price TD. 2002. The Seasonal Mobility Model for Prehistoric Herders in the South-Western Cape of South Africa Assessed by Isotopic Analysis of Sheep Tooth Enamel. Journal of Archaeological Science 29(9):917-932.

Balasse M, Obein G, Ughetto-Monfrin J, and Mainland I. 2012. Investigating seasonality and season of birth in past herds: a reference set of sheep enamel stable oxygen isotope ratios. Archaeometry 54(2):349-368.

Balasse M, Smith AB, Ambrose SH, and Leigh SR. 2003. Determining sheep birth seasonality by analysis of tooth enamel oxygen isotope ratios: The late stone age site of Kasteelberg (South Africa). Journal of Archaeological Science 30(2):205-215.

Bartholomew GA, and Birdsell JB. 1953. Ecology and the protohominids. American Anthropologist 55(4):481-498.

Behrensmeyer AK, and Reed KE. 2013. Reconstructing the habitats of *Australopithecus*: Paleoenvironments, site taphonomy, and faunas. In: Reed KE, Fleagle JG, and Leakey RE, editors. The Paleobiology of *Australopithecus*. London: Springer. p 41-60.

Behrensmeyer AK, Todd NE, Potts R, and McBrinn GE. 1997. Late Pliocene faunal turnover in the Turkana Basin, Kenya and Ethiopia. Science 278(5343):1589-1594.

Bennett K. 1990. Milankovitch cycles and their effects on species in ecological and evolutionary time. Paleobiology 16(01):11-21.

Blumenschine RJ, Bunn HT, Geist V, Ikawa-Smith F, Marean CW, Payne AG, Tooby J, and van der Merwe NJ. 1987. Characteristics of an early hominid scavenging niche [and comments and reply]. Current Anthropology 28(4):383-407.

Bobe R, and Behrensmeyer AK. 2004. The expansion of grassland ecosystems in Africa in relation to mammalian evolution and the origin of the genus *Homo*. Palaeogeography, Palaeoclimatology, Palaeoecology 207(3):399-420.

Bocherens H, Mashkour M, Billiou D, Pellé E, and Mariotti A. 2001. A new approach for studying prehistoric herd management in arid areas: intra-tooth isotopic analyses of archaeological caprine from Iran. Comptes Rendus de l'Académie des Sciences-Series IIA-Earth and Planetary Science 332(1):67-74.

Boisserie J-R. 2005. The phylogeny and taxonomy of Hippopotamidae (Mammalia: Artiodactyla): a review based on morphology and cladistic analysis. Zoological Journal of the Linnean Society 143(1):1-26.

Boisserie J-R, Lihoreau F, and Brunet M. 2005. The position of Hippopotamidae within Cetartiodactyla. Proceedings of the National Academy of Sciences 102(5):1537-1541.

Bonnefille R, and Mohammed U. 1994. Pollen-inferred climatic fluctuations in Ethiopia during the last 3000 years. Palaeogeography, Palaeoclimatology, Palaeoecology 109(2-4):331-343.

Boyde A. 1976. Amelogenesis and the structure of enamel. In: Cohen B, and Kramer I, editors. Scientific Foundations of Denistry. London: Heinemann. p 335-352.

Boyde A, Fortelius M, Lester K, and Martin L. 1988. Basis of the structure and development of mammalian enamel as seen by scanning electron microscopy. Scanning Microscopy 2:1479-1490.

Brockman DK, and van Schaik CP. 2005. Seasonality in primates: studies of living and extinct human and non-human primates: Cambridge University Press.

Bromage TG. 1989. Experimental confirmation of enamel incremental periodicity in the pigtailed macaque. American Journal of Physical Anthropology 78(2):197-197.

Bromage TG, and Schrenk F. 1999. African Biogeography, Climate Change & Human Evolution. Oxford: Oxford University Press.

Campisano CJ, and Feibel CS. 2008. Depositional environments and stratigraphic summary of the Pliocene Hadar formation at Hadar, Afar depression, Ethiopia. Geological Society of America Special Papers 446:179-201.

Cerling TE, Andanje SA, Blumenthal SA, Brown FH, Chritz KL, Harris JM, Hart JA, Kirera FM, Kaleme P, and Leakey LN. 2015. Dietary changes of large herbivores in the Turkana Basin, Kenya from 4 to 1 Ma. Proceedings of the National Academy of Sciences 112(37):11467-11472.

Cerling TE, Harris JM, MacFadden BJ, Leakey MG, Quade J, Eisenmann V, and Ehleringer JR. 1997. Global vegetation change through the Miocene/Pliocene boundary. Nature 389(6647):153-158.

Cerling TE, Levin NE, Quade J, Wynn JG, Fox DL, Kingston JD, Klein RG, and Brown FH. 2010. Comment on the paleoenvironment of *Ardipithecus ramidus*. Science 328(5982):1105.

Cleland EE, Chuine I, Menzel A, Mooney HA, and Schwartz MD. 2007. Shifting plant phenology in response to global change. Trends in Ecology and Evolution 22(7):357-365.

Coryndon S. 1978. Hippopotamidae. In: Maglio V, and Cooke H, editors. Evolution of African Mammals. Cambridge: Harvard University Press. p 483-495.

Craig H. 1961. Isotopic variations in meteoric waters. Science 133(3465):1702-1703.

Dansgaard W. 1964. Stable isotopes in precipitation. Tellus 16(4):436-468.

Dart R. 1925. *Australopithecus africanus*: the man-ape of South Africa. Nature 115:195-199.

Dean M. 1987. Growth layers and incremental markings in hard tissues; a review of the literature and some preliminary observations about enamel structure in *Paranthropus boisei*. Journal of Human Evolution 16(2):157-172.

deMenocal PB. 1995. Plio-Pleistocene African climate. Science 270(5233):53-59.

deMenocal PB. 2004. African climate change and faunal evolution during the Pliocene–Pleistocene. Earth and Planetary Science Letters 220(1-2):3-24.

deMenocal PB. 2011. Climate and human evolution. Science 331:540-542.

Dirks W, Bromage TG, and Agenbroad LD. 2012. The duration and rate of molar plate formation in Palaeoloxodon cypriotes and Mammuthus columbi from dental histology. Quaternary International 255:79-85.

Domínguez-Rodrigo M. 2014. Is the "Savanna Hypothesis" a dead concept for explaining the emergence of the earliest hominins? Current Anthropology 55(1):59-81.

Dongmann G, Nürnberg H, Förstel H, and Wagener K. 1974. On the enrichment of $H_2{}^{18}O$ in the leaves of transpiring plants. Radiation and Environmental Biophysics 11(1):41-52.

Dorst J, and Dandelot P. 1970. A field guide to the larger mammals of Africa. London: Collins London.

Drapeau M, Robe R, Wynn J, and Geraads D. 2014. The Omo Mursi Formation reconsidered: a window into the East African Pliocene. Journal of Human Evolution 75:64-79.

Elenga H, Schwartz D, and Vincens A. 1994. Pollen evidence of late Quaternary vegetation and inferred climate changes in Congo. Palaeogeography, Palaeoclimatology, Palaeoecology 109(2-4):345-356.

Engel M, and Hilding O. 1983. Mineralization of developing teeth. Scanning Electron Microscopy 4:1833-1845.

Estes R. 1991. The behavior guide to African mammals: University of California Press Berkeley.

Feibel CS. 1997. Debating the environmental factors in hominid evolution. GSA Today: A Publication of the Geological Society of America 7(3):1-7.

FitzGerald C. 1998. Do enamel microstructures have regular time dependency? Conclusions from the literature and a large-scale study. Journal of Human Evolution 35(4):371-386.

Flanagan L, and Ehleringer J. 1991. Stable isotope composition of stem and leaf water: applications to the study of plant water use. Functional Ecology 5(2):270-277.

Foley R. 1993. The influence of seasonality on hominid evolution. In: Ulijaszek S, and Strickland S, editors. Seasonality and Human Ecology. Cambridge: Cambridge University Press. p 17-37.

Foley R. 1994. Speciation, extinction and climatic change in hominid evolution. Journal of Human Evolution 26(4):275-289.

Foley R. 1995. The adaptive legacy of human evolution: A search for the environment of evolutionary adaptedness. Evolutionary Anthropology: Issues, News, and Reviews 4(6):194-203.

Fricke HC, Clyde WC, and O'Neil JR. 1998. Intra-tooth variations in $\delta^{18}O$ (PO_4) of mammalian tooth enamel as a record of seasonal variations in continental climate variables. Geochimica et Cosmochimica Acta 62(11):1839-1850.

Frost SR, Jablonski NG, and Haile-Selassie Y. 2014. Early Pliocene Cercopithecidae from Woranso-Mille (Central Afar, Ethiopia) and the origins of the *Theropithecus oswaldi* lineage. Journal of Human Evolution 76:39-53.

Fukuhara T. 1959. Comparative anatomical studies of the growth lines in the enamel of mammalian teeth. Acta Anatomica Nipponica 34:322-332.

Gadbury C, Todd L, Jahren AH, and Amundson R. 2000. Spatial and temporal variations in the isotopic composition of bison tooth enamel from the Early Holocene Hudson–Meng Bone Bed, Nebraska. Palaeogeography, Palaeoclimatology, Palaeoecology 157(1):79-93.

Gat JR. 1980. The isotopes of hydrogen and oxygen in precipitation. In: Fritz P, and Fontes J, editors. Handbook of Environmental Isotope Geochemistry Vol 1, The Terrestrial Environment. Amsterdam: Elservier. p 21-42.

Geraads D, Melillo S, and Haile-Selassie Y. 2009. Middle Pliocene Bovidae from hominid-bearing sites in the Woranso-Mille area, Afar region, Ethiopia. Palaeontologica Africana 44:57-68.

Grine FE. 1986. Ecological causality and the pattern of Plio-Pleistocene hominid evolution in Africa. South African Journal of Science 82(2):87-89.

Grine FE, Ungar PS, and Teaford MF. 2006. Was the Early Pliocene hominin'*Australopithecus' anamensis* a hard object feeder? South African Journal of Science 102:301-310.

Gustafson G, and Gustafson A. 1967. Microanatomy and histochemistry of enamel. In: Miles A, editor. The Structural and Chemical Organization of Teeth. New York: Academic Press. p 75-134.

Haile-Selassie Y, Deino A, Saylor B, Umer M, and Latimer B. 2007. Preliminary geology and paleontology of new hominid-bearing Pliocene localities in the central Afar region of Ethiopia. Anthropological Science 115(3):215-222.

Haile-Selassie Y, Saylor BZ, Deino A, Alene M, and Latimer BM. 2010. New hominid fossils from Woranso-Mille (Central Afar, Ethiopia) and taxonomy of early *Australopithecus*. American Journal of Physical Anthropology 141(3):406-417.

Hallin KA, Schoeninger MJ, and Schwarcz HP. 2012. Paleoclimate during Neandertal and anatomically modern human occupation at Amud and Qafzeh, Israel: the stable isotope data. Journal of Human Evolution 62(1):59-73.

Harris J, and Cerling T. 2002. Dietary adaptations of extant and Neogene African suids. Journal of Zoology 256:45-54.

Harris J, Cerling T, Leakey M, and Passey B. 2008. Stable isotope ecology of fossil hippopotamids from the Lake Turkana Basin of East Africa. Journal of Zoology 275(3):323-331.

Hays JD, Imbrie J, and Shackleton NJ. 1976. Variations in the Earth's orbit: pacemaker of the ice ages. Science 194:1121-1132.

Hewes GW. 1961. Food transport and the origin of hominid bipedalism. American Anthropologist 63(4):687-710.

Higgins P, and MacFadden BJ. 2004. "Amount Effect" recorded in oxygen isotopes of Late Glacial horse (*Equus*) and bison (*Bison*) teeth from the Sonoran and Chihuahuan deserts, southwestern United States. Palaeogeography, Palaeoclimatology, Palaeoecology 206(3):337-353.

Hillson S. 1992. Dental enamel growth, perikymata and hypoplasia in ancient tooth crowns. Journal of the Royal Society of Medicine 85(8):460-466.

Hillson S. 2005. Teeth, Second Editon. Cambridge: Cambridge University Press.

Hoefs J. 2009. Stable isotope geochemistry. Berlin: Springer

Hoppe KA, Stover SM, Pascoe JR, and Amundson R. 2004. Tooth enamel biomineralization in extant horses: implications for isotopic microsampling. Palaeogeography, Palaeoclimatology, Palaeoecology 206(3):355-365.

Hughen KA, Eglinton TI, Xu L, and Makou M. 2004. Abrupt tropical vegetation response to rapid climate changes. Science 304(5679):1955-1959.

Hunt KD. 1994. The evolution of human bipedality: ecology and functional morphology. Journal of Human Evolution 26(3):183-202.

Isbell LA, and Young TP. 1996. The evolution of bipedalism in hominids and reduced group size in chimpanzees: alternative responses to decreasing resource availability. Journal of Human Evolution 30(5):389-397.

Kappelman J, Swisher III CC, Fleagle JG, Yirga S, Bown TM, and Feseha M. 1996. Age of *Australopithecus afarensis* from Fejej, Ethiopia. Journal of Human Evolution 30(2):139-146.

Kierdorf H, Witzel C, Upex B, Dobney K, and Kierdorf U. 2012. Enamel hypoplasia in molars of sheep and goats, and its relationship to the pattern of tooth crown growth. Journal of Anatomy 220(5):484-495.

Kimbel WH, Lockwood CA, Ward CV, Leakey MG, Rak Y, and Johanson DC. 2006. Was *Australopithecus anamensis* ancestral to *A. afarensis*? A case of anagenesis in the hominin fossil record. Journal of Human Evolution 51(2):134-152.

Kingdon J. 2003. Lowly origin: where, when, and why our ancestors first stood up. Princeton: Princeton University Press.

Kingston JD, and Hill A. 2005. When it rains it pours: legends and truths of East African pluvials. In: Lieberman D, Smith RJ, and Kelley J, editors. Interpreting the Past: Essays on Human, Primate and Mammal Evolution. Hague: Brill Academic Publishers. p 189-205.

Kingston JD. 2005. Orbital controls on seasonality. In: Brockman D, and Van Schaik C, editors. Seasonality in Primates: Studies of Living and Extinct Human and Non-Human Primates. Cambridge: Cambridge University Press. p 519-542.

Kingston JD. 2007. Shifting adaptive landscapes: progress and challenges in reconstructing early hominid environments. American Journal of Physical Anthropology 134(S45):20-58.

Kingston JD, and Harrison T. 2007. Isotopic dietary reconstructions of Pliocene herbivores at Laetoli: Implications for early hominin paleoecology. Palaeogeography, Palaeoclimatology, Palaeoecology 243(3):272-306.

Kita NT, Huberty J, Kozdon R, Beard B, and Valley JW. 2011. High-precision SIMS oxygen, sulfur and iron stable isotope analyses of geological materials: accuracy, surface topography and crystal orientation. Surface and Interface Analysis 43(1-2):427-431.

Kita NT, Ushikubo T, Fu B, and Valley JW. 2009. High precision SIMS oxygen isotope analysis and the effect of sample topography. Chemical Geology 264(1):43-57.

Koch PL, Fisher DC, and Dettman D. 1989. Oxygen Isotope Variation in the Tusks of Extinct Proboscideans - a Measure of Season of Death and Seasonality. Geology 17(6):515-519.

Kohn MJ. 1996. Predicting animal $\delta^{18}O$: accounting for diet and physiological adaptation. Geochimica et Cosmochimica Acta 60(23):4811-4829.

Kohn MJ, Schoeninger MJ, and Valley JW. 1996. Herbivore tooth oxygen isotope compositions: Effects of diet and physiology. Geochimica et Cosmochimica Acta 60(20):3889-3896.

Kohn MJ, Schoeninger MJ, and Valley JW. 1998. Variability in oxygen isotope compositions of herbivore teeth: reflections of seasonality or developmental physiology? Chemical Geology 152(1-2):97-112.

Kohn MJ, and Welker JM. 2005. On the temperature correlation of $\delta^{18}O$ in modern precipitation. Earth and Planetary Science Letters 231(1):87-96.

Kolodny Y, Bar-Matthews M, Ayalon A, and McKeegan KD. 2003. A high spatial resolution $\delta^{18}O$ profile of a speleothem using an ion-microprobe. Chemical Geology 197(1):21-28.

Kullmer O, Sandrock O, Viola TB, Hujer W, Said H, and Seidler H. 2008. Suids, elephantoids, paleochronology, and paleoecology of the Pliocene hominid site Galili, Somali Region, Ethiopia. Palaios 23(7):452-464.

Laporte LF, and Zihlman AL. 1983. Plates, climate and hominoid evolution. South African Journal of Science 79(3):96-110.

Leakey MG, Feibel CS, McDougall I, and Walker A. 1995. New four-million-year-old hominid species from Kanapoi and Allia Bay, Kenya. Nature 376(6541):565-571.

Leakey MG, Feibel CS, McDougall I, Ward C, and Walker A. 1998. New specimens and confirmation of an early age for *Australopithecus anamensis*. Nature 393(6680):62-66.

Leakey MG, Spoor F, Brown FH, Gathogo PN, Kiarie C, Leakey LN, and McDougall I. 2001. New hominin genus from eastern Africa shows diverse middle Pliocene lineages. Nature 410(6827):433-440.

Lee-Thorp JA, Sponheimer M, and Luyt J. 2007. Tracking changing environments using stable carbon isotopes in fossil tooth enamel: an example from the South African hominin sites. Journal of Human Evolution 53(5):595-601.

Levin N, Cerling T, Passey B, Harris J, and Ehleringer J. 2006. A stable isotope aridity index for terrestrial environments. Proceedings of the National Academy of Sciences 103(30):11201-11205.

Levin NE, Brown FH, Behrensmeyer AK, Bobe R, and Cerling TE. 2011. Paleosol carbonates from the Omo Group: Isotopic records of local and regional environmental change in East Africa. Palaeogeography, Palaeoclimatology, Palaeoecology 307(1):75-89.

Levin NE, Haile-Selassie Y, Frost SR, and Saylor BZ. 2015. Dietary change among hominins and cercopithecids in Ethiopia during the early Pliocene. Proceedings of the National Academy of Sciences 112(40):12304-12309.

Longinelli A. 1984. Oxygen isotopes in mammal bone phosphate: a new tool for paleohydrological and paleoclimatological research? Geochimica et Cosmochimica Acta 48(2):385-390.

Luz B, and Kolodny Y. 1985. Oxygen isotope variations in phosphate of biogenic apatites, IV. Mammal teeth and bones. Earth and Planetary Science Letters 75(1):29-36.

Luz B, Kolodny Y, and Horowitz M. 1984. Fractionation of oxygen isotopes between mammalian bone-phosphate and environmental drinking water. Geochimica et Cosmochimica Acta 48(8):1689-1693.

Macho GA, Leakey M, Williamson D, and Jiang Y. 2003. Palaeoenvironmental reconstruction: evidence for seasonality at Allia Bay, Kenya, at 3.9 million years. Palaeogeography, Palaeoclimatology, Palaeoecology 199(1):17-30.

Macho GA, and Williamson DK. 2002. The effects of ecology on life history strategies and metabolic disturbances during development: an example from the African bovids. Biological Journal of the Linnean Society 75(2):271-279.

Maslin MA, and Trauth MH. 2009. Plio-Pleistocene East African pulsed climate variability and its influence on early human evolution. In: Grine F, Fleagle JG, and Leakey RE, editors. The First Humans–Origin and Early Evolution of the Genus Homo: Springer. p 151-158.

McCrea JM. 1950. On the isotopic chemistry of carbonates and a paleotemperature scale. The Journal of Chemical Physics 18(6):849-857.

Metcalfe JZ, and Longstaffe FJ. 2012. Mammoth tooth enamel growth rates inferred from stable isotope analysis and histology. Quaternary Research 77(3):424-432.

Metcalfe JZ, and Longstaffe FJ. 2014. Environmental change and seasonal behavior of mastodons in the Great Lakes region inferred from stable isotope analysis. Quaternary Research 82(2):366-377.

Meteorological Office. 1983. Tables of Temperature, Relative Humidity, Precipitation and Sunshine for the World: Part IV. Africa, the Atlantic Ocean South of 35°N and the Indian Ocean. . London: Her Majesty's Stationary Office.

Moore J. 1996. Savanna chimpanzees, referential models and the last common ancestor. In: McGrew WC, Marchant LF, and Nishida T, editors. Great Ape Societies. Cambridge: Cambridge University Press. p 275-292.

Moss-Salentijn L, Moss M, and Yuan MS-T. 1997. The ontogeny of mammalian enamel. In: Koeningswald W, and P S, editors. Tooth enamel microstructure. Rotterdam: A.A. Balkema. p 5-30.

Nelson SV. 2005. Paleoseasonality inferred from equid teeth and intra-tooth isotopic variability. Palaeogeography, Palaeoclimatology, Palaeoecology 222(1):122-144.

Nelson SV. 2007. Isotopic reconstructions of habitat change surrounding the extinction of *Sivapithecus,* a Miocene hominoid, in the Siwalik Group of Pakistan. Palaeogeography, Palaeoclimatology, Palaeoecology 243(1):204-222.

Niemitz C. 2010. The evolution of the upright posture and gait—a review and a new synthesis. Naturwissenschaften 97(3):241-263.

Orland IJ, Bar-Matthews M, Kita NT, Ayalon A, Matthews A, and Valley JW. 2009. Climate deterioration in the Eastern Mediterranean as revealed by ion microprobe analysis of a speleothem that grew from 2.2 to 0.9 ka in Soreq Cave, Israel. Quaternary Research 71(1):27-35.

Passey BH, and Cerling TE. 2002. Tooth enamel mineralization in ungulates: implications for recovering a primary isotopic time-series. Geochimica et Cosmochimica Acta 66(18):3225-3234.

Passey BH, Cerling TE, Schuster GT, Robinson TF, Roeder BL, and Krueger SK. 2005. Inverse methods for estimating primary input signals from time-averaged isotope profiles. Geochimica et Cosmochimica Acta 69(16):4101-4116.

Passey BH, Levin NE, Cerling TE, Brown FH, and Eiler JM. 2010. High-temperature environments of human evolution in East Africa based on bond ordering in paleosol carbonates. Proceedings of the National Academy of Sciences 107(25):11245-11249.

Payne RJ, and Wilson JD. 1999. Resource limitation in seasonal environments. Oikos 87(2):303-314.

Poage MA, and Chamberlain CP. 2001. Empirical relationships between elevation and the stable isotope composition of precipitation and surface waters: Considerations for studies of paleoelevation change. American Journal of Science 301(1):1-15.

Podlesak D, Torregrossa A, Ehleringer J, Dearing M, Passey B, and Cerling T. 2008. Turnover of oxygen and hydrogen isotopes in the body water, CO_2, hair, and enamel of a small mammal. Geochimica et Cosmochimica Acta 72:19-35.

Pokras EM, and Mix AC. 1987. Earth's precession cycle and Quaternary climatic change in tropical Africa. Nature 326:486-487.

Potts R. 1996. Evolution and climate variability. Science 273(5277):922.

Potts R. 1998a. Environmental hypotheses of hominin evolution. American Journal of Physical Anthropology 107(s27):93-136.

Potts R. 1998b. Variability selection in hominid evolution. Evolutionary Anthropology: Issues, News, and Reviews 7(3):81-96.

Potts R. 2012. Evolution and Environmental Change in Early Human Prehistory. Annual Review of Anthropology 41:151-167.

Potts R. 2013. Hominin evolution in settings of strong environmental variability. Quaternary Science Reviews 73:1-13.

Rayner R, Moon B, and Masters J. 1993. The Makapansgat Australopithecine environment. Journal of Human Evolution 24(3):219-231.

Reed KE. 1997. Early hominid evolution and ecological change through the African Plio-Pleistocene. Journal of Human Evolution 32(2):289-322.

Reed KE, and Fish JL. 2005. Tropical and temperate seasonal influences on human evolution. In: Brockman D, and Van Schaik C, editors. Seasonality in primates: studies of living and extinct human and non-human primates. Cambridge: Cambridge University Press. p 489-518.

Reich PB. 1995. Phenology of tropical forests: patterns, causes, and consequences. Canadian Journal of Botany 73(2):164-174.

Reith EJ, and Butcher EO. 1967. Microanatomy and histochemistry of amelogenesis. In: Miles A, editor. Structural and Chemical Organization of Teeth. New York: Academic Press. p 371-397.

Retallack G. 1994. The environmental factor approach to the interpretation of paleosols. In: Amundson R, Harden J, and Singer M, editors. Factors of soil formation: a fifieth annerversary perspective. Madison: Soil Science Society of America. p 31-64.

Retallack GJ. 2000. Depth to pedogenic carbonate horizon as a paleoprecipitation indicator?: Comment and Reply Geology 28(6):572.

Retallack GJ. 2005. Pedogenic carbonate proxies for amount and seasonality of precipitation in paleosols. Geology 33(4):333-336.

Robinson C, Fuchs P, Deutsch D, and Weatherell J. 1978. Four chemically distinct stages in developing enamel from bovine incisor teeth. Caries Research 12(1):1-11.

Rozanski K, Araguás-Araguás L, and Gonfiantini R. 1992. Relation between long-term trends of oxygen-18 isotope composition of precipitation and climate. Science 258:981-984.

Rozanski K, Araguás-Araguás L, and Gonfiantini R. 1993. Isotopic patterns in modern global precipitation. In: Swart P, Lohmann K, McKenzie J, and Savin E, editors. Climate Change in Continental Isotopic Records. Washington: Geophysical Monograph AGU. p 1-36.

Rozanski K, Araguás-Araguás L, and Gonfiantini R. 1996. Isotope patterns of precipitation in the East African Region. In: Johnson C, editor. The Limnology, Climatology, and Paleoclimatology of the East African Lakes. Amsterdam: Gordon and Breach. p 79-93.

Schoeninger MJ, Reeser H, and Hallin K. 2003. Paleoenvironment of *Australopithecus anamensis* at Allia Bay, East Turkana, Kenya: evidence from mammalian herbivore enamel stable isotopes. Journal of Anthropological Archaeology 22(3):200-207.

Sepulchre P, Ramstein G, Fluteau F, Schuster M, Tiercelin J-J, and Brunet M. 2006. Tectonic uplift and Eastern Africa aridification. Science 313(5792):1419-1423.

Sharp Z, and Cerling TE. 1998. Fossil isotope records of seasonal climate and ecology: straight from the horse's mouth. Geology 26(3):219-222.

Shellis R. 1984. Variations in growth of the enamel crown in human teeth and a possible relationship between growth and enamel structure. Archives of Oral Biology 29(9):697-705.

Souron A, Balasse M, and Boisserie J-R. 2012. Intra-tooth isotopic profiles of canines from extant *Hippopotamus amphibius* and late Pliocene hippopotamids (Shungura Formation, Ethiopia): insights into the seasonality of diet and climate. Palaeogeography, Palaeoclimatology, Palaeoecology 342:97-110.

Sponheimer M, and Lee-Thorp J. 2014. Hominin Paleodiets: The Contribution of Stable Isotopes. In: Henke W, and Tattersall I, editors. Handbook of Paleoanthropology. Berlin: Springer. p 1-27.

Sponheimer M, and Lee-Thorp JA. 1999. Oxygen isotopes in enamel carbonate and their ecological significance. Journal of Archaeological Science 26(6):723-728.

Stanley SM. 1995. Climatic forcing and the origin of the human genus. In: Stanley SM, editor. Effects of past global change in life. Washington DC: National Academy Press. p 233-243.

Suga S. 1982. Progressive mineralization pattern of developing enamel during the maturation stage. Journal of Dental Research 61:1532-1542.

Suga S. 1983. Comparative hisotology of the progressive mineralization pattern of developing enamel. In: Suga S, editor. Mechanisms of Tooth Enamel Formation. Toyko: Quintessence Publishing. p 167-203.

Tafforeau P, Bentaleb I, Jaeger J-J, and Martin C. 2007. Nature of laminations and mineralization in rhinoceros enamel using histology and X-ray synchrotron microtomography: potential implications for palaeoenvironmental isotopic studies. Palaeogeography, Palaeoclimatology, Palaeoecology 246(2):206-227.

Tojo B, and Ohno T. 1999. Continuous growth-line sequences in gastropod shells. Palaeogeography, Palaeoclimatology, Palaeoecology 145(1):183-191.

Trauth MH, Maslin MA, Deino AL, Strecker MR, Bergner AG, and Dühnforth M. 2007. High- and low-latitude forcing of Plio-Pleistocene East African climate and human evolution. Journal of Human Evolution 53(5):475-486.

Treble P, Schmitt AK, Edwards R, McKeegan KD, Harrison T, Grove M, Cheng H, and Wang Y. 2007. High resolution Secondary Ionisation Mass Spectrometry (SIMS) $\delta^{18}O$ analyses of Hulu Cave speleothem at the time of Heinrich Event 1. Chemical Geology 238(3):197-212.

Uno KT, Quade J, Fisher DC, Wittemyer G, Douglas-Hamilton I, Andanje S, Omondi P, Litoroh M, and Cerling TE. 2013. Bomb-curve radiocarbon measurement of recent biologic tissues and applications to wildlife forensics and stable isotope (paleo) ecology. Proceedings of the National Academy of Sciences 110(29):11736-11741.

Valley JW, Graham CM, Harte B, Eiler JM, and Kinny PD. 1998a. Ion microprobe analysis of oxygen, carbon, and hydrogen isotope ratios. In: McKibben M, Shanks W, III, and WI R, editors. Applications of Microanalytical Techniques to Understanding Mineralizing Processes: S.E.G. Review in Economic Geology. p 73-97.

Valley JW, Kinny PD, Schulze DJ, and Spicuzza MJ. 1998b. Zircon megacrysts from kimberlite: oxygen isotope variability among mantle melts. Contributions to Mineralogy and Petrology 133(1-2):1-11.

Valley JW, and Kita NT. 2009. *In situ* oxygen isotope geochemistry by ion microprobe. Secondary Ion Mass Spectrometry in the Earth Sciences (MAC Short Course) Canada: Mineralogical Association of Canada. p 19-63.

Van Couvering J. 2000. Fejej. In: Delson E, Tattersall I, Van Couvering J, and Brooks A, editors. Encyclopedia of human evolution and prehistory (2nd Edition). New York: Garland. p 267-268.

Verschuren D, Damsté JSS, Moernaut J, Kristen I, Blaauw M, Fagot M, Haug GH, van Geel B, De Batist M, and Barker P. 2009. Half-precessional dynamics of monsoon rainfall near the East African Equator. Nature 462(7273):637-641.

Verschuren D, Laird KR, and Cumming BF. 2000. Rainfall and drought in equatorial east Africa during the past 1,100 years. Nature 403(6768):410-414.

Vogel J. 1983. Isotopic evidence for the past climates and vegetation of southern Africa. Bothalia 14(3/4):391-394.

Vrba E, Denton G, Partridge T, and Burckle L. 1995. Paleoclimate and Evolution with Emphasis on Human Origins. New Haven: Yale University Press.

Vrba ES. 1988. Late Pliocene climatic events and hominid evolution. In: Grine F, editor. Evolutionary History of the "Robust" Australopithecines. New York: Aldine de Gruyter. p 405-426.

Walther G-R, Post E, Convey P, Menzel A, Parmesan C, Beebee TJ, Fromentin J-M, Hoegh-Guldberg O, and Bairlein F. 2002. Ecological responses to recent climate change. Nature 416(6879):389-395.

Ward CV. 2014. Taxonomic affinity of the Pliocene hominin fossils from Fejej, Ethiopia. Journal of Human Evolution 73:98-102.

Weidel BC, Ushikubo T, Carpenter SR, Kita NT, Cole JJ, Kitchell JF, Pace ML, and Valley JW. 2007. Diary of a bluegill (*Lepomis macrochirus*): daily $\delta^{13}C$ and $\delta^{18}O$ records in otoliths

by ion microprobe. Canadian Journal of Fisheries and Aquatic Sciences 64(12):1641-1645.

Weinmann JP, Wessinger GD, and Reed G. 1942. Correlation of chemical and histological investigations on developing enamel. Journal of Dental Research 21:171-182.

Wheeler PE. 1991. The influence of bipedalism on the energy and water budgets of early hominids. Journal of Human Evolution 21(2):117-136.

White TD, Ambrose SH, Suwa G, Su DF, DeGusta D, Bernor RL, Boisserie J-R, Brunet M, Delson E, Frost S et al. . 2009. Macrovertebrate Paleontology and the Pliocene Habitat of *Ardipithecus ramidus*. Science 326(5949):67-93.

White TD, WoldeGabriel G, Asfaw B, Ambrose S, Beyene Y, Bernor RL, Boisserie J-R, Currie B, Gilbert H, Haile-Selassie Y et al. . 2006. Asa Issie, Aramis and the origin of *Australopithecus*. Nature 440(7086):883-889.

Wood B, and Leakey M. 2011. The Omo-Turkana Basin Fossil Hominins and Their Contribution to Our Understanding of Human Evolution in Africa. Evolutionary Anthropology: Issues, News, and Reviews 20(6):264-292.

Wynn JG. 2000. Paleosols, stable carbon isotopes, and paleoenvironmental interpretation of Kanapoi, Northern Kenya. Journal of Human Evolution 39(4):411-432.

Wynn JG. 2004. Influence of Plio-Pleistocene aridification on human evolution: Evidence from paleosols of the Turkana Basin, Kenya. American Journal of Physical Anthropology 123(2):106-118.

Yurtsever Y, and Gat J. 1981. Stable isotope hydrology: Deuterium and Oxygen-18 in the water cycle. IAEA Technical Report Series 210. Atmospheric Waters:103-142.

Zazzo A, Balasse M, and Patterson WP. 2005. High-resolution δ 13 C intratooth profiles in bovine enamel: implications for mineralization pattern and isotopic attenuation. Geochimica et Cosmochimica Acta 69(14):3631-3642.

Zazzo A, Bendrey R, Vella D, Moloney A, Monahan F, and Schmidt O. 2012. A refined sampling strategy for intra-tooth stable isotope analysis of mammalian enamel. Geochimica et Cosmochimica Acta 84:1-13.

CHAPTER 5: DISCUSSION AND CONCLUSION

Results of stable isotope analyses on modern Koobi Fora and fossil Allia Bay fauna samples presented in this dissertation demonstrate 1) that Allia Bay 4Ma was more mesic with a greater amount of woody cover compared to today, 2) enamel does diagenetically alter and changes to the mineral structure correspond to changes in $\delta^{18}O$ values, and 3) the unaltered enamel regions indicate seasonal shifts in available $\delta^{18}O$ values recorded in tooth enamel of both browsers and grazers during enamel deposition. There appear to be two main patterns of seasonal variation in rainfall, either 1) periods when the local environment had a stable moisture regime with relatively little variation in the magnitude of difference in $\delta^{18}O_{en}$, or 2) periods of more extreme aridity resulting in greater marked seasonality intra-annually. There also is a possible shift in the baseline $\delta^{18}O_{en}$ values recorded by the hippos and suids 16-17‰ and 23-25‰ when the general pattern of the seasonal cycle recorded was similar but the amount of rainfall changed between a wetter and drier phase.

This dissertation highlights the importance of looking at human evolution in terms of smaller, more local sites and time scales. The interpretation of the larger region of the Turkana Basin over the last 4 Ma suggests that the region was as arid as today. But, this does not accurately characterize the paleoenvironment at Allia Bay or capture the amount of seasonal variation experienced within one site over a short period of time (i.e., 60 ka). During the time of *Au. anamensis*, the habitat at Allia Bay was most likely to have been a gallery forest along a permanent river channel or a Miombo woodland with areas of widely scattered trees. Both can be considered mosaic habitats, but possibly the biomass availability in each mosaic is differentially affected by varying seasonal rainfall patterns. Further, during the time that this hominin species inhabited the region, we see evidence for a variable seasonal environment and a shift in the baseline $\delta^{18}O_{en}$ values.

Kingston (2007) advocated that short-term ecological changes might match or even exceed the influence of long-term changes on evolution. Allia Bay fossil fauna SIMS generated $\delta^{18}O_{en}$ patterns serve as an example of the amount of variation in the seasonal paleoenvironment that can be experienced at the biological time scale. The baseline shift in $\delta^{18}O_{en}$ values suggest a transition between closed and open habitats accompanied by differences in rainfall, but with the seasonal cycle being maintained as the amplitude does not change for the hippos. Yet, during the driest phases recorded at Allia Bay by the browsers, there is a change in the seasonal cycle of rainfall with an increase in the magnitude of seasonality. SIMS high-resolution analysis of fossil enamel $\delta^{18}O$ patterns demonstrated in this dissertation provide a new scale of analysis in paleoenvironment reconstructions to address questions about seasonality not previously available to researchers to investigate how varied seasonal rainfall was in mosaic paleoenvironments. The Allia Bay fossil locality served as a pilot study to demonstrate the variation in seasonal rainfall patterns at hominin fossil localities; the next step is to expand the application of this method to other hominin fossil localities in East Africa.

Future Studies

By generating high-resolution $\delta^{18}O$ values from fossil fauna enamel, we demonstrate a method of controlling for enamel diagenesis and we provide a new scale of analysis for reconstructing the paleoenvironment during the lifetime of an individual animal. The SIMS capabilities available to researchers now allows for more nuanced questions about the relationship between the environment and human evolution. Several of these future studies are briefly discussed below.

SIMS analysis of $\delta^{13}C$

The next step in this larger paleoenvironment reconstruction project at Allia Bay is to analyze the $\delta^{13}C$ values in the same Allia Bay samples at WiscSIMS to 1) identify and control for

diagenetically altered $\delta^{13}C$ values and 2) reveal evidence of paleoecology complementary to the $\delta^{18}O$ values. Overall, high $\delta^{13}C$ values in large-bodied herbivores would indicate arid and open conditions whereas low values would indicate more closed, wooded environments (Kohn 2010). By investigating the $\delta^{18}O$ and $\delta^{13}C$ patterns with the high-resolution capability of SIMS in contrast to previously reported bulk data (i.e., a single value per tooth), the seasonal relationship between precipitation and the feeding ecology at the local site level within individual browsing and grazing fauna can be understood. The addition of high-resolution $\delta^{13}C$ patterns recorded in faunal enamel will be a first step at understanding how the biomass availability on a landscape changes the feeding behavior of an individual animal as fluctuations in seasonally available $\delta^{18}O_{ppt}$ occur. Most importantly, this will be at a biological time scale (during the duration of enamel deposition).

Australopithecus anamensis fossil localities

By conducting similar high-resolution SIMS analyses at other fossil localities contemporary to Allia Bay, the hypothesis of early *Australopithecus* as a hominin genus uniquely adapted to arid regions (Codron et al. 2008) can be further investigated. Some ecological indicators suggest that *Au. anamensis* could survive in a variety of ecosystems from wetter, closed woodlands with patches of open grassland to more arid woodland and shrubland regions (Wynn 2000). Prime fossil localities to investigate would include Kanapoi, Omo Mursi, and Woranso-Mille. Kanapoi has the most recovered *Au. anamensis* fossils and is a more arid environment compared to Allia Bay based on the bulk isotopic analysis of enamel. Based on the results of the Allia Bay high-resolution SIMS data, it would be expected that the more arid a site it, the more marked a seasonal shift (i.e., increased $\Delta^{18}O_{en}$) would be recorded in the fossil enamel. Although not a contemporary site of Allia Bay, the *Au. anamensis* locality of Woranso-Mille represents a wetter, but similarly open environment to Kanapoi. By analyzing the $\delta^{18}O$ and $\delta^{13}C$ in a wet/open environment compared to the wet/closed woodland of Allia Bay would be an

interesting site to better understand the seasonal relationship between $\delta^{18}O$ and $\delta^{13}C$ available on a paleolandscape. At Omo-Mursi, where no hominins have been recovered, the more mesic environment might suggest that the paleoenvironment had a more stable mildly seasonal habitat that was well-watered throughout the year with a constant biomass availability resulting in increased competition with closed-habitat species. The increase in competition in a stable well-watered environment might have pushed the adaptively flexible hominins into regions with increased variable seasonality.

Other fossil localities

Additionally, it would be interesting to conduct similar seasonal evaluation of intra-annual variation in rainfall ($\delta^{18}O$ analysis) and diet ($\delta^{13}C$ analysis) using SIMS to analyze fossil fauna at the *Au. afarensis* locality of Laetoli, Tanzania. A phylogenetic analysis supports the idea of a single evolving lineage beginning with the earlier *Ardipithecus ramidus* that was subsequently succeeded by *Au. anamensis*, which was in turn replaced by the later *Au. afarensis* (Haile-Selassie et al. 2010; Kimbel et al. 2006; White et al. 2006), documented at Laetoli (Leakey and Hay 1979). The addition of Laetoli, the famous footprint site, will result in site environment data for the two latter species to complement those from the earliest species.

The fossil fauna material from the Upper Laetolil Beds of Laetoli (~3.6-3.85 Ma) contain *Au. afarensis* remains. Previous characterization of the habitat, based on the lack of permanent rivers or lakes, concludes that the region was arid (Su and Harrison 2015). However, the identification of fossil springs and plant biomarkers at nearby Olduvai Gorge ~2 Ma) indicate that hominins had access to spring-fed wetlands on this patchwork landscape (Ashley et al. 2010; Ashley et al. 2009; Magill et al. 2016) making the Laetolil Beds an ideal comparison to Allia Bay. By testing the fossil fauna of the Laetolil Beds with SIMS high-resolution $\delta^{18}O$ and $\delta^{13}C$ analysis, we would be able to characterize the seasonal variation in rainfall and faunal diet in an environment with limited access to year-round water. In arid regions with limited access to

permanent water sources (i.e., the river at Allia Bay and fossil springs in the Olduvai/Laetoli region), seasonal shifts in available resource biomass on the landscape could have significant impact on the behaviors expressed by groups of early hominins (i.e., seasonal foraging, niche specialization).

Diagenesis and CLFM image fluorescence

This dissertation provided one new method, CLFM, to identify possible diagentically altered regions affected by mineral structure change by inclusions in enamel occurring post-depositional. After concluding this dissertation project, the best understanding of the relationship between CLFM imaging and diagenesis is that mineral structure changes to fossil enamel occur in all the zones that fluoresces for each CLFM laser line, but not each laser line identifies changes that alter the $\delta^{18}O_{en}$ values. The best-fit of the far-red fluorophore laser line corresponding to $\delta^{18}O_{en}$ values that have altered values from the expected pattern suggests that the minerals causing the fluorescent emissions in the far-red regions are likely the cause of the isotopic alteration. Until further research with electron microprobe analysis, far-red fluorophore zones are considered the cause of alteration to $\delta^{18}O_{en}$ values at Allia Bay. The particular incorporation of diagenetic material is highly dependent of site-specific characteristics of the soil matrix and groundwater, so further investigations must be conducted using CLFM images of fossil material to better understand how different fluorescing minerals impact $\delta^{18}O_{en}$ values. To specifically identify the diagenesis observed in the Allia Bay fossil fauna studied in this dissertation, electron microprobe analysis will need to be conducted similar to previous studies (Kohn et al. 1999).

While enamel has been presumed to be limitedly altered by diagenesis, the results of this dissertation confirm the previous CL enamel analysis identifying mineral structure changes (Schoeninger et al. 2003) and show that $\delta^{18}O_{en}$ values do alter in correlation with zones of mineral structure change. Enamel diagenesis does not occur only at the outer surface that is in contact with the burial environment, but also along macro-cracks, along the DEJ where the more organic

dentine is decomposing during fossilization causing exchanges with enamel, and throughout all the enamel. The established protocol of enamel sampling by ablating the outer surface of enamel and sampling from the internal layers for isotopic analysis should be used with caution in future studies unless through diagenetic analyses have been conducted.

Conclusion

Through traditional bulk stable isotope analysis of modern and fossil fauna enamel and high-resolution SIMS generated $\delta^{18}O_{en}$ patterns, this dissertation presented an assessment of the paleoenvironment at Allia Bay 3.97 Ma when Australopithecus anamensis occupied the Turkana Basin. By demonstrating that the local environment at Allia Bay was distinctly wetter and more closed compared to regional interpretations of the Turkana Basin, it is clear that local habitats surrounding Lake Turkana were distinct ecologically to the extent that different microclimates existed over the past 4Ma during the critical period of human evolution in East Africa. This project added a new method for paleoenvironment investigations, improving the scale of analysis from the duration of a single tooth developing (i.e., possibly multiple years of tooth formation) to individual enamel layer deposition (i.e. daily increments). While the complex process of enamel diagenesis is not understood completely, the results of this dissertation confirm previous questions about the relationship between mineral structure change and alteration to $\delta^{18}O_{en}$ values. Some evidence of mineral structure change (i.e., unknown far-red fluorophores identified by CLFM) do correlate with diagenesis of $\delta^{18}O_{en}$ values, while other inclusions (i.e., zonation in enamel associated with green and red fluorophores) have possibly limited impact to $\delta^{18}O_{en}$ values. Ultimately, this dissertation documented the first evidence of variation in $\delta^{18}O_{en}$ values associated with recording seasonality at Allia Bay and the need for early hominins to be adaptively flexible in a variable seasonal paleoenvironment.

References

Ashley GM, Barboni D, Dominguez-Rodrigo M, Bunn HT, Mabulla AZ, Diez-Martin F, Barba R, and Baquedano E. 2010. Paleoenvironmental and paleoecological reconstruction of a freshwater oasis in savannah grassland at FLK North, Olduvai Gorge, Tanzania. Quaternary Research 74(3):333-343.

Ashley GM, Tactikos JC, and Owen RB. 2009. Hominin use of springs and wetlands: paleoclimate and archaeological records from Olduvai Gorge (~ 1.79–1.74 Ma). Palaeogeography, Palaeoclimatology, Palaeoecology 272(1):1-16.

Codron D, Lee-Thorp JA, Sponheimer M, De Ruiter D, and Codron J. 2008. What insights can baboon feeding ecology provide for early hominin niche differentiation? International Journal of Primatology 29(3):757-772.

Haile-Selassie Y, Saylor BZ, Deino A, Alene M, and Latimer BM. 2010. New hominid fossils from Woranso-Mille (Central Afar, Ethiopia) and taxonomy of early *Australopithecus*. American Journal of Physical Anthropology 141(3):406-417.

Kimbel WH, Lockwood CA, Ward CV, Leakey MG, Rak Y, and Johanson DC. 2006. Was *Australopithecus anamensis* ancestral to *A. afarensis*? A case of anagenesis in the hominin fossil record. Journal of Human Evolution 51(2):134-152.

Kingston JD. 2007. Shifting adaptive landscapes: progress and challenges in reconstructing early hominid environments. American Journal of Physical Anthropology 134(S45):20-58.

Kohn MJ. 2010. Carbon isotope compositions of terrestrial C3 plants as indicators of (paleo)ecology and (paleo)climate. Proceedings of the National Academy of Sciences 107(46):19691-19695.

Kohn MJ, Schoeninger MJ, and Barker WW. 1999. Altered states: Effects of diagenesis on fossil tooth chemistry. Geochimica et Cosmochimica Acta 63(18):2737-2747.

Leakey MD, and Hay RL. 1979. Pliocene footprints in the Laetolil Beds at Laetoli, northern Tanzania. Nature 278(5702):317-323.

Magill CR, Ashley GM, Domínguez-Rodrigo M, and Freeman KH. 2016. Dietary options and behavior suggested by plant biomarker evidence in an early human habitat. Proceedings of the National Academy of Sciences:201507055.

Schoeninger MJ, Hallin K, Reeser H, Valley JW, and Fournelle J. 2003. Isotopic alteration of mammalian tooth enamel. International Journal of Osteoarchaeology 13(1-2):11-19.

Su DF, and Harrison T. 2015. The paleoecology of the Upper Laetolil Beds, Laetoli Tanzania: A review and synthesis. Journal of African Earth Sciences 101:405-419.

White TD, WoldeGabriel G, Asfaw B, Ambrose S, Beyene Y, Bernor RL, Boisserie J-R, Currie B, Gilbert H, Haile-Selassie Y et al. . 2006. Asa Issie, Aramis and the origin of *Australopithecus*. Nature 440(7086):883-889.

Wynn JG. 2000. Paleosols, stable carbon isotopes, and paleoenvironmental interpretation of Kanapoi, Northern Kenya. Journal of Human Evolution 39(4):411-432.